

**LONGSHORE CURRENT AND SEDIMENT TRANSPORT
DUE TO BREAKING WAVES AND ALONGSHORE
PRESSURE GRADIENT**

by

Ali Farhadzadeh, Nobuhisa Kobayashi and Mark B. Gravens

Research Report No. CACR- CACR-10-04
August 2010



Center for Applied Coastal Research
University of Delaware
Newark, DE 19716

ACKNOWLEDGEMENTS

This study was supported by the U.S. Army Corps of Engineers, Coastal and Hydraulics Laboratory under Contract No. W912BU-09-R-0031 and W912HZ-10-P-0234.

TABLE OF CONTENTS

LIST OF TABLES.....	iv
LIST OF FIGURES.....	v
ABSTRACT.....	x
CHAPTER 1 INTRODUCTION.....	1
CHAPTER 2 DATA ANALYSIS.....	4
2.1 EXPERIMENTAL SETUP.....	4
2.2 BATHYMETRY.....	6
2.3 FREE SURFACE ELEVATION.....	9
2.4 CROSS-SHORE AND LONGSHORE CURRENTS.....	16
2.5 SEDIMENT CONCENTRATION.....	22
2.6 LONGSHORE SEDIMENT TRANSPORT.....	27
CHAPTER 3 NUMERICAL MODEL COAST.....	30
3.1 COMBINED WAVE AND CURRENT MODEL IN WET ZONE.....	30
3.2 HYDRODYNAMIC MODEL FOR LONGSHORE CURRENT ONLY.....	40
3.3 SEDIMENT TRANSPORT MODEL IN WET ZONE.....	41
3.4 SEDIMENT TRANSPORT MODEL FOR LONGSHORE CURRENT ONLY.....	48

3.5	MODEL FOR IMPERMEABLE WET AND DRY ZONE.....	50
3.6	SEDIMENT TRANSPORT MODEL IN WET AND DRY ZONE.....	57
CHAPTER 4	COMPARISON WITH EXPERIMENT.....	62
4.1.	MODEL CALIBRATION.....	63
4.2.	COMPARISONS.....	65
4.3.	APPLICATIONS.....	82
CHAPTER 5	SUMMARY AND CONCLUSIONS.....	86
REFERENCES.....		90
APPENDIX A.....	TEST BC1.....	96
APPENDIX B.....	TEST BC2.....	120
APPENDIX C.....	TEST BC3.....	144
APPENDIX D.....	TEST BC4.....	161
APPENDIX E.....	TEST BC5.....	185

LIST OF TABLES

Table 2-1. Range of Wave height, Spectral Peak Period and Wave Set-down Measured at $x = 0$ and Test Duration for Five Tests	10
Table 2-2. Averaged Wave Height, Spectral Peak Period and Wave Set-down at $x = 0$ for Five Tests.....	11
Table 2-3. Cross-shore Location, Still Water Depth and Mean Cross-shore Velocity at $y = 0$ for Test BC1.....	18
Table 2-4. Range of Mean Cross-shore Velocity in Zone of Alongshore Uniformity for Four Tests with Waves.....	19
Table 2-5. Cross-shore Locations of ADV, Still Water Depth and Mean Longshore Velocity at $y = 0$ for Test BC1.....	20
Table 2-6. Range of Mean Longshore Velocities in Zone of Alongshore Uniformity for Five Tests	22
Table 2-7. Fitted Coefficients and Suspended Sediment Volume per Unit Horizontal Area Based on Exponential and Power-form Profiles at $y = 0$ for Test BC1.....	24
Table 2-8. Total Longshore Sediment Transport Data for Each Trap in Test BC1.....	28
Table 2-9. Total Longshore Sediment Transport Rate Q_{ly} (cm^3/s) across Surf and Swash Zones for Five Tests.....	29
Table 4-1. Recirculation Rate and Alongshore Gradient E of Mean Water Level for Five Tests.....	65

LIST OF FIGURES

Fig. 2-1. Layout of LSTF experimental setup.....	5
Fig. 2-2. Measured initial and final profiles and change in bottom elevation for test BC1.....	7
Fig. 2-3. Measured initial profiles for test BC1.....	8
Fig. 2-4. Averaged initial and final profiles in zone of alongshore uniformity for BC1.....	9
Fig. 2-5. Cross-shore and longshore variations of <i>RMS</i> wave height for test BC1.....	11
Fig. 2-6. Cross-shore and longshore variations of wave setup for test BC1.....	12
Fig. 2-7. Estimation of wave setup alongshore gradient for test BC1.....	13
Fig. 2-8. Estimation of wave setup alongshore gradient for test BC2.....	14
Fig. 2-9. Estimation of wave setup alongshore gradient for test BC3.....	14
Fig. 2-10. Estimation of wave setup alongshore gradient for test BC4.....	15
Fig. 2-11. Estimation of wave setup alongshore gradient for test BC5.....	15
Fig. 2-12. Cross-shore positioning of ADV and FOBS at $y = 0$ for test BC1.....	17
Fig. 2-13. Cross-shore and longshore variations of mean cross-shore velocity for test BC1.....	19
Fig. 2-14. Cross-shore and longshore variations of mean longshore velocity for test BC1.....	21
Fig. 2-15. Vertical distributions of mean concentration \bar{c} using exponential and power-form profiles for each FOBS for test BC1.....	23

Fig. 2-16. Sediment concentration data and power-form and exponential profiles at $y = 0$ for test BC1.....	25
Fig. 2-17. Comparison of suspended sediment volume per unit horizontal area using power-form and exponential profiles for all locations in test BC1.....	26
Fig. 2-18. Cross-shore and longshore distributions of suspended sediment volume per unit horizontal area using power-form and exponential profiles at all locations for test BC1.....	27
Fig. 2-19. Cross-shore distribution of total longshore sediment transport rate q_y for test BC1.....	29
Fig. 3-1. Definition sketch for incident irregular waves on beach.....	31
Fig. 3-2. Function $G_b(r)$ for wet and dry zone.....	54
Fig. 3-3. Transition from wet model ($x < x_r$) to wet and dry model ($x > x_{swl}$) for emerged impermeable structure ($R_c > 0$).....	55
Fig. 4-1. Empirical function $F(x)$ for cross-shore variation of wave setup alongshore gradient.....	64
Fig. 4-2. Measured and computed cross-shore variations of mean water level $\bar{\eta}$, free surface standard deviation σ_η , cross-shore current \bar{U} and longshore current \bar{V} for BC1.....	66
Fig. 4-3. Cross-shore variations of computed q_{sy} and q_{by} as well as measured and computed q_y for BC1.....	67

Fig. 4-4. Cross-shore variations of computed q_{sx} , q_{bx} and q_x for BC1.....	68
Fig. 4-5. Cross-shore variation of measure and computed suspended sediment volume per unit horizontal area for BC1.....	69
Fig. 4-6. Measured and computed cross-shore variations of mean water level $\bar{\eta}$, free surface standard deviation σ_η , cross-shore current \bar{U} and longshore current \bar{V} for BC2.....	70
Fig. 4-7. Cross-shore variations of computed q_{sy} and q_{by} as well as measured and computed q_y for BC2.....	71
Fig. 4-8. Cross-shore variations of computed q_{sx} , q_{bx} and q_x for BC2.....	72
Fig. 4-9. Cross-shore variation of measured and computed suspended sediment volume per unit horizontal area for BC2.....	73
Fig. 4-10. Cross-shore variations of measured and computed longshore current \bar{V} , computed q_{sy} and q_{by} as well as measured and computed q_y for BC3.....	74
Fig. 4-11. Cross-shore variation of computed suspended sediment volume per unit horizontal area for BC3.....	75
Fig. 4-12. Measured and computed cross-shore variations of mean water level $\bar{\eta}$, free surface standard deviation σ_η , cross-shore current \bar{U} and longshore current \bar{V} for BC4.....	76

Fig. 4-13. Cross-shore variations of computed q_{sy} and q_{by} as well as measured and computed q_y for BC4.....	77
Fig. 4-14. Cross-shore variations of computed q_{sx} , q_{bx} and q_x for BC4.....	78
Fig. 4-15. Cross-shore variation of measured and computed suspended sediment volume per unit horizontal area for BC4.....	79
Fig. 4-16. Measured and computed cross-shore variations of mean water level $\bar{\eta}$, free surface standard deviation σ_η , cross-shore current \bar{U} and longshore current \bar{V} for BC5.....	80
Fig. 4-17. Cross-shore variations of computed q_{sy} and q_{by} as well as measured and computed q_y for BC5.....	81
Fig. 4-18. Cross-shore variations of computed q_{sx} , q_{bx} and q_x for BC5.....	81
Fig. 4-19. Cross-shore variation of computed suspended sediment volume per unit horizontal area for BC5.....	82
Fig. 4-20. Computed cross-shore variations of \bar{V} , q_{sy} , q_{by} and q_y for $(E \times 10^4) =$ -1.2, -0.6, 0.0, 0.6 and 1.2.....	83
Fig. 4-21. Computed cross-shore variations of q_{sx} , q_{bx} and q_x for $(E \times 10^4) =$ -1.2, -0.6, 0.0, 0.6 and 1.2.....	84
Fig. 4-22. Computed cross-shore variations of longshore sediment transport volume per unit width, V_y for $(E_m \times 10^4) =$ 0.0, 0.6 and 1.2.....	85

ABSTRACT

Five tests were conducted in a wave basin with a recirculation system in the Large-scale Sediment Transport Facility (LSTF) of the US Army Engineer Research and Development Center to study sediment transport due to waves and currents. These five tests are explained and the analyzed data are presented for the subsequent comparison with the cross-shore numerical model CSHORE.

The effects of external currents on the wave-induced longshore current and sediment transport in the surf zone are examined using the above five tests and CSHORE which is extended to include the alongshore pressure gradient term in the longshore momentum equation and to allow oblique waves in the wet and dry zone on a beach. Analytical solutions for the case of current only are derived from the combined wave and current model and the sediment transport model in CSHORE.

The cross-shore variations of the wave setup, root-mean-square wave height, mean cross-shore and longshore velocities and total longshore sediment transport rate are predicted fairly well for the five tests with no and favorable pressure gradients. The cross-shore variation of the suspended sediment volume per unit area is predicted

only qualitatively partly because of the large scatter of the sediment volumes estimated from the measured sand concentrations.

The calibrated and verified CSHORE is used to compute cases of adverse and time-varying pressure gradients and extrapolate the experimental results for wider applications. The adverse alongshore pressure gradient is shown to reverse the longshore current in the outer surf zone. The tidal effect on longshore sediment transport is predicted to be minor if the tide generates the alongshore pressure gradient varying with time sinusoidally.

CHAPTER 1

INTRODUCTION

A quantitative understanding of longshore sediment transport in surf and swash zones on beaches under obliquely waves is essential for the design of shoreline erosion mitigation measures such as beach nourishment and sand bypassing (e.g., Kobayashi et al. 2007a). A large number of empirical formulas including the CERC formula (Coastal Engineering Manual 2002) have been proposed for predicting the total longshore sediment transport rate over the entire surf and swash zones as a function of the breaking wave characteristics, beach slope, and sediment diameter. Some of the formulas have been refined and may predict the total sediment rate within a factor of about two (Kamphuis 2002; van Rijn 2002). For practical applications in the United States, the CERC formula is normally calibrated for each project site. This engineering practice may be prudent but requires time and expense. Moreover, the performance of a project will need to be monitored because the formula calibrated for field conditions before the project may need to be recalibrated after the project.

Field and laboratory measurements on the distribution of longshore sediment transport across the surf and swash zones (Bodge and Dean 1987; Wang 1998; Miller 1999; Wang et al. 2002) indicated several distribution patterns depending on nearshore morphology (barred and plane beaches) and breaker type. The longshore sediment transport rate in the swash zone was found to contribute significantly to the total transport rate when incident waves collapsed on

the foreshore. Wang (1998) evaluated available formulas for predicting the local longshore sediment transport rate as a function of the cross-shore distance. The accuracy of these formulas is similar to the accuracy of the simpler CERC formula for the total transport rate. Consequently, use is rarely made of the cross-shore integration of the predicted local transport rate to estimate the total transport rate for practical applications. However, the local longshore sediment transport rate may be predicted more accurately now that longshore currents on natural beaches can be predicted fairly accurately (Ruessink et al. 2001).

A tidal current near a coastal inlet can be strong and its effect on longshore sediment transport needs to be included for the prediction of sediment transport near the inlet (Hanson et al. 2006). On the other hand, Apotsos et al. (2008a) examined the effect of the alongshore variation of wave setup on alongshore flows in the surf zone using field data collected onshore of a submarine canyon. The alongshore pressure gradient caused by the wave setup varying alongshore was shown to be capable of driving a strong longshore current. These studies indicate that the alongshore gradient of the mean water level caused by tides or wave setup can generate a strong longshore current and modify longshore sediment transport on beaches.

Longshore sediment transport due to breaking waves and external currents is investigated using the cross-shore numerical model CSHORE (Kobayashi et al. 2010) which is extended to include the alongshore pressure gradient of the mean water level. The extended CSHORE is compared with five tests conducted in the Large-scale Sediment Transport Facility by Gravens and Wang (2007). The external currents were varied by adjusting the alongshore recirculation of water. The direction of the recirculated currents was in the same direction as the wave-induced longshore current. The calibrated CSHORE is used to examine the cross-shore distributions of the longshore current and sediment transport rate for the external currents

flowing against the wave-induced current. Since a tidal current varies during the tidal cycle, the net effect of the tidal current on longshore sediment transport during one tidal cycle is examined to assess the degree of importance of the tidal current for the cumulative volume of longshore sediment transport.

The present report is organized in the following sequence.

In Chapter 2, the experiment of Gravens and Wang (2007) is explained and the bathymetry, wave, current and sediment transport data are analyzed for the five tests.

In Chapter 3, the numerical model CSHORE is modified to include alongshore pressure gradient and allow oblique waves in the wet and dry zone. The modified CSHORE is explained in detail.

In Chapter 4, CSHORE is calibrated for the alongshore pressure gradient associated with the recirculation system used in the experiment. The calibrated CSHORE is compared with the cross-shore distributions of the wave setup, wave height, cross-shore current, longshore current and longshore sediment transport rates for the five tests. The verified CSHORE is then used to examine the effects of alongshore pressure gradients that were not tested in the experiment.

Finally, the summary and conclusions of this study are presented. Additional tables and figures for the five tests are attached in Appendices A, B, C, D and E.

It is noted that the summary of this report will be presented in a journal paper that has been submitted by Farhadzadeh et al. (2010).

CHAPTER 2

DATA ANALYSIS

Gravens and Wang (2007) conducted a series of experiments in the Large-scale Sediment Transport Facilities (LSTF) basin of the US Army Engineer Research and Development Center. One of the experiments was designed to investigate sediment transport processes under waves and currents in the absence of a coastal structure. This experiment included five base tests BC1 to BC5. In the following, the experiment is explained first before the analysis of the bathymetry, free surface elevation, current and sediment transport data.

2.1. Experimental Setup

The base experiment by Gravens and Wang (2007) for sediment transport under combined waves and current in the absence of a coastal structure was conducted in a wave basin that was 50 m long, 30 m wide and 1.4 m deep. Fig. 2-1 depicts the experimental setup in the LSTF basin where the cross-shore coordinate x is positive onshore with $x = 0$ on the horizontal bottom of the basin and the longshore coordinate y is positive in the downwave direction with $y = 0$ approximately in the middle of the beach. The model beach consisted of uniform sand with a median diameter of 0.15 mm. The sediment specific gravity, fall velocity and porosity are 2.65, 1.65 cm/s, and 0.4, respectively (Kobayashi et al. 2007a). The cross-

shore width and longshore length of the beach were 18 m and 31 m, respectively. Unidirectional irregular waves were generated on the horizontal bottom seaward of the beach in the still water depth of 0.9 m. The wave angle was 10° relative to the shore normal at $x = 0$. This base experiment consisted of five tests BC1 to BC5. These tests were conducted on a quasi-equilibrium beach profile of alongshore uniformity in the middle of the beach.

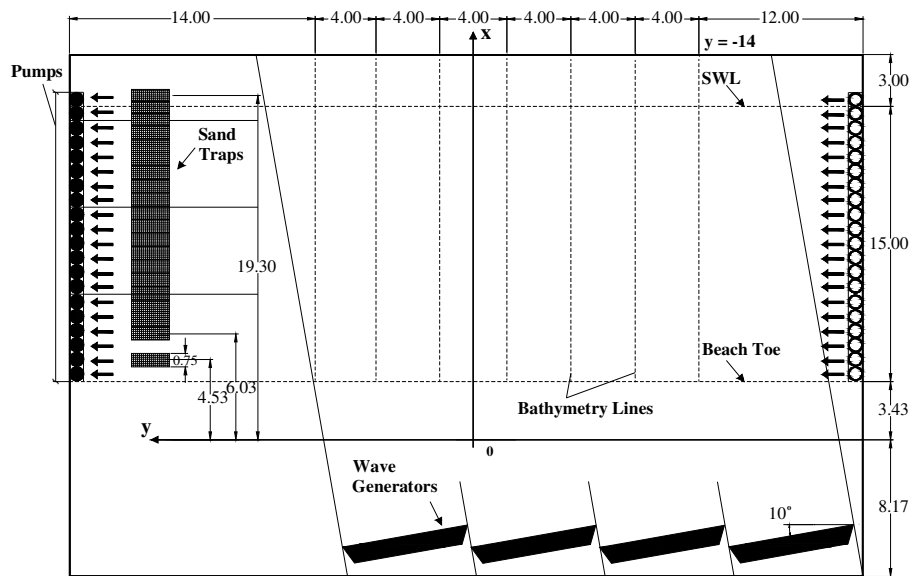


Fig. 2-1. Layout of LSTF experimental setup

In test BC1, the longshore water flux Q produced by the wave-driven longshore current was recirculated from the downstream end to the upstream end of the beach using 20 pumps at the downstream end situated over the cross-shore span of approximately $x = 4 - 19$ m. The initial beach profile for test BC1 was a quasi-equilibrium profile for given wave and sediment conditions. In test BC2, the longshore water flux was increased to $2Q$ to impose an external current while the wave conditions were kept the same. Test BC3 corresponded to test BC2 with no waves. In tests BC4 and BC5, the longshore water flux was $1.5Q$. The initial condition

for test BC4 was the final condition for test BC3 with bed forms generated by the longshore current only and oriented perpendicular to the shoreline. Test BC5 was a repeat of test BC4 to investigate the influence of antecedent bed forms (ripples). The assumption of alongshore uniformity will be shown later to be valid in the 10 m wide zone between $y = -6$ m and $y = 4$ m where the alongshore coordinate y is positive in the downwave direction with $y = 0$ near the center of the beach as shown in Fig. 2-1.

For each test, the free surface elevation, cross-shore and longshore velocities were measured at 10 cross-shore locations along an instrument bridge and 11 alongshore stations between $y = -10$ m and $y = 10$ m, except for tests BC3 and BC4 in which the instruments failed to collect the data at $y = -8$ m and $y = 8$ m. The velocities were measured at a distance of approximately $d/3$ with $d =$ still water depth above the local bottom. Data were recorded for 10 min at each alongshore station and then the instrument bridge was moved to the next alongshore station until the last station of the 11 stations. The sediment concentrations were measured at a number of elevations above the local bottom at several cross-shore locations along each of the 11 alongshore stations.

The total longshore sediment transport rate q_y was measured using 20 bottom traps placed at the downstream end of the basin as shown in Fig. 2-1.

The initial and final cross-shore bottom profiles were measured at the beginning and end of each test on a number of transects between $y = -10$ m and $y = 10$ m.

In the following, test BC1 is presented as an example. The analyzed data for each of the five tests are presented in tables and figures in Appendices A to E.

2.2. Bathymetry

The cross-shore profiles between $y = -10$ m and $y = 10$ m were measured from $x = 3.43$ m in water depth of about 0.70 m up to the dry zone well above the still water shoreline. The bottom elevation z_b is positive upward with $z_b = 0$ at the still water level (SWL). The bottom profile change during each test was about 2 cm. It should be noted that the measured profiles were smoothed to reduce irregularity caused by ripples. Fig. 2-2 shows the three-dimensional view of the smoothed initial and final profiles for test BC1 and the bottom elevation change during test BC1.

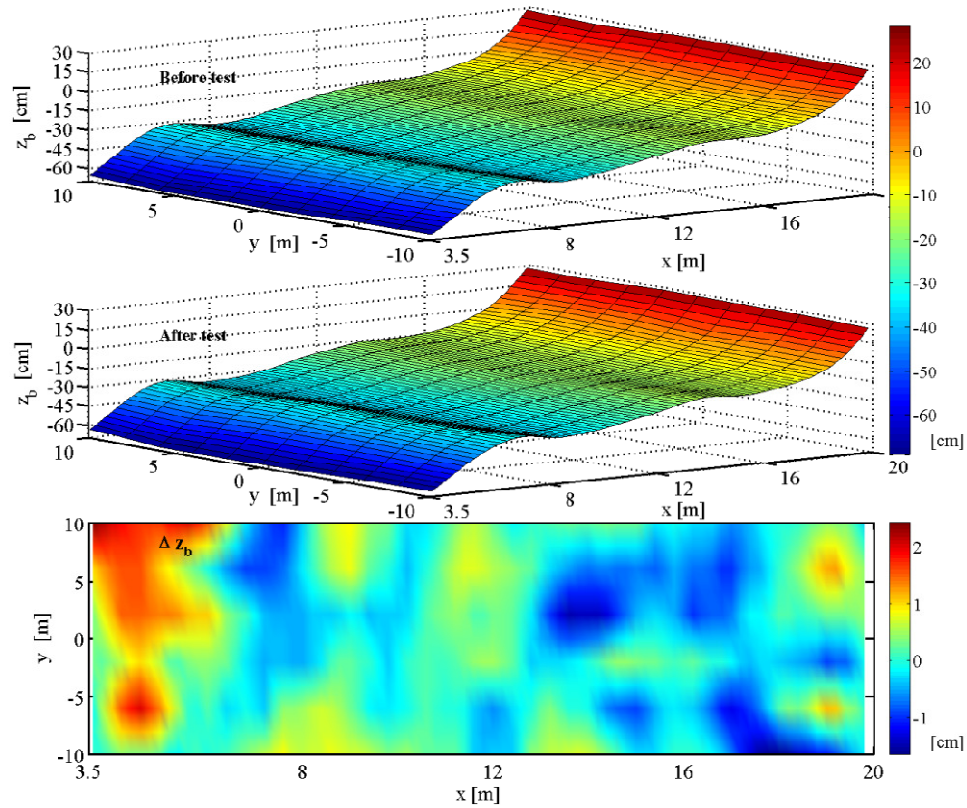


Fig. 2-2. Measured initial and final profiles and change in bottom elevation for test BC1

For each test, the profiles were measured at several alongshore stations. For tests BC1 and BC2, the alongshore spacing between profiles was 4 m. For the other tests, the longshore spacing was reduced to increase the alongshore resolution. Fig. 2-3 shows the initial cross-shore profiles at 6 longshore stations for test BC1. The measured profiles between $y = -10$ m and $y = 10$ m were almost uniform alongshore.

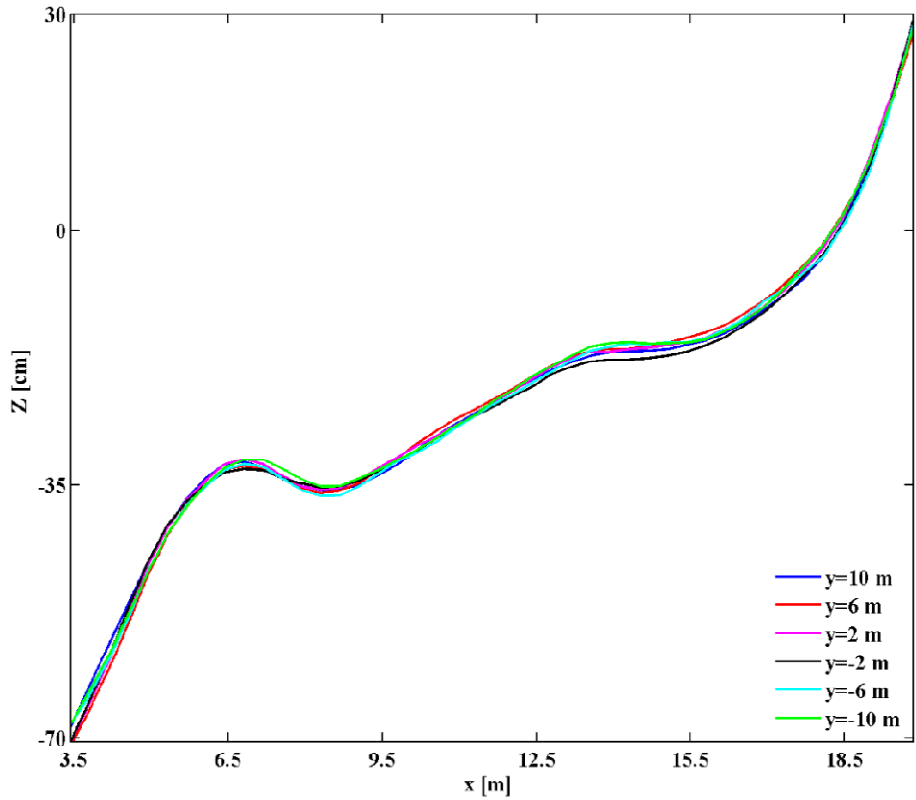


Fig. 2-3.Measured initial profiles for test BC1

The most offshore wave gauge, taken as the seaward boundary of the numerical model, was located at $x = 0$ where the water depth was 0.90 m. The initial bottom profiles were extrapolated linearly from $x = 3.43$ m (the seaward limit of the measured bottom profile) to $x = 0$ (see Fig. 2-1). Alongshore uniformity in the zone between $y = -6$ m and $y = 4$ m is assumed in the following comparison of the numerical model and the data. Therefore, the initial bottom

profiles in the zone of alongshore uniformity were averaged and used as input to the numerical model. Fig. 2-4 depicts the averaged initial and final profiles for test BC1. For tests BC1, BC2, BC4 and BC5, the maximum elevation difference among all the initial bottom profiles in this uniform zone was less than 2 cm. For test BC3 with no waves, the difference was less than 0.5 cm. The elevation difference between the averaged initial and final profiles of tests BC1-BC5 was about 2 cm. Fig. 2-4 depicts the averaged initial and final profiles which were quasi-equilibrium during test BC1.

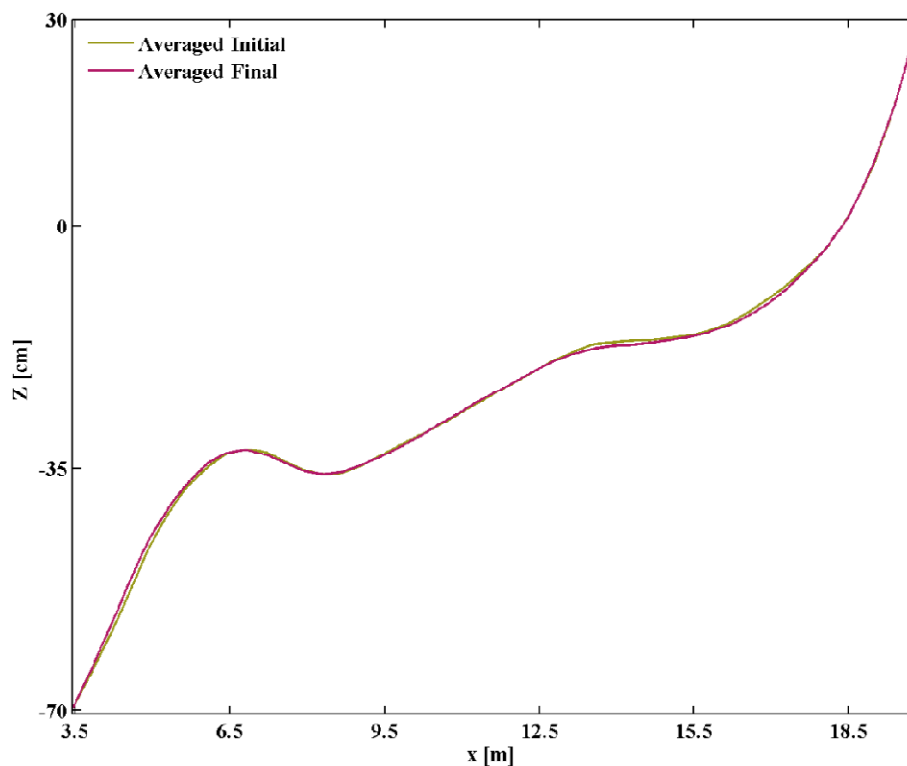


Fig. 2-4. Averaged initial and final profiles in zone of alongshore uniformity for BC1

2.3. Free Surface Elevation

The free surface elevation was measured using wave gauges mounted on the shore normal instrument bridge in the cross-shore direction. The data was collected for 10 min at

each of the 11 alongshore stations. The measured wave conditions were almost uniform in the zone of alongshore uniformity of $y = -6$ m to $y = 4$ m. Table 2-1 lists the range of the root-mean-square wave height H_{rms} , spectral peak period T_p and wave set-down ($-\bar{\eta}$) at the most offshore wave gauge located at $x = 0$ in the zone of alongshore uniformity as well as the test duration T_e for each of the five tests. It is noted that the free surface elevation is positive above SWL and the mean water level $\bar{\eta}$ is negative for wave set-down.

Table 2-1. Range of Wave height, Spectral Peak Period and Wave Set-down Measured at $x = 0$ and Test Duration for Five Tests

Test	BC1	BC2	BC3	BC4	BC5
H_{rms} (cm)	16.11 – 16.25	16.22 – 16.30	0.02 – 0.03	15.79 – 15.91	15.67 – 15.83
T_p (s)	1.46 – 1.47	1.46 – 1.48	0.49 – 0.69	1.46 – 1.48	1.47 – 1.48
$-\bar{\eta}$ (cm)	0.31 – 0.45	0.28 – 0.39	0.19 – 0.31	0.15 – 0.23	0.20 – 0.40
T_e (min)	165	150	195	148	150

For the comparison of the numerical model with the data, the wave parameters at $x = 0$ averaged in the zone of alongshore uniformity are used as input at the seaward boundary. Table 2-2 summarizes the input values used for each of the five tests. For test BC3, no waves were generated but $\bar{\eta}$ was negative perhaps because of the water recirculation.

Fig. 2-5 shows the cross-shore and alongshore variations of all the measured root-mean-square wave heights for test BC1. The wave height H_{rms} increased in the region of $x = 0 - 5.5$ m due to shoaling and decreased due to irregular wave breaking in the zone of $x = 5.5 - 8.5$ m (see Fig. 2-4 for the bottom profile). The broken waves shoaled slightly up to $x = 11.5$ m before increased wave breaking in very shallow water. The similar wave transformation occurred for tests BC2, BC4 and BC5. The measured free surface oscillations were very small

for test BC3. The zone of alongshore uniformity is indicated using the vertical gray lines in Fig. 2-5 and subsequent figures to justify the selection of this zone between $y = -6$ m to $y = 4$ m.

Table 2-2. Averaged Wave Height, Spectral Peak Period and Wave Set-down at $x = 0$ for Five Tests

Test	BC1	BC2	BC3	BC4	BC5
H_{rms} (cm)	16.2	16.3	0.0	15.9	15.7
T_p (s)	1.47	1.47	0.0	1.47	1.48
$\bar{\eta}$ (cm)	-0.36	-0.32	-0.25	-0.19	-0.31

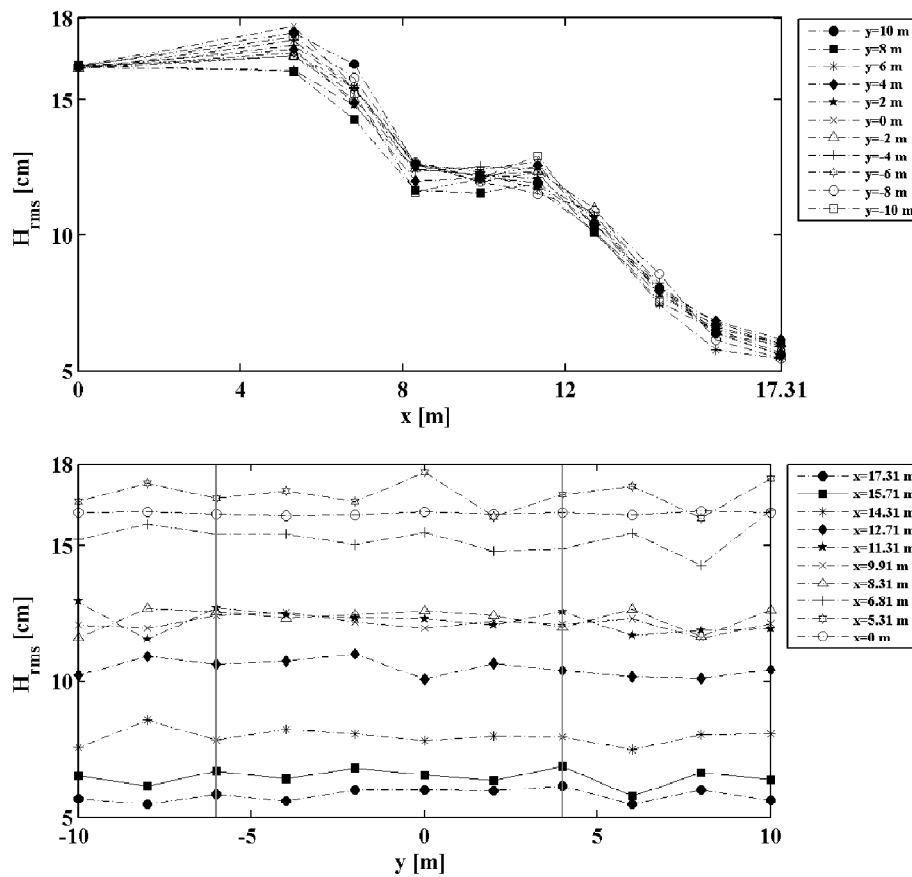


Fig. 2-5. Cross-shore and longshore variations of RMS wave height for test BC1

The cross-shore and alongshore variations of the wave setup $\bar{\eta}$ for test BC1 are depicted in Fig. 2-6. The wave setup increased onshore and reached its maximum at the most onshore wave gauge. This was the case with tests BC2, BC4 and BC5 as well. For test BC3, the mean water level was almost zero as no wave was generated.

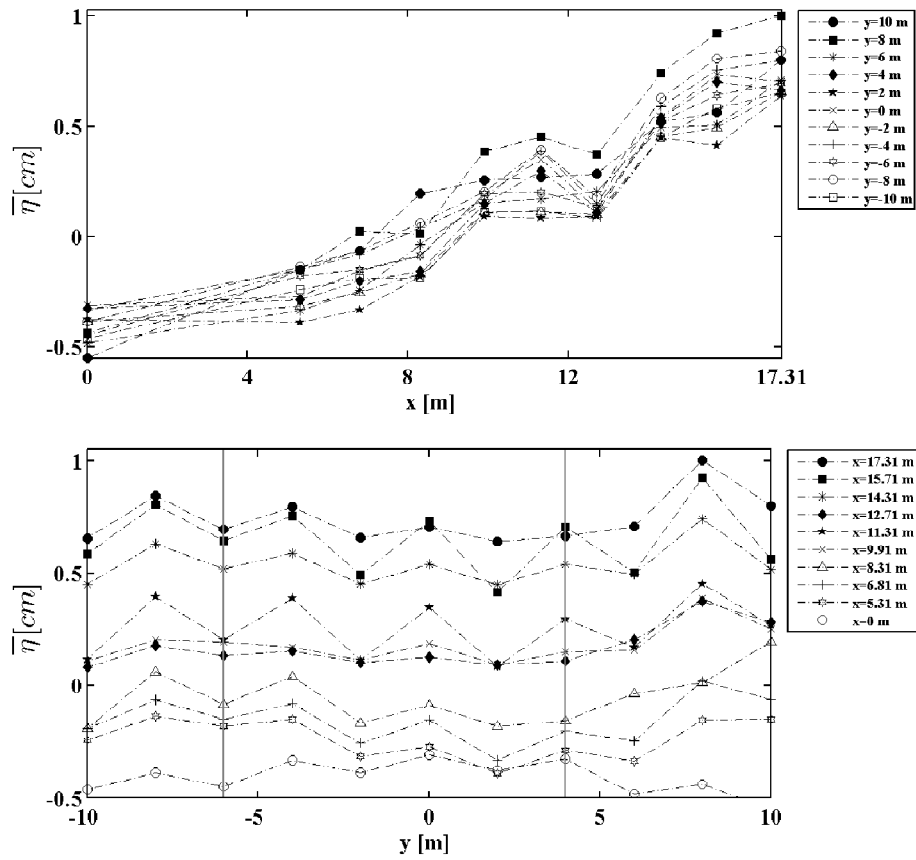


Fig. 2-6. Cross-shore and longshore variations of wave setup for test BC1

The numerical model CSHORE will be extended in Chapter 3 to include the alongshore pressure gradient term in the longshore momentum equation to estimate the external current generated by the recirculation system. To estimate the alongshore gradient of the wave setup for each test, the measured $\bar{\eta}$ at all cross-shore locations in the zone of alongshore uniformity is plotted as a function of y and a linear function in the form of $\bar{\eta} = (ay + b)$ is fitted to the data. Figs. 2-7 to 2-11 show the linear regression analysis of the measured wave setup for each of the five tests. The fitted value of a listed in each figure is the alongshore gradient of $\bar{\eta}$.

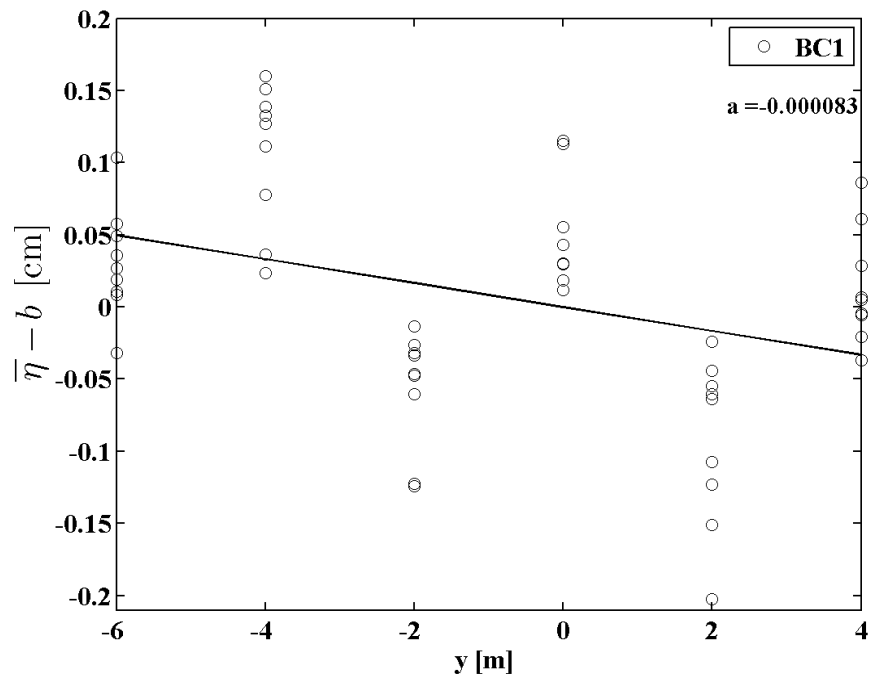


Fig. 2-7. Estimation of wave setup alongshore gradient for test BC1

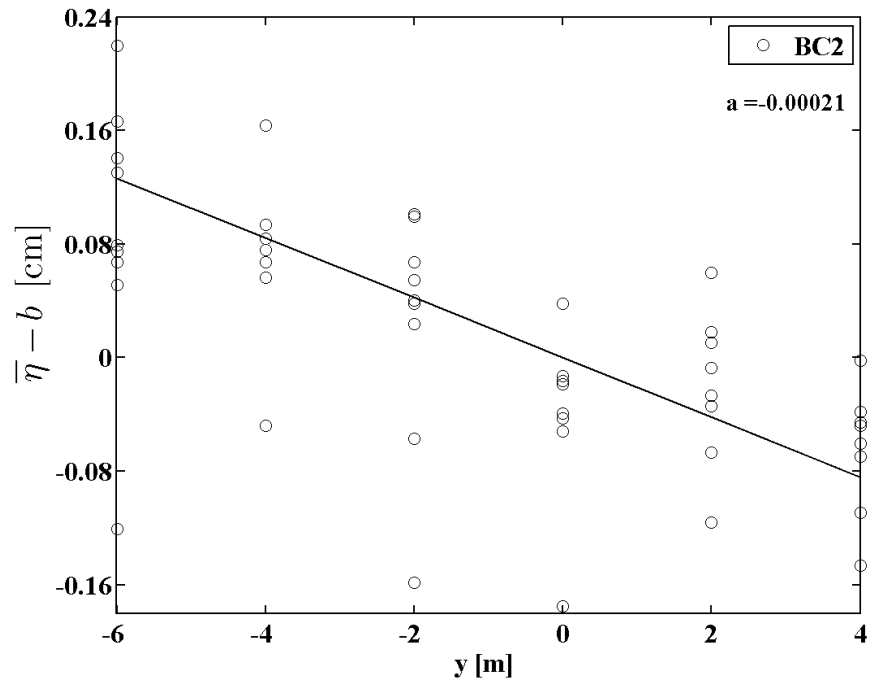


Fig. 2-8. Estimation of wave setup alongshore gradient for test BC2

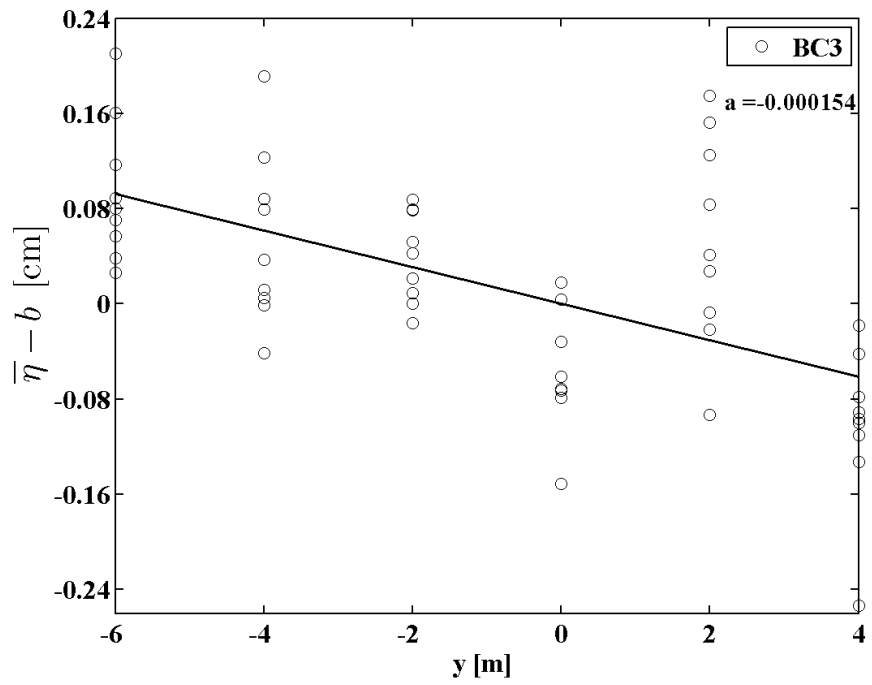


Fig. 2-9. Estimation of wave setup alongshore gradient for test BC3

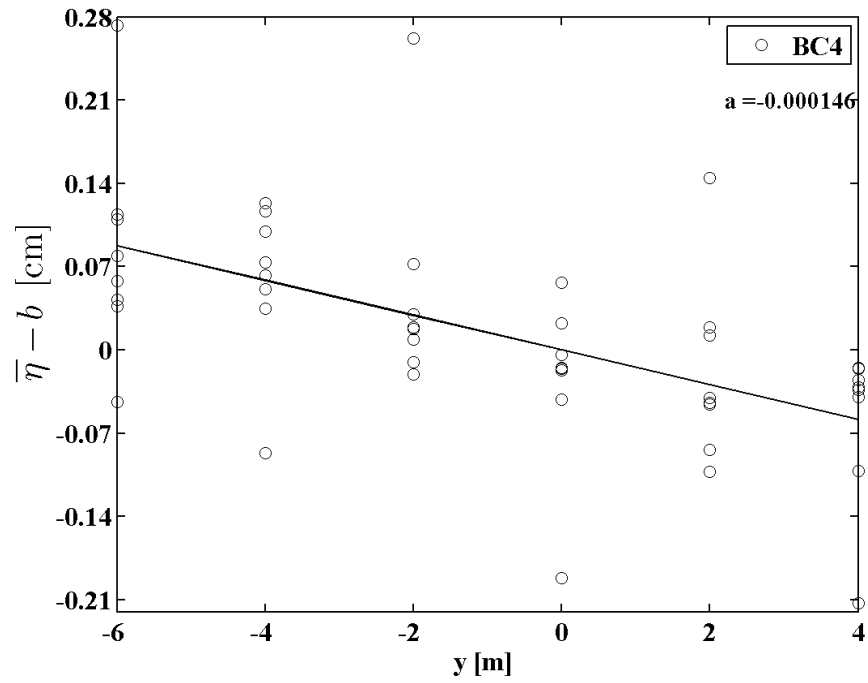


Fig. 2-10. Estimation of wave setup alongshore gradient for test BC4

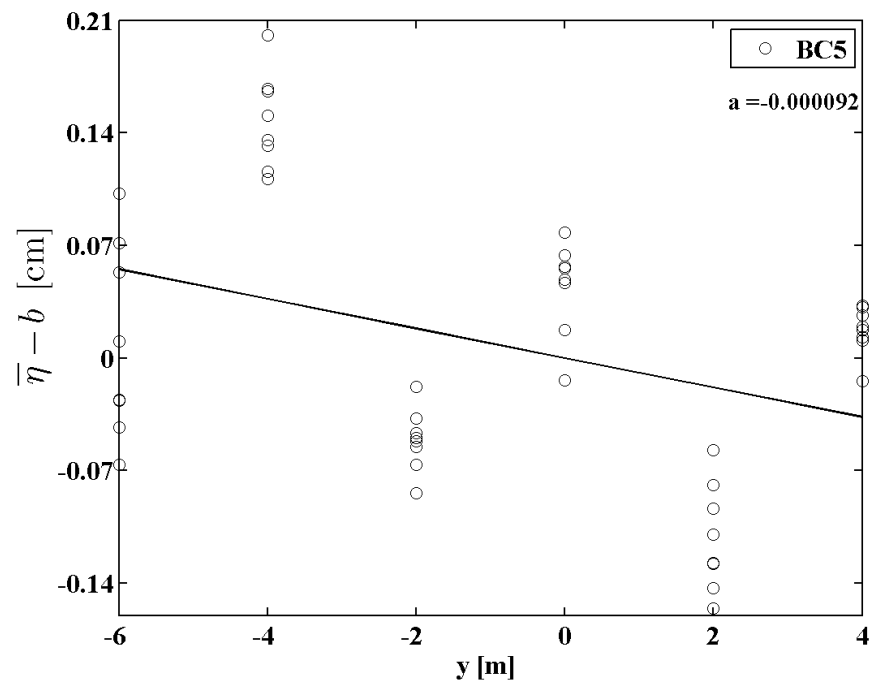


Fig. 2-11. Estimation of wave setup alongshore gradient for test BC5

The same regression analysis is also applied to the wave setup data at each cross-shore location for each test in order to estimate the cross-shore variation of the alongshore wave setup gradient. The attempt was unsuccessful because of the large scatter of the alongshore wave setup gradient. Tables A.4, B.4, C.3, D.4 and E.3 in Appendices A, B, C, D and E, respectively, present the coefficients a and b and the correlation coefficient CC between the data points and the fitted line for each cross-shore location for tests BC1, BC2, BC3, BC4 and BC5, respectively.

The data points in Figs. 2-7 to 2-11 are very scattered in the longshore direction. The difference of $\bar{\eta}$ over the alongshore distance of 10 m is on the order of 1 mm and is probably within the error of the free surface elevation measurement. Therefore, the alongshore gradient of wave setup could not be estimated reliably. Moreover, the recirculation system at the downstream end of the wave basin was situated over the cross-shore span of $x = 4 - 19$ m. Accordingly, the wave setup alongshore gradient must have been reduced in the zone of $x = 0 - 4$ m. The cross-shore variation of the alongshore wave setup gradient used for the computation will be explained in Chapter 4.

2.4. Cross-Shore and Longshore Currents

The velocity data was collected using 10 Acoustic Doppler Velocimeters (ADV) mounted on the instrument bridge. The velocity data was recorded in the same manner as the free surface data. The data was collected at an interval of 2 m in the region of $y = -10 - 10$ m. The velocities measured at a distance of approximately $d/3$ with $d =$ still water depth above the local bottom are assumed to correspond to the depth-averaged velocities. Fig. 2-12 shows the cross-shore positioning of the ADVs at $y = 0$ for test BC1. The locations of the Fiber Optic

Backscatter Sensors (FOBS) utilized to measure the sediment concentrations in the water column are also shown in this figure and will be explained in Section 2.5.

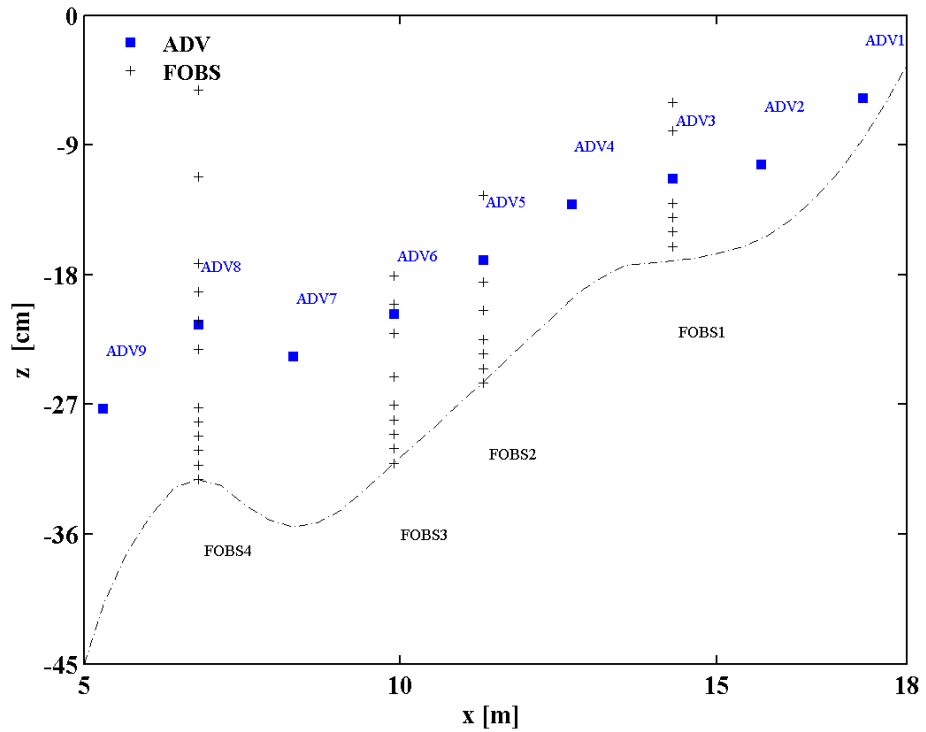


Fig. 2-12. Cross-shore positioning of ADV and FOBS at $y = 0$ for test BC1

Table 2-3 presents the ADV cross-shore locations, still water depth and mean cross-shore velocity \bar{U} at $y = 0$ for test BC1. The measured \bar{U} was negative and represented the offshore return (undertow) current.

Table 2-3. Cross-shore Location, Still Water Depth and Mean Cross-shore Velocity at $y = 0$ for Test BC1

ADV	x (m)	d (cm)	\bar{U} (cm/s)
10	2.81	74.13	NR
9	5.31	40.93	-3.40
8	6.81	32.20	-4.38
7	8.31	35.50	-5.80
6	9.91	31.07	-3.98
5	11.31	25.50	-3.71
4	12.71	19.69	-6.67
3	14.31	17.03	-8.26
2	15.71	15.50	-3.46
1	17.31	8.60	-4.77

NR = Not Reliable

Fig. 2-13 illustrates the cross-shore and long-shore variations of the mean cross-shore velocity \bar{U} . The measured \bar{U} was relatively uniform in the zone of alongshore uniformity. For test BC1, the offshore direction velocity increased from ADV9 ($x = 5.31$ m) to ADV7 ($x = 8.31$ m) over the offshore bar and then decreased up to ADV5 ($x = 11.31$ m) in the zone of reduced wave breaking (see Fig. 2-5). The offshore direction velocity increased from ADV5 to ADV3 ($x = 14.31$ m) and then decreased toward ADV1 ($x = 17.31$ m) due to the wave breaking on the stepped profile (see Fig. 2-12) and the decrease of H_{rms} (see Fig. 2-5). The cross-shore variations of \bar{U} for tests BC2, BC4 and BC5 are similar to those for BC1.

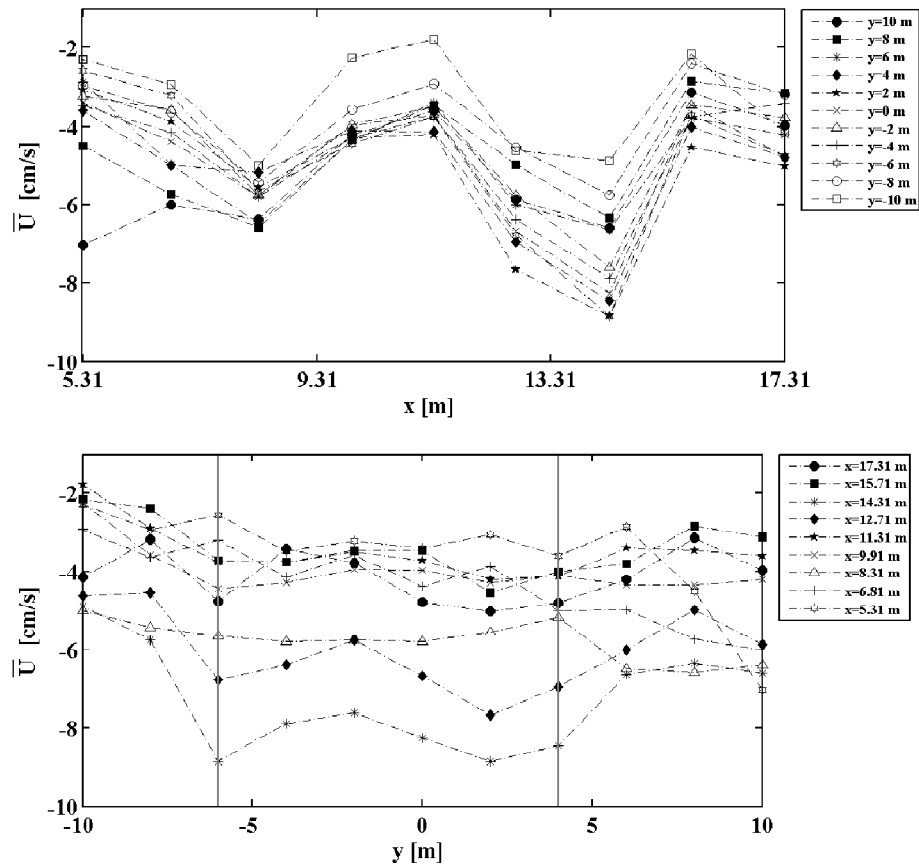


Fig. 2-13. Cross-shore and longshore variations of mean cross-shore velocity for test BC1

Table 2-4 summarizes the range of the cross-shore velocity \bar{U} at all cross-shore locations in the zone of alongshore uniformity for tests BC1, BC2, BC4 and BC5 with waves. The cross-shore velocities were in the similar range because the wave conditions were very similar as shown in Table 2-2.

Table 2-4. Range of Mean Cross-shore Velocity in Zone of Alongshore Uniformity for Four Tests with Waves

Test	BC1	BC2	BC4	BC5
$\bar{U}(cm/s)$	2.58 – 8.85	-0.07 – 8.90	1.35 – 8.07	1.77 – 7.48

Table 2-5 presents the ADV locations, still water depth d and mean longshore velocity at $y = 0$ for test BC1. Fig. 2-14 shows the cross-shore and longshore variations of the mean longshore velocity for test BC1. The longshore velocity increased from ADV9 up to ADV7 and then decreased up to ADV4. The longshore velocity increased again up to ADV2 where the longshore current velocity was the maximum. The longshore current was reduced at ADV1 as the water depth became smaller. The cross-shore variation of \bar{V} can be interpreted using the cross-shore variations of z_b (Fig. 2-12) and H_{rms} (Fig. 2-5) where \bar{V} tended to increase in the zones of intense wave breaking. The cross-shore variations of \bar{V} were similar for the four tests with waves except for test BC5 in which the longshore current velocity was the maximum at ADV8. The longshore velocity was relatively uniform in the zone of alongshore uniformity in the lower panel of Fig. 2-14.

Table 2-5. Cross-shore Locations of ADV, Still Water Depth and Mean Longshore Velocity at $y = 0$ for Test BC1

ADV	x (m)	d (cm)	\bar{V} (cm/s)
10	2.81	74.13	NR
9	5.31	40.93	2.83
8	6.81	32.20	9.98
7	8.31	35.50	13.36
6	9.91	31.07	12.59
5	11.31	25.50	10.54
4	12.71	19.69	8.75
3	14.31	17.03	14.40
2	15.71	15.50	16.32
1	17.31	8.60	13.86

Table 2-6 summarizes the range of the measured mean longshore velocity \bar{V} in the zone of alongshore uniformity for tests BC1-BC5. The mean longshore velocities were positive and in the downwave (water recirculation) direction for all the tests. The mean longshore velocity was the largest in test BC2 with an external current of 5 to 10 cm/s across the surf zone. The recirculation rate was the same for test BC3 (no wave) and test BC2 with waves. The external current velocity for tests BC4 and BC5 varied between 2 to 5 cm/s across the surf zone. The measured longshore velocity across the surf zone was the smallest for test BC1 with no external current.

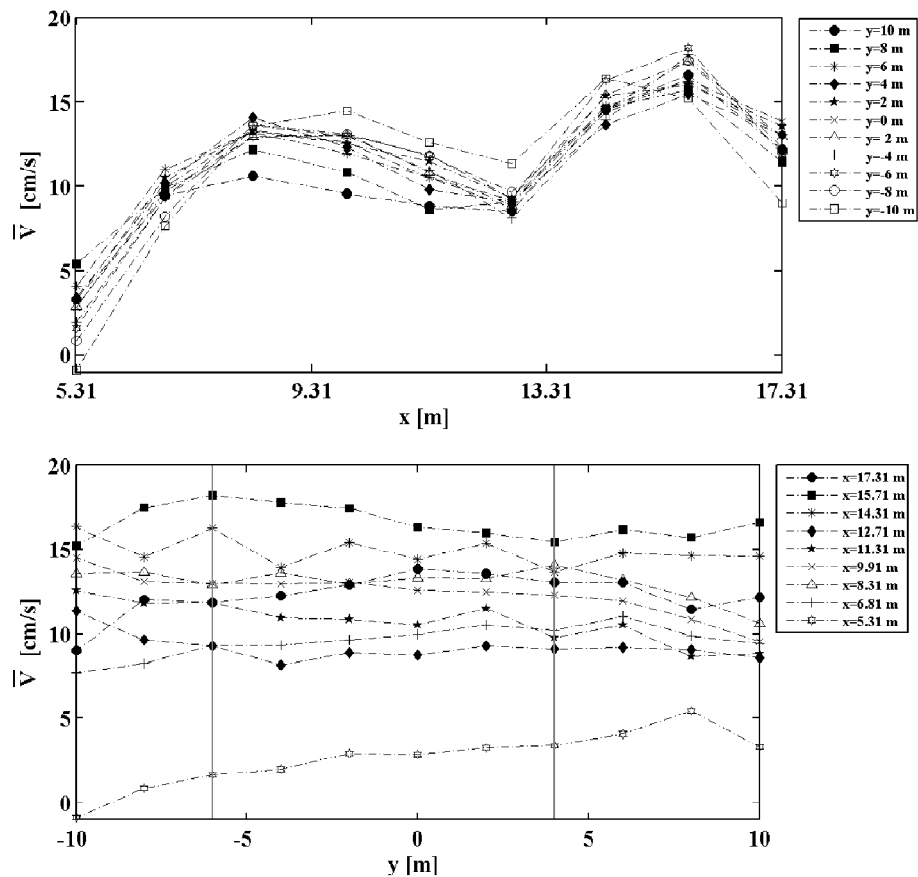


Fig. 2-14. Cross-shore and longshore variations of mean longshore velocity for test BC1

Table 2-6. Range of Mean Longshore Velocities in Zone of Alongshore Uniformity for Five Tests

Test	BC1	BC2	BC3	BC4	BC5
$\bar{V}(cm/s)$	1.67 – 18.23	0.62 – 23.86	0.00 – 21.04	4.41 – 20.35	5.04 – 23.24

2.5. Sediment Concentration

The sediment concentration data along each alongshore station was collected using a number of FOBS placed vertically at 6 cross-shore locations for tests BC1 and BC2 and at 3 locations for test BC4. As an example, the positioning of FOBS in test BC1 is shown in Fig. 2-12. The lowest elevation of the concentration measurement was 1 cm above the local bottom. For test BC3 with no waves, sediment suspension was weak under longshore current alone and no meaningful data was obtained. The sediment concentration data was not collected for test BC5 which was a repeat of test BC4.

The measured concentration profile at each location was fitting by the following exponential and power-form functions

$$\bar{c} = \bar{c}_b \exp(-z_m / l_c) \quad \text{for } z_m \geq 0 \quad (2-1)$$

$$\bar{c} = \bar{c}_a (z_a / z_m)^m \quad \text{for } z_m \geq z_a \quad (2-2)$$

where z_m = elevation above the local bottom; \bar{c}_b , l_c , \bar{c}_a and m = fitted coefficients at each location; and z_a = lowest elevation 1 cm of the power-form profile. Kobayashi et al. (2005) showed that their sediment concentration data could be fitted by the power-form and exponential profiles equally well. Kobayashi et al. (2007a) analyzed different concentration

data from the LSTF basin and concluded that the power-form fitted better than the exponential profile. Fig. 2-15 shows the fitted concentration profiles using Eqs. (2-1) and (2-2) for test BC1. Eq. (2-2) fitted slightly better than Eq. (2-1).

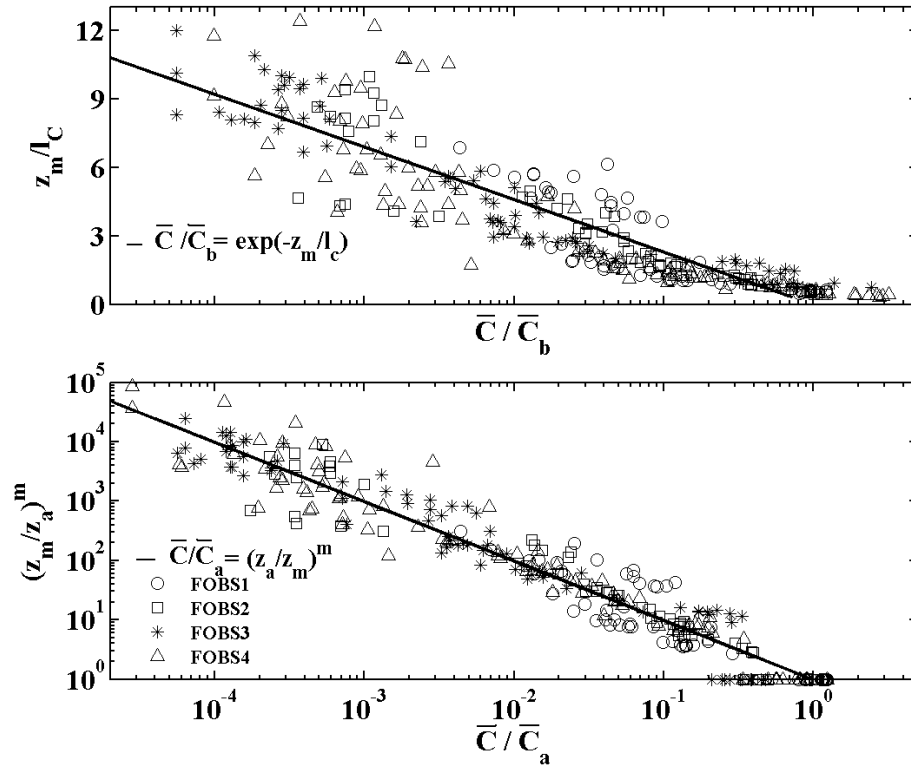


Fig. 2-15. Vertical distributions of mean concentration \bar{c} using exponential and power-form profiles for each FOBS for test BC1

The suspended sediment volume per unit horizontal area, V_s , at each location is obtained by integrating the fitted profiles over the water column

$$V_s = \int_{z_a}^{\bar{h}} \bar{c}_a \left(\frac{z_a}{z_m} \right)^m dz_m = \frac{\bar{c}_a z_a}{m-1} \left[1 - \left(\frac{z_a}{\bar{h}} \right)^{m-1} \right] \quad (2-3)$$

$$V_s = \int_0^{\bar{h}} \bar{c}_b \exp(-z_m / l_c) dz_m = \bar{c}_b l_c \left[1 - \exp\left(-\frac{\bar{h}}{l_c}\right) \right] \quad (2-4)$$

Table 2-7 lists the FOBS cross-shore locations, mean water depth \bar{h} , fitted coefficients, suspended sediment volume per unit horizontal area, and the correlation coefficient for both exponential and power-form profiles at $y = 0$ for test BC1. The correlation coefficient CC between the data and the fitted profile tends to be higher for the power-form profile than the exponential form for test BC1.

Table 2-7. Fitted Coefficients and Suspended Sediment Volume per Unit Horizontal Area

Based on Exponential and Power-form Profiles at $y = 0$ for Test BC1

$y = 0$ m		Exponential				Power			
x (m)	\bar{h} (cm)	c_b (g/l)	l_c (cm)	V_s (cm)	CC	c_a (g/l)	m	V_s (cm)	CC
6.81	32.05	13.74	2.22	0.0073	0.90	45.97	3.02	0.0086	0.99
9.91	31.26	3.57	1.30	0.0008	0.93	8.40	3.68	0.0012	0.78
11.31	25.85	3.84	1.72	0.0014	0.96	8.58	3.05	0.0016	0.98
14.31	17.58	5.80	1.93	0.0025	0.86	5.31	1.93	0.0020	0.99

Fig. 2-16 depicts the sediment concentration data and the fitted profiles for test BC1. The blue line representing the power-form profile appears to fit to the data better than the red line of the exponential profile.

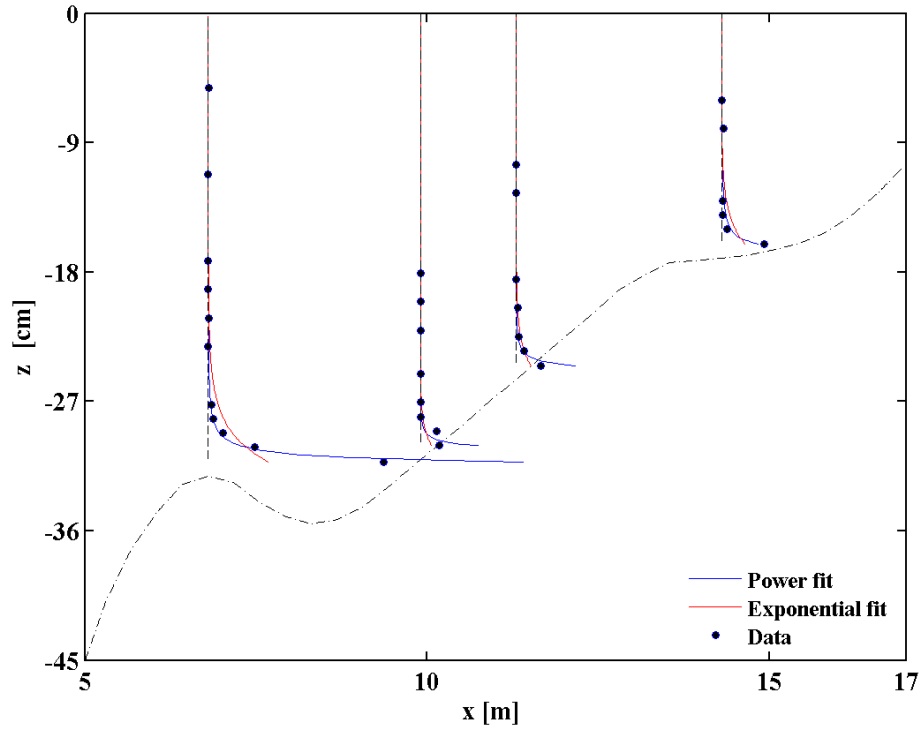


Fig. 2-16. Sediment concentration data and power-form and exponential profiles at $y = 0$ for test BC1

Fig. 2-17 shows the comparison of the suspended sediment volumes calculated using Eqs. (2-3) and (2-4) for all locations in test BC1 where the solid line is the perfect agreement and the dotted lines indicate the deviation of a factor of 2. The suspended sediment volumes using the two fitted profiles remain within a factor of 2. Consequently, both volumes are used in the following to judge the degree of uncertainty related to the fitted profiles.

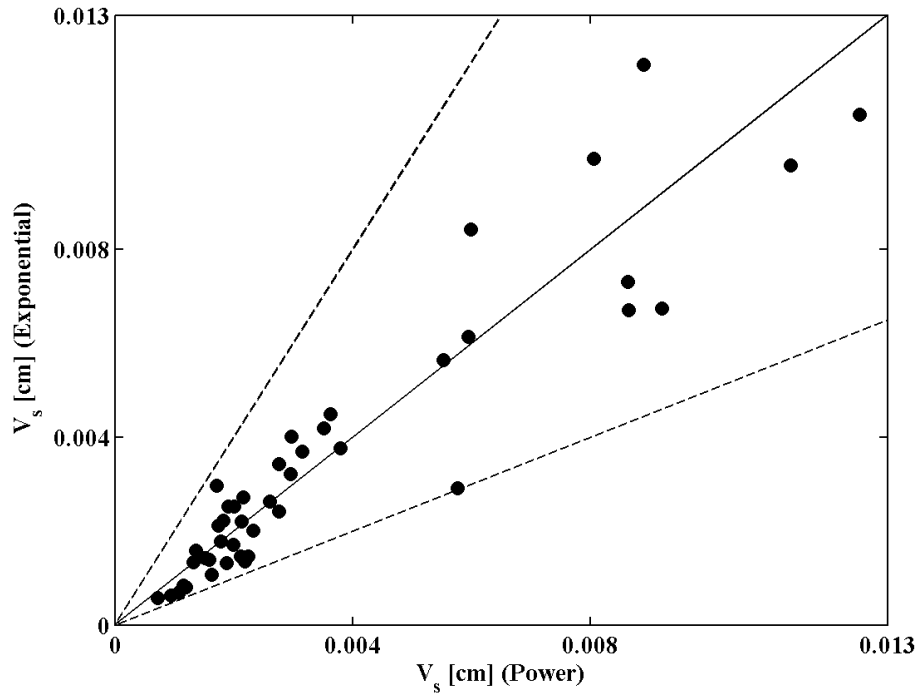


Fig. 2-17. Comparison of suspended sediment volume per unit horizontal area using power-form and exponential profiles for all locations in test BC1

Fig. 2-18 depicts the cross-shore and longshore distributions of V_s for test BC1 where the exponential and power-form profiles are indicated using red and blue symbols respectively. For tests BC1, BC2 and BC4, the maximum V_s was measured in the outer surf zone where spilling breakers occurred. The suspended sediment volume decreased onshore and slightly increased in the inner surf zone. The longshore variation of V_s is relatively constant in the zone of alongshore uniformity but the scatter of V_s is about a factor of 2 partly because of the difficulty in measuring sand concentrations accurately.

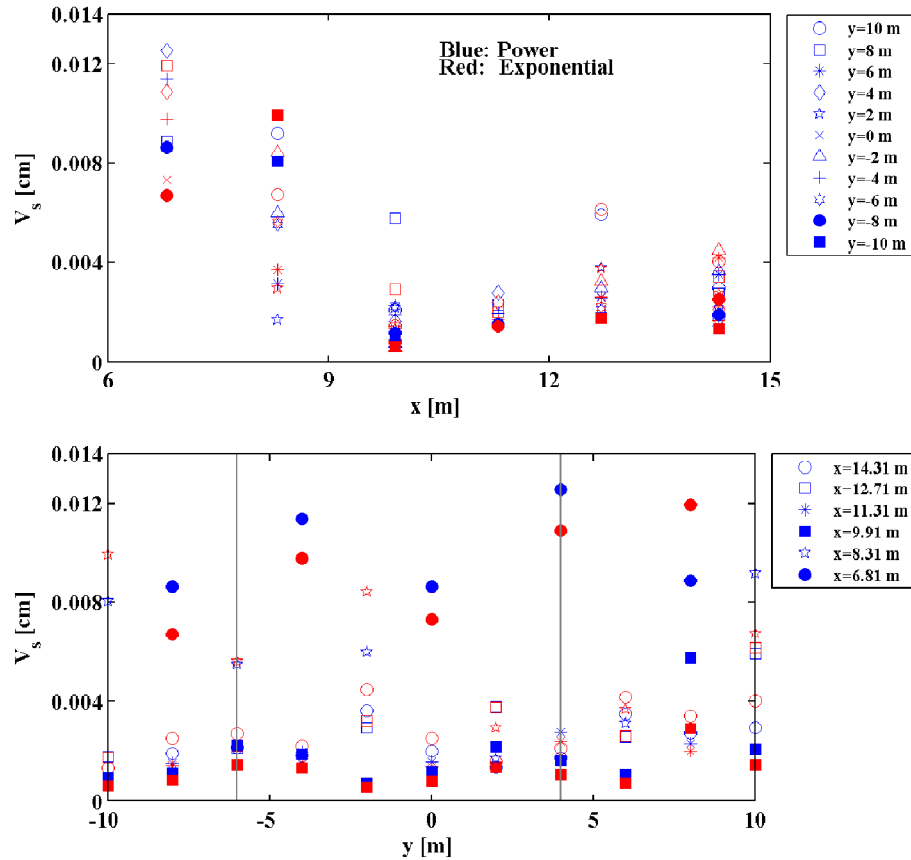


Fig. 2-18. Cross-shore and longshore distributions of suspended sediment volume per unit horizontal area using power-form and exponential profiles at all locations for test BC1

2.6. Longshore Sediment Transport

The cross-shore distribution of the total longshore sediment transport rate q_y was measured using twenty 0.75-m wide bottom traps, positioned at the downstream end of the wave basin as shown in Fig. 2-1. Table 2-8 presents the data corresponding to the cross-shore distribution of the total (suspended sediment and bed load) longshore sediment rate (sediment volume with no void) for test BC1. The data provided in the table is plotted in Fig. 2-19. The longshore sediment rate tended to increase onshore and increased rapidly from $q_y = 0.023$ to $0.072 \text{ cm}^2/\text{s}$ near the still water shoreline $x = 17.31$ (Trap 17) and 18.73 m (Trap 19). The

maximum longshore sediment rates of $q_y = 0.118$ and $0.094 \text{ cm}^2/\text{s}$ for tests BC2 and BC5, respectively, occurred at $x = 18.06 \text{ m}$ (Trap 18). The maximum rates of $q_y = 0.005$ and $0.081 \text{ cm}^2/\text{s}$ for tests BC3 and BC4, respectively were recorded at $x = 15.06 \text{ m}$ (Trap 14). The total longshore sediment rate Q_{ty} is calculated by integrating the measured q_y with respect to x . The calculated Q_{ty} is tabulated in Table 2-9. The calculated values of Q_{ty} are very similar for the three tests BC2, BC4 and BC5 with external currents. For test BC1 with no external current, Q_{ty} was significantly less than those of the tests with the external currents, demonstrating the significant role of the external current in the longshore sediment transport. The value of Q_{ty} for test BC3 is much less than the other tests indicating the dominant effect of breaking waves on sediment suspension.

Table 2-8. Total Longshore Sediment Transport Data for Each Trap in Test BC1

Trap No.	Dist. to Shoreline (m)	x (m)	q_y (cm^2/s)
1	13.88	4.56	0.006
2	12.38	6.06	0.013
3	11.63	6.81	0.021
4	10.88	7.56	0.016
5	10.13	8.31	0.014
6	9.38	9.06	0.012
7	8.63	9.81	0.015
8	7.88	10.56	0.030
9	7.13	11.31	0.025
10	6.38	12.06	0.037
11	5.63	12.81	0.043
12	4.88	13.56	0.039
13	4.13	14.31	0.031
14	3.38	15.06	0.032
15	2.63	15.81	0.030
16	1.88	16.56	0.031
17	1.13	17.31	0.023
18	0.38	18.06	0.065
19	-0.30	18.73	0.072
20	-0.90	19.33	0.001

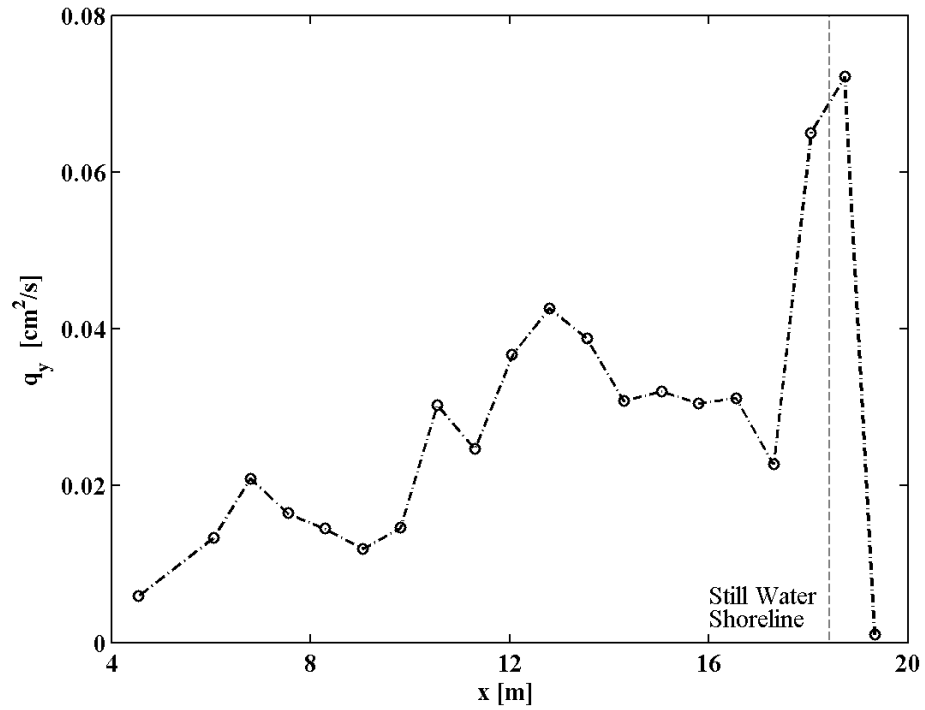


Fig. 2-19. Cross-shore distribution of total longshore sediment transport rate q_y for test BC1

Table 2-9. Total Longshore Sediment Transport Rate Q_{ty} (cm³/s) across Surf and Swash Zones for Five Tests

Test	BC1	BC2	BC3	BC4	BC5
Q_{ty} (cm ³ /s)	41.8	77.8	1.0	75.4	77.9

CHAPTER 3

NUMERICAL MODEL CSHORE

The cross-shore numerical model CSHORE assumes longshore uniformity and uses the time-averaged continuity, cross-shore momentum, longshore momentum, wave energy, and roller energy equations to predict the cross-shore variations of the mean and standard deviation of the free surface elevation and depth-averaged cross-shore and longshore velocities (Kobayashi et al. 2007a, 2009b and Kobayashi 2009). CSHORE is extended in the following to include the alongshore pressure gradient of the mean water level in the longshore momentum equation. Analytical solutions are obtained for the longshore current and sediment transport in the absence of waves. The wet and dry model, initially developed for normally incident waves, is also extended for the case of oblique waves. The sediment transport model for the wet and dry zone is modified to account for obliquely incident waves.

3.1. Combined Wave and Current Model in Wet Zone

Fig. 3-1 shows obliquely incident irregular waves on an essentially straight shoreline where alongshore uniformity is assumed. The cross-shore coordinate x is positive onshore and

the longshore coordinate y is positive in the downwave direction. The beach is assumed to be impermeable. The depth-averaged cross-shore and longshore velocities are denoted by U and V , respectively. Incident waves are assumed to be unidirectional with $\theta =$ incident angle relative to the shore normal. The height and period of the irregular waves are represented by the root-mean-square wave height H_{rms} and the representative wave period, which is taken as the spectral peak period T_p , specified at the seaward boundary located at $x = 0$. The location of the seaward boundary is normally taken to be outside the surf zone so that wave set-down or setup is very small at $x=0$. The incident wave angle θ at $x=0$ is assumed to be in the range of $|\theta| < 80^\circ$ to ensure that the incident waves propagate landward.

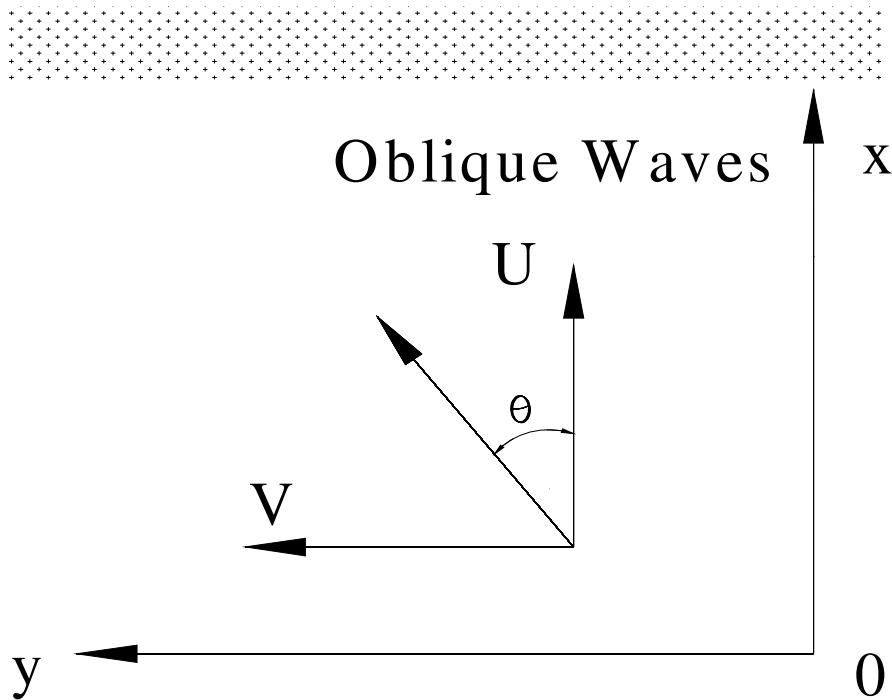


Fig. 3-1. Definition sketch for incident irregular waves on beach

The mean water depth \bar{h} with the overbar indicating time-averaging is given by

$$\bar{h} = (\bar{\eta} + S - z_b) \quad (3-1)$$

where $\bar{\eta}$ = wave setup above the still water level (SWL); S = storm tide above the datum $z = 0$; and z_b = bottom elevation above the datum. The storm tide S is assumed to be uniform in the computation domain and is specified as input at $x=0$. Linear wave and current theory for wave refraction (e.g., Phillips 1977; Mei 1989; Dalrymple 1988) is used to predict the spatial variations of H_{rms} and θ . The dispersion relation for linear waves is expressed as

$$\omega^2 = kg \tanh(k\bar{h}) \quad ; \quad \omega_p = \omega + k(Q_x \cos \theta + Q_y \sin \theta) / \bar{h} \quad (3-2)$$

where ω = intrinsic angular frequency; k = wave number; g = gravitational acceleration; ω_p = absolute angular frequency given by $\omega_p = 2\pi / T_p$; Q_x and Q_y = time-averaged volume flux per unit width in the x and y directions, respectively, and θ = incident wave angle. Eq. (3-2) can be solved iteratively to obtain k and ω for known $\omega_p, \bar{h}, \theta, Q_x$ and Q_y . The phase velocity C and the group velocity C_g are given by

$$C = \omega / k \quad ; \quad C_g = nC \quad ; \quad n = \frac{1}{2} \left[1 + \frac{2k\bar{h}}{\sinh(2k\bar{h})} \right] \quad (3-3)$$

The cross-shore model CSHORE computes the wave and current fields simultaneously. The depth-integrated continuity equation of water requires that the cross-shore volume flux Q_x is constant and equal to the wave overtopping rate q_o at the landward end of the computation domain. The time averaged volume fluxes are expressed as

$$Q_x = \bar{h}\bar{U} + \frac{g\sigma_\eta^2}{C} \cos \theta + q_r \cos \theta = q_o \quad (3-4)$$

$$Q_y = \bar{h}\bar{V} + \frac{g\sigma_\eta^2}{C} \sin \theta + q_r \sin \theta \quad (3-5)$$

where \bar{U} and \bar{V} = mean cross-shore and longshore velocity respectively. \bar{U} is negative and offshore because $\cos \theta > 0$ if $q_o = 0$ (no wave overtopping); σ_η = standard deviation of the free surface elevation η ; and q_r = volume flux of a roller on the front of a breaking wave. The wave-induced volume flux per unit width in the direction of wave propagation is given by $g\sigma_\eta^2/C$ in Eqs. (3-4) and (3-5). If the incident wave angle θ is small, Eq. (3-5) can be approximated by $Q_y \simeq \bar{h}\bar{V}$ for most applications.

For the case of alongshore uniformity, Snell's law is used to obtain the wave angle θ

$$k \sin \theta = \text{constant} \quad (3-6)$$

The constant value is obtained from the values of θ , \bar{h} and T_p specified at the seaward boundary $x = 0$ located outside the surf zone where ω can be approximated by ω_p in Eq. (3-2). Reflected waves are neglected in this model.

For the case of no wind, the cross-shore and longshore momentum equations are expressed as

$$\frac{d}{dx} \left(S_{xx} + \rho \frac{Q_x^2}{\bar{h}} \right) = -\rho g \bar{h} \frac{d\bar{\eta}}{dx} - \tau_{bx} \quad (3-7)$$

$$\frac{d}{dx} \left(S_{xy} + \rho \frac{Q_x Q_y}{\bar{h}} \right) = -\rho g \bar{h} S_\eta - \tau_{by} \quad (3-8)$$

where S_η = alongshore gradient of mean water level given by $S_\eta = \frac{\partial \bar{\eta}}{\partial y}$ which must be independent of y for the case of alongshore uniformity, S_{xx} = cross-shore radiation stress; ρ = water density; τ_{bx} = cross-shore bottom stress; S_{xy} = shear component of the radiation stress; and τ_{by} = longshore bottom stress. The alongshore pressure gradient S_η of the mean water level is added in Eq. (3-8) to account for an external alongshore current where the external current may be tidal. Linear wave theory for progressive waves is used to estimate S_{xx} and S_{xy} as

$$S_{xx} = (nE + M_r) \cos^2 \theta + E \left(n - \frac{1}{2} \right) ; \quad S_{xy} = (nE + M_r) \cos \theta \sin \theta \quad (3-9)$$

with

$$n = C_g / C \quad ; \quad E = \rho g \sigma_\eta^2 \quad ; \quad M_r = \rho C q_r \quad (3-10)$$

where C_g = linear wave group velocity; E = specific wave energy with the root-mean-square wave height defined as $H_{rms} = \sqrt{8} \sigma_\eta$; and M_r = momentum flux of a roller propagating with the phase velocity C .

The time-averaged bottom shear stresses in Eqs. (3-7) and (3-8) are written as

$$\tau_{bx} = \frac{1}{2} \rho f_b \overline{UU_a} \quad ; \quad \tau_{by} = \frac{1}{2} \rho f_b \overline{VU_a} \quad ; \quad U_a = (U^2 + V^2)^{0.5} \quad (3-11)$$

where U = depth-averaged cross-shore velocity; V = depth-averaged longshore velocity; f_b = bottom friction factor; and the overbar indicates time averaging. The bottom friction factor f_b is of the order of 0.01 on sand beaches but should be calibrated using longshore current data because of the sensitivity of longshore currents to f_b . The equivalency of the time and

probabilistic averaging is assumed to express τ_{bx} and τ_{by} in terms of the mean and standard deviation of the depth-averaged velocities U and V expressed as

$$U = \sigma_T F_U \quad ; \quad V = \sigma_T F_V \quad ; \quad U_a = \sigma_T F_a \quad ; \quad F_a = (F_U^2 + F_V^2)^{0.5} \quad (3-12)$$

with

$$F_U = U_* + r \cos \theta \quad ; \quad F_V = V_* + r \sin \theta \quad ; \quad U_* = \frac{\bar{U}}{\sigma_T} \quad ; \quad V_* = \frac{\bar{V}}{\sigma_T} \quad (3-13)$$

where \bar{U} and \bar{V} = depth-averaged cross-shore and longshore currents; σ_T = standard deviation of the oscillatory (assumed Gaussian) depth-averaged velocity U_T with zero mean; and r = Gaussian variable defined as $r = U_T/\sigma_T$ whose probability density function is given by

$$f(r) = \frac{1}{\sqrt{2\pi}} \exp\left(-\frac{r^2}{2}\right) \quad (3-14)$$

Linear progressive wave theory is used locally to express U_T in terms of the oscillatory free surface elevation $(\eta - \bar{\eta})$

$$U_T = \frac{C}{h} (\eta - \bar{\eta}) \quad (3-15)$$

which yields the standard deviation σ_T of the oscillatory velocity U_T

$$\sigma_T = C \sigma_* \quad ; \quad \sigma_* = \sigma_\eta / \bar{h} \quad (3-16)$$

It is noted that that $U_* = \bar{U} / \sigma_T$ and $V_* = \bar{V} / \sigma_T$ are normally of the order of unity or less.

The standard deviations of U and V are given by

$$\sigma_U = \sigma_T \cos \theta \quad ; \quad \sigma_V = \sigma_T |\sin \theta| \quad (3-17)$$

where $\cos \theta > 0$ but $\sin \theta$ can be negative. Substitution of Eq. (3-12) into Eq. (3-11) yields

$$\tau_{bx} = \frac{1}{2} \rho f_b \sigma_T^2 G_{bx} \quad ; \quad \tau_{by} = \frac{1}{2} \rho f_b \sigma_T^2 G_{by} \quad (3-18)$$

with

$$G_{bx} = \int_{-\infty}^{\infty} F_U F_a f(r) dr \quad ; \quad G_{by} = \int_{-\infty}^{\infty} F_V F_a f(r) dr \quad (3-19)$$

which must be integrated numerically.

The wave action equation for the case of alongshore uniformity becomes

$$\frac{d}{dx} \left[\frac{E}{\omega} \left(C_g \cos \theta + \frac{Q_x}{h} \right) \right] = - \frac{D_B + D_f}{\omega} \quad (3-20)$$

which reduces to the wave energy equation if ω is constant and $Q_x=0$

$$\frac{dF_x}{dx} = -D_B - D_f \quad ; \quad F_x = EC_g \cos \theta \quad (3-21)$$

where F_x = cross-shore energy flux based on linear progressive wave theory; and D_B and D_f = energy dissipation rates due to wave breaking and bottom friction, respectively. Eq. (3-20) is used to compute σ_η .

The energy dissipation rate D_B due to wave breaking in Eq. (3-20) is estimated using the formula by Battjes and Stive (1985), which was modified by Kobayashi et al. (2005) to account for the local bottom slope and to extend the computation to the lower swash zone. The modified formula is expressed as

$$D_B = \frac{\rho g a_s Q H_B^2}{4T} ; \quad \frac{Q-1}{\ln Q} = \left(\frac{H_{rms}}{H_m} \right)^2 ; \quad (3-22)$$

$$H_m = \frac{0.88}{k} \tanh \left(\frac{\gamma k \bar{h}}{0.88} \right) ; \quad a_s = \frac{2\pi S_b}{3k \bar{h}} \geq 1$$

where a_s = slope effect parameter; Q = fraction of breaking waves; H_B = breaker height used to estimate D_B ; T = intrinsic wave period given by $T = 2\pi/\omega$ with ω obtained using Eq. (3-2);

$H_{rms} = \sqrt{8}\sigma_\eta$ = local root-mean-square wave height; H_m = local depth-limited wave height;

γ = empirical breaker ratio parameter; and S_b = local bottom slope given by

$S_b = \left(\frac{\partial z_b}{\partial x} \cos \theta + \frac{\partial z_b}{\partial y} \sin \theta \right)$ where $\frac{\partial z_b}{\partial y} = 0$ for the case of alongshore uniformity. The

parameter a_s is the ratio between the wave length ($2\pi/k$) and the horizontal length ($3\bar{h}/S_b$) imposed by the small depth and relatively steep slope where the lower limit of $a_s = 1$ corresponds to the formula by Battjes and Stive (1985) who also assumed $H_B = H_m$. The fraction Q is zero for no wave breaking and unity when all waves break. The requirement of $0 \leq Q \leq 1$ implies $H_{rms} \leq H_m$ but H_{rms} can become larger than H_m in very shallow water.

When $H_{rms} > H_m$, use is made of $Q = 1$ and $H_B = H_{rms}$. In addition, the upper limit of $\sigma_* = \sigma_\eta / \bar{h}$ is imposed as $\sigma_* \leq 1$ in very shallow water (Kobayashi et al. 1998). The breaker ratio parameter γ in Eq. (3-22) is typically in the range of $\gamma = 0.5 - 1.0$ (Kobayashi et al. 2007a) but should be calibrated to obtain a good agreement with the measured cross-shore variation of σ_η if such data is available. An option is provided in CSHORE (Kobayashi 2009) to estimate γ using the empirical formula developed by Apotsos et al. (2008b) using field data.

On the other hand, the energy dissipation rate D_f due to bottom friction in Eq. (3-20) is expressed as

$$D_f = \frac{1}{2} \rho f_b \overline{U_a^3} \quad (3-23)$$

Substitution of U_a given in Eq. (3-12) into Eq. (3-23) yields

$$D_f = \frac{1}{2} \rho f_b \sigma_r^3 G_f \quad ; \quad G_f = \int_{-\infty}^{\infty} F_a^3 f(r) dr \quad (3-24)$$

where $f(r)$ is given by Eq. (3-14).

The energy equation for the roller is based on that used by Ruessink et al. (2001)

$$\frac{d}{dx} (\rho C^2 q_r \cos \theta) = D_B - D_r \quad (3-25)$$

$$D_r = \rho g \beta_r q_r \quad ; \quad \beta_r = (0.1 + S_b) \geq 0.1$$

where the roller dissipation rate D_r is assumed to equal the rate of work to maintain the roller on the wave-front slope β_r of the order of 0.1. Use is made of the empirical formula for β_r proposed by Kobayashi et al. (2005) who included the local bottom slope effect. If the roller is neglected, $q_r = 0$ and Eq. (3-25) yields $D_r = D_B$. The roller effect improves the agreement for the longshore current (Kobayashi et al. 2007a).

Eqs. (3-4) – (3-25) are the same as those used by Kobayashi et al. (2007a) who assumed $Q_x = q_o = 0$ in Eq. (3-4) and used linear shallow-water wave theory with $C = (g \bar{h})^{0.5}$ in Eq. (3-15). Substitution of Eqs. (3-16) and (3-17) into Eq. (3-4) yields the following equation of the mean cross-shore current:

$$\bar{U} = -\frac{g\bar{h}}{C^2}\sigma_U\sigma_* \left(1 + \frac{Cq_r}{g\sigma_\eta^2}\right) + \frac{Q_x}{\bar{h}} \quad (3-26)$$

Approximate analytical equations of G_{bx} , G_{by} and G_f given by Eqs. (3-19) and (3-24) are obtained by Kobayashi et al. (2009a) to reduce the computation time and improve the numerical stability. The function F_a given in Eq. (3-12) with Eq. (3-13) is rewritten as

$$F_a = \left[(r - r_m)^2 + F_m^2 \right]^{0.5} \quad (3-27)$$

with

$$r_m = -(U_* \cos \theta + V_* \sin \theta) \quad ; \quad F_m = V_* \cos \theta - U_* \sin \theta \quad (3-28)$$

Eq. (3-27) is approximated as

$$F_a = (r - r_m) + |F_m| \quad \text{for } r \geq 0 \quad (3-29)$$

$$F_a = -(r - r_m) + |F_m| \quad \text{for } r < 0$$

Substituting Eq. (3-29) into Eqs. (3-19) and (3-24) and integrating the resulting equations analytically, the following approximate expressions for G_{bx} , G_{by} and G_f are obtained

$$G_{bx} = \sqrt{\frac{2}{\pi}} (U_* - r_m \cos \theta) + U_* |F_m| \quad (3-30)$$

$$G_{by} = \sqrt{\frac{2}{\pi}} V_* (1 + \sin^2 \theta) + V_* |F_m| \quad (3-31)$$

$$G_f = 2\sqrt{\frac{2}{\pi}} + (1 + U_*^2 + V_*^2) |F_m| + \sqrt{\frac{2}{\pi}} (U_*^2 + V_*^2 + 2r_m^2) \quad (3-32)$$

which depends on $\sin\theta$ ($\cos\theta > 0$ assumed), r_m and F_m where Eq. (3-28) yields $U_* = -(r_m \cos\theta + F_m \sin\theta)$ and $V_* = (F_m \cos\theta - r_m \sin\theta)$. It is noted that Eq. (3-31) satisfies $G_{by} = 0$ for $\bar{V} = 0$ unlike the slightly different approximate equation given by Kobayashi et al. (2009a).

For the case of normally incident waves, $\sin\theta = 0$ and $V_* = 0$, Eqs. (3-30) – (3-32) yield $G_{bx} = 1.6 U_*$, $G_{by} = 0$, and $G_f = (1.6 + 2.4 U_*^2)$. For this case, G_{bx} and G_f given by Eqs. (3-19) and (3-24) can be integrated analytically as presented by Kobayashi et al. (2007b) who approximated the analytical expressions of G_{bx} and G_f as $G_{bx} = 1.64 U_*$ and $G_f = (1.6 + 2.6 U_*^2)$. These approximate equations are very similar to the above equations obtained from Eqs. (3-30) and (3-32).

3.2. Hydrodynamic Model for Longshore Current Only

For the case of no wave, $\sigma_\eta = 0$, $q_r = 0$ (no roller) and $q_o = 0$ (no wave overtopping). An analytical solution for longshore current can be derived from the combined wave and current model. Eqs. (3-4) and (3-5) are respectively reduced to

$$Q_x = \bar{h} \bar{U} \quad (3-33)$$

$$Q_y = \bar{h} \bar{V} \quad (3-34)$$

The continuity equation is reduced to $Q_x = 0$ and $\bar{U} = 0$. Since the cross-shore radiation stress $S_{xx} = 0$, Eq. (3-7) is modified as

$$\tau_{bx} = -\rho g \bar{h} \frac{d\bar{\eta}}{dx} \quad (3-35)$$

The cross-shore bottom stress τ_{bx} given by Eq. (3-11) yields $\tau_{bx} = 0$ in the absence of waves under the condition of no flux at the landward boundary. Eq. (3-35) reduces to

$$\bar{\eta} = 0 \quad (3-36)$$

For $Q_x = 0$ and $S_{xy} = 0$, the longshore momentum equation given by Eq. (3-8) becomes

$$\tau_{by} = -\rho g \bar{h} S_\eta \quad (3-37)$$

The longshore bottom stress τ_{by} given by Eq. (3-11) is modified as

$$\tau_{by} = \frac{1}{2} \rho f_b \bar{V} |\bar{V}| \quad (3-38)$$

Equating Eqs. (3-38) and (3-39), the longshore current is given by

$$\bar{V} = \left[\frac{2g\bar{h}}{f_b} (-S_\eta) \right]^{0.5} \quad \text{for } S_\eta < 0 \quad (3-39)$$

$$\bar{V} = - \left[\frac{2g\bar{h}}{f_b} S_\eta \right]^{0.5} \quad \text{for } S_\eta > 0 \quad (3-40)$$

where the longshore current \bar{V} driven by the alongshore gradient S_η of $\bar{\eta}$ flows in the direction of the decreasing $\bar{\eta}$.

3.3. Sediment Transport Model in Wet Zone

The combined wave and current model CSHORE predicts the spatial variations of the hydrodynamic variables used in the following sediment transport model for given beach profile, water level and seaward wave conditions at $x = 0$. The bottom sediment is assumed to

be uniform and characterized by d_{50} = median diameter; w_f = sediment fall velocity; and s = sediment specific gravity.

First, the spatial variation of the degree of sediment movement is estimated using the critical Shields parameter ψ_c (Madsen and Grant 1976) which is taken as $\psi_c = 0.05$. The instantaneous bottom shear stress τ'_b is assumed to be given by $\tau'_b = 0.5 \rho f_b U_a^2$ with U_a given in Eq. (3-11). The sediment movement is assumed to occur when τ'_b exceeds the critical shear stress, $\rho g(s-1)d_{50} \psi_c$. The probability P_b of sediment movement can be shown to be the same as the probability of $(r - r_m)^2 > F_b^2 = (R_b^2 - F_m^2)$ where $R_b = [2g(s-1)d_{50}\psi f_b^{-1}]^{0.5} / \sigma_T$ and r_m and F_m are defined in Eq. (3-28). For the Gaussian variable r given by Eq. (3-14), P_b is given by

$$P_b = \frac{1}{2} \operatorname{erfc} \left(\frac{F_b - r_m}{\sqrt{2}} \right) + \frac{1}{2} \operatorname{erfc} \left(\frac{F_b + r_m}{\sqrt{2}} \right) \quad \text{for } F_b^2 > 0 \quad (3-41)$$

and $P_b = 1$ for $F_b^2 \leq 0$ where erfc is the complementary error function. The value of P_b computed from $x = 0$ located outside the surf zone increases landward and fluctuates in the surf and swash zones, depending on the presence of a bar or a terrace that increases the local fluid velocity.

Second, the spatial variation of the degree of sediment suspension is estimated using the experimental finding of Kobayashi et al. (2005) who showed that the turbulent velocities measured in the vicinity of the bottom were related to the energy dissipation rate due to bottom friction. Representing the magnitude of the instantaneous turbulent velocity by $(D'_f / \rho)^{1/3}$ with $D'_f = 0.5 \rho f_b U_a^3$ in light of Eq. (3-23), the probability P_s of sediment

suspension is assumed to be the same as the probability of $(D_f' / \rho)^{1/3}$ exceeding the sediment fall velocity w_f . The probability P_s is then equal to the probability of $(r - r_m)^2 > F_s^2 = (R_s^2 - F_m^2)$ with $R_s = [(2/f_b)^{1/3} w_f / \sigma_T]$ and is given by

$$P_s = \frac{1}{2} \operatorname{erfc} \left(\frac{F_s - r_m}{\sqrt{2}} \right) + \frac{1}{2} \operatorname{erfc} \left(\frac{F_s + r_m}{\sqrt{2}} \right) \quad \text{for } F_s^2 > 0 \quad (3-42)$$

and $P_s = 1$ for $F_s^2 \leq 0$. If $P_s > P_b$, use is made of $P_s = P_b$ assuming that sediment suspension occurs only when sediment movement occurs. Fine sands on beaches tend to be suspended once their movement is initiated.

Third, the suspended sediment volume V_s per unit horizontal bottom area is estimated by modifying the sediment suspension model by Kobayashi and Johnson (2001)

$$V_s = P_s \frac{e_B D_r + e_f D_f}{\rho g (s-1) w_f} (1 + S_{bx}^2)^{0.5} (1 + S_{by}^2)^{0.5} \quad ; \quad S_{bx} = \frac{\partial z_b}{\partial x} \quad ; \quad S_{by} = \frac{\partial z_b}{\partial y} \quad (3-43)$$

where S_{bx} = cross-shore bottom slope; S_{by} = longshore bottom slope; and e_B and e_f = suspension efficiencies for the energy dissipation rates D_r and D_f due to wave breaking and bottom friction, respectively. Use has been made of $e_B = 0.005$ and $e_f = 0.01$ as typical values in the computation of berm and dune erosion but the value of e_B is uncertain and should be calibrated if V_s is measured (Kobayashi et al. 2007a). The sediment suspension probability P_s in Eq. (3-43) ensures that $V_s = 0$ if $P_s = 0$. The term involving S_{bx} and S_{by} is the actual bottom area per unit horizontal bottom area and essentially unity except for very steep slopes. For the case of alongshore uniformity, $S_{by} = 0$. The cross-shore and longshore suspended sediment transport rates q_{sx} and q_{sy} are expressed as

$$q_{sx} = a_x \bar{U} V_s \quad ; \quad q_{sy} = \bar{V} V_s \quad ; \quad a_x = \left[a + (S_{bx} / \tan \phi)^{0.5} \right] \geq a \quad (3-44)$$

where a = empirical suspended load parameter and ϕ = angle of internal friction of the sediment with $\tan \phi = 0.63$ for sand (Bailard 1981). The parameter a accounts for the onshore suspended sediment transport due to the positive correlation between the time-varying cross-shore velocity and suspended sediment concentration. The value of a increases to unity as the positive correlation decreases to zero. For the three small-scale equilibrium profile tests conducted by Kobayashi et al. (2005), a was of the order of 0.2. The effect of the cross-shore bottom slope on a_x was included by Kobayashi et al. (2009b) to increase berm and dune erosion. For $S_{bx} \leq 0$, $a_x = a$. The cross-shore suspended sediment transport rate q_{sx} is negative (offshore) because the return (undertow) current \bar{U} is negative (offshore). On the other hand, the longshore suspended sediment transport rate q_{sy} in Eq. (3-44) neglects the correlation between the time-varying longshore velocity and suspended sediment concentration, which appears to be very small if the longshore current \bar{V} is sufficiently large. Payo et al. (2009) verified Eq. (3-44) using velocities and sand concentrations measured along 20 transects at the Field Research Facility at Duck, North Carolina during a storm in 1997.

Fourth, the formulas for the cross-shore and longshore bedload transport rates q_{bx} and q_{by} are devised somewhat intuitively because bedload in the surf zone has never been measured. The time-averaged rates q_{bx} and q_{by} are tentatively expressed as

$$q_{bx} = B_b \overline{(U^2 + V^2)} U \quad ; \quad q_{by} = B_b \overline{(U^2 + V^2)} V \quad (3-45)$$

where B_b = empirical parameter. Eq. (3-45) may be regarded as a quasi-steady application of the formula of Meyer-Peter and Mueller (e.g., Ribberink 1998). Substitution of U and V given in Eq. (3-12) with Eqs. (3-13) and (3-14) into Eq. (3-45) yields

$$q_{bx} = B_b \sigma_T^3 (b_* + U_* V_*^2 + 2F_m \sin \theta) \quad (3-46)$$

$$q_{by} = B_b \sigma_T^3 [V_* (1 + U_*^2 + V_*^2) - 2r_m \sin \theta] \quad (3-47)$$

where $b_* = (3U_*^3 + U_*^3)$ and F_m and r_m are defined in Eq. (3-28).

Eqs. (3-46) and (3-47) yield $q_{bx} = b_* B \sigma_T^3$ and $q_{by} = 0$ for normally incident waves with $\sin \theta = 0$ and $V_* = 0$. The expressions of B_b and b_* are obtained by requiring that $q_{bx} = b_* B \sigma_T^3$ reduces to the onshore bedload formula proposed by Kobayashi et al. (2008) for normally incident waves, which synthesized existing data and simple formulas. The proposed formulas are written as

$$q_{bx} = \frac{bP_b}{g(s-1)} \sigma_T^3 (1 + U_* V_*^2 + 2F_m \sin \theta) G_s(S_{bx}) \quad (3-48)$$

$$q_{by} = \frac{bP_b}{g(s-1)} \sigma_T^3 [V_* (1 + U_*^2 + V_*^2) - 2r_m \sin \theta] G_s(S_{by}) \quad (3-49)$$

where b = empirical bedload parameter; and G_s = bottom slope function. The sediment movement probability P_b given in Eq. (3-41) accounts for the initiation of sediment movement. It is noted that $b_* = 1$ in Eq. (3-48) to compensate for the limitations of Eq. (3-45) and the Gaussian distribution of the horizontal velocity used in Eqs. (3-13) and (3-14) as discussed by Kobayashi et al. (2008) who calibrated $b = 0.002$ using available laboratory data for nonbreaking waves.

The bottom slope function $G_s(S_{bx})$ was introduced by Kobayashi et al. (2008) to account for the effect of the steep cross-shore slope S_{bx} on the bedload transport rate and is expressed as

$$G_s(S_{bx}) = \tan \phi / (\tan \phi + S_{bx}) \quad \text{for} \quad -\tan \phi < S_{bx} < 0 \quad (3-50)$$

$$G_s(S_{bx}) = (\tan \phi - 2S_{bx}) / (\tan \phi - S_{bx}) \quad \text{for} \quad 0 < S_{bx} < \tan \phi \quad (3-51)$$

where $G_s = 1$ for $S_{bx} = 0$. Eq. (3-50) corresponds to the functional form of G_s used by Bagnold (1966) for steady stream flow on a downward slope with $S_{bx} < 0$ where the downward slope increases q_{bx} . Eq. (3-51) ensures that G_s approaches negative infinity as the upward slope S_{bx} approaches $\tan \phi = 0.63$ for sand. Eqs. (3-50) and (3-51) reduce to $G_s = (1 - S_{bx} / \tan \phi)$ for $|S_{bx}| \ll \tan \phi$. Eq. (3-43) with G_s given by Eqs. (3-50) and (3-51) implies that the bedload transport rate q_{bx} is positive (onshore) for $S_{bx} < (\tan \phi)/2$ and negative (offshore) for $S_{bx} > (\tan \phi) / 2$. Use is made of $|G_s| < G_m = 10$ to avoid an infinite value in the computation. The computed profile change is not very sensitive to the assumed value of G_m because the beach profile changes in such a way to reduce a very steep slope except in the region of scarping (e.g., Seymour et al. 2005). The effect of the longshore bottom slope S_{by} is included in Eq. (3-49) using the same bottom slope function $G_s(S_{by})$ but has never been validated for lack of suitable data.

The landward marching computation of the time-averaged model in the wet zone ends at the cross-shore location $x = x_r$ where the mean water depth \bar{h} is less than 0.1 cm. No reliable data exists for suspended sand and bedload transport rates in the zone which is wet and dry intermittently. In the absence of wave overtopping [$q_o = 0$ in Eq. (3-4)], the following simple procedure was proposed by Kobayashi et al. (2008) to deal with the zone with the bottom

slope $S_{bx} > \tan \phi$. The cross-shore total sediment transport rate $q_x = (q_{sx} + q_{bx})$ at $x = x_r$ is denoted by q_{xr} . If q_{xr} is negative (offshore), q_x is extrapolated linearly to estimate q_x on the scarped face with $S_{bx} > \tan \phi$

$$q_x = q_{xr} (x_e - x) / (x_e - x_r) \quad \text{for } x_r < x < x_e \quad (3-52)$$

where x_e = landward limit of the scarping zone with $S_{bx} > \tan \phi$. The extrapolated q_x is in the range of $q_{xr} \leq q_x \leq 0$ and the scarping zone is eroded due to the offshore sediment transport. This simple procedure is effective for a high and wide dune, that is typical in the Netherlands (e.g., van Gent et al. 2006), but does not allow onshore sediment transport due to overwash. The model for the wet and dry zone in Section 3.5 has been developed to predict wave overtopping and overwash of dunes.

Finally, the beach profile change is computed using the continuity equation of bottom sediment

$$(1 - n_p) \frac{\partial z_b}{\partial t} + \frac{\partial q_x}{\partial x} + \frac{\partial q_y}{\partial y} = 0 \quad (3-53)$$

where n_p = porosity of the bottom sediment which is normally taken as $n_p = 0.4$; t = slow morphological time for the change of the bottom elevation z_b ; and $q_y = (q_{sy} + q_{by})$ = longshore total sediment transport rate. For the case of alongshore uniformity, the third term in Eq. (3-53) is zero. Eq. (3-53) is solved using an explicit Lax-Wendroff numerical scheme (e.g., Nairn and Southgate 1993) to obtain the bottom elevation at the next time level. This computation procedure is repeated starting from the initial bottom profile until the end of a profile evolution test. The computation time is of the order of 10^{-3} of the test duration.

3.4. Sediment Transport Model for Longshore Current Only

The hydrodynamic model for the case of no waves and no cross-shore flux is presented in Section 3.2. Longshore sediment transport due to the longshore current \bar{V} is analyzed in the following.

The sediment movement occurs when the absolute bottom shear stress due to longshore current $|\tau'_b| = 0.5\rho f_b \bar{V}^2$ exceeds the critical shear stress, $\rho g(s-1)d_{50}\psi_c$. The criteria for sediment movement due to the longshore current \bar{V} , which can be positive or negative, can be written as $P_b = 1$ for $|\bar{V}| > V_{cb}$ and $P_b = 0$ for $|\bar{V}| < V_{cb}$ with

$$V_{cb} = \left[\frac{2g(s-1)d_{50}\psi_c}{f_b} \right]^{0.5} \quad (3-54)$$

where V_{cb} is the critical longshore current speed for sediment movement.

Sediment suspension is assumed to take place when the turbulence velocity due to the bottom shear stress $(|D_f|/\rho)^{1/3}$ with $|D_f| = 0.5\rho f_b |\bar{V}|^3$ exceeds the sediment fall velocity w_f . The sediment suspension criteria for longshore current only is expressed as $P_s = 1$ for $|\bar{V}| > V_{cs}$ and $P_s = 0$ for $|\bar{V}| < V_{cs}$ where the critical longshore current speed V_{cs} for sediment suspension is given by

$$V_{cs} = w_f \left(\frac{2}{f_b} \right)^{1/3} \quad (3-55)$$

If $V_{cs} < V_{cb}$, use is made of $V_{cs} = V_{cb}$ because sediment suspension occurs only when sediment movement occurs.

The suspended sediment volume per unit area, V_s , given by Eq. (3-43) where for the case of longshore current only and alongshore uniformity, $D_r = 0$ and $S_{by} = 0$. Eq. (3-43) is modified as

$$V_s = \frac{e_f f_b |\bar{V} - \bar{V}_{cs}|^3}{2g(s-1)w_f} (1 + S_{bx}^2)^{0.5} > 0 \quad \text{for } |\bar{V}| > V_{cs} \quad (3-56)$$

$$V_s = 0 \quad \text{for } |\bar{V}| < V_{cs}$$

where the probability of sediment suspension under the time-varying wave velocities is replaced by V_{cs} given by Eq. (3-55).

The suspended sediment transport rates given by Eq. (3-44) with $\bar{U} = 0$ are reduced to

$$q_{sx} = 0 \quad ; \quad q_{sy} = \bar{V}V_s \quad (3-57)$$

The bed load rates given by Eqs. (3-48) and (3-49) for the case of no wave ($\sigma_T = 0$) are modified as

$$q_{bx} = 0 \quad (3-58)$$

$$q_{by} = \frac{b(\bar{V} - V_{cb})^3}{g(s-1)} > 0 \quad \text{for } \bar{V} > V_{cb}$$

$$q_{by} = 0 \quad \text{for } |\bar{V}| < V_{cb} \quad (3-59)$$

$$q_{by} = \frac{b(\bar{V} + V_{cb})^3}{g(s-1)} < 0 \quad \text{for } \bar{V} < (-V_{cb})$$

where the probability of sediment movement is replaced by V_{cb} given by Eq. (3-54) as is the case with sediment transport in steady flow (e.g. Ribberink 1998).

3.5. Model for Impermeable Wet and Dry Zone

A time-averaged probabilistic model was developed by Kobayashi et al (2010) to predict the cross-shore variations of the wet probability and the mean and standard deviation of the water depth and cross-shore velocity in the wet and dry zone. The model was limited to normally incident waves and alongshore uniformity. It is extended here to obliquely incident waves. A sediment transport model in the wet and dry zone is conceptually the same as the sediment transport model in the wet zone.

The incident wave angle θ in the wet and dry zone is assumed to be small $[(\sin \theta)^2 \ll 1]$ due to wave refraction so that the cross-shore hydrodynamics may approximately be predicted by the wet and dry zone model for normally incident waves. The time-averaged cross-shore continuity and momentum equations derived from the nonlinear shallow-water wave equations for the case of $(\sin \theta)^2 \ll 1$

$$\frac{d}{dx}(\overline{hU}) = 0 \quad (3-60)$$

$$\frac{d}{dx} \left(\overline{hU^2} + \frac{g}{2} \overline{h^2} \right) = -gS_{bx} \bar{h} - \frac{1}{2} f_b \overline{|U|U} \quad ; \quad S_{bx} = \frac{dz_b}{dx} \quad (3-61)$$

The wave energy equation corresponding to Eqs. (3-60) and (3-61) was given by Kobayashi and Wurjanto (1992) who used it to estimate the rate of wave energy dissipation due to wave

breaking. The wave energy equation is not used in CSHORE because no formula is available to estimate the time-averaged energy dissipation rate in the wet and dry zone.

The assumption for the Gaussian distribution assumed in Eq. (3-14) has simplified the cross-shore model CSHORE in the wet zone significantly. The assumption of the exponential distribution of the instantaneous water depth h is made to simplify the cross-shore model in the wet and dry zone. The probability density function $f(h)$ is expressed as

$$f(h) = \frac{P_w^2}{h} \exp\left(-P_w \frac{h}{\bar{h}}\right) \quad \text{for } h > 0 \quad (3-62)$$

with

$$P_w = \int_0^{\infty} f(h) dh \quad ; \quad \bar{h} = \int_0^{\infty} h f(h) dh \quad (3-63)$$

where P_w = wet probability for the water depth $h > 0$; and \bar{h} = mean water depth for the wet duration only. The dry probability of $h = 0$ is equal to $(1 - P_w)$. The mean water depth for the entire duration is equal to $P_w \bar{h}$. The overbar in Eqs. (3-60) and (3-61) indicates averaging for the wet duration only. The free surface elevation $(\eta - \bar{\eta})$ above MWL is equal to $(h - \bar{h})$.

The standard deviations of η and h are the same and given by

$$\frac{\sigma_\eta}{\bar{h}} = \left(\frac{2}{P_w} - 2 + P_w \right)^{0.5} \quad (3-64)$$

which yields $\sigma_\eta = \bar{h}$ for $P_w = 1$. This equality was supported by the depth measurements in the lower swash zone by Kobayashi et al. (1998) who assumed $P_w = 1$ in Eq. (3-62).

The instantaneous cross-shore velocity U and longshore velocity V for the case of $(\sin \theta)^2 \ll 1$ may be related to the depth h as follows

$$U = \alpha\sqrt{gh} + U_s \quad ; \quad V = \alpha\sqrt{gh} \sin \theta_1 \quad (3-65)$$

where α = positive constant exceeding unity; and U_s = steady velocity which is allowed to vary with x ; and θ_1 = wave angle at the still water shoreline located at $x = x_{SWL}$. The angle θ_1 is used to represent the alongshore component of wave uprush velocity. The steady velocity U_s is intended to account for offshore return flow on the seaward slope and the downward velocity increase on the landward slope. Holland et al. (1991) measured the bore speed and flow depth on a barrier island using video techniques and obtained $\alpha \approx 2$ where the celerity and fluid velocity of the bore are assumed to be approximately the same. Tega and Kobayashi (1996) computed wave overtopping of dunes using the nonlinear shallow-water wave equations and showed $\alpha \approx 2$ for the computed U and h . As a result, use is made of $\alpha = 2$ as a first approximation. Eq. (3-65) implies that the velocities U and V increase monotonically with the increase of h at given x . Eq. (3-65) yields $U = U_s$ and $V = 0$ when $h = 0$, which may be acceptable in view of the very small depth in the wet and dry zone. Using Eqs. (3-65) and (3-62), the mean and standard deviation of U and V can be expressed as

$$\bar{U} = \frac{\sqrt{\pi}}{2} \alpha (P_w g \bar{h})^{0.5} + P_w U_s \quad ; \quad \bar{V} = \frac{\sqrt{\pi}}{2} \alpha (P_w g \bar{h})^{0.5} \sin \theta_1 \quad (3-66)$$

$$\sigma_U^2 = \alpha^2 g \bar{h} - 2(\bar{U} - U_s)(\bar{U} - P_w U_s) + P_w (\bar{U} - U_s)^2 \quad ; \quad \sigma_V = \alpha \sqrt{g \bar{h}} \left[1 - \frac{\pi}{4} P_w (2 - P_w) \right]^{0.5} |\sin \theta_1| \quad (3-67)$$

Eq. (3-65) for the case of $(\sin \theta_1)^2 \ll 1$ is substituted into Eqs. (3-60) and (3-61) which are averaged for the wet duration using Eq. (3-62). The continuity equation (3-60) yields

$$\frac{3\sqrt{\pi}\alpha}{4}\bar{h}\left(\frac{g\bar{h}}{P_w}\right)^{0.5} + U_s\bar{h} = q_o \quad (3-68)$$

where q_o = wave overtopping rate predicted in the following.

After lengthy algebra, the cross-shore momentum equation (3-61) is expressed as

$$\frac{d}{dx}\left(B\frac{g\bar{h}^2}{P_w} + \frac{q_o^2}{\bar{h}}\right) = -gS_{bx}\bar{h} - \frac{f_b}{2}\alpha^2 g\bar{h}G_b(r_s) \quad (3-69)$$

with

$$B = \left(2 - \frac{9\pi}{16}\right)\alpha^2 + 1 \quad ; \quad r_s = \frac{3\sqrt{\pi}}{4}\frac{U_s\bar{h}}{q_o - U_s\bar{h}} \quad (3-70)$$

The function $G_b(r_s)$ in Eq. (3-69) with $r = r_s$ for simplicity is given by

$$G_b(r) = 1 + \sqrt{\pi}r + r^2 \quad \text{for } r \geq 0 \quad (3-71)$$

$$G_b(r) = 2\exp(-r^2) - r^2 - 1 + \sqrt{\pi}r[2\text{erf}(r) + 1] \quad \text{for } r < 0 \quad (3-72)$$

where erf is the error function. The function G_b increases monotonically with the increase of r and $G_b = 0$ and 1 for $r = -0.94$ and 0.0, respectively, as shown in Fig. 3-2. For $r < -1.5$, $G_b \simeq -(1 + \sqrt{\pi}r + r^2)$.

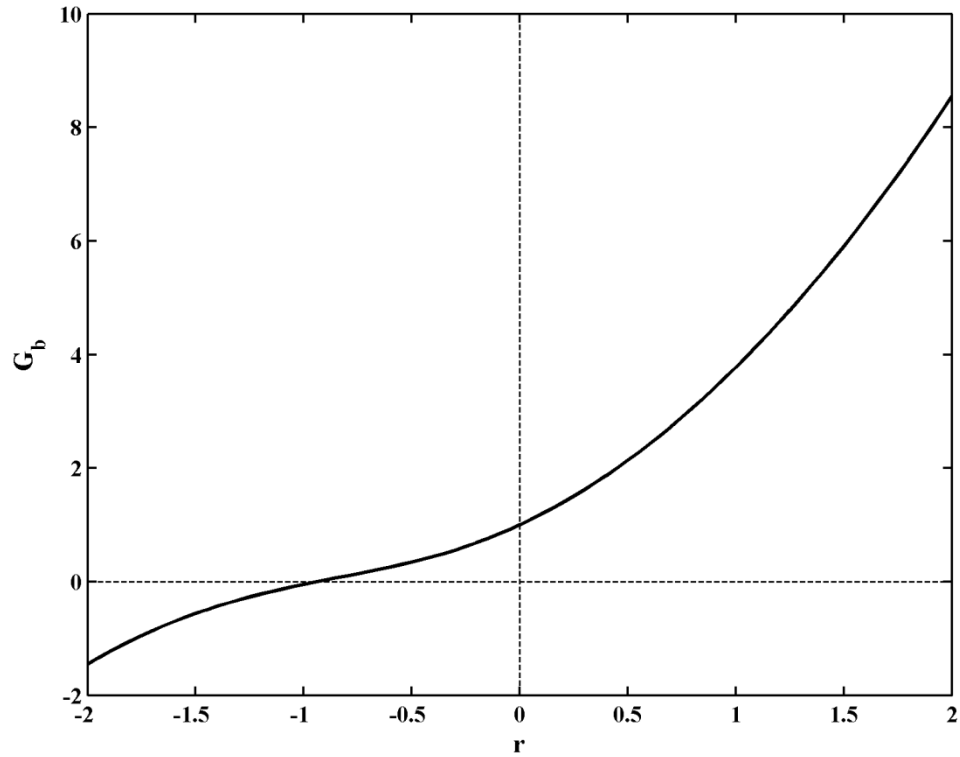


Fig. 3-2. Function $G_b(r)$ for wet and dry zone

Eqs. (3-68) and (3-69) are used to predict the cross-shore variations of \bar{h} and U_s for assumed q_o where $\sigma_\eta, \bar{U}, \bar{V}, \sigma_U$ and σ_V are computed using Eqs. (3-64), (3-66) and (3-67). It is necessary to estimate the wet probability P_w empirically. To simplify the integration of the momentum equation (3-69), the following formula is adopted:

$$P_w = \left[(1 + A_o) \left(\frac{\bar{h}_1}{\bar{h}} \right)^n - A_o \left(\frac{\bar{h}_1}{\bar{h}} \right)^3 \right]^{-1} ; \quad A_o = \frac{q_o^2}{Bg\bar{h}_1^3} \quad \text{for } x \leq x_c \quad (3-73)$$

where \bar{h}_1 = mean water depth at the location of $P_w = 1$; n = empirical parameter for P_w ;

A_o = parameter related to the wave overtopping rate q_o normalized by the depth \bar{h}_1 where

water is present always. The transition location x_l from the wet ($P_w = 1$ always) zone to the wet and dry ($P_w < 1$) zone may be taken at $x = x_{SWL}$ where x_{SWL} is the cross-shore location of the still water shoreline of an emerged slope (see Fig. 3-3). Eq. (3-73) is assumed to be valid on the seaward slope and crest in the region of $x \leq x_c$ where x_c = cross-shore location of the highest bottom elevation or landward end of the horizontal crest of a structure in Fig. 3-3.

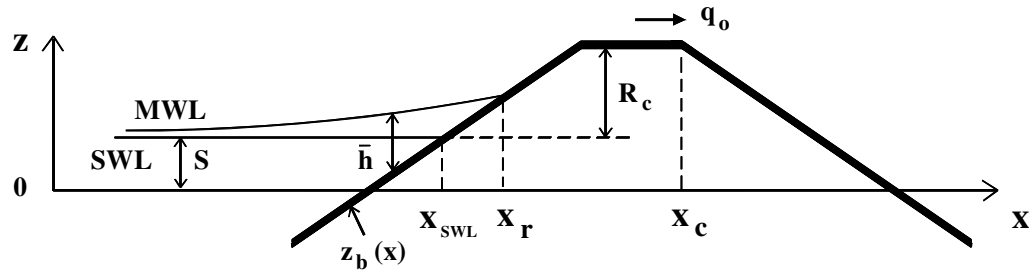


Fig. 3-3. Transition from wet model ($x < x_r$) to wet and dry model ($x > x_{SWL}$) for emerged impermeable structure ($R_c > 0$)

Integration of Eq. (3-69) for P_w given by Eq. (3-73) with $\bar{h} = \bar{h}_1$ at $x = x_1 = x_{SWL}$ yields $\bar{h}(x)$ for $x_1 \leq x \leq x_c$

$$B_n (1 + A_o) \bar{h}_1 \left[\left(\frac{\bar{h}_1}{\bar{h}} \right)^{n-1} - 1 \right] = z_b(x) - z_b(x_1) + \frac{\alpha^2}{2} \int_{x_1}^x f_b G_b dx \quad (3-74)$$

where $B_n = B(2-n)/(n-1)$; and $z_b(x)$ = bottom elevation at the cross-shore location x .

The mean water depth \bar{h} at given x is computed by solving Eq. (3-74) iteratively where the bottom friction factor f_b is allowed to vary with x and the function G_b given by Eqs. (3-71) and (3-72) depends on r_s defined in Eq. (3-70). The empirical parameter n is taken to be in

the range of $1 < n < 2$ so that $B_n > 0$. The formula for n calibrated using the 107 tests of wave overtopping and overflow on a dike by Farhadzadeh et al. (2007) was expressed as $n = 1.01 + 0.98 [\tanh(A_o)]^{0.3}$ where $1.01 \leq n \leq 1.99$.

The wave overtopping rate q_o is predicted by imposing $U_s = 0$ in Eq. (3-68) at the location of x_c

$$q_o = \frac{3\sqrt{\pi}\alpha}{4} \bar{h}_c \left(\frac{g\bar{h}_c}{P_c} \right)^{0.5} \quad \text{at } x = x_c \quad (3-75)$$

where \bar{h}_c and P_c are the computed mean depth \bar{h} and wet probability P_w at x_c .

On the slope landward of the crest, the wet probability P_w is assumed to be constant and equal to P_c

$$P_w = P_c \quad \text{for } x \geq x_c \quad (3-76)$$

Substituting Eq. (3-76) into Eq. (3-69) and integrating the resulting equation from x_c to x , the mean depth $\bar{h}(x)$ on the landward slope in the region of $x > x_c$ is expressed as

$$\frac{\bar{h}}{\bar{h}_c} - 1 + \frac{9\pi\alpha^2}{64B} \left[\left(\frac{\bar{h}_c}{\bar{h}} \right)^2 - 1 \right] = \frac{P_c}{2B\bar{h}_c} \left[z_b(x_c) - z_b(x) - \frac{\alpha^2}{2} \int_{x_c}^x f_b G_b dx \right] \quad (3-77)$$

where the bottom elevation $z_b(x)$ decreases with the landward increase of x in the region of $x > x_c$. Eq. (3-77) is solved iteratively to compute \bar{h} at given x .

For assumed q_o , the landward marching computation of \bar{h} , σ_η , \bar{U} , \bar{V} , σ_U and σ_V is initiated using the wet model in Section 3.1 from the seaward boundary $x=0$ to the landward limit located at $x = x_r$ which corresponds to the location where the computed \bar{h} or σ_η becomes negative or \bar{h} becomes less than 0.1 cm for an emerged crest as shown in Fig. 3-3. The landward marching computation is continued using the wet and dry model in this section from the location of $x = x_{SWL}$ where $\bar{h} = \bar{h}_1$ in Eq. (3-74) to the landward end of the computation domain or until the mean depth \bar{h} becomes less than 0.001 cm. Then, the rate q_o is computed using Eq. (3-75). This landward computation starting from $q_o = 0$ is repeated until the difference between the computed and assumed values of q_o is less than 1%. This convergency is normally obtained after several iterations. The computed values of $\bar{h}, \sigma_\eta, \bar{U}, \bar{V}, \sigma_U$ and σ_V by the two different models in the overlapping zone of $x_{SWL} < x < x_r$ (see Fig. 3-3) are averaged to smooth the transition from the wet zone to the wet and dry zone.

3.6. Sediment Transport Model in Wet and Dry Zone

The sediment transport model for the wet zone in Section 3.3 is adjusted for the wet and dry zone. Obliquely incident waves with $(\sin \theta_1)^2 \ll 1$ and alongshore uniformity are assumed here. The Gaussian velocity distribution has been assumed in Section 3.3, whereas U and V in the wet and dry zone is expressed in Eq. (3-65) along with the exponential distribution of h given by Eq. (3-62). It is noted that the wet and dry zone exists only in the presence of waves. Consequently, there is no wet and dry zone for the case of longshore current only.

First, the movement of sediment particles is assumed to occur when the instantaneous bottom shear stress given by $0.5\rho f_b(U^2 + V^2)$ exceeds the critical shear stress $\rho g(s-1)d_{50}\psi_c$ as assumed for Eq. (3-41). Assuming $(\sin \theta_1)^2 \ll 1$ and $(U^2 + V^2) \approx U^2$, the probability P_b of sediment movement is the same as the probability of $|U| > U_{cb}$ where $U_{cb} = [2g(s-1)d_{50}\psi_c f_b^{-1}]^{0.5}$. Using Eqs. (3-62) and (3-65), P_b can be shown to be given by

$$P_b = P_w \quad \text{for } U_s > U_{cb} \quad (3-78)$$

$$P_b = P_w \exp\left[-\frac{P_w (U_{cb} - U_s)^2}{\alpha^2 g \bar{h}}\right] \quad \text{for } |U_s| \leq U_{cb} \quad (3-79)$$

$$P_b = P_w \left\{ 1 - \exp\left[-\frac{P_w (U_{cb} + U_s)^2}{\alpha^2 g \bar{h}}\right] + \exp\left[-\frac{P_w (U_{cb} - U_s)^2}{\alpha^2 g \bar{h}}\right] \right\} \quad \text{for } -U_s > U_{cb} \quad (3-80)$$

where the upper limit of P_b is the wet probability P_w because no sediment movement occurs during the dry duration.

Second, sediment suspension is assumed to occur when the instantaneous turbulent velocity estimated as $(f_b/2)^{1/3}|U|$ exceeds the sediment fall velocity w_f as assumed for Eq. (3-42). The probability P_s of sediment suspension is then the same as the probability of $|U| > U_{cs}$ where $U_{cs} = w_f(2/f_b)^{1/3}$. The probability P_s is then given by

$$P_s = P_w \quad \text{for } U_s > U_{cs} \quad (3-81)$$

$$P_s = P_w \exp \left[-\frac{P_w (U_{cs} - U_s)^2}{\alpha^2 g \bar{h}} \right] \quad \text{for } |U_s| \leq U_{cs} \quad (3-82)$$

$$P_s = P_w \left\{ 1 - \exp \left[-\frac{P_w (U_{cs} + U_s)^2}{\alpha^2 g \bar{h}} \right] + \exp \left[-\frac{P_w (U_{cs} - U_s)^2}{\alpha^2 g \bar{h}} \right] \right\} \quad \text{for } -U_s > U_{cs} \quad (3-83)$$

which reduce to Eqs. (3-78) – (3-80) if U_{cs} is replaced by U_{cb} . If $P_s > P_b$, use is made of $P_s = P_b$ because sediment suspension occurs only when sediment movement occurs.

Third, the suspended sediment volume V_s per unit horizontal bottom area in the wet zone is estimated using Eq. (3-43) with $S_{by} = 0$ for alongshore uniformity. In the wet and dry zone, V_s is assumed to be given by (Kobayashi et al. 2010)

$$V_s = P_s V_{Bf} (1 + S_{bx}^2)^{0.5} \quad (3-84)$$

where V_{Bf} = potential suspended sediment volume on a horizontal bottom ($S_{bx} = 0$) when $P_s = 1$. The value of V_{Bf} is assumed to be constant and chosen so that the suspended sediment volume V_s is continuous at $x = x_{SWL}$ at the seaward end of the wet and dry zone. The assumption of constant V_{Bf} may be reasonable because suspended sediment in the swash zone tends to remain suspended during wave uprush and downrush. It is noted that P_s given by Eqs. (3-81) – (3-83) decreases landward with the decrease of P_w . However, Eq. (3-84) for the time-averaged suspended sediment volume V_s has not been verified for lack of available data.

Kobayashi et al. (2010) estimated the cross-shore suspended sediment transport rate q_{sx} using Eq. (3-44) for the wet zone

$$q_{sx} = a_x \bar{U} V_s \quad ; \quad a_x = \left[a + (S_{bx} / \tan \phi)^{0.5} \right] \geq a \quad (3-85)$$

Likewise, the longshore sediment transport rate q_{sy} is estimated using the equation for the wet zone

$$q_{sy} = \bar{V} V_s \quad (3-86)$$

Eq. (3-85) was found to underpredict major wave overwash in the three small-scale tests conducted by Figlus et al. (2009) to investigate the transition from minor to major wave overwash of dunes constructed of fine sand. For these tests, suspended load was computed to be dominant. In order to account for the wave overtopping rate q_o explicitly, Eq. (3-85) is modified as

$$q_{sx} = (a_x \bar{U} + a_o U_o) V_s \quad ; \quad U_o = q_o / \bar{h} \quad (3-87)$$

where a_o = empirical parameter with $a_o = 0$ in Eq. (3-85); and U_o = onshore current due to q_o , which is significant only in the zone of the very small depth \bar{h} . The parameter a_x is the same as in Eq. (3-85). The calibrated value for the three tests by Figlus et al. (2009) was in the range of $a_o = 1.3 - 1.8$. However, the range of $a_o = 0.1 - 0.5$ was necessary for the minor wave overwash data used by Kobayashi et al. (2010) to calibrate Eqs. (3-84) and (3-85). The accurate prediction of wave overtopping and overwash is very difficult because of the small water depth and large velocity in the zone which is wet intermittently.

The cross-shore and longshore bedload transport rates q_{bx} and q_{by} are estimated using Eq. (3-48) and (3-49) with $S_{by} = 0$, $\theta = \theta_1$ and $(\sin \theta)^2 \ll 1$ for which

$\sigma_T = (\sigma_U^2 + \sigma_V^2)^{0.5} \approx \sigma_U$. Neglecting the small terms in these equations, q_{bx} and q_{by} are simplified as

$$q_{bx} = \frac{b P_b \sigma_U^3}{g (s-1)} G_s (S_{bx}) \quad (3-88)$$

$$q_{by} = \frac{b P_b \sigma_U^3}{g (s-1)} [V_* (1 + U_*^2) + 2U_* \sin \theta_1] \quad (3-89)$$

where the bottom slope function $G_s (S_{bx})$ is given by Eqs. (3-50) and (3-51), and the standard deviation σ_U is given by Eq. (3-67) for the wet and dry zone. The parameter b in the wet and dry zone is chosen so that the value of q_{bx} is continuous at $x = x_{SWL}$.

Finally, the sediment transport rates q_{sx} , q_{bx} , q_{sy} and q_{by} computed for the wet zone and the wet and dry zone are averaged in the overlapping zone of $x_{SWL} < x < x_r$ for the smooth transition between the two zones in the same way as the smooth transition of the hydrodynamic variables as explained in Section 3.5. The linear extrapolation for the case of no overwash given by Eq. (3-52) for scarping is not applied now that the sediment transport in the wet and dry zone is predicted. The continuity equation of bottom sediment given by Eq. (3-53)

with $\frac{\partial q_y}{\partial y} = 0$ is solved numerically to obtain the bottom elevation at the next time level. The

total transport rates in the x and y directions are given by $q_x = (q_{sx} + q_{bx})$ and $q_y = (q_{sy} + q_{by})$, respectively.

CHAPTER 4

COMPARISONS WITH EXPERIMENT

The extended CSHORE in Chapter 3 is compared with the analyzed data of the base experiment in Chapter 2. The base experiment consisted of five tests BC1 to BC5. The offshore boundary of the CSHORE computation is taken at $x = 0$ in water depth of 0.9 m. The still water shoreline is located at $x_l = 18.4$ m. The measured values of H_{rms} , T_p and $\bar{\eta}$ at $x = 0$ for each test are specified as input. The wave angle is $\theta = 10^\circ$ at $x = 0$. Test BC1 approximately corresponds to the spilling wave test in Kobayashi et al. (2007a) who calibrated three empirical parameters in CSHORE for this test. The calibrated values of $\gamma = 1.0$ in Eq. (3-22), $f_b = 0.02$ in Eq. (3-11) and $e_B = 0.002$ in Eq. (3-43) are used for the following computations for the five tests. The cross-shore grid spacing of the finite difference method used in CSHORE is taken as 2 cm to provide a sufficient resolution near the shoreline.

In Chapter 2, the measured values of $\bar{\eta}$, σ_η , \bar{U} and \bar{V} for the five tests are examined to determine the zone of alongshore uniformity. The velocities measured at a distance of approximately $d/3$ ($d =$ still water depth) above the local bottom are assumed to correspond to the depth-averaged velocities used in CSHORE. All the measured values in the zone of alongshore uniformity ($y = -6$ m and $y = -4$ m) are used in the following comparisons to

indicate the degree of data variability. The alongshore averaged bottom profile in this zone is used as the initial profile (see Fig. 2-4 for test BC1). The averaged wave conditions at $x = 0$ (see Table 2-2) are used as the offshore wave condition in the following computations.

4.1. Model Calibration

The attempt to estimate the alongshore gradient S_η using the measured wave setup in the zone of alongshore uniformity in Section 2.3 was not successful mostly because of the difficulty in measuring wave setup within an error of 0.1 mm. In addition, the recirculation system at the downstream end was situated over the cross-shore span of $x = 4 - 19$ m as shown in Fig. 4-1. As a result, the functional form S_η in Eq. (3-8) is assumed and calibrated

$$S_\eta = EF(x) \text{ for } x \geq 0 \quad ; \quad F(x) = 0.5 \left[1 + \tanh \left(\frac{x - x_0}{\Delta x} \right) \right] \quad (4-1)$$

where S_η increases from zero at $x = 0$ to E at $x = 9$ m for the calibrated values of $x_0 = 6$ m and $\Delta x = 1$ m. The cross-shore variation of the empirical function $F(x)$ is shown in Fig. 4-1. The calibrated value of E for each test is listed in Table 4-1 where $E = 0$ for BC1 with no external current and the recirculation rate Q . The calibrated value of E is proportional to the recirculation rate $(\beta - 1) Q$ with $\beta = 1.0, 1.5$ and 2.0 associated with the external current except for BC3 with no wave. The calibrated values of E for tests BC2 and BC3 are the same perhaps because the recirculation rates were the same.

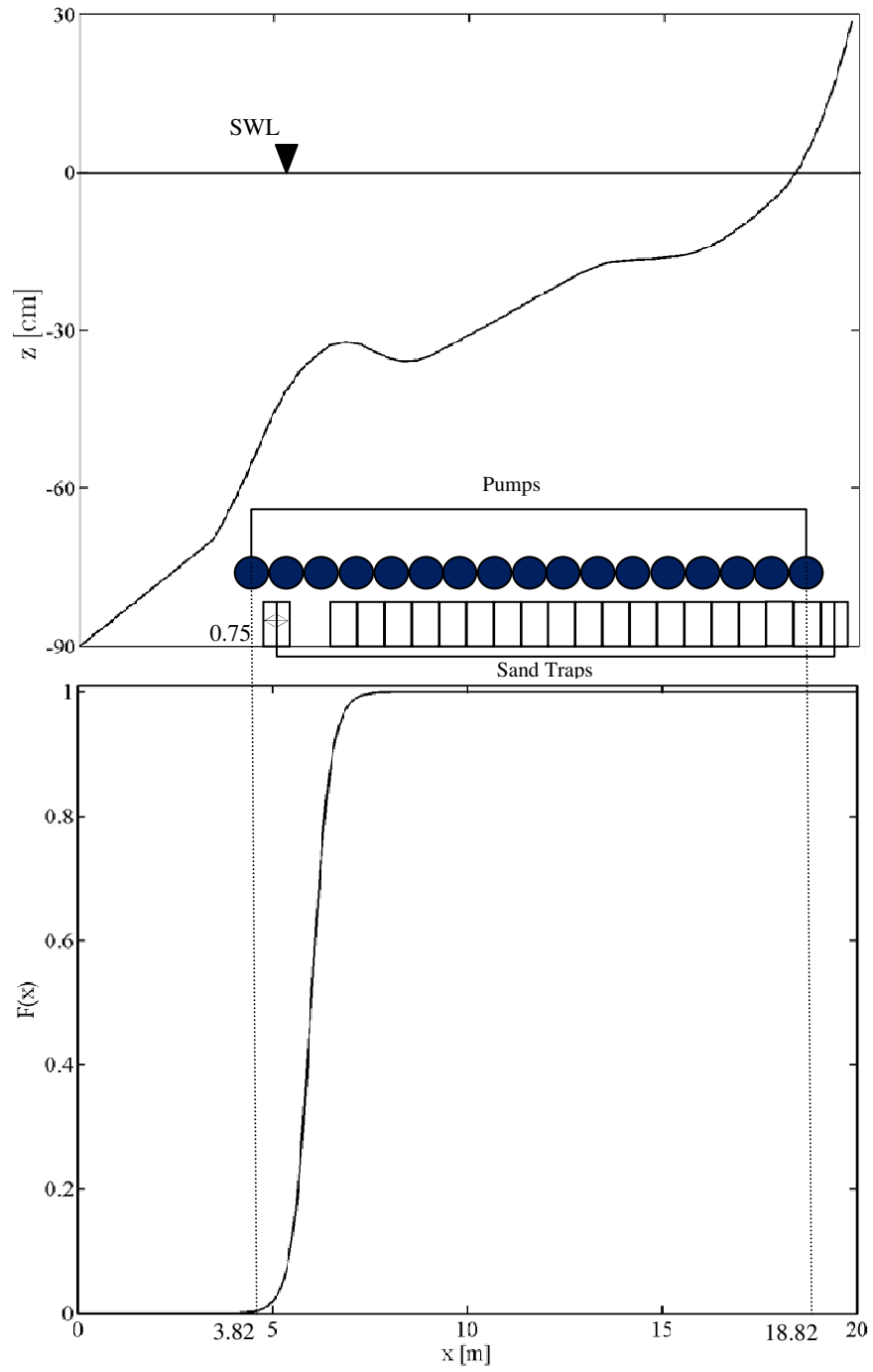


Fig. 4-1. Empirical function $F(x)$ for cross-shore variation of wave setup alongshore gradient

Table 4-1. Recirculation Rate and Alongshore Gradient E of Mean Water Level for Five Tests

Test	BC1	BC2	BC3	BC4	BC5
Recirculation Rate	Q	$2Q$	$2Q$	$1.5Q$	$1.5Q$
$E \times 10^4$	0.0	-1.2	-1.2	-0.6	-0.6

4.2. Comparisons

Fig. 4-2 shows the measured and computed cross-shore variations of $\bar{\eta}, \bar{\sigma}_\eta, \bar{U}$ and \bar{V} for BC1. The difference between the measured and computed values is generally larger than the alongshore variability of the measured $\bar{\eta}, \bar{\sigma}_\eta, \bar{U}$ and \bar{V} . The offshore return current \bar{U} and the longshore current \bar{V} become the maximum near the shoreline. The wet and dry zone added to CSHORE is very narrow for this experiment where the landward end of the beach was located at $x = 19.8$ m. The computed cross-shore variation approaches zero at the upper limit of wave runup on the initial beach profile $z_b(x)$ plotted in the top panel of Fig. 4-2. The prediction of no wave overtopping at $x = 19.8$ m is consistent with no wave overtopping observed in this experiment.

Fig. 4-3 depicts the computed cross-shore variations of q_{sy} and q_{by} as well as the measured and computed cross-shore variations of q_y for BC1 where q_{sy} , q_{by} and q_y are expressed as the sediment volume (no void) per unit width per unit time. The longshore suspended sediment transport rate q_{sy} , and the longshore bed load transport rate q_{by} , and the longshore total sediment transport rate q_y increase onshore and peak near the shoreline. The suspended sediment transport rate is predicted to be about five times larger than the longshore

bed load transport rate for test BC1. The peak of q_y near the still water shoreline located at $x = 18.4$ m is predicted fairly well.

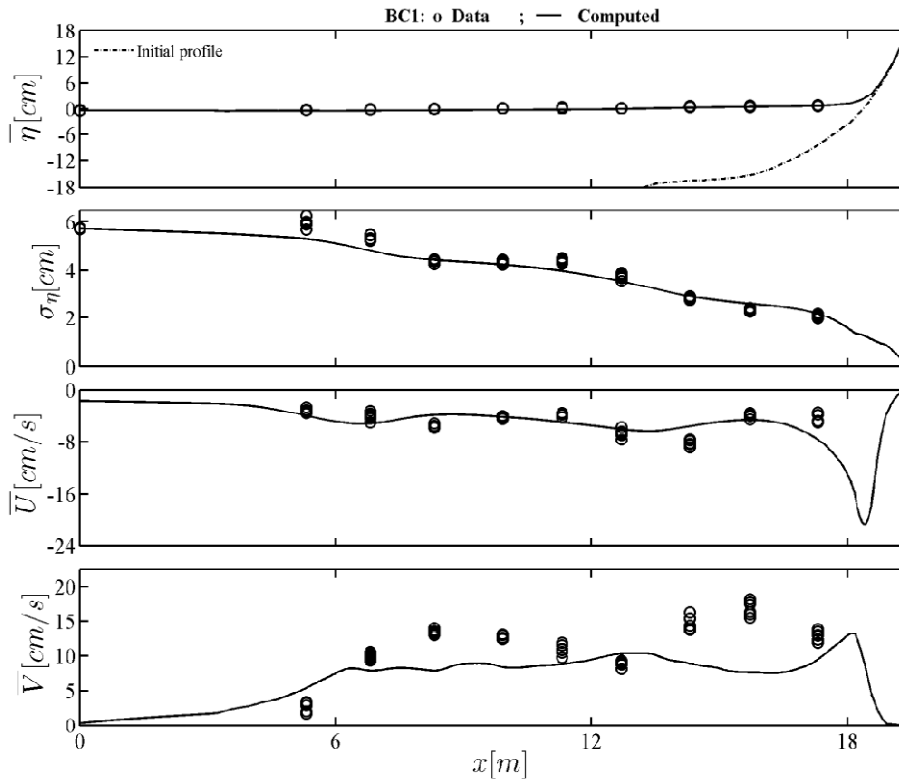


Fig. 4-2. Measured and computed cross-shore variations of mean water level $\bar{\eta}$, free surface standard deviation σ_{η} , cross-shore current \bar{U} and longshore current \bar{V} for BC1

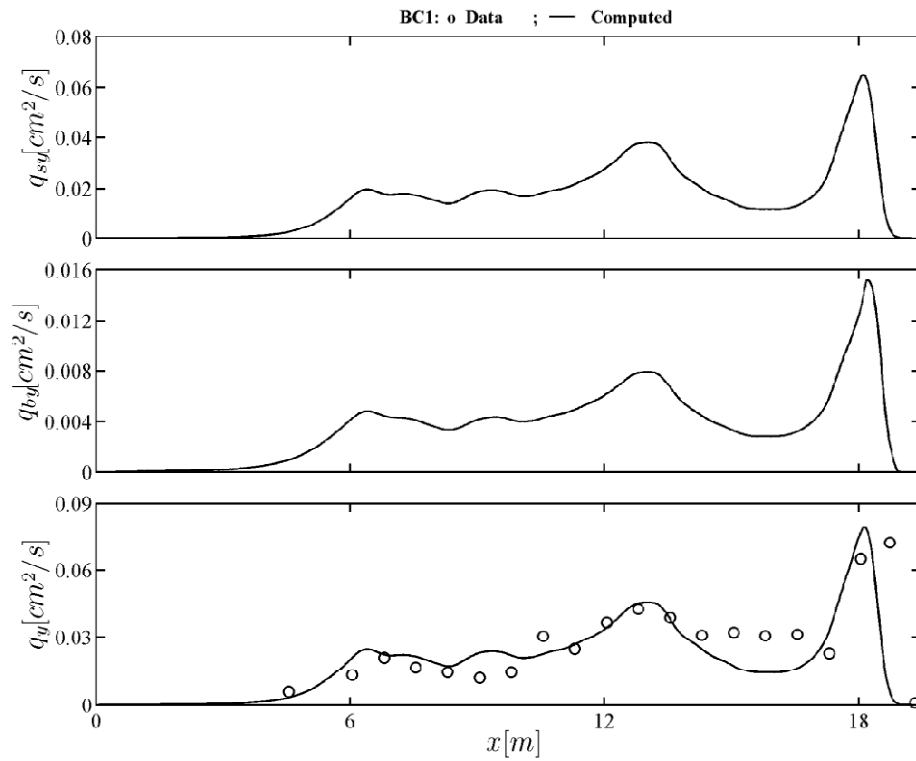


Fig. 4-3. Cross-shore variations of computed q_{sy} and q_{by} as well as measured and computed q_y for BC1

Fig. 4-4 shows the cross-shore variations of computed q_{sx} , q_{bx} and q_x for test BC1. The cross-shore suspended sediment transport rate q_{sx} is negative (offshore) as the mean cross-shore velocity \bar{U} is negative (offshore) as shown in Fig. 4-2. The offshore suspended sediment transport rate q_{sx} increases onshore gradually and becomes the maximum near the shoreline. The offshore suspended sediment transport rate and the onshore bed load transport rate are similar and cancel out except near the shoreline where the offshore suspended sediment transport rate becomes the maximum. The computed beach profile evolution indicates a quasi-equilibrium profile apart from limited erosion near the shoreline.

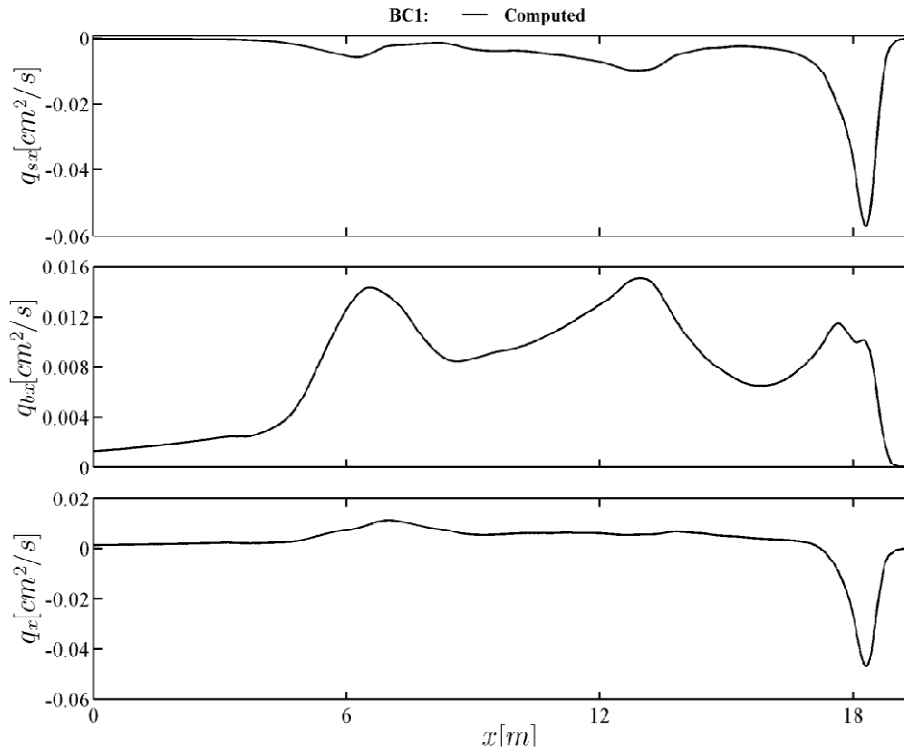


Fig. 4-4. Cross-shore variations of computed q_{sx} , q_{bx} and q_x for BC1

Fig. 4-5 depicts the cross-shore variation of the computed suspended sediment volume per horizontal unit area, V_s , computed with the measured values of V_s at all locations within the zone of alongshore uniformity. In view of the scatter of data points, the agreement is relatively good in the region of $x = 10 - 14.5$ m but the measured values of V_s in the outer surf zone are significantly underpredicted for the adopted efficiency $e_B = 0.002$ due to wave breaking. To improve the agreement, the value of e_B would need to be increased to about 0.01 in the outer surf zone where the previously calibrated range was $e_B = 0.002 - 0.01$ (Kobayashi 2009).

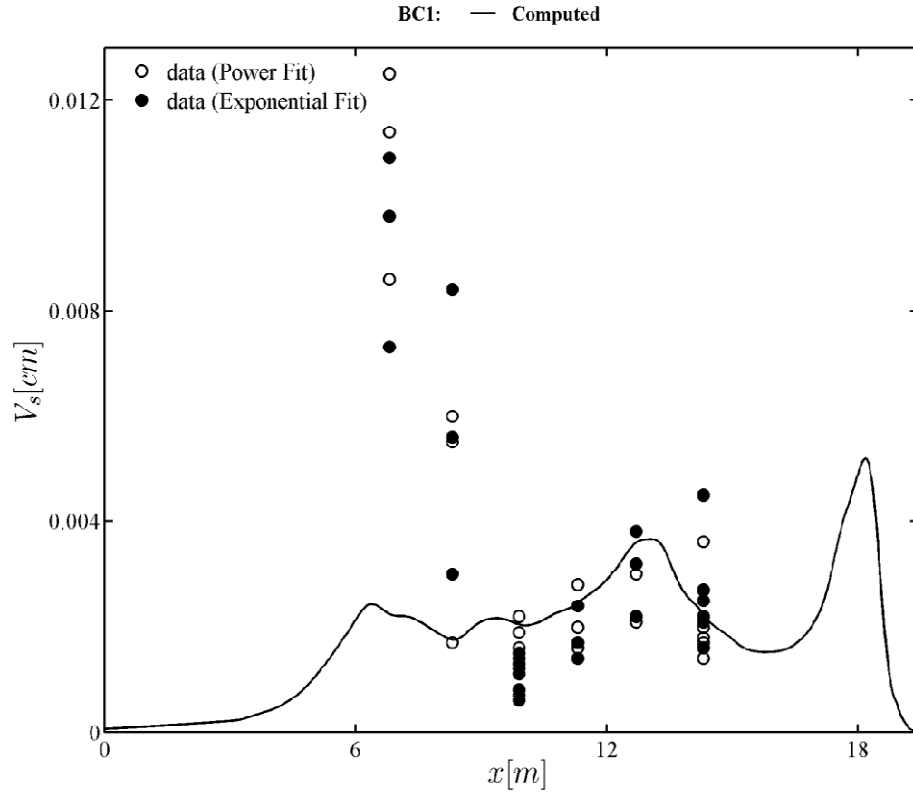


Fig. 4-5. Cross-shore variation of measure and computed suspended sediment volume per unit horizontal area for BC1

Figs. 4-6 to 4-9 show the same comparisons for test BC2. The measured and computed cross-shore variations of $\bar{\eta}$, σ_η and \bar{U} for test BC2 in Fig. 4-6 are very similar to those for test BC1 because these quantities are not sensitive to the alongshore gradient S_η added in the longshore momentum equation which affects the longshore current \bar{V} . The measured and computed values of \bar{V} increase with the increase of $(-S_\eta)$ in Eq. (3-8) due to the increase from $E = 0$ for BC1 to $(-E) = 1.2 \times 10^{-4}$ for test BC2.

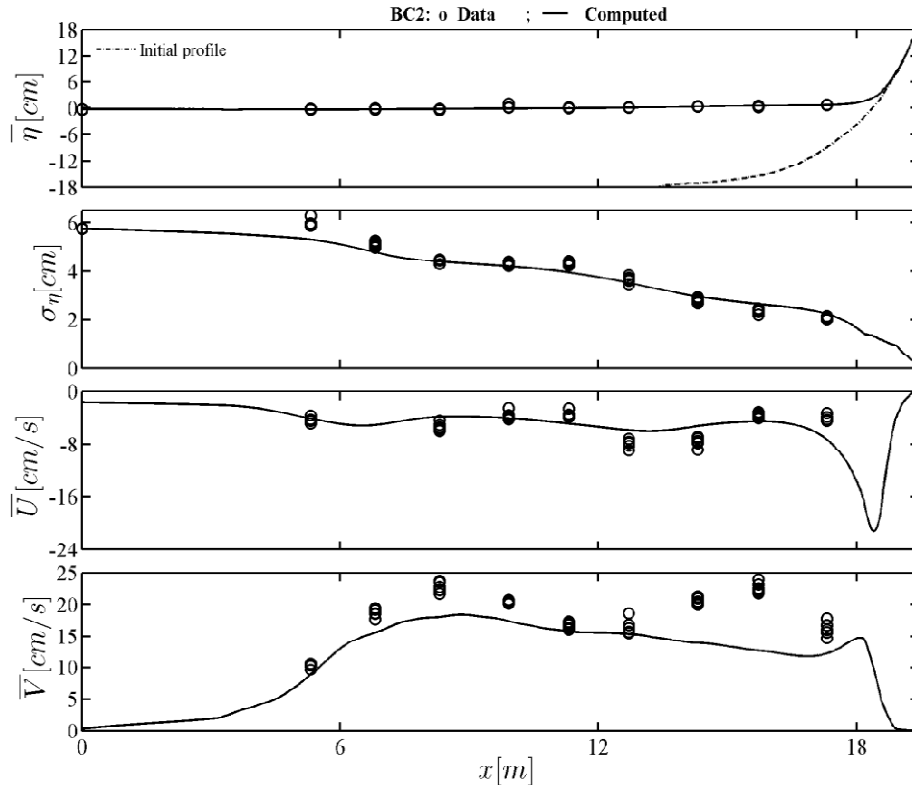


Fig. 4-6. Measured and computed cross-shore variations of mean water level $\bar{\eta}$, free surface standard deviation σ_{η} , cross-shore current \bar{U} and longshore current \bar{V} for BC2

Fig. 4-7 depicts the cross-shore variations of the longshore sediment transport rates for test BC2. The longshore suspended sediment transport rate q_{sy} is about five times larger than the longshore bed load transport rate q_{by} . The increase of \bar{V} for test BC2 causes the similar increase of both q_{sy} and q_{by} . The agreement between the measured and computed q_y for test BC2 is not as good as the agreement for test BC1 shown in Fig. 4-3 perhaps because of the simple functional form of S_{η} assumed in Eq. (4-1).

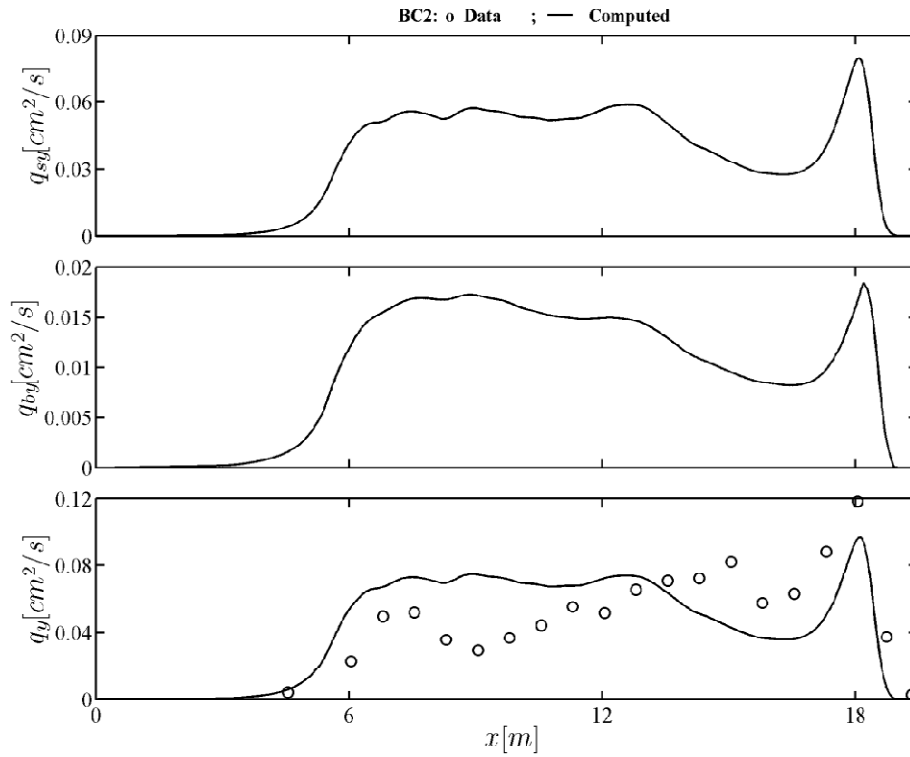


Fig. 4-7. Cross-shore variations of computed q_{sy} and q_{by} as well as measured and computed q_y for BC2

The cross-shore variations of the computed cross-shore sediment transport rates for test BC2 depicted in Fig. 4-8 are similar to those for test BC1 in Fig. 4-4 because the alongshore gradient S_η affects the cross-shore sediment transport processes only indirectly.

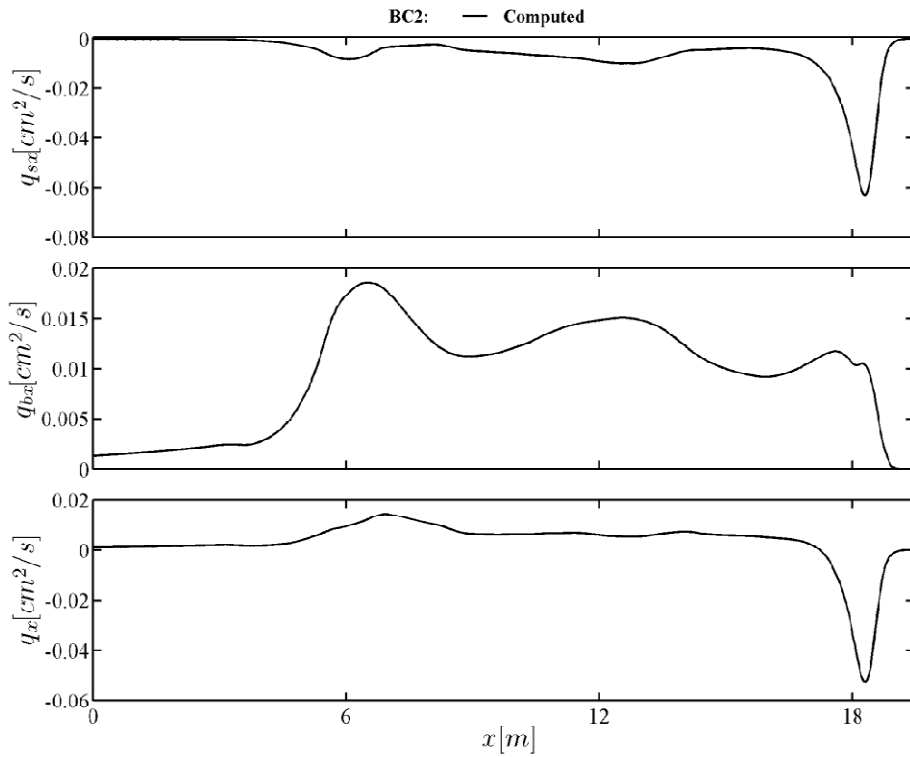


Fig. 4-8. Cross-shore variations of computed q_{sx} , q_{bx} and q_x for BC2

The comparison of the measured and computed V_s for test BC2 is shown in Fig. 4-9. The underprediction in the outer surf zone is reduced in comparison to Fig. 4-5 but the overprediction in the middle surf zone is increased.

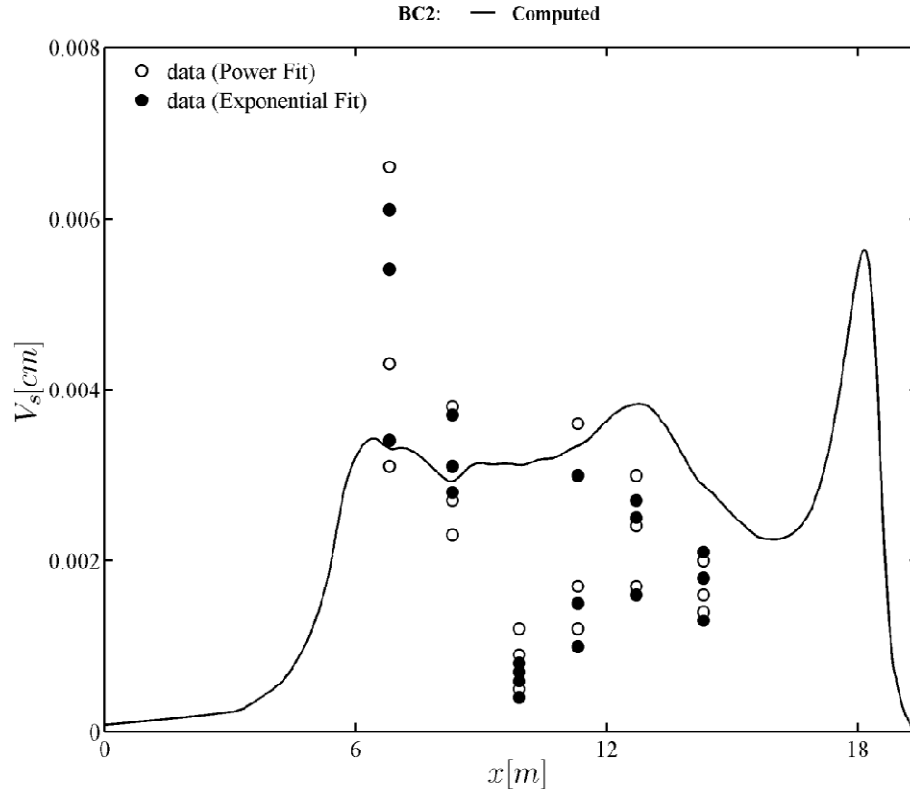


Fig. 4-9. Cross-shore variation of measured and computed suspended sediment volume per unit horizontal area for BC2

As for BC3 with no wave, the direct comparison with CSHORE is not possible because CSHORE requires input waves. The simple analytical solution for the longshore current in absence of waves is presented in Section 3.2. The longshore sediment transport rates due to the longshore current only are presented in Section 3.4. Eqs. (3-39) is used to predict the cross-shore distribution of the longshore current $\bar{V}(x)$. The longshore suspended sediment transport rate q_{sy} and the longshore bed load transport rate q_{by} are predicted using Eqs. (3-57) and (3-59), respectively. Fig. 4-10 compares the measured and computed cross-shore variations of \bar{V} and q_y for test BC3 together with the computed q_{sy} and q_{by} . The agreement for

\bar{V} is similar to those in Figs. 4-2 and 4-6, indicating the generality of the alongshore momentum equation given by Eq. (3-8). The agreement for q_y is poor partly because of the very small measured values for test BC3 and partly because of the empirical nature of the sediment transport formulas used for the case of the longshore current only.

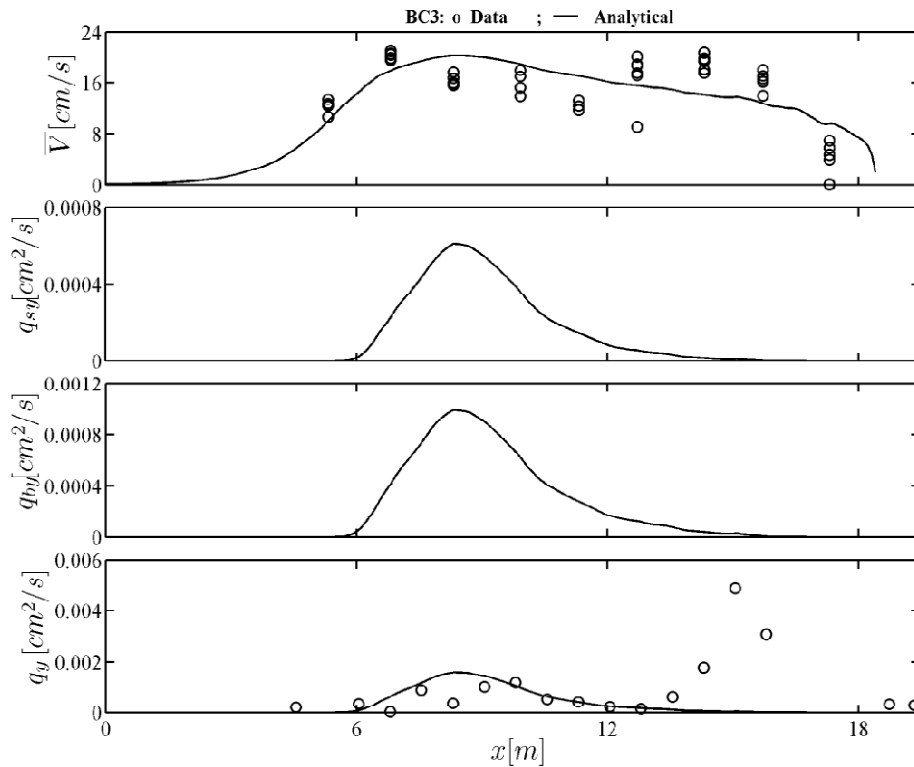


Fig. 4-10. Cross-shore variations of measured and computed longshore current \bar{V} , computed q_{sy} and q_{by} as well as measured and computed q_y for BC3

Fig. 4-11 shows the cross-shore variation of V_s based on the analytical solution given by Eq. (3-56). The sediment suspension is predicted to occur only in the zone of $x = 6 - 16$ m in the absence of waves. The values of V_s for tests BC1 and BC2 are more than 100 times greater than that of test BC3 with no breaking waves for sediment suspension.

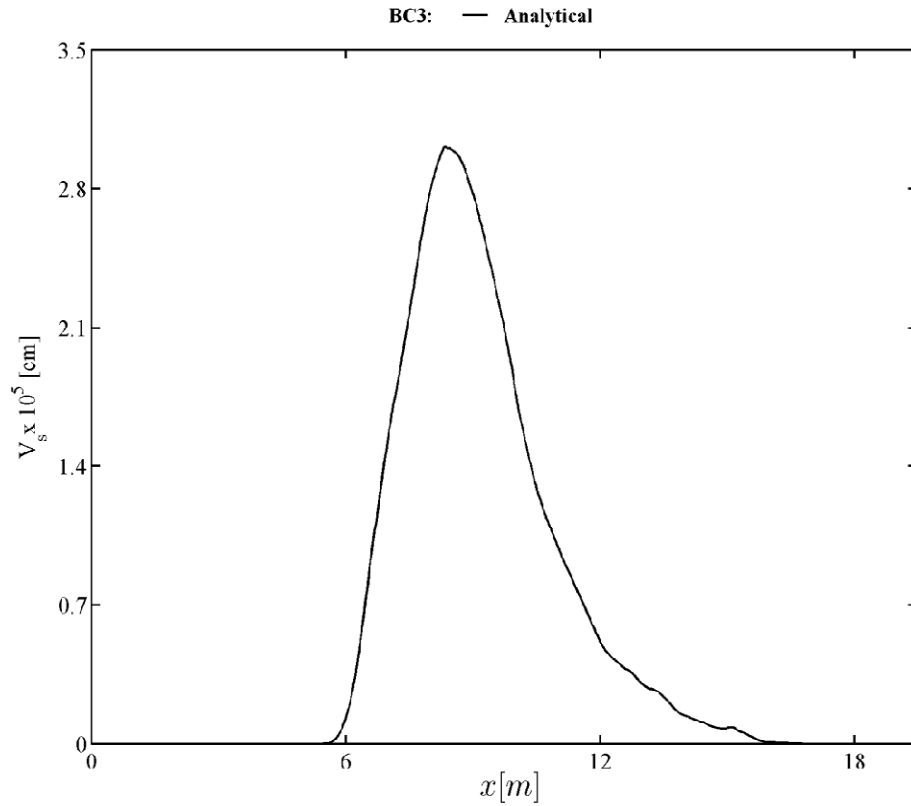


Fig. 4-11. Cross-shore variation of computed suspended sediment volume per unit horizontal area for BC3

The comparisons for test BC4 are shown in Figs. 4-12 to 4-15. The measured and computed cross-shore variations of $\bar{\eta}$, σ_η and \bar{U} in Fig. 4-12 are very similar to those of BC1 and BC2 plotted in Figs. 4-2 and 4-6. The measured and computed values of \bar{V} for test BC4 are slightly smaller than those for BC2 due to the smaller alongshore gradient of the mean water level. Consequently, the measured and computed q_y in Fig. 4-13 are smaller than those for BC2 shown in Fig. 4-7. It is noted that the computed q_{sy} , q_{by} and q_y exhibit numerical

fluctuations associated with bottom irregularities (bed forms). Test BC4 was conducted on the final profile of test BC3 where bed forms generated by the current only were oriented normal to the shoreline unlike wave-generated bed forms oriented parallel to the shoreline.

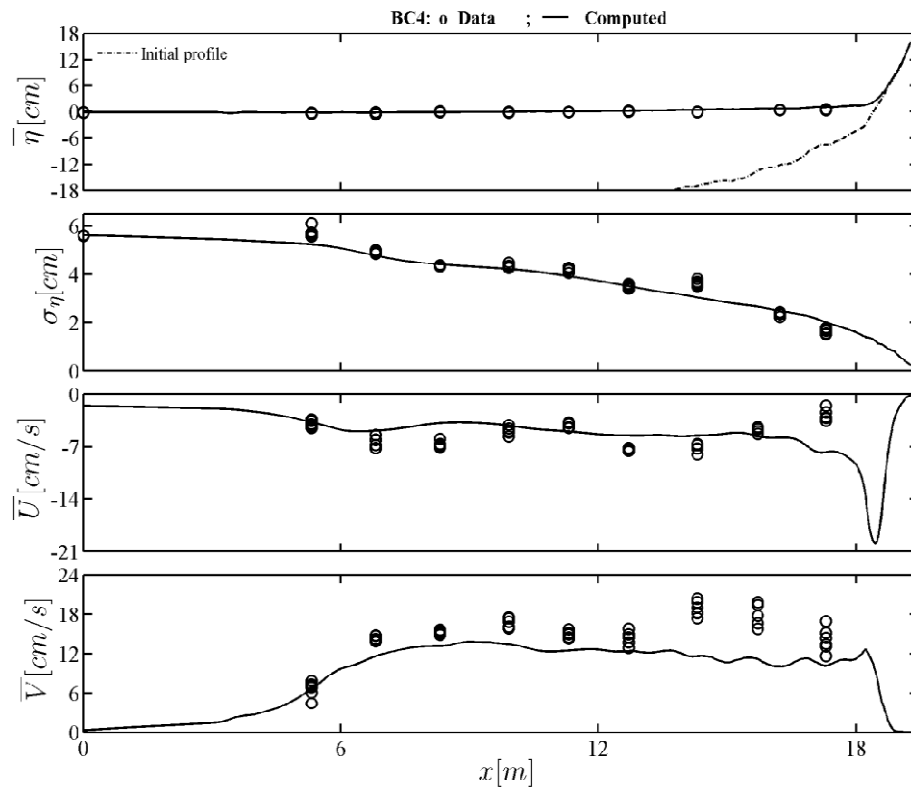


Fig. 4-12. Measured and computed cross-shore variations of mean water level $\bar{\eta}$, free surface standard deviation σ_{η} , cross-shore current \bar{U} and longshore current \bar{V} for BC4

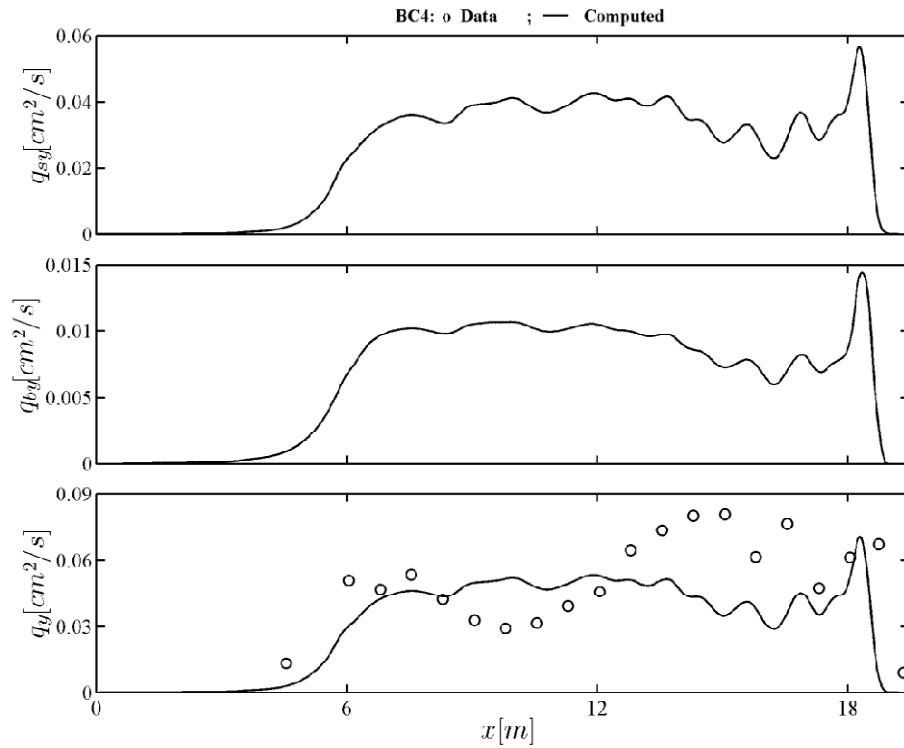


Fig. 4-13. Cross-shore variations of computed q_{sy} and q_{by} as well as measured and computed q_y for BC4

The cross-shore variations of the computed cross-shore sediment transport rates for BC4 plotted in Fig. 4-14 are similar to those in Fig. 4-4 for BC1 and in Fig. 4-8 for BC2. The cross-shore sediment transport rates are affected very little by the alongshore pressure gradient.

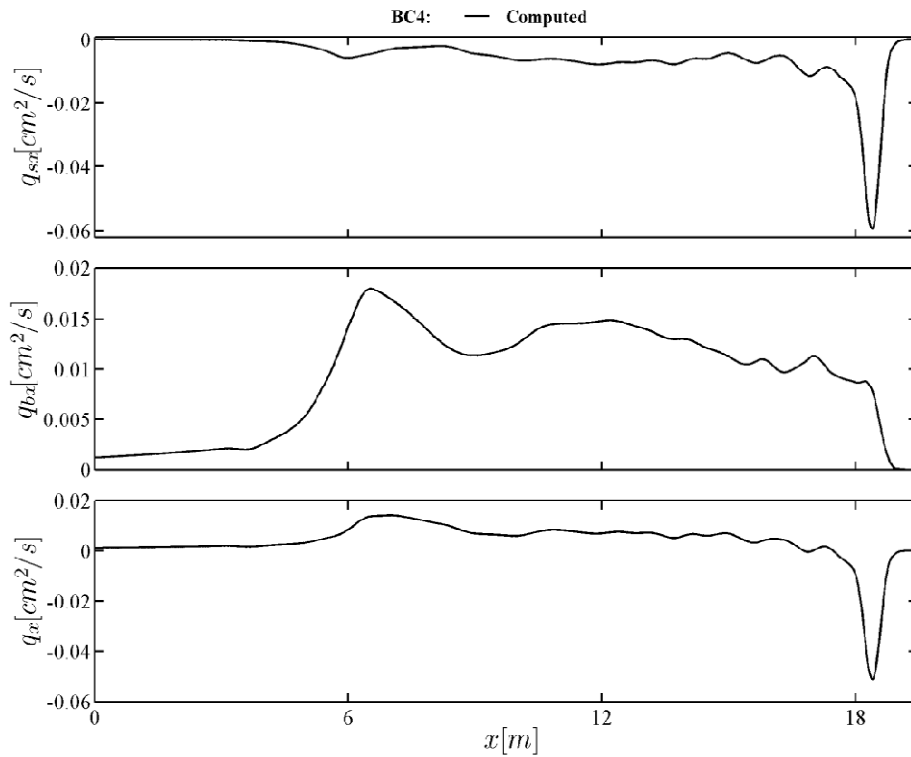


Fig. 4-14. Cross-shore variations of computed q_{sx} , q_{bx} and q_x for BC4

Fig. 4-15 shows the cross-shore variations of the measured and computed suspended sediment volumes V_s for test BC4 in comparison with those in Fig. 4-5 and 4-9 for tests BC1 and BC2. The measured and computed V_s for test BC4 are of the same order of magnitude within the scatter of data points.

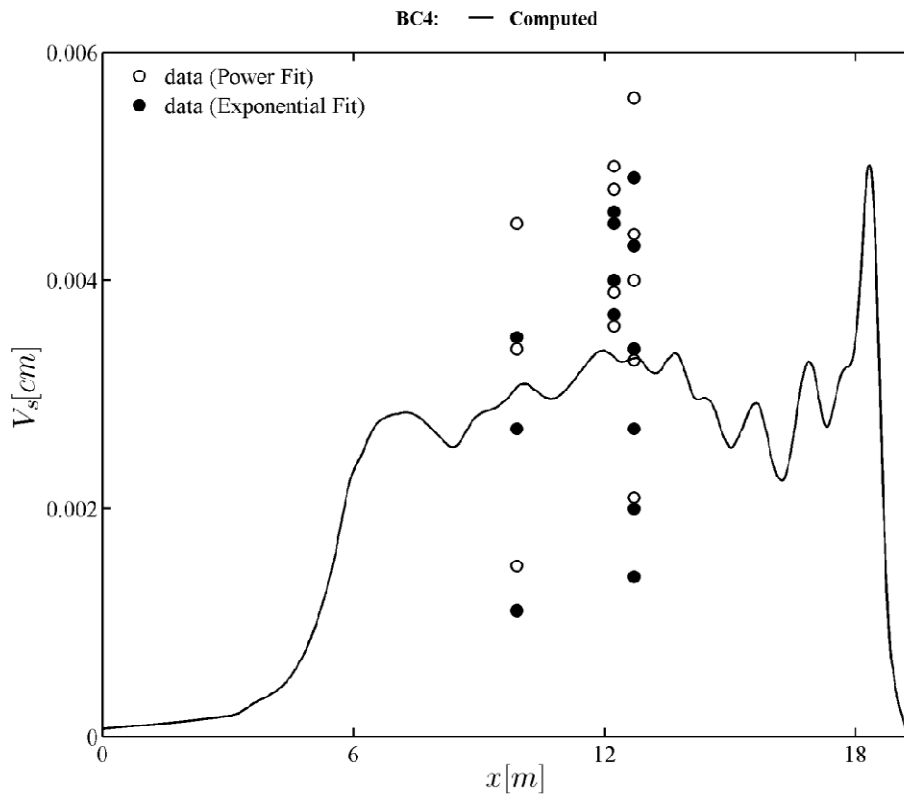


Fig. 4-15. Cross-shore variation of measured and computed suspended sediment volume per unit horizontal area for BC4

Test BC5 is a repeat of test BC4 where the initial bottom profile for test BC5 was the final bottom profile with wave-induced ripples of test BC4. Therefore, the computed and measured hydrodynamic variables and sediment transport rates plotted in Figs. 4-16 to 4-19 for test BC5 are very similar to those in Figs. 4-12 to 4-15 for test BC4. The difference of the two tests was the current-generated and wave-generated (ripple crest parallel to the shoreline) bed forms on the initial profiles. The orientation difference of the bed forms caused no

detectable difference in these figures perhaps because bed forms may appear to be two-dimensional but are three dimensional in reality.

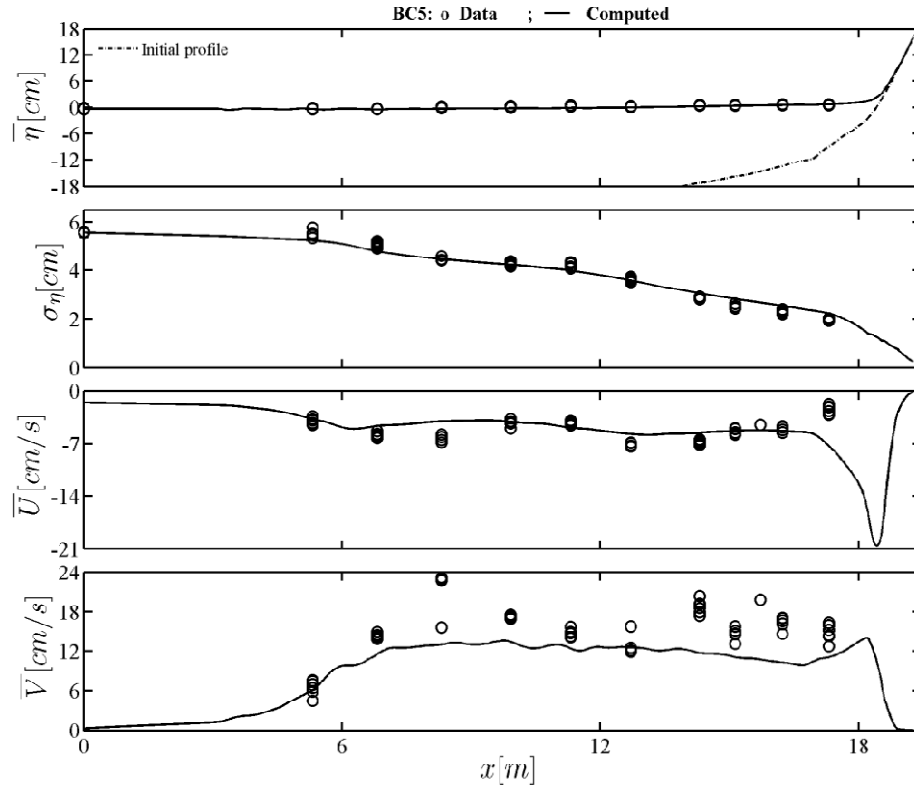


Fig. 4-16. Measured and computed cross-shore variations of mean water level $\bar{\eta}$, free surface standard deviation σ_{η} , cross-shore current \bar{U} and longshore current \bar{V} for BC5

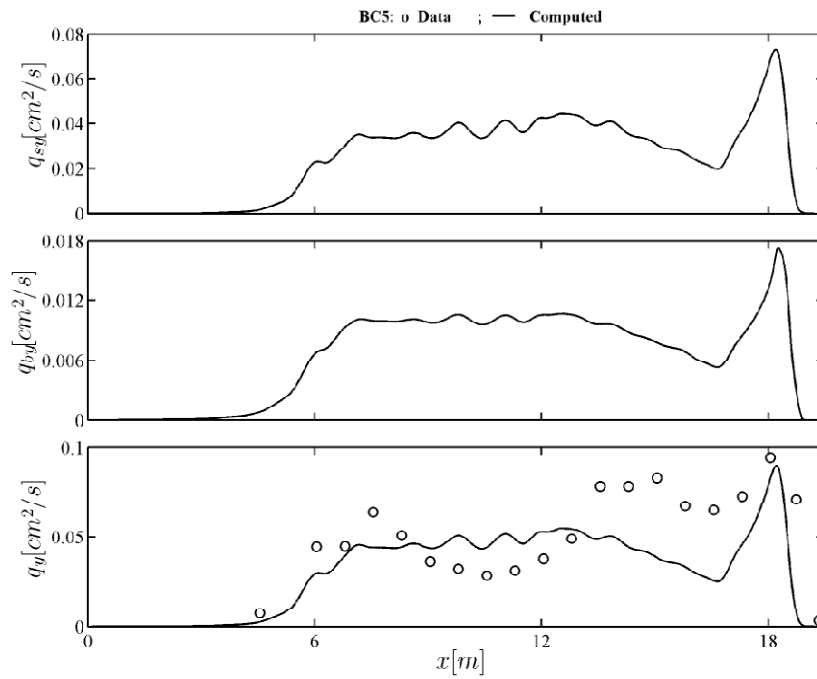


Fig. 4-17. Cross-shore variations of computed q_{sy} and q_{by} as well as measured and computed

q_y for BC5

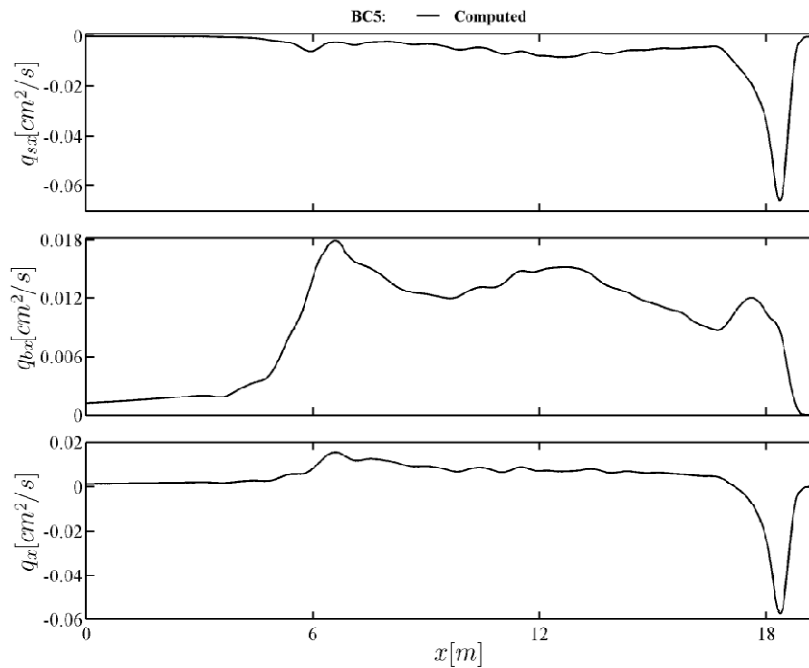


Fig. 4-18. Cross-shore variations of computed q_{sx} , q_{bx} and q_x for BC5

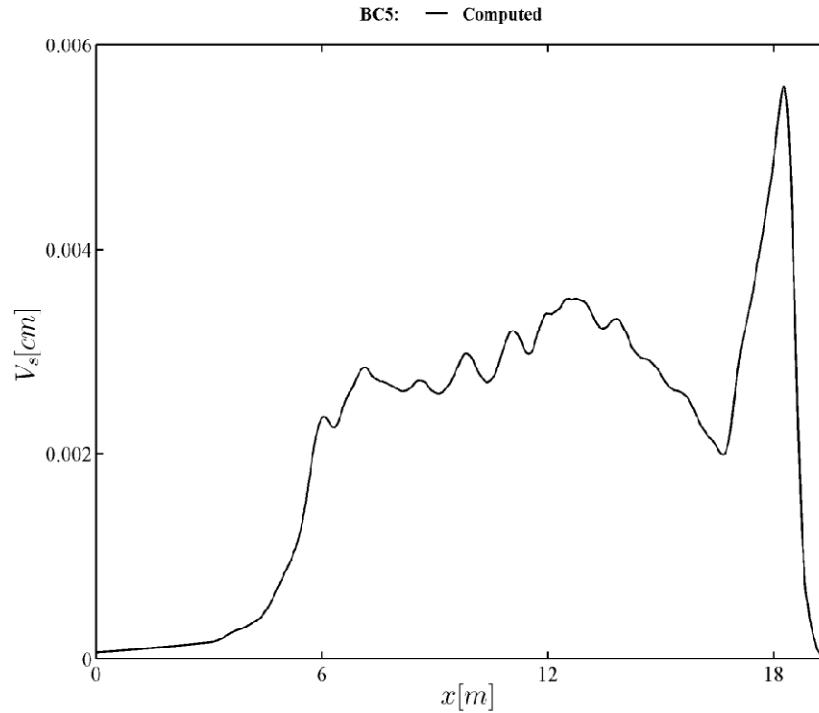


Fig. 4-19. Cross-shore variation of computed suspended sediment volume per unit horizontal area for BC5

4.3. Applications

The comparisons of CSHORE with the five tests listed in Table 4-1 are limited to the case of $E = 0$ (no pressure gradient) and $E < 0$ (favorable pressure gradient). The effects of the pressure gradient term in Eq. (3-8) on the cross-shore variations of \bar{V} and q_y is examined using the input to CSHORE for test BC1. The alongshore pressure gradient S_η given by Eq. (4-1) can be adjusted by changing the dimensionless constant E .

Fig. 4-20 shows the computed cross-shore variations of \bar{V} , q_{sy} , q_{by} and q_y for $(E \times 10^4) = -1.2, -0.6, 0.0, 0.6$ and 1.2 where $\bar{V} < 0$ in the upwave direction. The cross-shore variation of \bar{V} is affected by the gradient S_η term more in the outer surf zone because this term in Eq.

(3-8) is proportional to the mean water depth \bar{h} . The radiation stress term in Eq. (3-8) becomes dominant in the inner surf zone where \bar{h} is small. It is noted that the form of Eq. (4-1) is devised in such a way that S_η and \bar{V} approach zero well outside the surf zone. The longshore suspended sediment transport rate q_{sy} , the longshore bed load transport rate q_{by} and the total sediment transport rate q_y are also affected by the gradient S_η term more in the outer surf zone where they may become negative (upwave directed). The longshore suspended sediment transport rate q_{sy} is about four times larger than the longshore bed load transport rate q_{by} . Fig. 4-20 indicates that the external current modifies the cross-shore distribution of q_y significantly if it is as large as the wave-induced current.

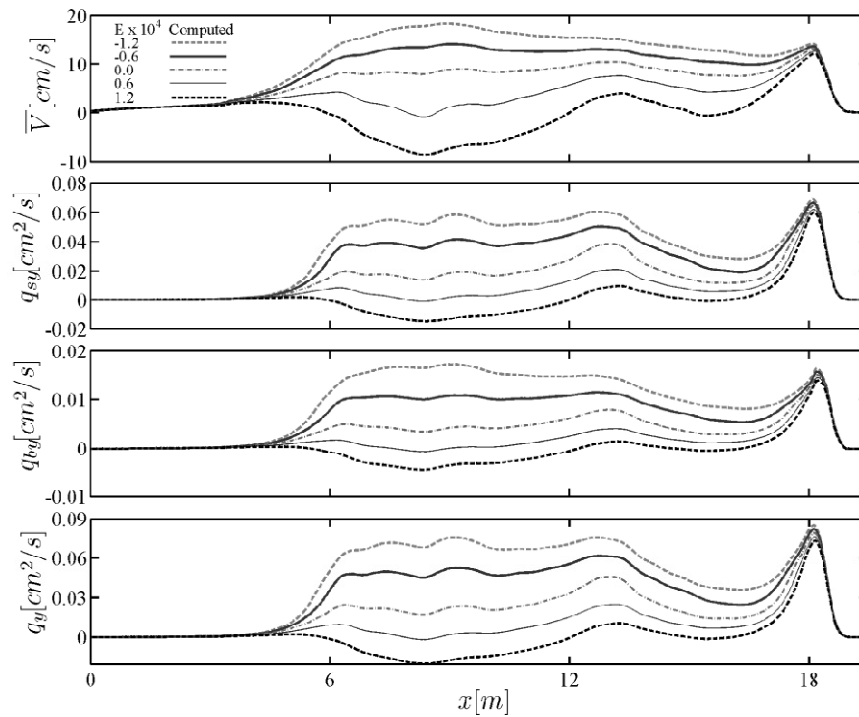


Fig. 4-20. Computed cross-shore variations of \bar{V} , q_{sy} , q_{by} and q_y for $(E \times 10^4) = -1.2, -0.6, 0.0, 0.6$ and 1.2

Fig. 4-21 depicts the computed cross-shore sediment transport rates q_{sx} , q_{bx} and q_x for the five different values of E . These quantities are less sensitive to the values of E because the cross-shore sediment transport rates are affected by E and S_η indirectly through \bar{V} . The longshore current \bar{V} modifies the energy dissipation rate due to bottom friction and the resulting suspended sediment volume and cross-shore suspended sediment transport rate q_{sx} . The longshore current \bar{V} affects the cross-shore bed load transport rate q_{bx} given by Eq. (3-48). These indirect effects are relatively small in Fig. 4-21.

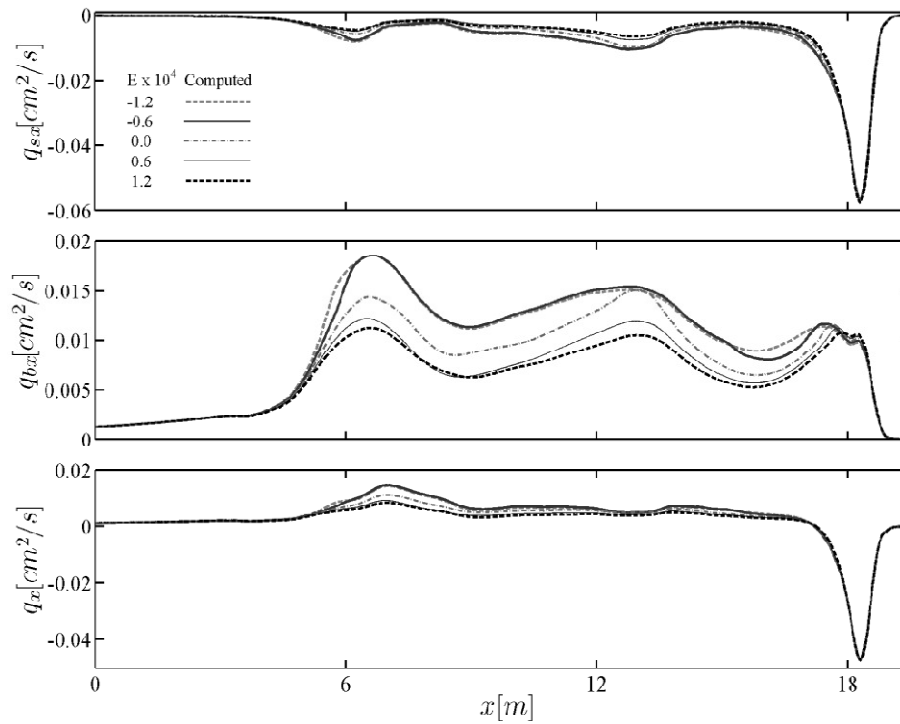


Fig. 4-21. Computed cross-shore variations of q_{sx} , q_{bx} and q_x for $(E \times 10^4) = -1.2, -0.6, 0.0, 0.6$ and 1.2

If the external current is caused by tides, the alongshore pressure gradient may vary during one tidal cycle. To simulate the effect of the tidal oscillation for BC1, E in Eq. (4-1) is

replaced by $E = E_m \sin(2\pi t / T_t)$ with $t =$ tidal time; and $T_t =$ tidal period which is taken as the test duration of 165 min for BC1. The computed q_y is integrated over the tidal period to obtain the longshore sediment transport volume V_y per unit width during one tidal cycle. The computed cross-shore variations of V_y for $(E_m \times 10^4) = 0.0, 0.6$ and 1.2 are shown in Fig. 4-22. The tidal oscillation reduces its net effect on the longshore sediment transport during one tidal cycle. The computed V_y in the outer surf zone increases slightly with the increase of E_m . This slight increase may be smaller than the error of CSHORE. This finding is convenient for practical applications because the alongshore pressure gradient is difficult to estimate on natural beaches. Fig. 4-22 indicates that the sinusoidal tidal effect may be neglected for tide-averaged longshore sediment transport.

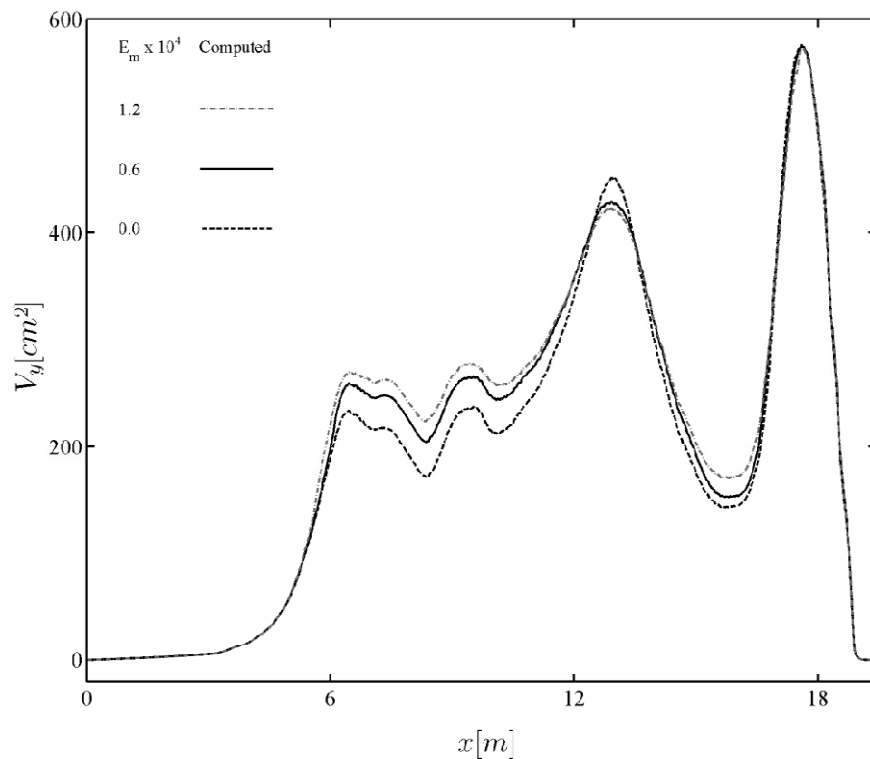


Fig. 4-22. Computed cross-shore variations of longshore sediment transport volume per unit width, V_y for $(E_m \times 10^4) = 0.0, 0.6$ and 1.2

CHAPTER 5

SUMMARY AND CONCLUSIONS

Extensive data analyses were performed for the laboratory experiment conducted by Gravens and Wang (2007) in the Large-scale Sediment Transport Facility of the US Army Engineer Research and Development Center. The experiment included five tests BC1 to BC5. The generated irregular waves were unidirectional with an incident angle of 10° at the seaward boundary. The longshore water fluxes of Q , $2Q$, $2Q$, $1.5Q$ and $1.5Q$ in tests BC1 to BC5, respectively, were recirculated from the downstream end to the upstream end of the beach where Q was the wave-driven longshore water flux for test BC1. Test BC3 was conducted under no wave condition. For each test, the initial and final bottom profiles, free surface elevation η , cross-shore current \bar{U} , and longshore current \bar{V} were measured at several cross-shore locations along a number of longshore stations. The vertical distribution of suspended sediment concentrations was measured at a number of cross-shore locations and longshore stations for three tests. The total longshore sediment transport rate q_y was measured using bottom traps placed at the downstream end of the wave basin for all the five tests.

The measured values of the mean water level $\bar{\eta}$, free surface standard deviation σ_{η} , \bar{U} and \bar{V} for the five tests have been examined to determine the zone of alongshore uniformity which was a 10 m wide zone in the middle of the beach. The averaged initial bottom profile and offshore wave conditions in the zone of alongshore uniformity have been used as input to the numerical model. The measured cross-shore variation of the root-mean-square wave height $H_{rms} = \sqrt{8}\sigma_{\eta}$ has been shown to be related to the quasi-equilibrium bottom profile z_b for four tests BC1, BC2, BC4 and BC5 with waves. An attempt has been made to estimate the alongshore gradient of $\bar{\eta}$ using a regression analysis of the measured $\bar{\eta}$. The attempt was unsuccessful because of the large scatter of the alongshore wave setup gradient caused by the very small difference of $\bar{\eta}$ over the alongshore distance of 10 m. The measured longshore and cross-shore currents have been interpreted in light of the measured cross-shore variations of z_b and H_{rms} for the four tests.

The sediment concentrations measured at a number of elevations at each cross-shore location was fitted by exponential and power-form functions. The correlation between the data and the fitted profiles was higher for the power-form distribution than the exponential distribution. The suspended sediment volume per unit horizontal area, V_s , at each location was obtained by integrating the fitted profiles vertically. The suspended sediment volumes using the two fitted profiles were similar within the difference less than a factor of 2.

The measured total longshore sediment transport rate q_y was integrated across the surf and swash zones to obtain the total longshore sediment transport rate Q_{ty} which was very similar for tests BC2, BC4 and BC5 with combined waves and external current. For test BC1

with no external current, Q_{ty} was reduced by about one half. For test BC3 with no waves, Q_{ty} was reduced almost by a factor of 100.

The cross-shore numerical model CSHORE has been extended to include the alongshore pressure gradient term in the longshore momentum equation. An analytical solution for longshore current has been derived from the combined wave and current model for the case of no waves. Analytical solutions have also been derived for longshore suspended sediment and bed load transport due to the longshore current only by modifying the formulas for the longshore suspended sediment and bed load transport rates under the combined waves and currents. Oblique waves in the wet and dry zone have been included in CSHORE for the case of small incident wave angles in the wet and dry zone. The longshore velocity and sediment transport rate in the wet and dry zone are computed and compared with the measured longshore current and sediment transport rate which were large near the shoreline. The alongshore gradient S_η of wave set up in the basin with the recirculating system was expressed in a simple functional form and calibrated for the five tests.

The extended CSHORE has been compared with the five tests. The cross-shore variations of $\bar{\eta}$, $\bar{\sigma}_\eta$, \bar{U} , \bar{V} and q_y are predicted fairly well for tests BC1, BC2, BC4 and BC5 with similar irregular waves and different recirculation rates. The analytical solutions for longshore current and longshore sediment transport rates have been compared with the data of test BC3. The agreement for the longshore current is good for all the five tests. The longshore suspended sediment transport rate is predicted to be much greater than the longshore bed load transport rate for the four tests with waves. For test BC3, the longshore suspended sediment and bed load transport rates are predicted to be of the same order of magnitude. The computed

suspended sediment volume V_s has been compared with the measured volume for tests BC1, BC2 and BC4. The agreement is only qualitative partly because of the large scatter of the measured volumes. The computed cross-shore distributions of the cross-shore sediment transport rates are consistent with the quasi-equilibrium beach profiles in this experiment except that the computed offshore suspended sediment transport rate is too large near the shoreline.

The longshore recirculation of water in the wave basin modifies the alongshore pressure gradient which affects mostly the longshore current \bar{V} and the total longshore sediment transport rate q_y in the outer surf zone on the beach. The experiment was limited to favorable alongshore pressure gradients in the direction of the wave-induced longshore current. The extended CSHORE is used to examine the effects of adverse and time-varying alongshore pressure gradients on the wave-induced longshore current and sediment transport. The adverse pressure gradient is shown to be capable of reversing the direction of the longshore current and sediment transport. The sinusoidal variation of the pressure gradient during one tidal cycle reduces its net effect on the cumulative longshore sediment transport significantly. It may be of interest to consider asymmetric temporal variations of the pressure gradient but no data is presently available to verify such predictions.

REFERENCES

- Apotsos, A., Raubenheimer, B., Elgar, S., and Guza, R.T. (2008a). "Wave-driven setup and alongshore flows onshore of a submarine canyon." *J. Geophys. Res.*, 113, C07025, doi:10.1029/2007JC004514.
- Apotsos, A., Raubenheimer, B., Elgar, S., and Guza, R.T. (2008b). "Testing and calibrating parametric wave transformation models on natural beaches." *Coastal Eng.*, 55, 224-235.
- Bagnold, R.A. (1966). "An approach to the sediment transport problem from general physics." U.S. Geol. Surv., Prof. Paper 422-I.
- Bailard, J.A. (1981). "An energetics total load sediment transport model for a plane sloping beach." *J. Geophys. Res.*, 86, 10,938-10,954.
- Battjes, J.A., and Stive, M.J.F. (1985). "Calibration and verification of a dissipation model for random breaking waves." *J. Geophys. Res.*, 90(C5), 9159-9167.
- Bodge, K. R., and Dean, R. G. (1987). "Short-term impoundment of longshore transport." *Proc., Coast. Sediments'87*, ASCE, Reston, Va., 468-483.

- Coastal Engineering Manual. (2002). Part III, U.S. Army Engineer Research and Development Center, Vicksburg, Miss.
- Dalrymple, R.A. (1988). "Model for refraction of water waves." *J. Waterway, Port, Coastal, Ocean Eng.*, 114(4), 423-435.
- Farhadzadeh, A., Kobayashi, N., and Gravens, M.B. (2010). "Longshore Sediment Transport due to Breaking Waves and External Current." *J. Waterway, Port, Coastal, Ocean Eng.* (submitted).
- Farhadzadeh, A., Kobayashi, N., Melby, J.A., and Ricottilli, C. (2007). "Experiments and numerical modeling of wave overtopping and overflow on dikes." Research Rep. No. CACR-07-02, Center for Applied Coastal Research, Univ. of Delaware, Newark, Del.
- Figlus, J., Kobayashi, N., Gralher, C., and Iranzo, V. (2009). "Experimental and numerical study on transition from minor to major wave overwash." Research Rep. No. CACR-09-04, Center for Applied Coastal Research, Univ. of Delaware, Newark, Del.
- Gravens, M.B., and Wang, P. (2007). "Data report: Laboratory testing of longshore sand transport by waves and currents; Morphology change behind headland structures," Rep. No. ERDC/CHL TR-07-8, Coastal and Hydraulics Laboratory, US Army Engineer Research and Development Center, Vicksburg, Ms.

- Hanson, H., Larson, M., Kraus, N.C., and Gravens, M.B. (2006). "Shoreline response to detached breakwaters and tidal current: Comparison of numerical and physical models." Coastal Engineering 2006, Proc. 30th Coastal Engineering Conf., World Scientific, Singapore, 3630-3642.
- Holland, K.T., Holman, R.A., and Sallenger, A.H., Jr. (1991). "Estimation of overwash bore velocities using video techniques." Proc. Coastal Sediments'91, ASCE, Reston, Va., 489-497.
- Kamphuis, J. W. (2002). "Alongshore transport rate of sand." Coastal Engineering 2002, Proc., 28th Coastal Engineering Conf., ASCE, Reston, Va., 2478-2490.
- Kobayashi, N.(2009). "Documentation of cross-shore numerical model CSHORE 2009." Research Rep. No. CACR-09-06, Center for Applied Coastal Research, Univ. of Delaware, Newark, Del.
- Kobayashi, N., and Johnson, B.D. (2001). "Sand suspension, storage, advection, and settling in surf and swash zones." J. Geophys. Res., 106, 9363-9376.
- Kobayashi, N., and Wurjanto, A. (1992). "Irregular wave setup and run-up on beaches." J. Waterway, Port, Coastal, Ocean Eng., 118(4), 368-386.
- Kobayashi, N., Agarwal, A., and Johnson, B.D. (2007a). "Longshore current and sediment transport on beaches." J. Waterway, Port, Coastal, Ocean Eng., 133(4), 296-304.

- Kobayashi, N., Payo, A., and Johnson, B.D. (2009a). "Suspended sand and bedload transport on beaches." Handbook of Coastal and Ocean Engineering, World Scientific, Singapore, Chapter 28, 807-823.
- Kobayashi, N., Payo, A., and Schmied, L. (2008). "Cross-shore suspended sand and bedload transport on beaches." J. Geophys. Res., 113, C07001, doi:10.1029/2007JC004203.
- Kobayashi, N., Zhao, H., and Tega, Y. (2005). "Suspended sand transport in surf zones." J. Geophys. Res., 110, C12009, doi:10.1029/2004JC002853.
- Kobayashi, N., Buck, M., Payo, A., and Johnson, B.D. (2009b). "Berm and dune erosion during a storm." J. Waterway, Port, Coastal, Ocean Eng., 135(1), 1-10.
- Kobayashi, N., Herrman, M.N., Johnson, B.D., and Orzech, M.D. (1998). "Probability distribution of surface elevation in surf and swash zones." J. Waterway, Port, Coastal, Ocean Eng., 124(3), 99-107.
- Kobayashi, N., Meigs, L.E., Ota, T., and Melby, J.A. (2007b). "Irregular breaking wave transmission over submerged porous breakwaters." J. Waterway, Port, Coastal, Ocean Eng., 133(2), 104-116.
- Kobayashi, N., Farhadzadeh, A., Melby, J., Johnson, B., and Gravens, M. (2010). "Wave overtopping of levees and overwash of dunes." J. Coastal Res., 26(5), in press.

- Madsen, O.S., and Grant, W.D. (1976). "Quantitative description of sediment transport by waves." Coastal Engineering 1976, Proc. 15th Coastal Engineering Conf., ASCE, Reston, Va., 1093-1112.
- Mei, C.C. (1989). The applied dynamics of ocean surface waves. World Scientific, Singapore.
- Miller, H. C. (1999). "Field measurements of longshore sediment transport during storms." Coastal Eng., 36, 301-321.
- Nairn, R.B., and Southgate, H.N. (1993). "Deterministic profile modeling of nearshore processes. Part 2. Sediment transport and beach profile development." Coastal Eng., 19, 57-96.
- Payo, A., Kobayashi, N., and Yamada, F. (2009). "Suspended sand transport along pier depression." J. Waterway, Port, Coastal, Ocean Eng., 135(5), 245-249.
- Phillips, O.M. (1977). The dynamics of the upper ocean. Cambridge Univ. Press, Cambridge, U.K.
- Ribberink, J.S. (1998). "Bed-load transport for steady flow and unsteady oscillatory flows." Coastal Eng., 34, 59-82.
- Ruessink, B.G., Miles, J.R., Feddersen, F., Guza, R.T., and Elgar, S. (2001). "Modeling the alongshore current on barred beaches." J. Geophys. Res., 106(C10), 22,451-22,463.

- Seymour, R., Guza, R.T., O'Reilly, W., and Elgar, S. (2005). "Rapid erosion of a small southern California beach fill." *Coastal Eng.*, 52, 151-158.
- Tega, Y. and Kobayashi, N. (1996). "Wave overwash of subaerial dunes." *Coastal Engineering 1996, Proc. 25th Coastal Engineering Conf.*, ASCE, Reston, Va., 4148-4160.
- van Gent, M.R.A., Coeveld, E.M., Walstra, D.J.R., van de Graaff, J., Steetzel, H.J., and Boers, M. (2006). "Dune erosion tests to study the influence of wave periods." *Coastal Engineering 2006, Proc. 30th Coastal Engineering Conf.*, World Scientific, Singapore, 2779-2791.
- van Rijn, L. C. (2002). "Longshore sand transport." *Coastal Engineering 2002, Proc. 28th Coastal Engineering Conf.*, ASCE, Reston, Va., 2439-2451.
- Wang, P. (1998). "Longshore sediment flux in water column and across surf zone." *J. Waterway, Port, Coastal, Ocean Eng.*, 124(3), 108-117.
- Wang, P., Ebersole, B. A., Smith, E. R., and Johnson, B. D. (2002). "Temporal and spatial variations of surf-zone currents and suspended sediment concentration." *Coastal Eng.*, 46, 175-211.

APPENDIX A

TEST BC1

Appendix A contains the tables and figures for test BC1.

Table A. 1. Still water depth, wave setup, root-mean-square wave height and peak period at given cross-shore and longshore locations for test BC1

<i>y= 10 m</i>					<i>y= 8 m</i>				
<i>x (m)</i>	<i>d (cm)</i>	$\bar{\eta}$ (cm)	$H_{rms}(cm)$	T_p (s)	<i>x (m)</i>	<i>d (cm)</i>	$\bar{\eta}$ (cm)	$H_{rms}(cm)$	T_p (s)
0.00	90.00	-0.55	16.21	1.47	0.00	90.00	-0.44	16.29	1.46
5.31	41.07	-0.15	17.48	1.50	5.31	41.63	-0.15	16.02	1.49
6.81	31.87	-0.06	16.31	1.50	6.81	32.17	0.02	14.27	1.50
8.31	35.73	0.20	12.63	1.50	8.31	35.93	0.01	11.66	1.58
9.91	31.72	0.25	12.14	1.59	9.91	31.26	0.39	11.58	1.58
11.31	25.20	0.27	11.95	1.59	11.31	24.93	0.46	11.89	1.58
12.71	19.54	0.29	10.44	1.60	12.71	19.26	0.37	10.12	1.59
14.31	16.60	0.52	8.07	1.72	14.31	16.43	0.74	8.05	1.86
15.71	15.29	0.56	6.38	1.84	15.71	14.78	0.93	6.65	1.86
17.31	8.87	0.80	5.60	1.85	17.31	8.17	1.00	6.00	1.86

<i>y= 6 m</i>					<i>y= 4 m</i>				
<i>x (m)</i>	<i>d (cm)</i>	$\bar{\eta}$ (cm)	$H_{rms}(cm)$	T_p (s)	<i>x (m)</i>	<i>d (cm)</i>	$\bar{\eta}$ (cm)	$H_{rms}(cm)$	T_p (s)
0.00	90.00	-0.48	16.14	1.48	0.00	90.00	-0.32	16.21	1.47
5.31	42.20	-0.33	17.19	1.51	5.31	41.67	-0.29	16.88	1.48
6.81	32.47	-0.24	15.46	1.50	6.81	32.00	-0.20	14.89	1.43
8.31	36.13	-0.04	12.66	1.50	8.31	35.90	-0.16	12.01	1.49
9.91	30.80	0.16	12.30	1.50	9.91	30.80	0.15	12.10	1.50
11.31	24.67	0.17	11.68	1.50	11.31	25.07	0.30	12.58	1.58
12.71	18.97	0.21	10.18	1.50	12.71	19.09	0.11	10.40	1.62
14.31	16.27	0.50	7.47	1.60	14.31	16.30	0.54	7.94	1.72
15.71	14.26	0.50	5.80	1.86	15.71	14.61	0.70	6.86	1.85
17.31	7.47	0.71	5.46	1.91	17.31	7.87	0.66	6.15	1.85

<i>y= 2 m</i>					<i>y= 0 m</i>				
<i>x (m)</i>	<i>d (cm)</i>	$\bar{\eta}$ (cm)	H_{rms} (cm)	T_p (s)	<i>x (m)</i>	<i>d (cm)</i>	$\bar{\eta}$ (cm)	H_{rms} (cm)	T_p (s)
0.00	90.00	-0.38	16.16	1.47	0.00	90.00	-0.31	16.25	1.47
5.31	41.13	-0.39	16.07	1.50	5.31	40.93	-0.27	17.71	1.50
6.81	31.53	-0.33	14.79	1.52	6.81	32.20	-0.15	15.48	1.51
8.31	35.67	-0.18	12.41	1.57	8.31	35.50	-0.09	12.61	1.49
9.91	30.79	0.09	12.22	1.51	9.91	31.07	0.19	11.98	1.50
11.31	25.47	0.09	12.10	1.58	11.31	25.50	0.35	12.30	1.48
12.71	19.21	0.09	10.66	1.57	12.71	19.69	0.13	10.10	1.49
14.31	16.33	0.45	7.97	1.71	14.31	17.03	0.54	7.81	1.59
15.71	14.96	0.42	6.36	1.85	15.71	15.50	0.73	6.54	1.86
17.31	8.27	0.64	6.00	1.95	17.31	8.60	0.70	6.03	1.93

<i>y= -2 m</i>					<i>y= -4 m</i>				
<i>x (m)</i>	<i>d (cm)</i>	$\bar{\eta}$ (cm)	H_{rms} (cm)	T_p (s)	<i>x (m)</i>	<i>d (cm)</i>	$\bar{\eta}$ (cm)	H_{rms} (cm)	T_p (s)
0.00	90.00	-0.38	16.14	1.47	0.00	90.00	-0.33	16.11	1.47
5.31	40.73	-0.31	16.63	1.50	5.31	41.37	-0.15	17.03	1.46
6.81	32.87	-0.25	15.01	1.48	6.81	32.53	-0.08	15.43	1.49
8.31	35.33	-0.17	12.46	1.48	8.31	35.93	0.04	12.33	1.49
9.91	31.34	0.11	12.21	1.48	9.91	31.41	0.17	12.53	1.49
11.31	25.53	0.11	12.33	1.57	11.31	25.53	0.39	12.47	1.48
12.71	20.18	0.10	11.00	1.49	12.71	19.98	0.15	10.75	1.58
14.31	17.73	0.45	8.06	1.63	14.31	16.67	0.59	8.23	1.59
15.71	16.03	0.50	6.80	1.86	15.71	15.52	0.76	6.40	1.60
17.31	8.93	0.66	6.02	1.88	17.31	8.47	0.80	5.60	1.89

<i>y = -6 m</i>					<i>y = -8 m</i>				
<i>x (m)</i>	<i>d (cm)</i>	$\bar{\eta}$ (cm)	H_{rms} (cm)	T_p (s)	<i>x (m)</i>	<i>d (cm)</i>	$\bar{\eta}$ (cm)	H_{rms} (cm)	T_p (s)
0.00	90.00	-0.45	16.15	1.46	0.00	90.00	-0.39	16.24	1.47
5.31	42.00	-0.18	16.73	1.52	5.31	41.97	-0.14	17.30	1.46
6.81	32.20	-0.15	15.42	1.50	6.81	31.90	-0.06	15.79	1.45
8.31	36.53	-0.08	12.56	1.48	8.31	35.87	0.06	12.69	1.57
9.91	31.48	0.20	12.43	1.58	9.91	31.35	0.21	11.96	1.47
11.31	25.53	0.20	12.70	1.58	11.31	25.47	0.40	11.55	1.49
12.71	19.79	0.14	10.62	1.50	12.71	19.41	0.18	10.91	1.59
14.31	15.60	0.52	7.83	1.72	14.31	15.50	0.63	8.58	1.59
15.71	15.01	0.64	6.70	1.74	15.71	15.07	0.81	6.16	1.60
17.31	8.00	0.70	5.84	1.88	17.31	8.00	0.84	5.46	1.89

<i>y = -10 m</i>				
<i>x (m)</i>	<i>d (cm)</i>	$\bar{\eta}$ (cm)	H_{rms} (cm)	T_p (s)
0.00	90.00	-0.46	16.21	1.47
5.31	41.93	-0.24	16.62	1.49
6.81	31.60	-0.19	15.21	1.56
8.31	35.20	-0.19	11.59	1.42
9.91	31.23	0.11	12.09	1.58
11.31	25.40	0.12	12.93	1.57
12.71	19.02	0.08	10.22	1.49
14.31	15.40	0.45	7.54	1.74
15.71	15.12	0.58	6.52	1.88
17.31	8.00	0.66	5.68	1.89

Table A.2. Still water depth, mean cross-shore and longshore velocity at given cross-shore and longshore locations for test BC1

x (m)	$y=10$ m			$y=8$ m		
	d (cm)	\bar{U} (cm/s)	\bar{V} (cm/s)	d (cm)	\bar{U} (cm/s)	\bar{V} (cm/s)
2.81	72.50	NR	NR	73.56	NR	NR
5.31	41.07	-7.03	3.29	41.63	-4.50	5.43
6.81	31.87	-6.00	9.42	32.17	-5.73	9.87
8.31	35.73	-6.37	10.62	35.93	-6.58	12.21
9.91	31.72	-4.20	9.59	31.26	-4.35	10.86
11.31	25.20	-3.60	8.82	24.93	-3.46	8.67
12.71	19.54	-5.87	8.56	19.26	-4.98	9.06
14.31	16.60	-6.60	14.59	16.43	-6.35	14.65
15.71	15.29	-3.11	16.60	14.78	-2.85	15.72
17.31	8.87	-3.97	12.20	8.17	-3.15	11.48

x (m)	$y=6$ m			$y=4$ m		
	d (cm)	\bar{U} (cm/s)	\bar{V} (cm/s)	d (cm)	\bar{U} (cm/s)	\bar{V} (cm/s)
2.81	74.63	NR	NR	74.38	NR	NR
5.31	42.20	-2.86	4.08	41.67	-3.59	3.40
6.81	32.47	-4.99	11.05	32.00	-5.00	10.21
8.31	36.13	-6.48	13.22	35.90	-5.17	14.06
9.91	30.80	-4.35	11.96	30.80	-4.11	12.32
11.31	24.67	-3.39	10.55	25.07	-4.13	9.79
12.71	18.97	-6.01	9.19	19.09	-6.95	9.11
14.31	16.27	-6.63	14.77	16.30	-8.45	13.67
15.71	14.26	-3.80	16.20	14.61	-4.01	15.48
17.31	7.47	-4.21	13.06	7.87	-4.80	13.05

	<i>y</i> = 2 <i>m</i>			<i>y</i> = 0 <i>m</i>		
<i>x</i> (<i>m</i>)	<i>d</i> (<i>cm</i>)	\bar{U} (<i>cm/s</i>)	\bar{V} (<i>cm/s</i>)	<i>d</i> (<i>cm</i>)	\bar{U} (<i>cm/s</i>)	\bar{V} (<i>cm/s</i>)
2.81	74.13	NR	NR	74.13	NR	NR
5.31	41.13	-3.06	3.27	40.93	-3.40	2.83
6.81	31.53	-3.87	10.53	32.20	-4.38	9.98
8.31	35.67	-5.54	13.28	35.50	-5.80	13.36
9.91	30.79	-4.28	12.51	31.07	-3.98	12.59
11.31	25.47	-4.21	11.52	25.50	-3.71	10.54
12.71	19.21	-7.66	9.31	19.69	-6.67	8.75
14.31	16.33	-8.85	15.36	17.03	-8.26	14.40
15.71	14.96	-4.54	16.03	15.50	-3.46	16.32
17.31	8.27	-5.01	13.57	8.60	-4.77	13.86

	<i>y</i> = -2 <i>m</i>			<i>y</i> = -4 <i>m</i>		
<i>x</i> (<i>m</i>)	<i>d</i> (<i>cm</i>)	\bar{U} (<i>cm/s</i>)	\bar{V} (<i>cm/s</i>)	<i>d</i> (<i>cm</i>)	\bar{U} (<i>cm/s</i>)	\bar{V} (<i>cm/s</i>)
2.81	74.13	NR	NR	73.15	NR	NR
5.31	40.73	-3.22	2.90	41.37	-3.48	1.99
6.81	32.87	-3.58	9.68	32.53	-4.15	9.35
8.31	35.33	-5.75	13.00	35.93	-5.79	13.62
9.91	31.34	-3.94	13.08	31.41	-4.30	12.96
11.31	25.53	-3.50	10.88	25.53	-3.76	10.96
12.71	20.18	-5.76	8.87	19.98	-6.38	8.15
14.31	17.73	-7.60	15.41	16.67	-7.87	13.96
15.71	16.03	-3.45	17.45	15.52	-3.76	17.83
17.31	8.93	-3.76	12.93	8.47	-3.41	12.28

	<i>y= -6 m</i>			<i>y= -8 m</i>		
<i>x (m)</i>	<i>d (cm)</i>	\bar{U} (cm/s)	\bar{V} (cm/s)	<i>d (cm)</i>	\bar{U} (cm/s)	\bar{V} (cm/s)
2.81	72.17	NR	NR	72.17	NR	NR
5.31	42.00	-2.58	1.67	41.97	-2.94	0.87
6.81	32.20	-3.19	9.36	31.90	-3.64	8.22
8.31	36.53	-5.65	12.94	35.87	-5.44	13.67
9.91	31.48	-4.45	13.04	31.35	-3.58	13.11
11.31	25.53	-3.75	11.88	25.47	-2.91	11.83
12.71	19.79	-6.78	9.31	19.41	-4.55	9.65
14.31	15.60	-8.84	16.27	15.50	-5.74	14.52
15.71	15.01	-3.71	18.23	15.07	-2.40	17.47
17.31	8.00	-4.76	11.87	8.00	-3.18	12.07

	<i>y= -10 m</i>		
<i>x (m)</i>	<i>d (cm)</i>	\bar{U} (cm/s)	\bar{V} (cm/s)
2.81	72.17	NR	NR
5.31	41.93	-2.28	-0.90
6.81	31.60	-2.93	7.68
8.31	35.20	-4.99	13.56
9.91	31.23	-2.25	14.51
11.31	25.40	-1.77	12.60
12.71	19.02	-4.63	11.35
14.31	15.40	-4.87	16.37
15.71	15.12	-2.15	15.23
17.31	8.00	-4.15	9.02

Table A. 2. Mean water depth, fitted profile coefficients, suspended sediment volume per unit horizontal area and correlation coefficient at given cross-shore and longshore locations for test BC1

<i>y=10 m</i>		<i>Exponential</i>				<i>Power</i>			
<i>x (m)</i>	\bar{h} (cm)	c_b (g/l)	l_c (cm)	V_s (cm)	<i>CC</i>	c_a (g/l)	<i>m</i>	V_s (cm)	<i>CC</i>
8.31	35.93	13.33	2.14	0.0068	0.96	49.60	3.04	0.0092	0.93
9.91	31.97	9.90	1.03	0.0015	0.88	15.27	3.75	0.0021	0.72
12.71	19.82	62.10	0.85	0.0062	0.99	23.47	2.48	0.0059	1.00
14.31	17.12	22.58	1.14	0.0040	0.93	7.88	1.93	0.0030	0.98

<i>y=8 m</i>		<i>Exponential</i>				<i>Power</i>			
<i>x (m)</i>	\bar{h} (cm)	c_b (g/l)	l_c (cm)	V_s (cm)	<i>CC</i>	c_a (g/l)	<i>m</i>	V_s (cm)	<i>CC</i>
6.81	32.19	36.43	1.61	0.0119	0.92	46.46	2.98	0.0089	1.00
9.91	31.65	17.91	1.09	0.0029	0.95	51.67	4.42	0.0058	1.00
11.31	25.39	5.05	1.82	0.0020	0.96	11.97	2.95	0.0023	0.98
14.31	17.17	9.10	1.76	0.0034	0.87	7.15	1.90	0.0028	0.98

<i>y=6 m</i>		<i>Exponential</i>				<i>Power</i>			
<i>x (m)</i>	\bar{h} (cm)	c_b (g/l)	l_c (cm)	V_s (cm)	<i>CC</i>	c_a (g/l)	<i>m</i>	V_s (cm)	<i>CC</i>
8.31	36.10	5.38	2.66	0.0037	0.82	17.28	3.07	0.0032	1.00
9.91	30.96	3.76	1.17	0.0007	0.96	7.81	3.75	0.0011	0.85
12.71	19.18	4.89	2.24	0.0026	0.93	4.67	1.54	0.0026	1.00
14.31	16.76	10.12	1.87	0.0042	0.89	10.74	2.11	0.0035	1.00

<i>y=4 m</i>		<i>Exponential</i>				<i>Power</i>			
<i>x (m)</i>	\bar{h} (cm)	<i>c_b (g/l)</i>	<i>l_c (cm)</i>	<i>V_s (cm)</i>	<i>CC</i>	<i>c_a (g/l)</i>	<i>m</i>	<i>V_s (cm)</i>	<i>CC</i>
6.81	31.80	17.07	2.51	0.0109	0.90	57.72	2.74	0.0125	0.98
9.91	30.95	6.35	1.11	0.0011	0.90	12.32	3.88	0.0016	0.73
11.31	25.36	8.30	1.50	0.0024	0.97	17.22	3.36	0.0028	0.98
14.31	16.84	5.33	1.82	0.0021	0.86	4.33	1.86	0.0017	0.98

<i>y=2 m</i>		<i>Exponential</i>				<i>Power</i>			
<i>x (m)</i>	\bar{h} (cm)	<i>c_b (g/l)</i>	<i>l_c (cm)</i>	<i>V_s (cm)</i>	<i>CC</i>	<i>c_a (g/l)</i>	<i>m</i>	<i>V_s (cm)</i>	<i>CC</i>
8.31	35.49	3.55	3.07	0.0030	0.75	7.94	2.75	0.0017	1.00
9.91	30.88	5.40	1.38	0.0014	0.92	15.71	3.74	0.0022	1.00
12.71	19.30	30.15	0.95	0.0038	0.99	12.50	2.21	0.0038	1.00
14.31	16.78	3.63	1.94	0.0016	0.86	3.42	1.87	0.0014	0.98

<i>y=0 m</i>		<i>Exponential</i>				<i>Power</i>			
<i>x (m)</i>	\bar{h} (cm)	<i>c_b (g/l)</i>	<i>l_c (cm)</i>	<i>V_s (cm)</i>	<i>CC</i>	<i>c_a (g/l)</i>	<i>m</i>	<i>V_s (cm)</i>	<i>CC</i>
6.81	32.05	13.74	2.22	0.0073	0.90	45.97	3.02	0.0086	0.99
9.91	31.26	3.57	1.30	0.0008	0.93	8.40	3.68	0.0012	0.78
11.31	25.85	3.84	1.72	0.0014	0.96	8.58	3.05	0.0016	0.98
14.31	17.58	5.80	1.93	0.0025	0.86	5.31	1.93	0.0020	0.99

<i>y=-2 m</i>		<i>Exponential</i>				<i>Power</i>			
<i>x (m)</i>	\bar{h} (cm)	<i>c_b (g/l)</i>	<i>l_c (cm)</i>	<i>V_s (cm)</i>	<i>CC</i>	<i>c_a (g/l)</i>	<i>m</i>	<i>V_s (cm)</i>	<i>CC</i>
8.31	35.17	13.00	2.55	0.0084	0.92	29.65	2.87	0.0060	0.97
9.91	31.46	1.98	1.49	0.0006	0.97	4.18	3.20	0.0007	0.88
12.71	20.28	5.47	2.38	0.0032	0.96	6.29	1.71	0.0030	1.00
14.31	18.19	13.86	1.60	0.0045	0.89	13.59	2.39	0.0036	1.00

<i>y=-4 m</i>		<i>Exponential</i>				<i>Power</i>			
<i>x (m)</i>	\bar{h} (cm)	<i>c_b (g/l)</i>	<i>l_c (cm)</i>	<i>V_s (cm)</i>	<i>CC</i>	<i>c_a (g/l)</i>	<i>m</i>	<i>V_s (cm)</i>	<i>CC</i>
6.81	32.45	14.72	2.59	0.0098	0.87	48.59	2.61	0.0114	1.00
9.91	31.58	7.77	1.11	0.0013	0.98	13.82	3.81	0.0019	0.90
11.31	25.92	5.36	1.59	0.0017	0.97	11.76	3.24	0.0020	0.98
14.31	17.26	5.52	1.84	0.0022	0.86	4.47	1.84	0.0018	0.98

<i>y=-6 m</i>		<i>Exponential</i>				<i>Power</i>			
<i>x (m)</i>	\bar{h} (cm)	<i>c_b (g/l)</i>	<i>l_c (cm)</i>	<i>V_s (cm)</i>	<i>CC</i>	<i>c_a (g/l)</i>	<i>m</i>	<i>V_s (cm)</i>	<i>CC</i>
8.31	36.45	10.07	2.29	0.0056	0.87	35.66	3.45	0.0055	0.99
9.91	31.68	9.28	1.07	0.0015	0.99	17.65	3.99	0.0022	0.96
12.71	19.93	5.61	1.81	0.0022	0.96	5.93	2.00	0.0021	1.00
14.31	16.12	8.26	1.62	0.0027	0.88	6.55	2.09	0.0022	0.99

<i>y=-8 m</i>		<i>Exponential</i>				<i>Power</i>			
<i>x (m)</i>	\bar{h} (cm)	<i>c_b (g/l)</i>	<i>l_c (cm)</i>	<i>V_s (cm)</i>	<i>CC</i>	<i>c_a (g/l)</i>	<i>m</i>	<i>V_s (cm)</i>	<i>CC</i>
6.81	31.84	10.59	2.50	0.0067	0.87	40.21	2.76	0.0086	1.00
9.91	31.56	3.44	1.36	0.0008	0.92	7.66	3.53	0.0011	0.76
11.31	25.86	4.35	1.62	0.0014	0.95	8.48	3.11	0.0015	0.99
14.31	16.13	8.05	1.57	0.0025	0.88	5.65	2.06	0.0019	0.98

<i>y=-10 m</i>		<i>Exponential</i>				<i>Power</i>			
<i>x (m)</i>	\bar{h} (cm)	<i>c_b (g/l)</i>	<i>l_c (cm)</i>	<i>V_s (cm)</i>	<i>CC</i>	<i>c_a (g/l)</i>	<i>m</i>	<i>V_s (cm)</i>	<i>CC</i>
8.31	35.01	23.46	1.90	0.0099	0.95	27.03	2.25	0.0081	0.97
9.91	31.34	2.57	1.35	0.0006	0.96	6.42	3.59	0.0009	0.83
12.71	19.11	3.11	2.33	0.0018	0.93	2.98	1.48	0.0018	1.00
14.31	15.85	2.61	2.16	0.0013	0.93	2.19	1.44	0.0013	0.99

Table A. 4. Coefficients a and b corresponding to wave setup longshore gradient and correlation coefficient CC between data and fitted line at given cross-shore location for tests BC1

x	a	b	CC
0	7.96E-05	-0.0035	0.58
5.31	-0.00017	-0.0028	0.73
6.81	-0.00013	-0.0021	0.55
8.31	-0.00014	-0.0012	0.61
9.91	-5.40E-05	0.0015	0.48
11.31	-2.92E-05	0.0024	0.09
12.71	-4.02E-05	0.0012	0.67
14.31	-3.33E-05	0.0051	0.22
15.71	-6.97E-05	0.0062	0.19
17.31	-8.23E-05	0.0069	0.55

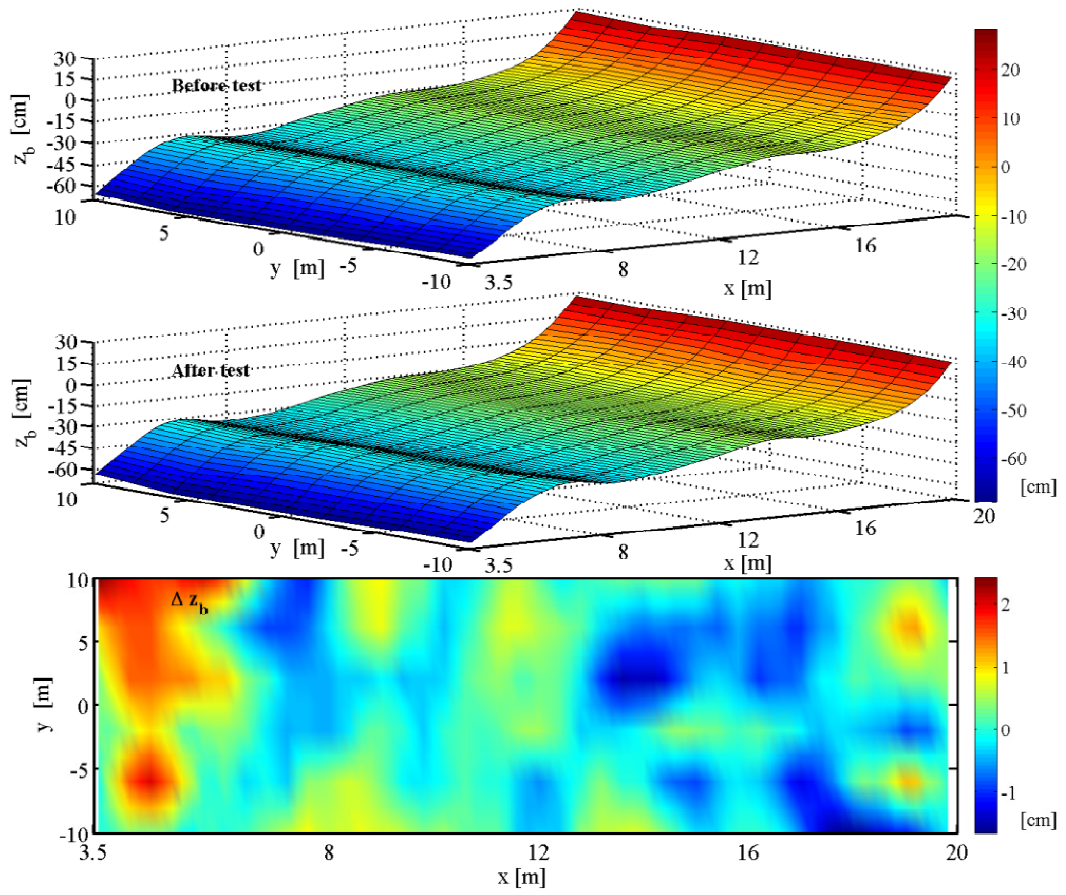


Fig. A-1. Measured initial and final profiles and change in bottom elevation for test BC1

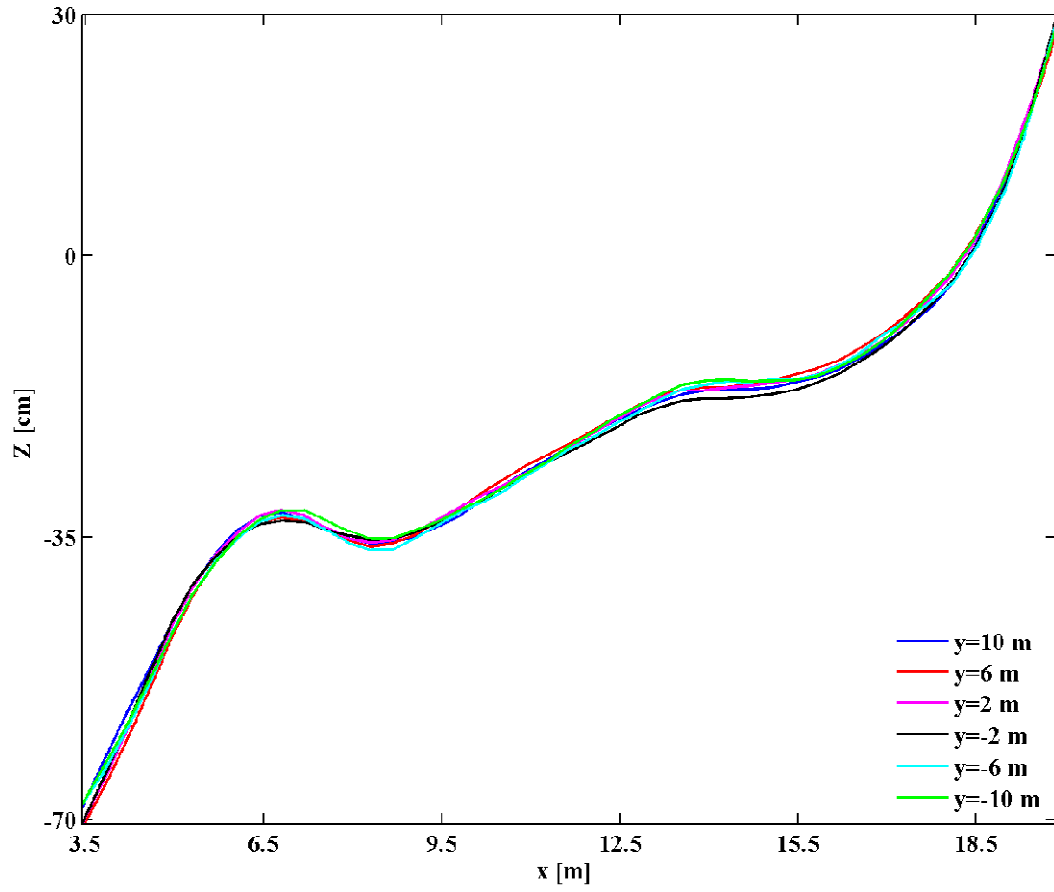


Fig. A-2. Measured initial cross-shore profiles for test BC1

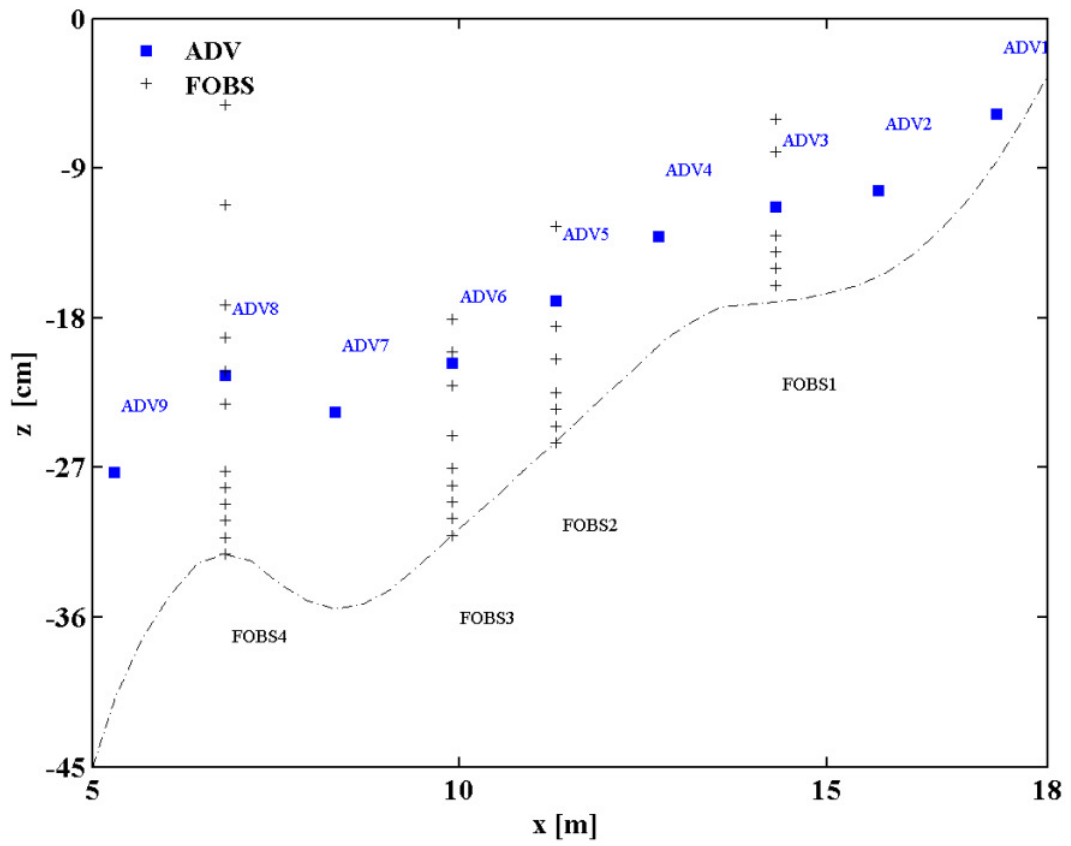


Fig. A-3. Cross-shore positioning of ADVs and FOBS at $y = 0$ for test BC1

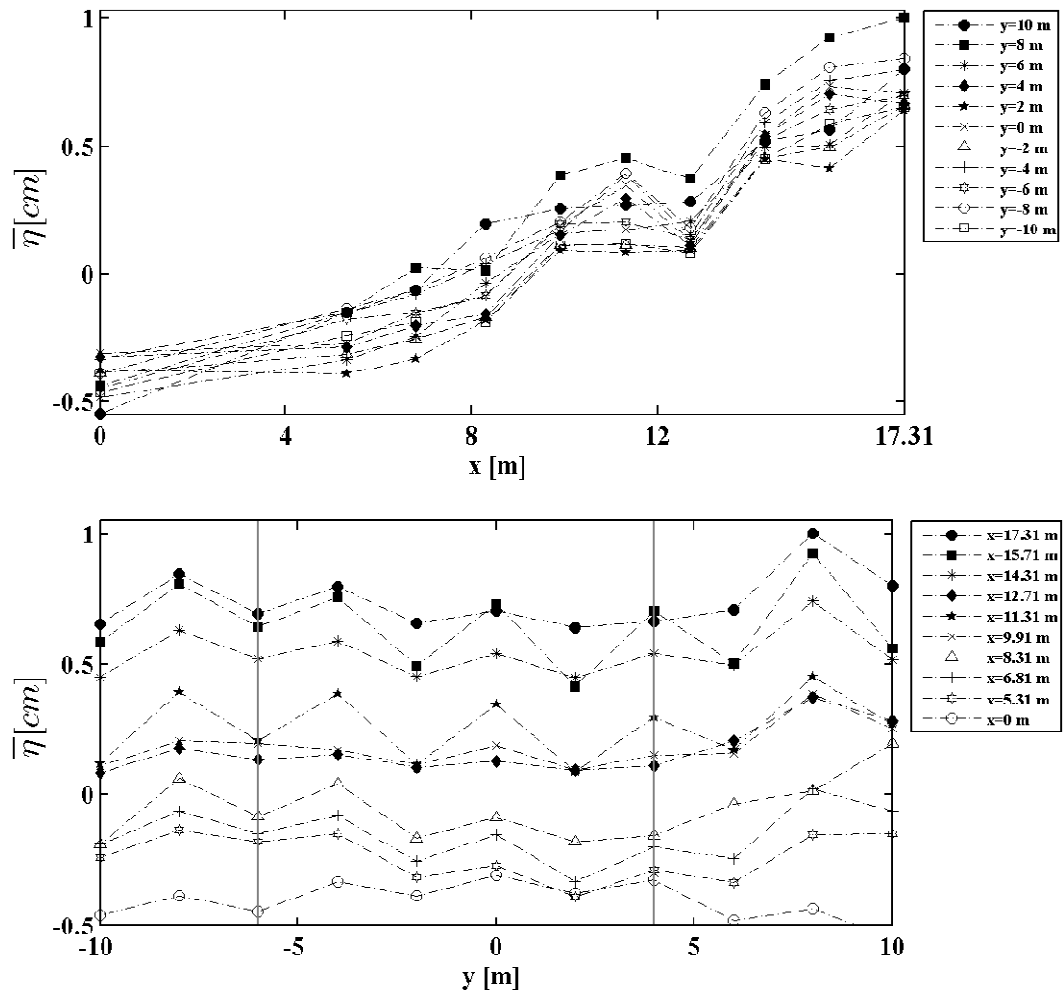


Fig. A-4. Cross-shore and longshore variations of wave setup for test BC1

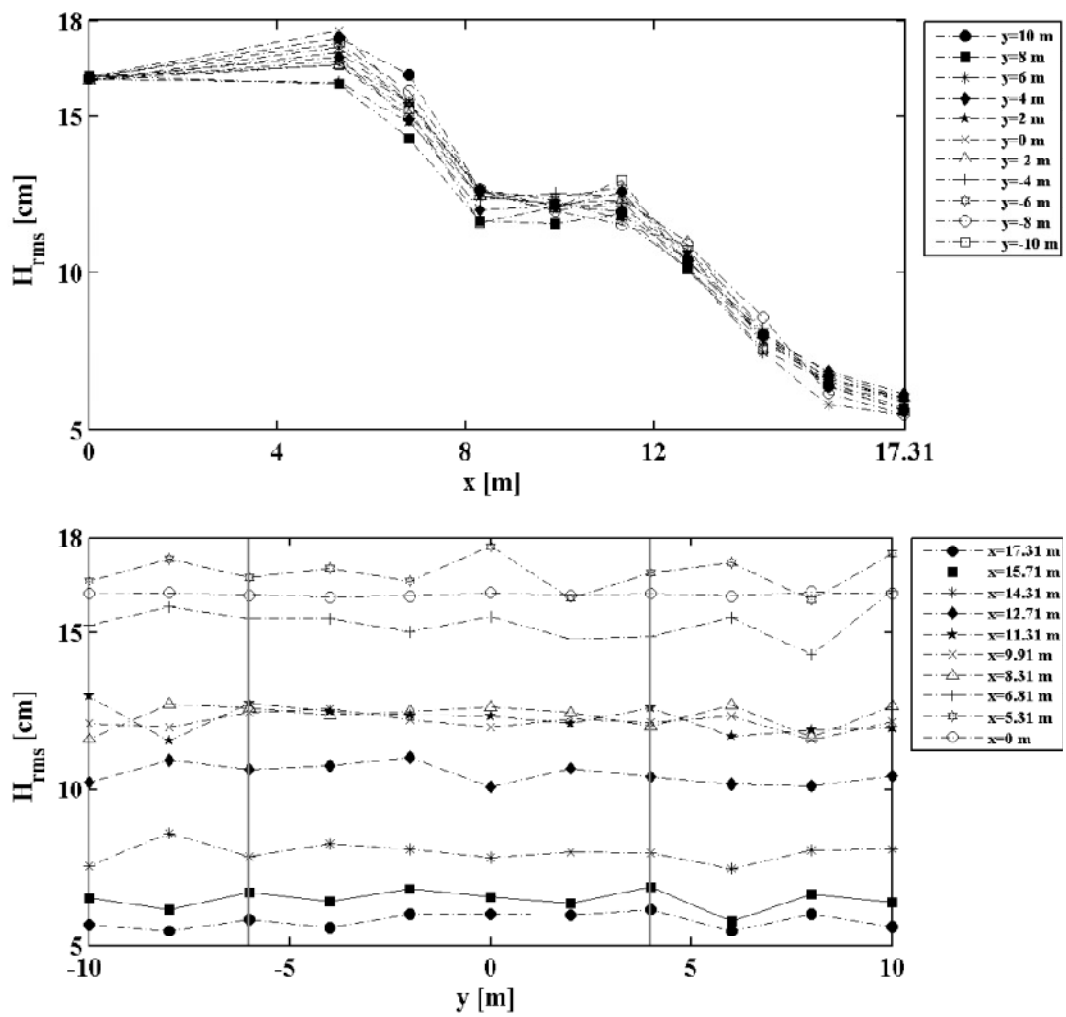


Fig. A-5. Cross-shore and longshore variations of *RMS* wave height for test BC1

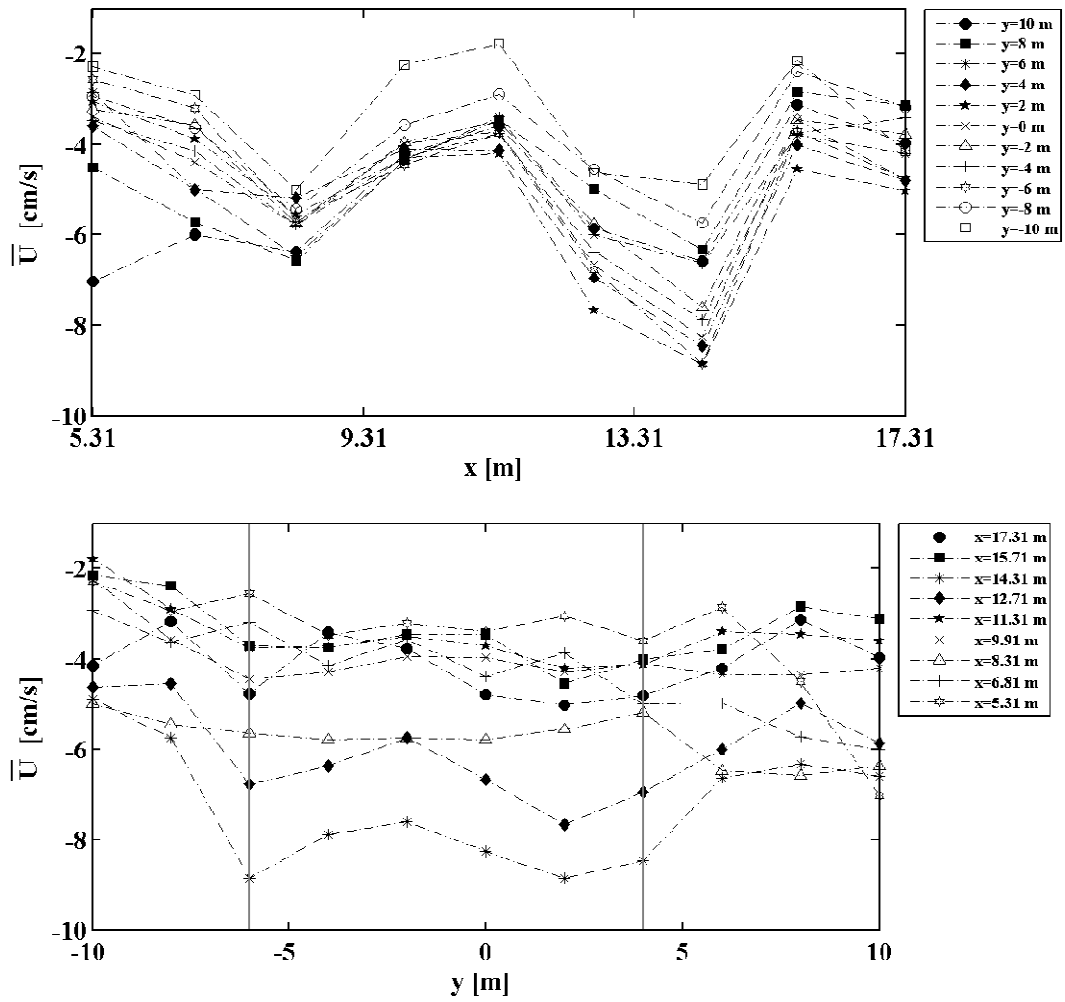


Fig. A-6. Cross-shore and longshore variations of mean cross-shore velocity for test BC1

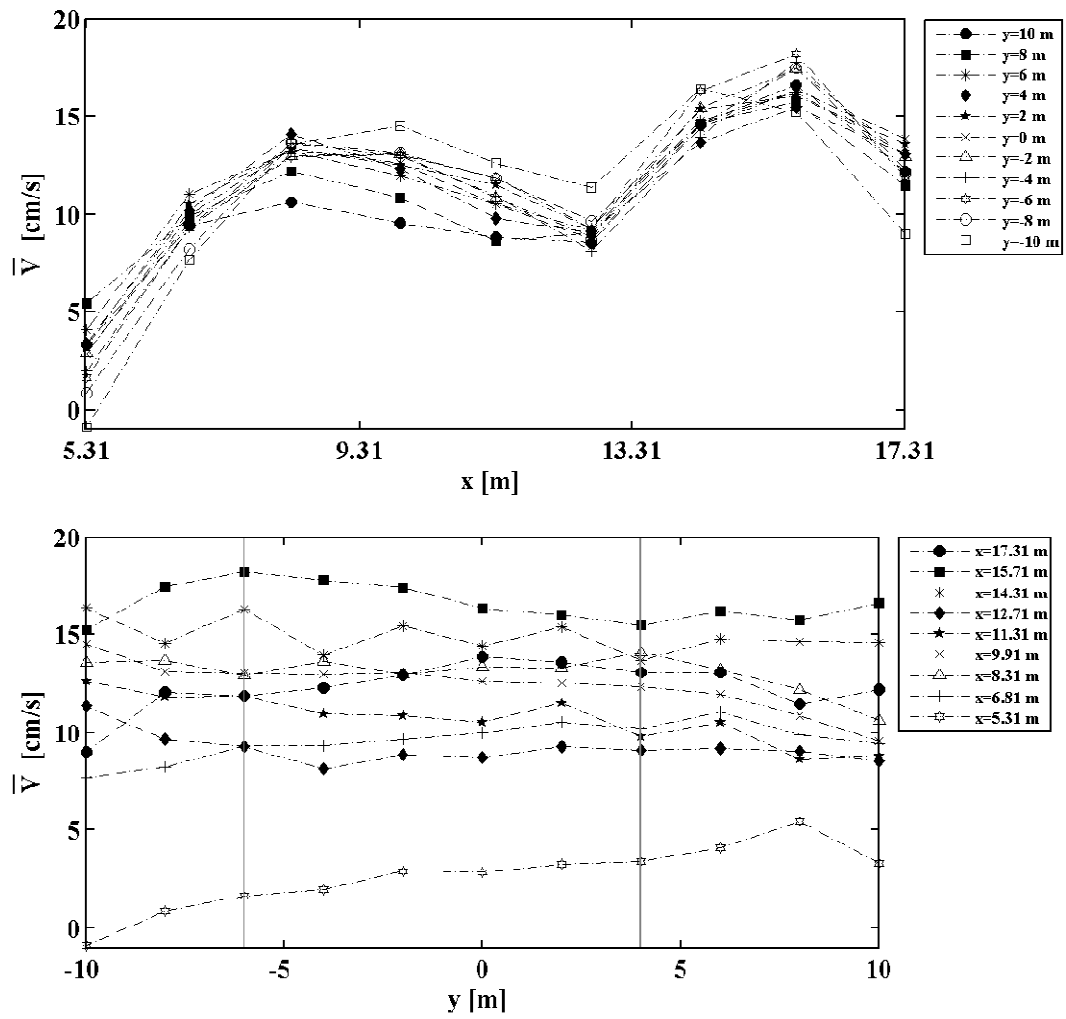


Fig. A-7. Cross-shore and longshore variations of mean longshore velocity for test BC1

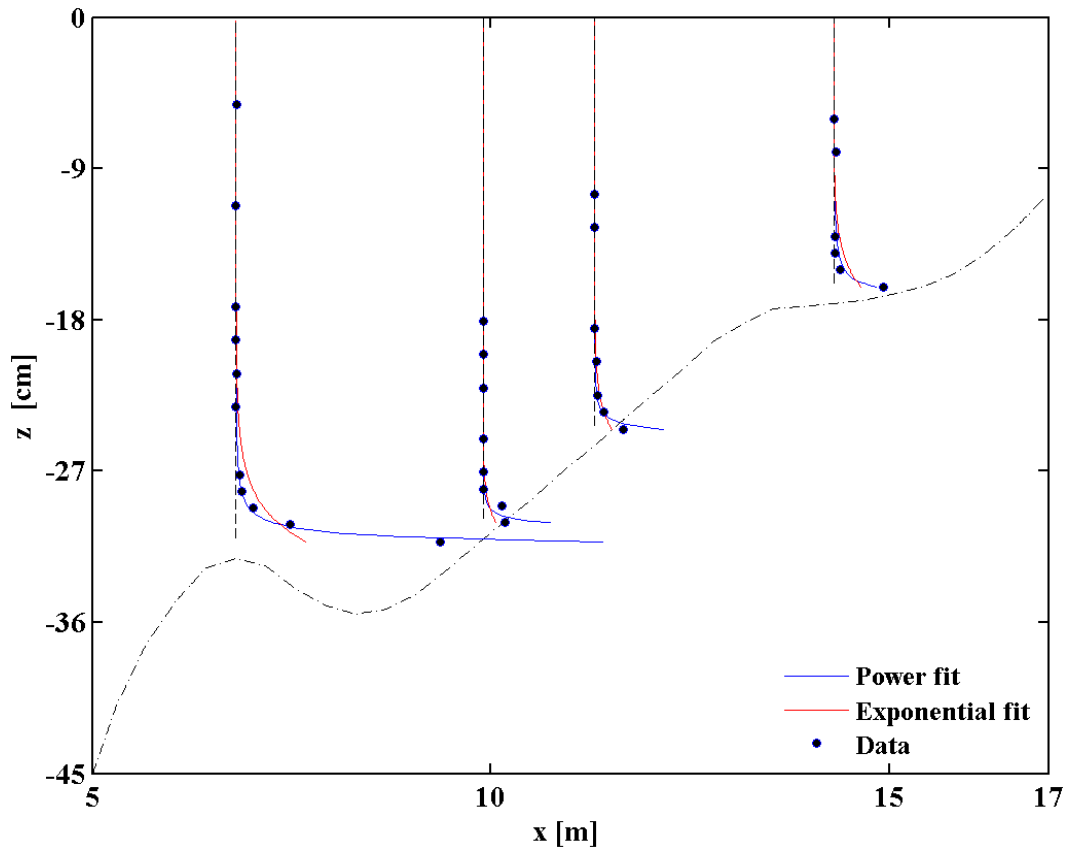


Fig. A-8. Sediment concentration data and power-form and exponential profiles at $y = 0$ for test BC1

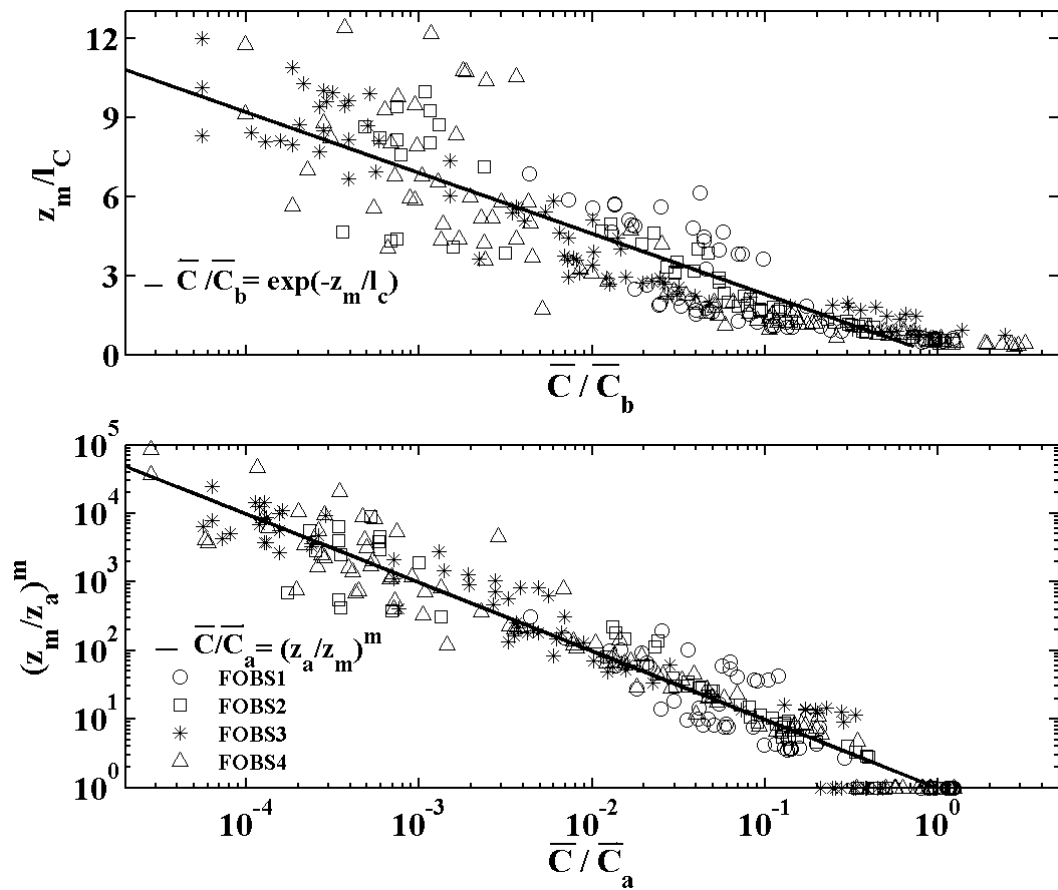


Fig. A-9. Vertical distributions of mean concentration \bar{c} using exponential and power-form profiles for each FOBS for test BC1

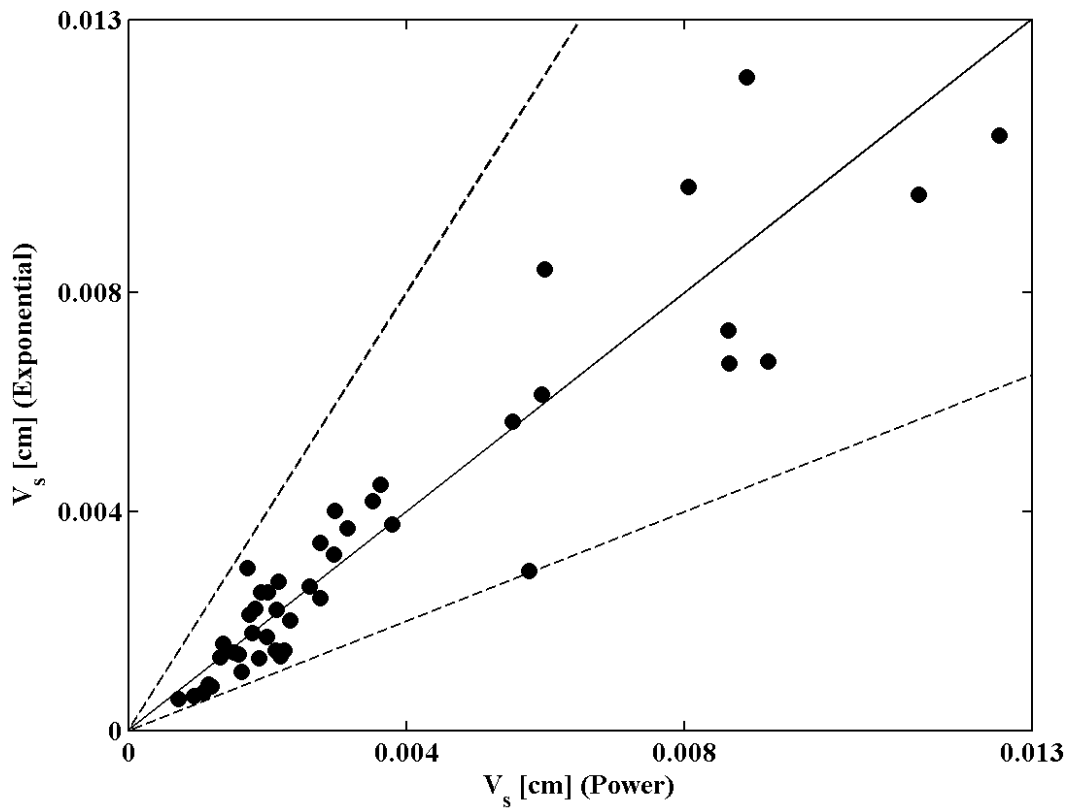


Fig. A-10. Comparison of suspended sediment volume per unit horizontal area using power-form and exponential profiles for all locations in test BC1

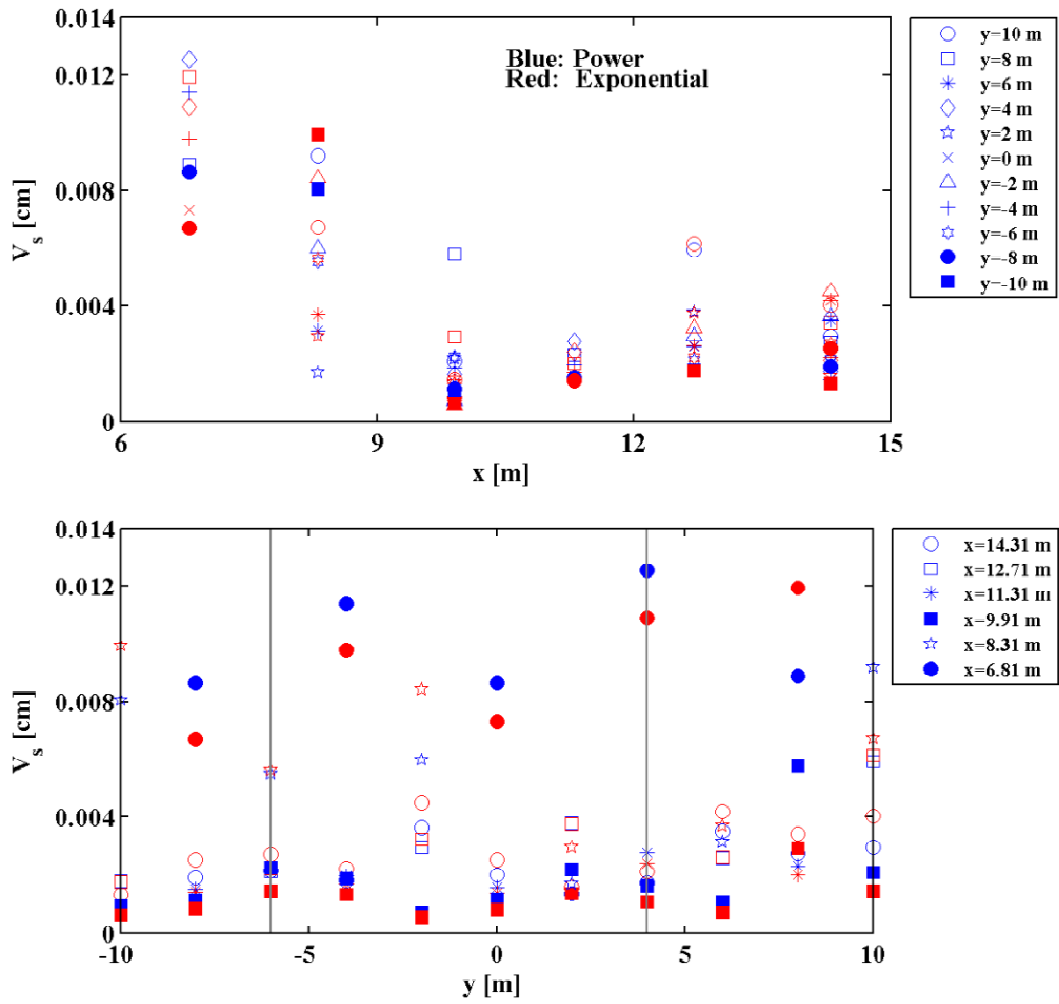


Fig. A-11. Cross-shore and longshore distributions of suspended sediment volume per unit horizontal area using power-form and exponential profiles at all locations for test BC1

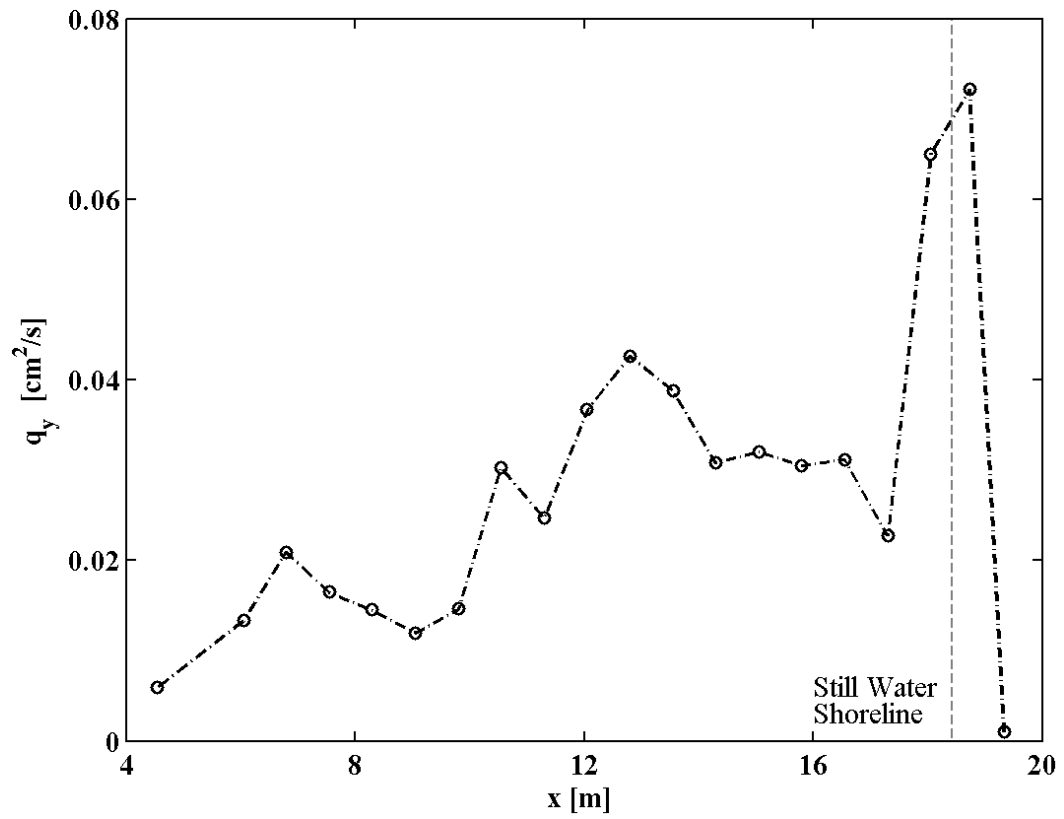


Fig. A-12. Cross-shore distribution of total longshore sediment transport rate q_y for test BC1

APPENDIX B

TEST BC2

Appendix B contains the tables and figures for test BC2.

Table B.1. Still water depth, wave setup, root-mean-square wave height and peak period at given cross-shore and longshore locations for test BC2

<i>y = 10 m</i>					<i>y = 8 m</i>				
<i>x (m)</i>	<i>d (cm)</i>	$\bar{\eta}$ (cm)	$H_{rms}(cm)$	T_p (s)	<i>x (m)</i>	<i>d (cm)</i>	$\bar{\eta}$ (cm)	$H_{rms}(cm)$	T_p (s)
0.00	90.00	-0.41	16.13	1.47	0.00	90.00	-0.40	16.22	1.47
5.31	39.13	-0.19	16.91	1.49	5.31	40.27	-0.25	16.21	1.47
6.81	32.07	-0.13	15.04	1.49	6.81	32.73	-0.15	13.91	1.57
8.31	35.40	-0.07	12.48	1.49	8.31	35.67	-0.21	11.99	1.58
9.91	31.59	-0.03	12.11	1.50	9.91	31.25	0.18	11.78	1.58
11.31	24.67	0.05	11.75	1.59	11.31	24.30	0.19	12.14	1.58
12.71	19.54	0.14	9.86	1.60	12.71	19.13	0.22	10.38	1.59
14.31	16.23	0.24	7.87	1.72	14.31	16.55	0.50	8.39	1.72
15.71	15.41	0.33	6.10	1.85	15.71	15.12	0.46	6.69	1.85
17.31	9.40	0.73	5.40	1.86	17.31	8.73	0.88	5.99	1.86

<i>y = 6 m</i>					<i>y = 4 m</i>				
<i>x (m)</i>	<i>d (cm)</i>	$\bar{\eta}$ (cm)	$H_{rms}(cm)$	T_p (s)	<i>x (m)</i>	<i>d (cm)</i>	$\bar{\eta}$ (cm)	$H_{rms}(cm)$	T_p (s)
0.00	90.00	-0.37	16.11	1.47	0.00	90.00	-0.30	16.25	1.48
5.31	41.40	-0.34	17.27	1.55	5.31	40.57	-0.38	16.64	1.46
6.81	33.40	-0.29	14.60	1.50	6.81	32.43	-0.28	14.23	1.48
8.31	35.93	-0.23	12.38	1.50	8.31	35.97	-0.42	12.22	1.42
9.91	30.91	0.06	11.96	1.49	9.91	31.02	0.01	12.28	1.48
11.31	23.93	0.01	11.85	1.56	11.31	24.47	-0.08	12.33	1.48
12.71	18.72	0.14	9.98	1.51	12.71	19.01	0.02	10.23	1.59
14.31	16.87	0.35	7.43	1.74	14.31	17.30	0.31	8.04	1.72
15.71	14.82	0.42	6.05	1.75	15.71	15.10	0.19	6.70	1.85
17.31	8.07	0.74	5.41	1.86	17.31	8.23	0.59	6.08	1.85

<i>y = 2 m</i>					<i>y = 0 m</i>				
<i>x (m)</i>	<i>d (cm)</i>	$\bar{\eta}$ (cm)	<i>H_{rms}(cm)</i>	<i>T_p (s)</i>	<i>x (m)</i>	<i>d (cm)</i>	$\bar{\eta}$ (cm)	<i>H_{rms}(cm)</i>	<i>T_p (s)</i>
0.00	90.00	-0.28	16.22	1.47	0.00	90.00	-0.30	16.30	1.47
5.31	39.73	-0.41	16.62	1.53	5.31	40.20	-0.39	17.76	1.49
6.81	31.47	-0.39	14.63	1.48	6.81	32.27	-0.24	14.78	1.49
8.31	36.00	-0.31	12.56	1.49	8.31	35.83	-0.55	12.17	1.57
9.91	31.12	0.04	11.95	1.57	9.91	31.36	NR	12.00	1.49
11.31	25.00	-0.05	12.17	1.57	11.31	25.17	-0.07	11.99	1.50
12.71	19.30	0.08	10.21	1.57	12.71	19.84	0.07	10.46	1.58
14.31	17.73	0.33	7.58	1.69	14.31	17.63	0.34	8.05	1.57
15.71	15.37	0.36	6.57	1.86	15.71	15.64	0.30	6.57	NR
17.31	8.40	0.70	5.72	1.88	17.31	8.90	0.68	5.88	1.88

<i>y = -2 m</i>					<i>y = -4 m</i>				
<i>x (m)</i>	<i>d (cm)</i>	$\bar{\eta}$ (cm)	<i>H_{rms}(cm)</i>	<i>T_p (s)</i>	<i>x (m)</i>	<i>d (cm)</i>	$\bar{\eta}$ (cm)	<i>H_{rms}(cm)</i>	<i>T_p (s)</i>
0.00	90.00	-0.29	16.28	1.46	0.00	90.00	-0.33	16.25	1.47
5.31	40.67	-0.31	16.59	1.52	5.31	40.97	-0.25	16.93	1.48
6.81	33.07	-0.33	14.10	1.56	6.81	32.67	-0.11	14.39	1.44
8.31	35.67	-0.27	12.57	1.42	8.31	35.77	-0.42	12.72	1.57
9.91	31.59	0.17	12.14	1.58	9.91	31.62	0.97	12.39	1.41
11.31	25.33	0.05	12.55	1.49	11.31	25.43	0.05	12.58	1.58
12.71	20.37	0.13	10.53	1.48	12.71	20.12	0.17	10.83	1.58
14.31	17.53	0.38	8.22	1.75	14.31	16.87	0.43	7.80	1.58
15.71	15.91	0.44	6.84	1.88	15.71	15.59	0.39	6.26	1.74
17.31	9.40	0.75	5.81	1.88	17.31	9.22	0.78	5.67	1.88

<i>y= -6 m</i>					<i>y= -8 m</i>				
<i>x (m)</i>	<i>d (cm)</i>	$\bar{\eta}$ (cm)	<i>H_{rms}(cm)</i>	<i>T_p (s)</i>	<i>x (m)</i>	<i>d (cm)</i>	$\bar{\eta}$ (cm)	<i>H_{rms}(cm)</i>	<i>T_p (s)</i>
0.00	90.00	-0.39	16.30	1.47	0.00	90.00	-0.39	16.14	1.46
5.31	41.27	-0.21	16.69	1.50	5.31	41.73	-0.25	17.20	1.50
6.81	32.27	-0.21	14.88	1.57	6.81	31.77	-0.15	14.57	1.48
8.31	35.87	-0.15	12.66	1.42	8.31	35.20	-0.37	12.70	1.56
9.91	31.66	0.20	12.51	1.58	9.91	31.26	NR	11.03	1.48
11.31	25.53	0.12	12.30	1.49	11.31	25.37	0.03	11.99	1.59
12.71	19.86	0.14	9.75	1.50	12.71	19.34	0.15	11.13	1.59
14.31	16.20	0.43	8.03	1.70	14.31	15.57	0.42	7.70	1.59
15.71	15.26	0.50	6.92	1.73	15.71	15.20	0.47	5.97	1.69
17.31	9.03	0.77	5.80	1.38	17.31	9.12	0.79	5.63	1.89

<i>y= -10 m</i>				
<i>x (m)</i>	<i>d (cm)</i>	$\bar{\eta}$ (cm)	<i>H_{rms}(cm)</i>	<i>T_p (s)</i>
0.00	90.00	-0.41	16.20	1.47
5.31	42.20	-0.31	16.34	1.50
6.81	31.27	-0.35	14.55	1.52
8.31	34.53	-0.24	11.50	1.51
9.91	30.86	0.06	12.79	1.57
11.31	25.20	-0.01	12.04	1.49
12.71	18.82	0.03	9.62	1.58
14.31	14.93	0.26	8.22	1.62
15.71	15.15	0.30	6.56	1.88
17.31	9.20	0.70	5.49	1.88

Table B.2. Still water depth, mean cross-shore and longshore velocity at given cross-shore and longshore locations for test BC2

x (m)	$y=10$ m			$y=8$ m		
	d (cm)	\bar{U} (cm/s)	\bar{V} (cm/s)	d (cm)	\bar{U} (cm/s)	\bar{V} (cm/s)
2.81	70.37	NR	1.37	72.17	-1.90	0.81
5.31	39.13	-2.98	6.73	40.27	-3.33	9.02
6.81	32.07	NR	13.99	32.73	NR	15.89
8.31	35.40	-1.19	20.70	35.67	-2.55	21.70
9.91	31.59	0.83	21.42	31.25	-0.24	21.86
11.31	24.67	1.43	18.42	24.30	-0.42	18.08
12.71	19.54	-2.96	17.67	19.13	-4.67	16.55
14.31	16.23	-3.72	23.63	16.55	-5.67	21.36
15.71	15.41	-1.47	26.42	15.12	-2.27	23.28
17.31	9.40	-3.56	21.04	8.73	-4.07	17.93

x (m)	$y=6$ m			$y=4$ m		
	d (cm)	\bar{U} (cm/s)	\bar{V} (cm/s)	d (cm)	\bar{U} (cm/s)	\bar{V} (cm/s)
2.81	73.97	-1.74	0.05	74.05	0.07	0.62
5.31	41.40	-3.03	9.44	40.57	-3.60	10.19
6.81	33.40	NR	16.82	32.43	NR	17.63
8.31	35.93	-3.38	22.67	35.97	-4.38	21.69
9.91	30.91	-2.16	20.94	31.02	-2.52	20.24
11.31	23.93	-1.92	16.97	24.47	-2.61	16.07
12.71	18.72	-5.83	16.06	19.01	-7.75	15.48
14.31	16.87	-5.74	21.50	17.30	-6.90	20.26
15.71	14.82	-2.47	23.52	15.10	-3.14	21.73
17.31	8.07	-3.35	17.16	8.23	-4.49	16.66

	<i>y= 2 m</i>			<i>y= 0 m</i>		
<i>x (m)</i>	<i>d (cm)</i>	\bar{U} (cm/s)	\bar{V} (cm/s)	<i>d (cm)</i>	\bar{U} (cm/s)	\bar{V} (cm/s)
2.81	74.13	-1.20	NR	73.97	-2.71	NR
5.31	39.73	-4.43	10.57	40.20	-4.27	10.34
6.81	31.47	NR	18.56	32.27	NR	18.49
8.31	36.00	-5.08	22.70	35.83	-5.67	22.21
9.91	31.12	-3.59	20.70	31.36	-3.71	20.12
11.31	25.00	-3.52	16.73	25.17	-3.65	16.26
12.71	19.30	-7.62	16.23	19.84	-8.22	15.68
14.31	17.73	-7.49	21.06	17.63	-6.89	20.46
15.71	15.37	-3.39	22.48	15.64	-3.50	22.25
17.31	8.40	-4.27	15.61	8.90	-3.26	14.66

	<i>y= -2 m</i>			<i>y= -4 m</i>		
<i>x (m)</i>	<i>d (cm)</i>	\bar{U} (cm/s)	\bar{V} (cm/s)	<i>d (cm)</i>	\bar{U} (cm/s)	\bar{V} (cm/s)
2.81	73.81	-1.95	NR	73.24	-2.03	NR
5.31	40.67	-4.49	10.25	40.97	-4.34	10.39
6.81	33.07	NR	19.16	32.67	NR	19.40
8.31	35.67	-5.45	23.42	35.77	-5.94	22.69
9.91	31.59	-4.08	20.63	31.62	-3.83	20.32
11.31	25.33	-3.55	16.97	25.43	-3.61	16.87
12.71	20.37	-7.16	16.77	20.12	-7.19	15.58
14.31	17.53	-7.75	20.89	16.87	-7.08	19.98
15.71	15.91	-3.69	22.08	15.59	-3.89	23.86
17.31	9.40	-4.30	15.57	9.22	-3.83	17.68

	<i>y= -6 m</i>			<i>y= -8 m</i>		
<i>x (m)</i>	<i>d (cm)</i>	\bar{U} (cm/s)	\bar{V} (cm/s)	<i>d (cm)</i>	\bar{U} (cm/s)	\bar{V} (cm/s)
2.81	72.66	-2.65	NR	72.42	-1.73	NR
5.31	41.27	-4.81	9.60	41.73	-4.24	9.40
6.81	32.27	NR	19.14	31.77	NR	18.83
8.31	35.87	-5.73	23.67	35.20	-5.60	23.44
9.91	31.66	-4.25	20.68	31.26	-4.94	20.67
11.31	25.53	-3.94	17.22	25.37	-3.45	17.44
12.71	19.86	-8.90	18.56	19.34	-6.60	17.58
14.31	16.20	-8.81	21.20	15.57	-6.01	22.89
15.71	15.26	-4.08	23.10	15.20	-3.02	24.93
17.31	9.03	-4.33	16.01	9.12	-3.78	17.70

	<i>y= -10 m</i>		
<i>x (m)</i>	<i>d (cm)</i>	\bar{U} (cm/s)	\bar{V} (cm/s)
2.81	72.17	NR	NR
5.31	42.20	-4.24	8.12
6.81	31.27	NR	18.81
8.31	34.53	-6.83	24.89
9.91	30.86	-3.73	21.91
11.31	25.20	-3.73	18.55
12.71	18.82	-9.78	21.06
14.31	14.93	-7.62	22.65
15.71	15.15	-3.85	23.92
17.31	9.20	-3.72	15.56

Table B.2. Mean water depth, fitted profile coefficients, suspended sediment volume per unit horizontal area and correlation coefficient at given cross-shore and longshore locations for test BC2

<i>y=10 m</i>		<i>Exponential</i>				<i>Power</i>			
<i>x (m)</i>	\bar{h} (cm)	c_b (g/l)	l_c (cm)	V_s (cm)	<i>CC</i>	c_a (g/l)	<i>m</i>	V_s (cm)	<i>CC</i>
6.81	31.94	17.43	1.84	0.0070	0.98	30.75	2.80	0.0065	0.87
9.91	31.57	5.17	1.44	0.0014	0.97	14.58	3.52	0.0022	0.85
11.31	24.72	7.59	1.88	0.0032	0.90	16.38	2.87	0.0033	1.00
14.31	16.47	33.73	0.76	0.0026	0.98	15.94	3.51	0.0024	1.00

<i>y=8 m</i>		<i>Exponential</i>				<i>Power</i>			
<i>x (m)</i>	\bar{h} (cm)	c_b (g/l)	l_c (cm)	V_s (cm)	<i>CC</i>	c_a (g/l)	<i>m</i>	V_s (cm)	<i>CC</i>
8.31	35.45	2.47	3.63	0.0026	0.76	10.49	2.66	0.0024	1.00
9.91	31.43	2.39	1.42	0.0006	0.97	3.74	2.95	0.0007	0.86
12.71	19.36	40.89	0.86	0.0041	0.99	38.53	3.88	0.0051	1.00
14.31	17.05	21.12	0.91	0.0024	0.97	12.06	3.04	0.0022	1.00

<i>y=6 m</i>		<i>Exponential</i>				<i>Power</i>			
<i>x (m)</i>	\bar{h} (cm)	c_b (g/l)	l_c (cm)	V_s (cm)	<i>CC</i>	c_a (g/l)	<i>m</i>	V_s (cm)	<i>CC</i>
6.81	33.11	19.09	1.77	0.0073	0.93	51.06	3.24	0.0087	0.99
9.91	30.96	1.91	1.50	0.0006	0.97	4.54	3.26	0.0008	0.87
11.31	23.94	9.08	1.46	0.0025	0.97	18.69	3.45	0.0029	0.98
14.31	17.21	21.40	0.87	0.0022	0.98	17.25	3.61	0.0025	1.00

<i>y=4 m</i>		<i>Exponential</i>				<i>Power</i>			
<i>x (m)</i>	\bar{h} (cm)	<i>c_b (g/l)</i>	<i>l_c (cm)</i>	<i>V_s (cm)</i>	<i>CC</i>	<i>c_a (g/l)</i>	<i>m</i>	<i>V_s (cm)</i>	<i>CC</i>
8.31	35.55	3.93	3.36	0.0037	0.88	18.56	2.85	0.0038	1.00
9.91	31.03	3.07	1.23	0.0006	0.94	6.13	3.73	0.0009	0.79
12.71	19.03	18.67	1.02	0.0027	0.99	17.77	3.25	0.0030	0.99
14.31	17.61	9.08	1.02	0.0013	0.96	6.15	2.84	0.0013	0.99

<i>y=2 m</i>		<i>Exponential</i>				<i>Power</i>			
<i>x (m)</i>	\bar{h} (cm)	<i>c_b (g/l)</i>	<i>l_c (cm)</i>	<i>V_s (cm)</i>	<i>CC</i>	<i>c_a (g/l)</i>	<i>m</i>	<i>V_s (cm)</i>	<i>CC</i>
6.81	31.07	5.76	2.36	0.0034	0.89	12.18	2.50	0.0031	0.99
9.91	31.16	1.93	1.19	0.0004	0.96	3.36	3.57	0.0005	0.84
11.31	24.95	12.23	1.37	0.0030	0.98	25.15	3.64	0.0036	0.97
14.31	18.06	16.83	0.87	0.0018	0.98	14.22	3.65	0.0020	1.00

<i>y=0 m</i>		<i>Exponential</i>				<i>Power</i>			
<i>x (m)</i>	\bar{h} (cm)	<i>c_b (g/l)</i>	<i>l_c (cm)</i>	<i>V_s (cm)</i>	<i>CC</i>	<i>c_a (g/l)</i>	<i>m</i>	<i>V_s (cm)</i>	<i>CC</i>
8.31	35.29	37.68	0.75	0.0028	0.99	16.65	3.33	0.0027	1.00
9.91	32.18	1.31	1.53	0.0004	0.96	2.41	3.05	0.0004	0.86
12.71	19.91	8.21	1.19	0.0016	0.99	7.86	2.78	0.0017	0.97
14.31	17.97	20.72	0.86	0.0021	0.97	11.50	3.23	0.0020	1.00

<i>y=-2 m</i>		<i>Exponential</i>				<i>Power</i>			
<i>x (m)</i>	\bar{h} (cm)	<i>c_b (g/l)</i>	<i>l_c (cm)</i>	<i>V_s (cm)</i>	<i>CC</i>	<i>c_a (g/l)</i>	<i>m</i>	<i>V_s (cm)</i>	<i>CC</i>
6.81	32.73	17.66	1.55	0.0054	0.94	21.46	2.88	0.0043	1.00
9.91	31.75	3.12	1.39	0.0008	0.96	7.90	3.55	0.0012	0.84
11.31	25.39	4.98	1.54	0.0015	0.96	10.09	3.28	0.0017	0.98
14.31	17.91	15.43	0.91	0.0018	0.97	8.49	3.03	0.0016	1.00

<i>y=-4 m</i>		<i>Exponential</i>				<i>Power</i>			
<i>x (m)</i>	\bar{h} (cm)	<i>c_b (g/l)</i>	<i>l_c (cm)</i>	<i>V_s (cm)</i>	<i>CC</i>	<i>c_a (g/l)</i>	<i>m</i>	<i>V_s (cm)</i>	<i>CC</i>
8.31	35.35	3.85	2.95	0.0031	0.79	10.01	2.68	0.0023	1.00
9.91	32.60	2.79	1.40	0.0007	0.93	3.57	2.95	0.0007	0.79
12.71	20.29	8.71	1.50	0.0025	0.98	11.29	2.80	0.0024	0.98
14.31	17.30	15.43	0.91	0.0018	0.97	8.49	3.03	0.0016	1.00

<i>y=-6 m</i>		<i>Exponential</i>				<i>Power</i>			
<i>x (m)</i>	\bar{h} (cm)	<i>c_b (g/l)</i>	<i>l_c (cm)</i>	<i>V_s (cm)</i>	<i>CC</i>	<i>c_a (g/l)</i>	<i>m</i>	<i>V_s (cm)</i>	<i>CC</i>
6.81	32.06	11.11	2.26	0.0061	0.87	28.89	2.64	0.0066	1.00
9.91	31.87	1.22	1.68	0.0004	0.97	2.12	2.85	0.0004	0.88
11.31	25.65	2.87	1.65	0.0010	0.95	6.66	3.17	0.0012	0.99
14.31	16.63	20.20	0.80	0.0018	0.98	6.23	2.64	0.0014	1.00

<i>y=-8 m</i>		<i>Exponential</i>				<i>Power</i>			
<i>x (m)</i>	\bar{h} (cm)	<i>c_b (g/l)</i>	<i>l_c (cm)</i>	<i>V_s (cm)</i>	<i>CC</i>	<i>c_a (g/l)</i>	<i>m</i>	<i>V_s (cm)</i>	<i>CC</i>
8.31	34.83	4.20	2.74	0.0030	0.83	13.62	2.99	0.0026	1.00
9.91	32.24	0.67	1.67	0.0002	0.99	1.17	2.84	0.0002	0.92
12.71	19.49	16.28	1.34	0.0039	0.93	23.95	3.21	0.0041	1.00
14.31	15.99	8.59	1.17	0.0016	0.93	5.06	2.29	0.0014	0.99

<i>y=-10 m</i>		<i>Exponential</i>				<i>Power</i>			
<i>x (m)</i>	\bar{h} (cm)	<i>c_b (g/l)</i>	<i>l_c (cm)</i>	<i>V_s (cm)</i>	<i>CC</i>	<i>c_a (g/l)</i>	<i>m</i>	<i>V_s (cm)</i>	<i>CC</i>
6.81	30.91	7.93	2.34	0.0046	0.88	19.09	2.52	0.0047	1.00
9.91	30.92	6.36	1.23	0.0013	0.99	15.69	3.89	0.0021	0.96
11.31	25.19	5.75	1.50	0.0017	0.96	13.00	3.43	0.0020	0.98
14.31	15.19	30.01	0.77	0.0024	0.98	9.56	2.84	0.0020	1.00

Table B. 4. Coefficients a and b corresponding to wave setup longshore gradient and correlation coefficient CC between data and fitted line at given cross-shore location for tests BC2

x	a	b	CC
0	8.71E-05	-0.0031	0.79
5.31	-0.00021	-0.0035	0.93
6.81	-0.00016	-0.0028	0.59
8.31	-0.00018	-0.0037	0.50
9.91	-4.42E-04	0.0032	0.40
11.31	-1.97E-04	-0.0001	0.93
12.71	-1.34E-04	0.0009	0.90
14.31	-1.37E-04	0.0036	0.97
15.71	-2.60E-04	0.0034	0.89
17.31	-1.76E-04	0.0069	0.90

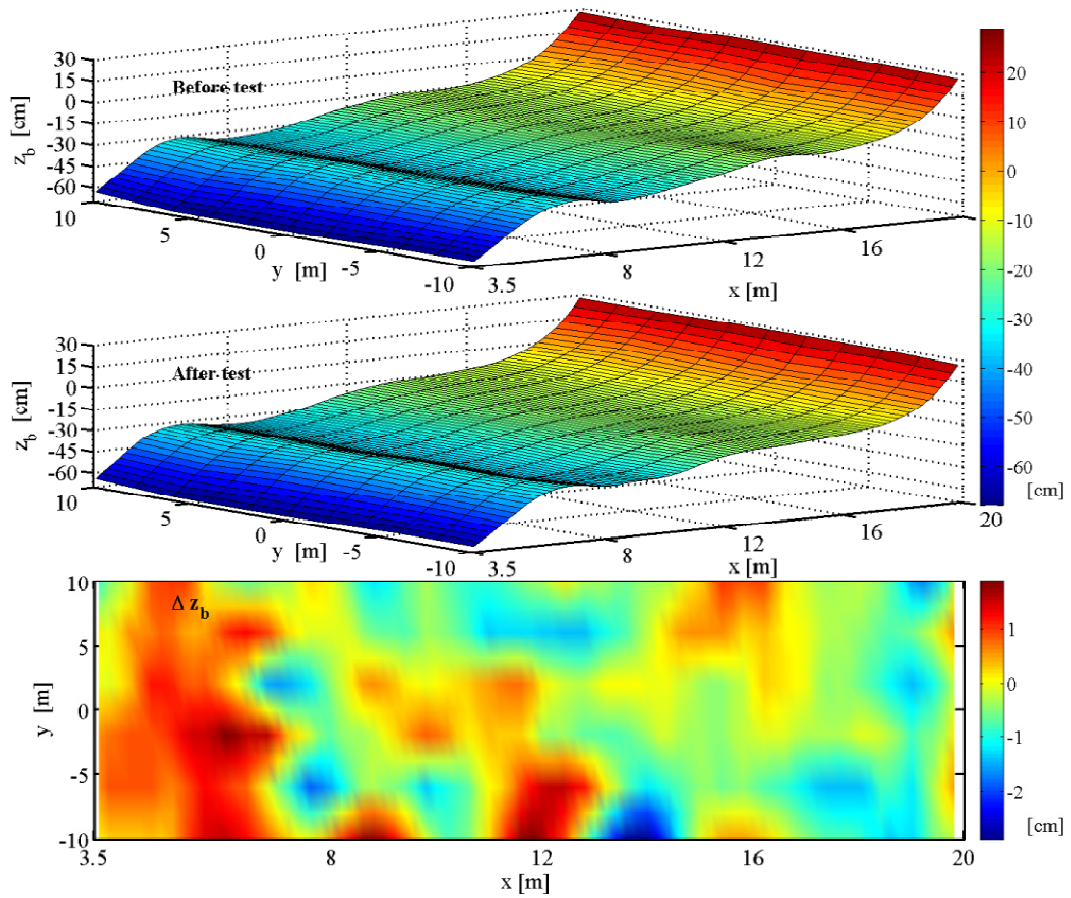


Fig. B-1. Measured initial and final profiles and change in bottom elevation for test BC2

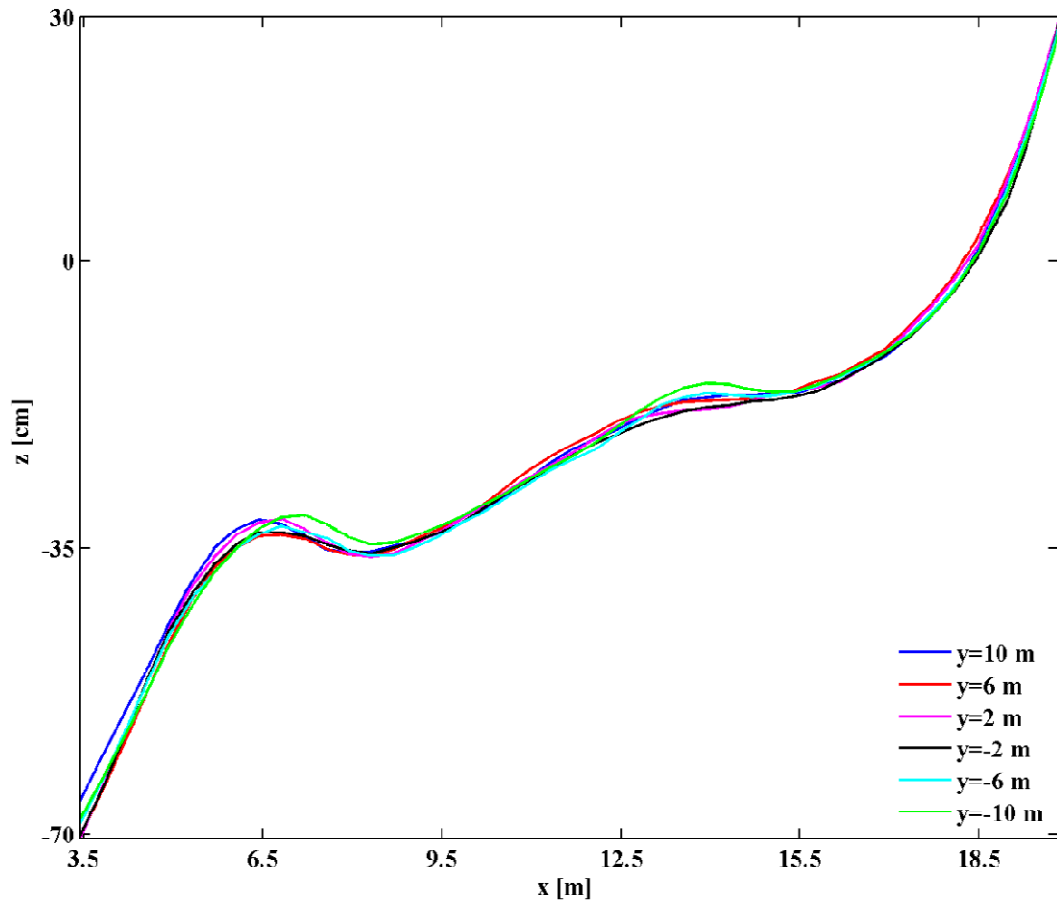


Fig. B-2. Measured initial cross-shore profiles for test BC2

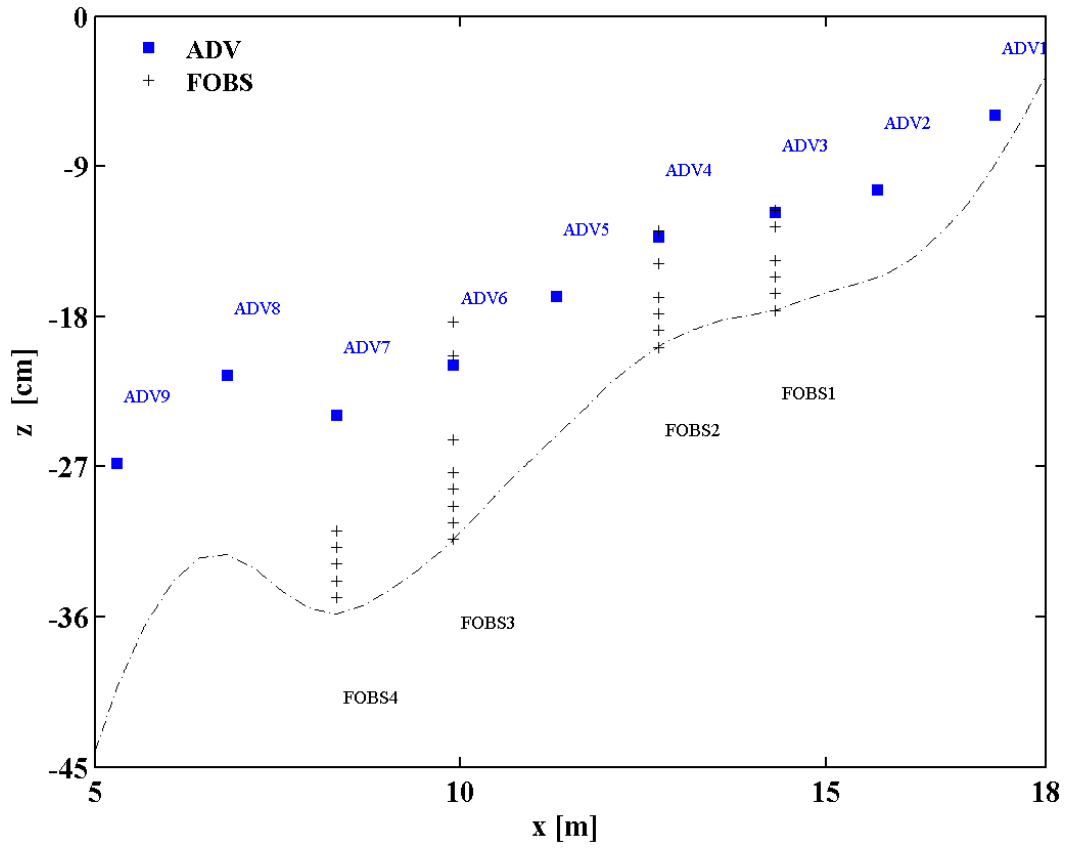


Fig. B-3. Cross-shore positioning of ADVs and FOBS at $y = 0$ for test BC2

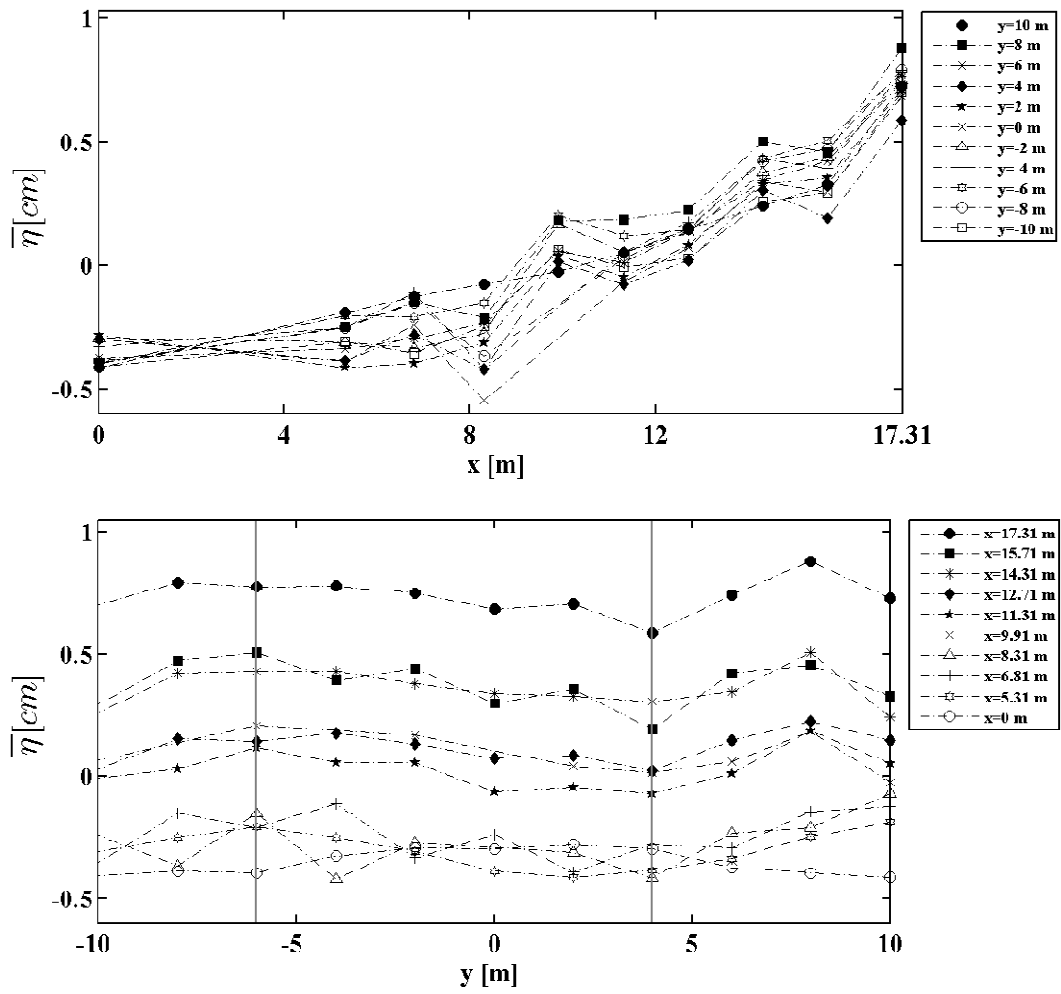


Fig. B-4. Cross-shore and longshore variations of wave setup for test BC2

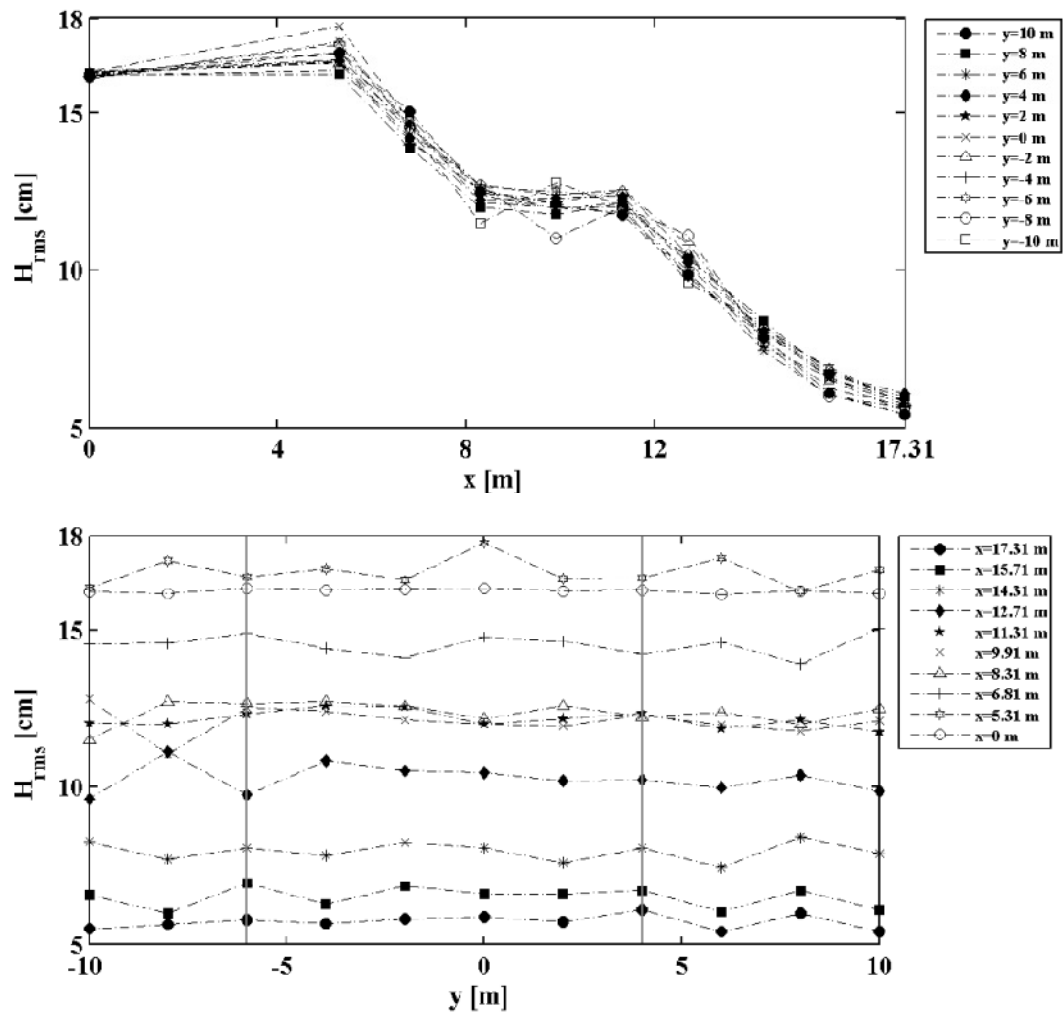


Fig. B-5. Cross-shore and longshore variations of *RMS* wave height for test BC2

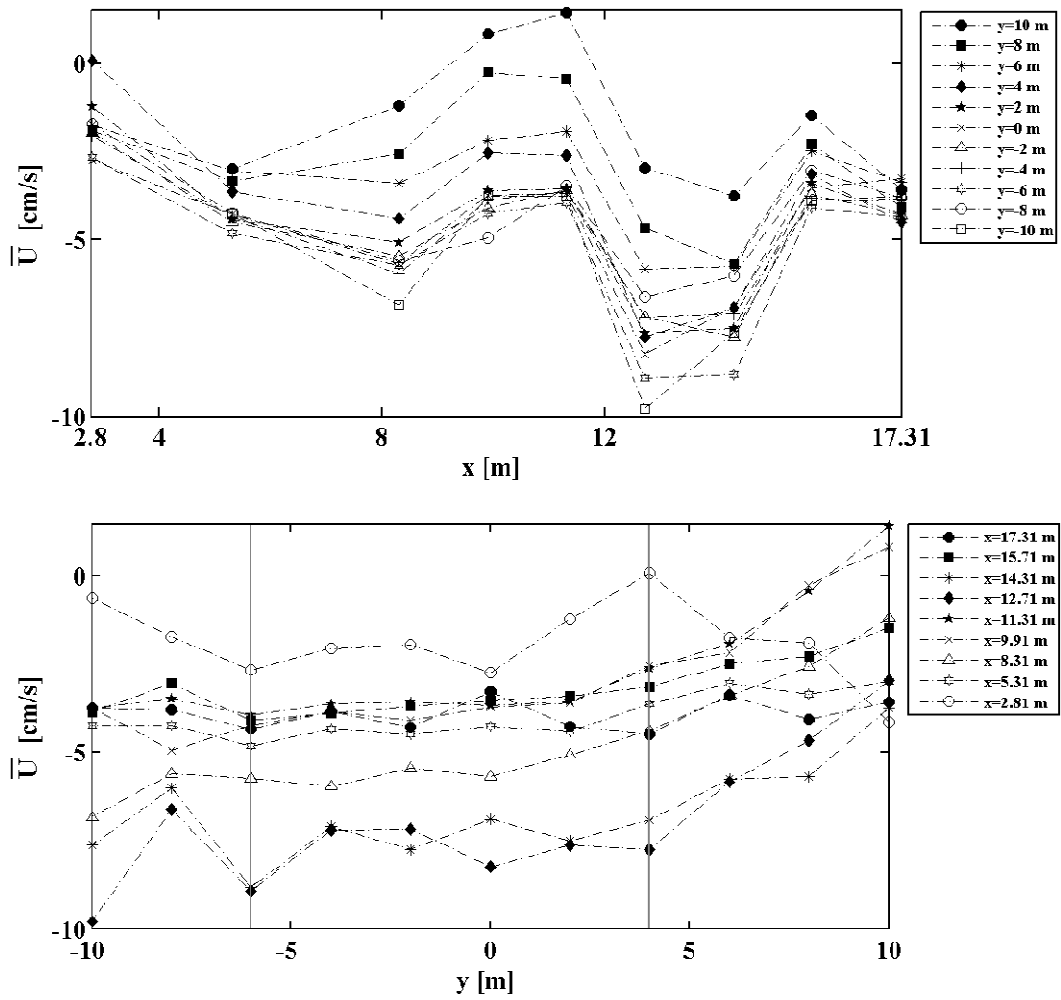


Fig. B-6. Cross-shore and longshore variations of mean cross-shore velocity for test BC2

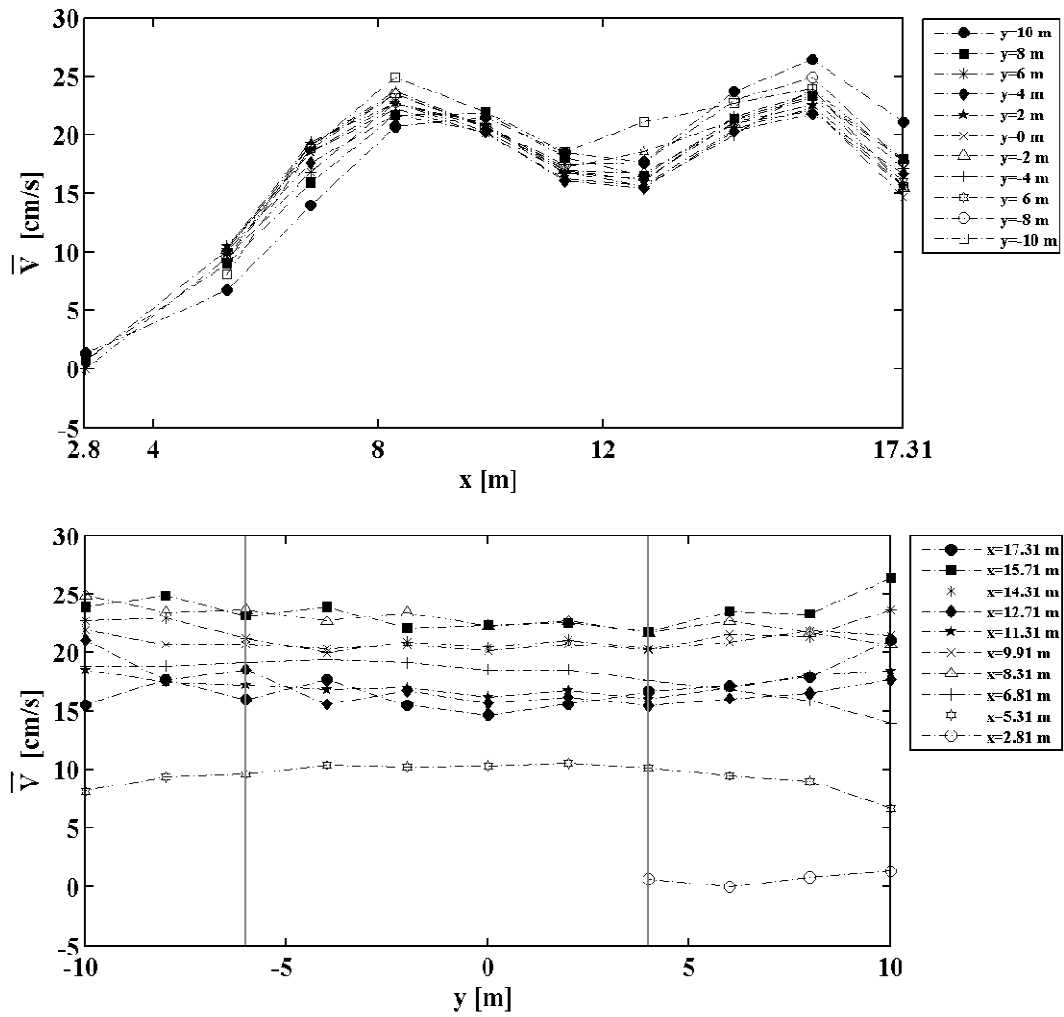


Fig. B-7. Cross-shore and longshore variations of mean longshore velocity for test BC2

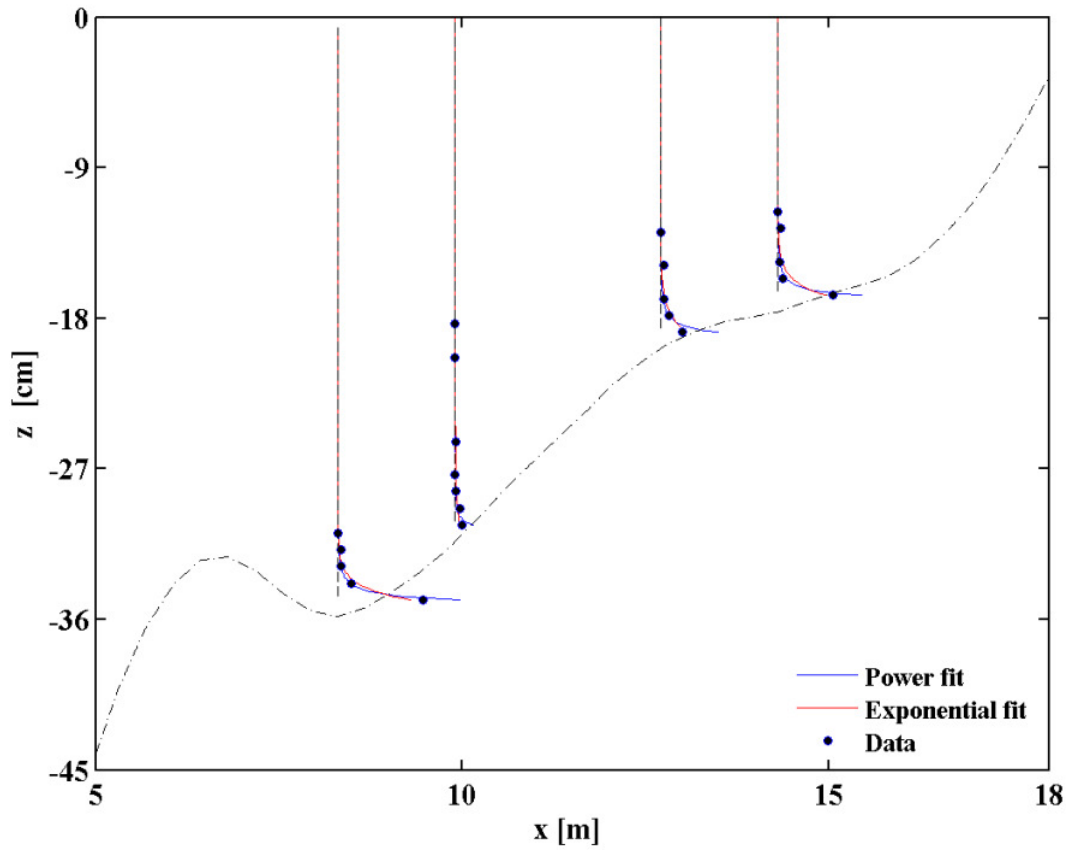


Fig. B- 8. Sediment concentration data and power-form and exponential profiles at $y = 0$ for test BC2

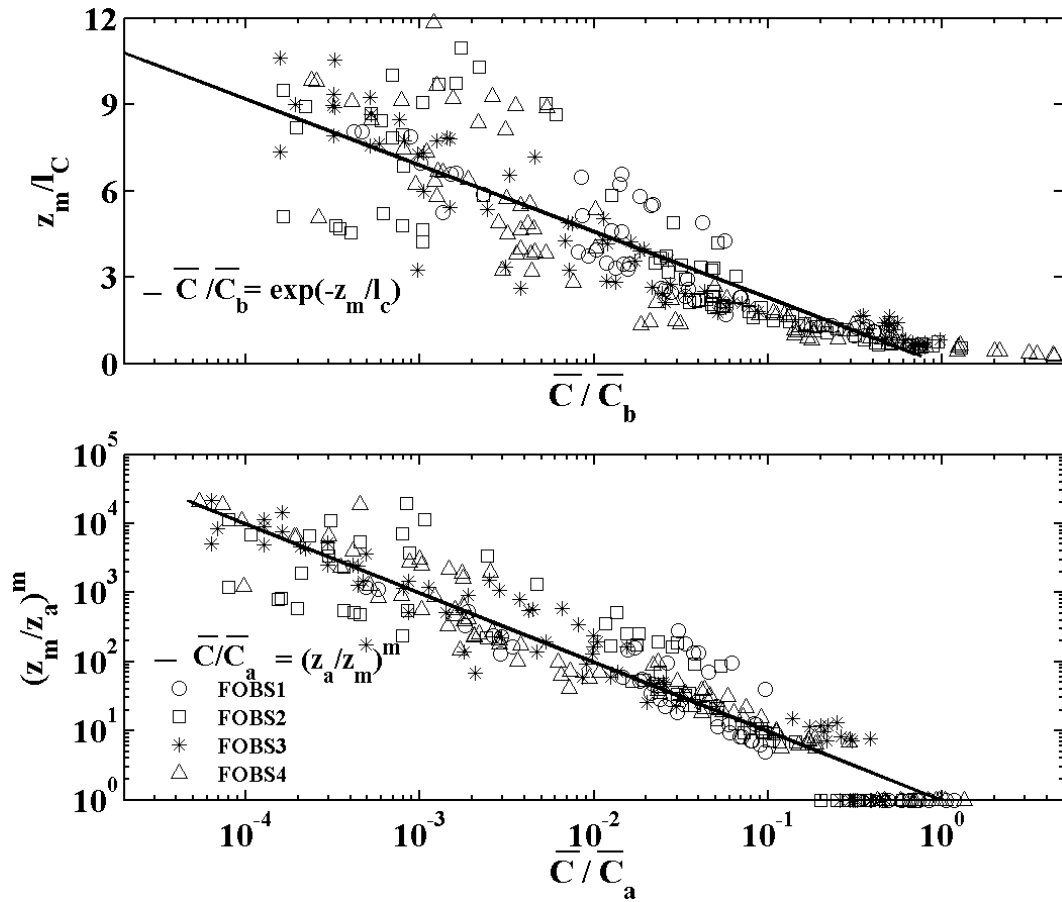


Fig. B-9. Vertical distributions of mean concentration \bar{C} using exponential and power-form profiles for each FOBS for test BC2

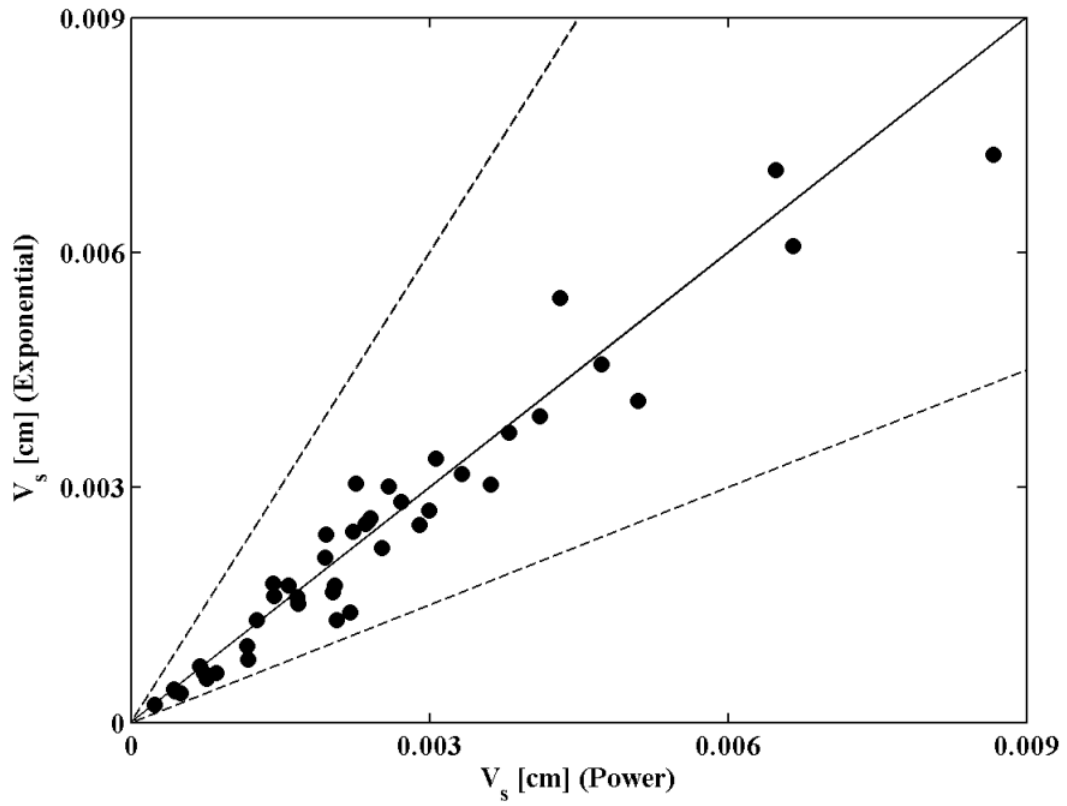


Fig. B- 10. Comparison of suspended sediment volume per unit horizontal area using power-form and exponential profiles for all locations in test BC2

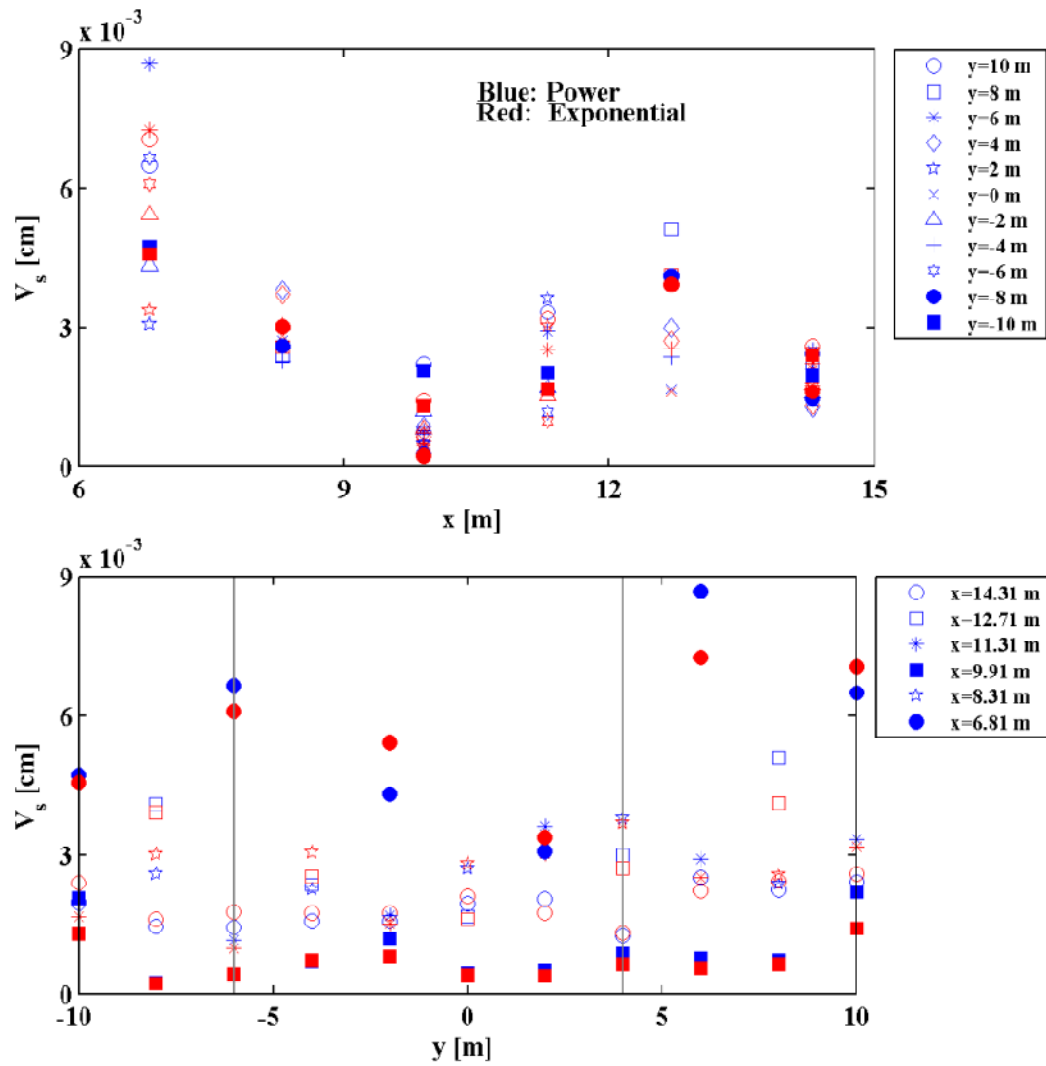


Fig. B-11. Cross-shore and longshore distributions of suspended sediment volume per unit horizontal area using power-form and exponential profiles at all locations for test BC2

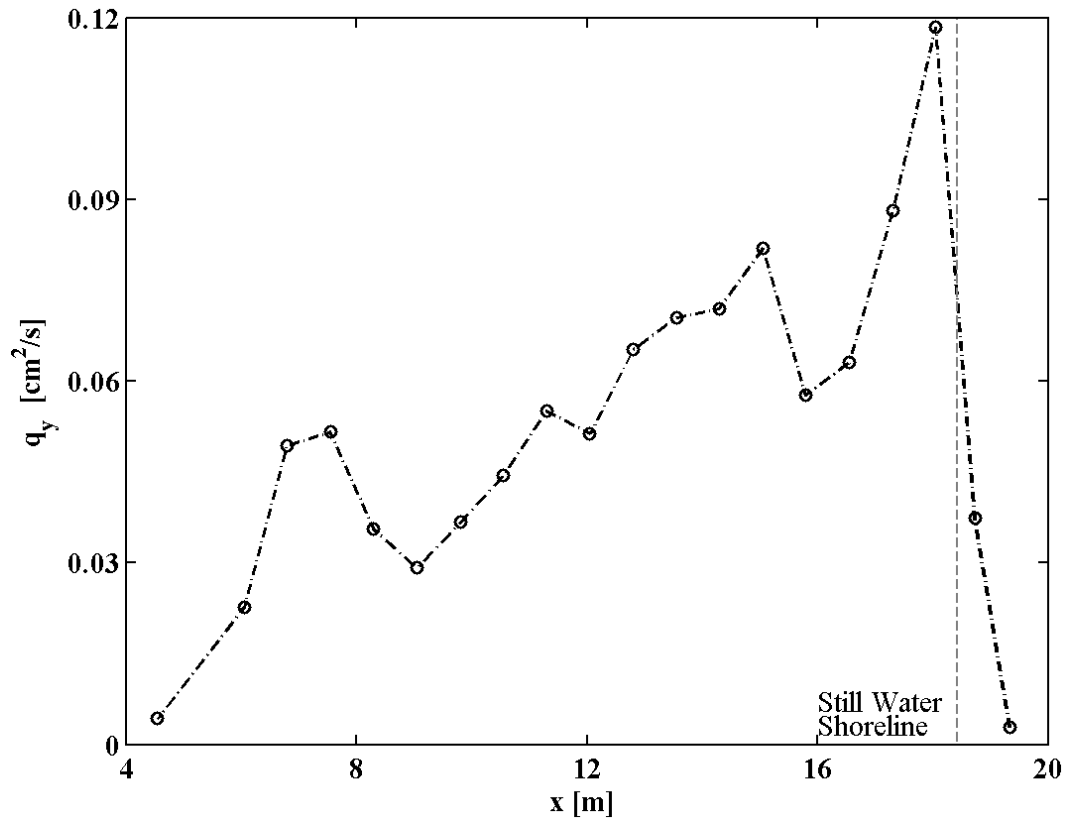


Fig. B-12. Cross-shore distribution of total longshore sediment transport rate q_y for test BC2

APPENDIX C

TEST BC3

Appendix C contains the tables and figures for test BC3.

Table C.1. Still water depth, wave setup, root-mean-square wave height and peak period at given cross-shore and longshore locations for test BC3

<i>y= 10 m</i>					<i>y= 8 m (interpolated)</i>				
<i>x (m)</i>	<i>d (cm)</i>	$\bar{\eta}$ (cm)	H_{rms} (cm)	T_p (s)	<i>x (m)</i>	<i>d (cm)</i>	$\bar{\eta}$ (cm)	H_{rms} (cm)	T_p (s)
0.00	90.00	-0.33	0.03	0.57	0.00	90.00	-0.25	0.02	0.58
5.31	42.54	-0.15	0.07	0.83	5.31	42.28	-0.17	0.06	0.71
6.81	31.93	0.16	0.09	1.07	6.81	32.59	0.19	0.07	1.69
8.31	34.67	-0.11	0.03	0.70	8.31	35.32	-0.13	0.04	0.91
9.91	30.72	-0.20	0.18	1.12	9.91	30.58	-0.15	0.11	0.96
11.31	23.87	-0.34	0.07	0.64	11.31	24.90	-0.23	0.06	0.73
12.71	18.04	0.02	0.08	0.65	12.71	18.29	-0.03	0.07	0.68
14.31	15.10	0.24	0.05	0.54	14.31	15.33	0.11	0.04	0.52
15.13	14.60	-0.11	0.08	2.78	15.13	15.13	-0.05	0.06	1.71
16.23	13.17	-0.52	0.06	0.67	16.23	12.07	-0.40	0.04	0.68
17.31	8.44	0.11	0.06	0.83	17.31	8.32	0.04	0.05	0.73

<i>y = 6 m</i>					<i>y = 4 m</i>				
<i>x (m)</i>	<i>d (cm)</i>	$\bar{\eta}$ (cm)	H_{rms} (cm)	T_p (s)	<i>x (m)</i>	<i>d (cm)</i>	$\bar{\eta}$ (cm)	H_{rms} (cm)	T_p (s)
0.00	90.00	-0.18	0.02	0.59	0.00	90.00	-0.24	0.03	0.69
5.31	42.12	-0.19	0.05	0.58	5.31	43.20	-0.30	0.05	0.58
6.81	33.31	0.21	0.05	2.30	6.81	33.00	-0.18	0.07	2.90
8.31	35.20	-0.14	0.06	1.12	8.31	34.93	-0.18	0.06	0.64
9.91	30.66	-0.09	0.05	0.80	9.91	29.66	-0.31	0.10	1.61
11.31	25.80	-0.13	0.06	0.83	11.31	24.73	-0.44	0.05	0.61
12.71	18.99	-0.08	0.05	0.72	12.71	20.20	-0.16	0.05	0.73
14.31	16.27	-0.02	0.03	0.50	14.31	16.40	0.07	0.03	0.55
15.13	15.13	0.00	0.05	0.63	15.13	16.00	-0.20	0.05	0.66
16.23	11.77	-0.28	0.02	0.69	16.23	12.43	-0.54	0.03	0.71
17.31	7.36	-0.03	0.04	0.62	17.31	8.02	0.03	0.04	0.85

<i>y = 2 m</i>					<i>y = 0 m</i>				
<i>x (m)</i>	<i>d (cm)</i>	$\bar{\eta}$ (cm)	H_{rms} (cm)	T_p (s)	<i>x (m)</i>	<i>d (cm)</i>	$\bar{\eta}$ (cm)	H_{rms} (cm)	T_p (s)
0.00	90.00	-0.19	0.02	0.57	0.00	90.00	-0.31	0.03	0.49
5.31	42.93	-0.15	0.05	0.54	5.31	41.77	-0.27	0.06	0.56
6.81	32.38	0.23	0.05	0.96	6.81	33.13	-0.07	0.08	2.33
8.31	35.00	-0.16	0.08	1.91	8.31	35.53	-0.12	0.06	0.71
9.91	30.45	-0.19	0.06	0.53	9.91	30.51	-0.29	0.10	1.70
11.31	24.87	-0.13	0.07	0.36	11.31	24.87	-0.37	0.05	0.61
12.71	19.20	-0.07	0.07	0.70	12.71	22.36	-0.06	0.06	0.98
14.31	16.38	-0.01	0.03	0.56	14.31	17.28	0.10	0.04	0.55
15.13	16.20	-0.04	0.06	0.53	15.13	15.50	-0.16	0.05	0.82
16.23	12.37	-0.32	0.03	0.66	16.23	12.33	-0.52	0.03	0.77
17.31	8.13	-0.02	0.04	0.87	17.31	8.56	0.11	0.04	0.85

<i>y= -2 m</i>					<i>y= -4 m</i>				
<i>x (m)</i>	<i>d (cm)</i>	$\bar{\eta}$ (cm)	$H_{rms}(cm)$	T_p (s)	<i>x (m)</i>	<i>d (cm)</i>	$\bar{\eta}$ (cm)	$H_{rms}(cm)$	T_p (s)
0.00	90.00	-0.20	0.02	0.55	0.00	90.00	-0.28	0.03	0.68
5.31	41.47	-0.11	0.06	0.46	5.31	40.68	-0.15	0.07	0.59
6.81	32.53	0.16	0.07	0.81	6.81	32.53	0.27	0.07	0.93
8.31	34.73	-0.13	0.07	1.08	8.31	35.20	-0.13	0.02	0.70
9.91	30.44	-0.17	0.05	0.89	9.91	30.48	-0.14	0.12	1.25
11.31	24.87	-0.31	0.06	0.80	11.31	25.13	-0.30	0.06	0.64
12.71	21.21	-0.02	0.07	2.70	12.71	20.58	0.02	0.08	0.93
14.31	18.36	0.07	0.04	0.50	14.31	15.93	0.21	0.04	0.79
15.13	16.23	-0.10	0.06	0.79	15.13	16.83	-0.13	0.06	0.67
16.23	10.97	-0.36	0.03	0.87	16.23	12.17	-0.49	0.04	0.60
17.31	6.98	-0.01	0.05	1.18	17.31	7.41	0.15	0.05	0.67

<i>y= -6 m</i>					<i>y= -8 m (interpolated)</i>				
<i>x (m)</i>	<i>d (cm)</i>	$\bar{\eta}$ (cm)	$H_{rms}(cm)$	T_p (s)	<i>x (m)</i>	<i>d (cm)</i>	$\bar{\eta}$ (cm)	$H_{rms}(cm)$	T_p (s)
0.00	90.00	-0.28	0.03	0.61	0.00	90.00	-0.29	0.03	0.69
5.31	41.98	-0.03	0.07	0.48	5.31	41.96	-0.06	0.06	0.50
6.81	33.71	0.29	0.07	0.54	6.81	32.80	0.23	0.07	0.77
8.31	36.33	-0.05	0.09	0.62	8.31	36.41	-0.09	0.09	0.74
9.91	31.65	-0.10	0.07	0.63	9.91	31.81	-0.11	0.08	0.59
11.31	24.67	-0.25	0.07	0.63	11.31	24.42	-0.29	0.08	0.64
12.71	20.10	0.01	0.07	0.87	12.71	20.22	-0.01	0.07	0.81
14.31	16.08	0.17	0.04	0.55	14.31	16.51	0.16	0.04	0.56
15.13	16.30	-0.09	0.09	1.13	15.13	14.57	-0.10	0.12	1.04
16.23	14.03	-0.42	0.04	0.73	16.23	13.33	-0.42	0.08	0.85
17.31	7.25	-0.06	0.06	0.85	17.31	7.91	-0.08	0.09	0.83

<i>y = -10 m</i>				
<i>x (m)</i>	<i>d (cm)</i>	$\bar{\eta}$ (cm)	H_{rms} (cm)	T_p (s)
0.00	90.00	-0.29	0.03	0.77
5.31	42.32	-0.09	0.06	0.53
6.81	32.54	0.17	0.06	1.00
8.31	36.07	-0.12	0.09	0.86
9.91	31.57	-0.13	0.10	0.54
11.31	24.73	-0.33	0.09	0.64
12.71	20.36	-0.02	0.07	0.74
14.31	16.13	0.15	0.04	0.57
15.13	14.93	-0.12	0.14	0.96
16.23	12.23	-0.42	0.12	0.97
17.31	8.67	-0.09	0.11	0.81

Table C. 2. Still water depth, mean cross-shore and longshore velocity at given cross-shore and longshore locations for test BC3

x (m)	$y=10$ m			$y=8$ m		
	d (cm)	\bar{U} (cm/s)	\bar{V} (cm/s)	d (cm)	\bar{U} (cm/s)	\bar{V} (cm/s)
2.81	69.88	NR	0.64	71.27	NR	3.25
5.31	42.54	0.81	6.62	42.28	1.52	10.20
6.81	31.93	5.16	15.58	32.59	3.50	17.89
8.31	34.67	3.72	15.41	35.32	2.28	15.07
9.91	30.72	5.94	19.52	30.58	1.75	11.52
11.31	23.87	NR	NR	24.90	NR	12.08
12.71	18.04	4.56	20.88	18.29	1.49	18.10
14.31	15.10	4.29	23.91	15.33	1.99	18.01
15.71	14.01	4.09	24.02	13.75	3.38	19.63
17.31	8.44	-0.18	5.84	8.32	-0.02	0.52

x (m)	$y=6$ m			$y=4$ m		
	d (cm)	\bar{U} (cm/s)	\bar{V} (cm/s)	d (cm)	\bar{U} (cm/s)	\bar{V} (cm/s)
2.81	72.66	0.45	4.29	74.30	1.50	2.03
5.31	42.12	1.32	11.63	43.20	0.96	12.61
6.81	33.31	2.33	19.77	33.00	1.23	19.63
8.31	35.20	0.68	16.06	34.93	-0.27	15.94
9.91	30.66	2.23	16.53	29.66	NR	NR
11.31	25.80	1.76	NR	24.73	2.22	13.26
12.71	18.99	0.26	20.05	20.20	-1.07	17.18
14.31	16.27	0.85	19.86	16.40	0.49	18.15
15.71	13.94	1.75	19.30	14.11	0.81	16.27
17.31	7.36	0.73	10.98	8.02	-0.09	6.96

	<i>y= 2 m</i>			<i>y= 0 m</i>		
<i>x (m)</i>	<i>d (cm)</i>	\bar{U} (cm/s)	\bar{V} (cm/s)	<i>d (cm)</i>	\bar{U} (cm/s)	\bar{V} (cm/s)
2.81	74.46	1.24	0.00	74.63	0.63	NR
5.31	42.93	0.24	12.34	41.77	0.04	13.38
6.81	32.38	0.34	20.43	33.13	-0.41	19.93
8.31	35.00	-1.00	15.62	35.53	-1.48	15.98
9.91	30.45	0.40	13.90	30.51	-1.28	NR
11.31	24.87	-1.60	NR	24.87	2.21	12.37
12.71	19.20	-1.90	18.91	22.36	-2.41	17.61
14.31	16.38	-0.76	19.82	17.28	-0.89	17.62
15.71	14.27	0.76	16.71	12.98	0.91	13.98
17.31	8.13	0.18	4.01	8.56	-0.04	0.13

	<i>y= -2 m</i>			<i>y= -4 m</i>		
<i>x (m)</i>	<i>d (cm)</i>	\bar{U} (cm/s)	\bar{V} (cm/s)	<i>d (cm)</i>	\bar{U} (cm/s)	\bar{V} (cm/s)
2.81	72.83	-0.59	1.76	74.30	1.39	0.66
5.31	41.47	-0.50	12.75	40.68	-0.68	12.44
6.81	32.53	-0.98	21.04	32.53	-1.72	20.56
8.31	34.73	-1.98	16.75	35.20	-2.37	16.77
9.91	30.44	-0.34	15.25	30.48	-0.85	17.07
11.31	24.87	NR	NR	25.13	NR	NR
12.71	21.21	-2.42	20.16	20.58	-3.49	18.79
14.31	18.36	-1.89	19.47	15.93	-2.07	19.79
15.71	12.75	-0.38	16.17	14.27	-0.63	17.13
17.31	6.98	-0.03	0.03	7.41	0.07	4.80

	<i>y= -6 m</i>			<i>y= -8 m</i>		
<i>x (m)</i>	<i>d (cm)</i>	\bar{U} (cm/s)	\bar{V} (cm/s)	<i>d (cm)</i>	\bar{U} (cm/s)	\bar{V} (cm/s)
2.81	74.30	NR	NR	74.46	NR	NR
5.31	41.98	-0.73	10.61	41.96	-1.02	10.20
6.81	33.71	-1.51	20.94	32.80	-2.19	19.63
8.31	36.33	-2.85	17.71	36.41	-3.28	18.42
9.91	31.65	-1.29	18.03	31.81	-1.78	19.32
11.31	24.67	1.42	11.67	24.42	NR	NR
12.71	20.10	-4.21	9.14	20.22	-5.07	17.77
14.31	16.08	-2.91	20.72	16.51	-3.19	22.04
15.71	14.73	-0.82	18.13	15.23	-1.01	19.56
17.31	7.25	-0.60	5.85	7.91	-0.84	6.03

	<i>y= 10 m</i>		
<i>x (m)</i>	<i>d (cm)</i>	\bar{U} (cm/s)	\bar{V} (cm/s)
2.81	74.63	NR	NR
5.31	42.32	0.04	5.23
6.81	32.54	-2.17	18.60
8.31	36.07	-3.51	18.73
9.91	31.57	-1.84	19.62
11.31	24.73	NR	NR
12.71	20.36	-4.06	16.57
14.31	16.13	-4.48	23.23
15.71	13.93	-2.00	22.66
17.31	8.67	-0.12	8.76

Table C.3. Coefficients a and b corresponding to wave setup longshore gradient and correlation coefficient CC between data and fitted line at given cross-shore locations for tests BC3

x	a	b	CC
0	4.75E-05	-0.0024	0.37
5.31	-0.00021	-0.0019	0.80
6.81	-0.00038	0.0008	0.73
8.31	-0.00011	-0.0014	0.89
9.91	-1.89E-04	-0.0022	0.85
11.31	-7.15E-05	-0.0031	0.26
12.71	-1.66E-04	-0.0006	0.93
14.31	-1.58E-04	0.0009	0.77
15.13	-5.48E-05	-0.0012	0.36
16.23	-4.10E-05	-0.0044	0.17
17.31	1.09E-05	0.0003	0.05

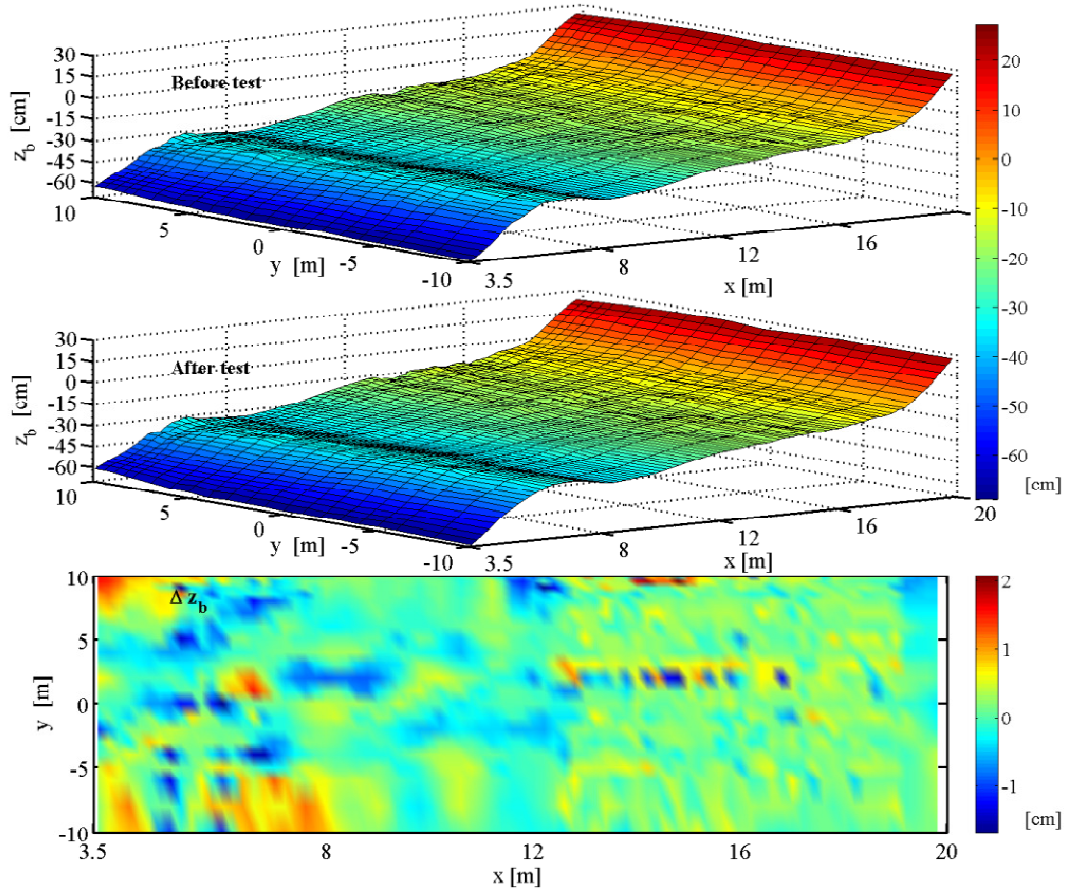


Fig. C-1. Measured initial and final profiles and change in bottom elevation for test BC3

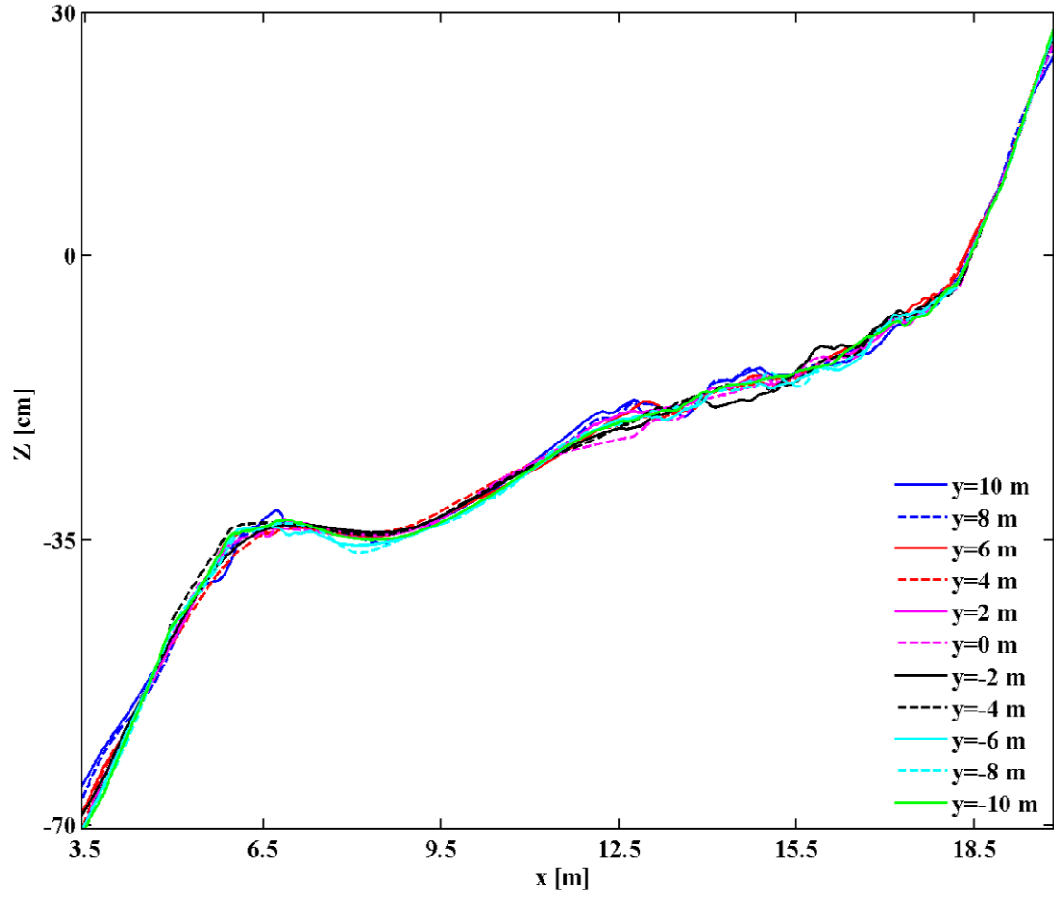


Fig. C-2. Measured initial cross-shore profiles for test BC3

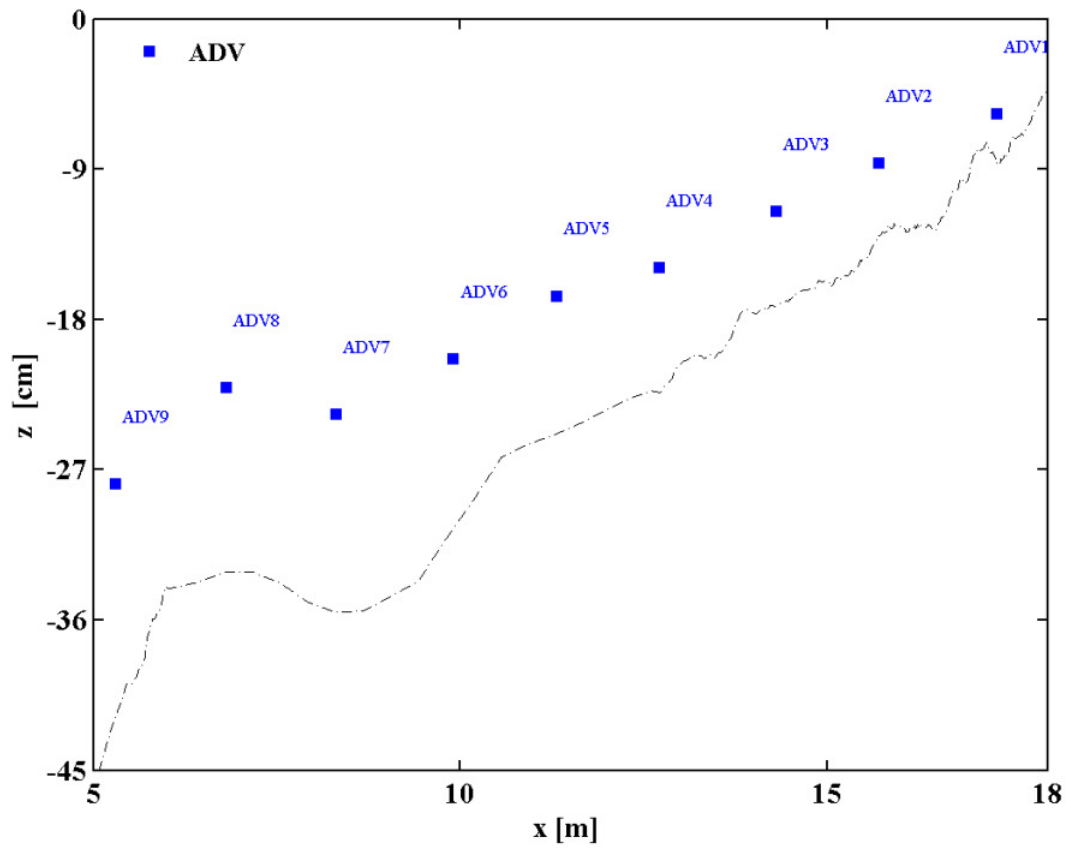


Fig. C-3. Cross-shore positioning of ADVs at $y = 0$ for test BC3

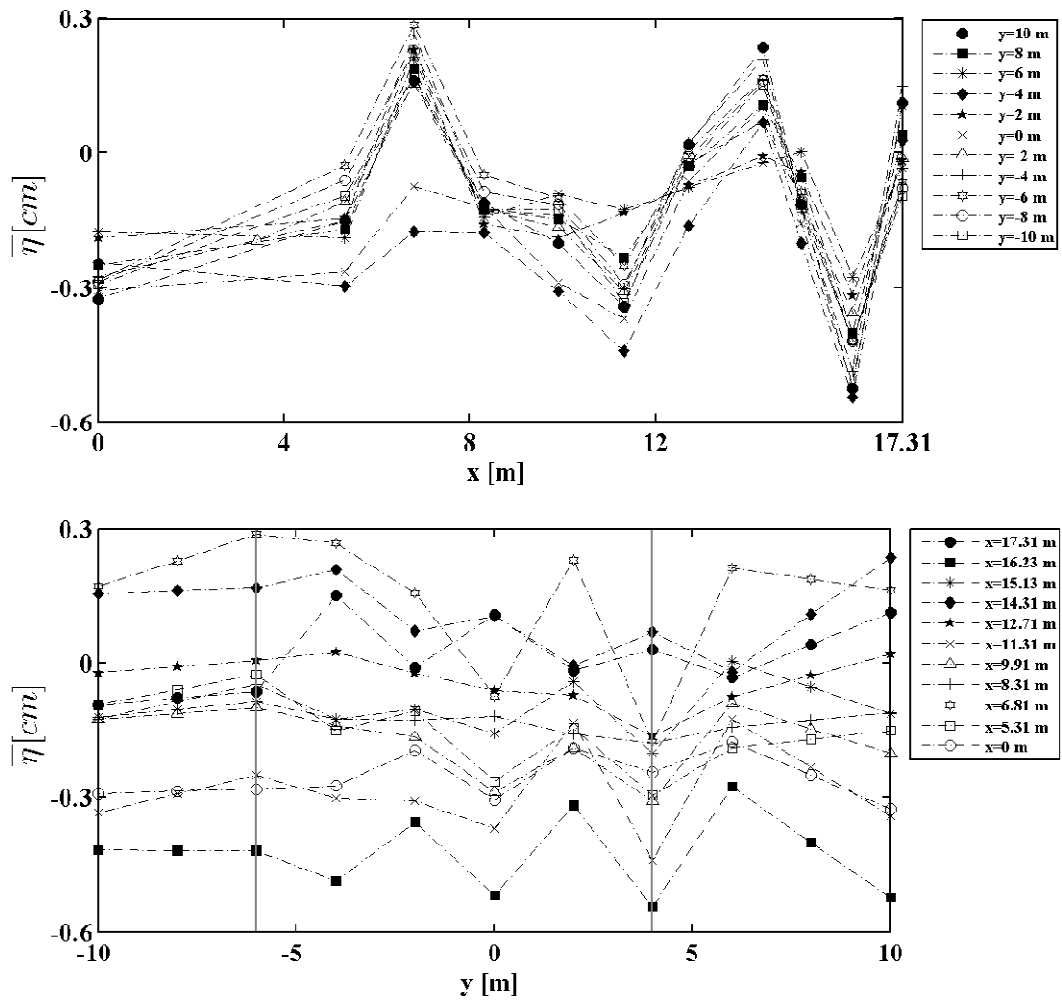


Fig. C-4. Cross-shore and longshore variations of wave setup for test BC3

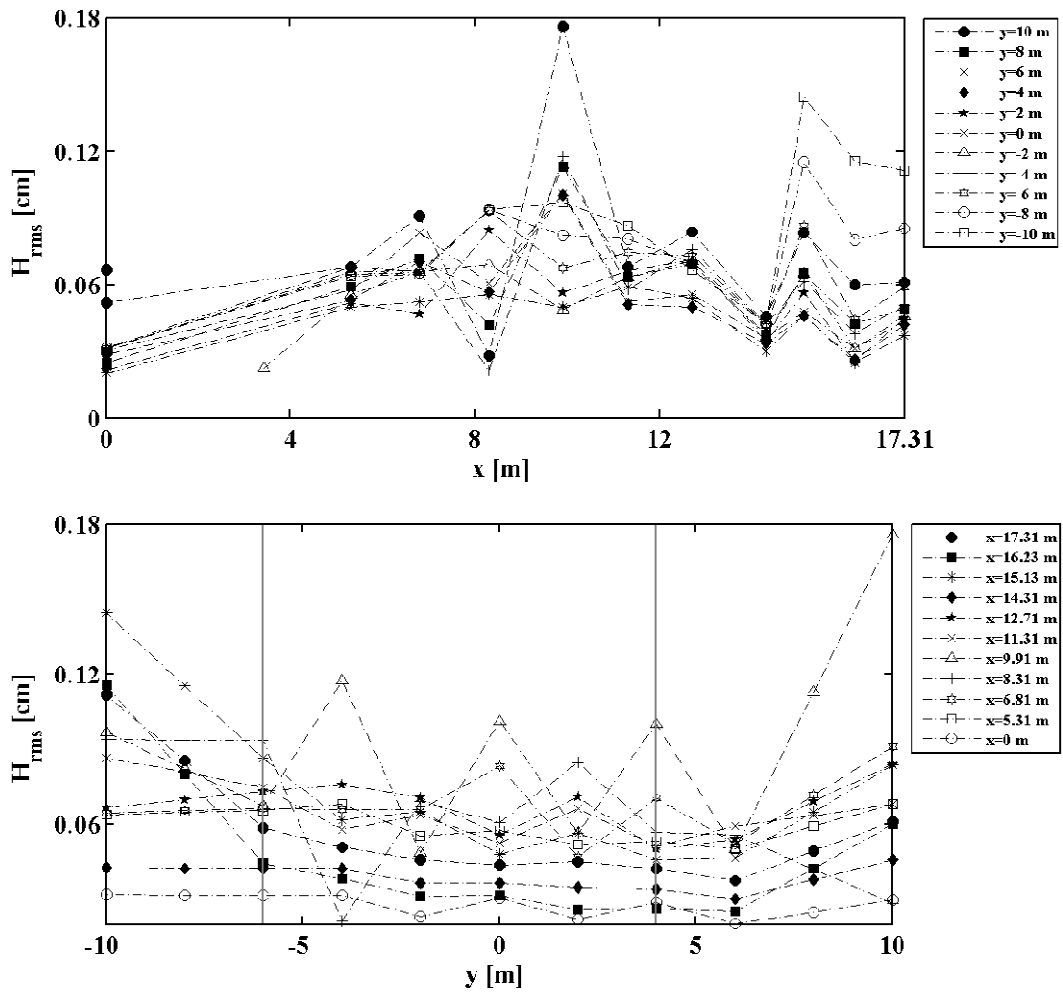


Fig. C-5. Cross-shore and longshore variations of *RMS* wave height for test BC3

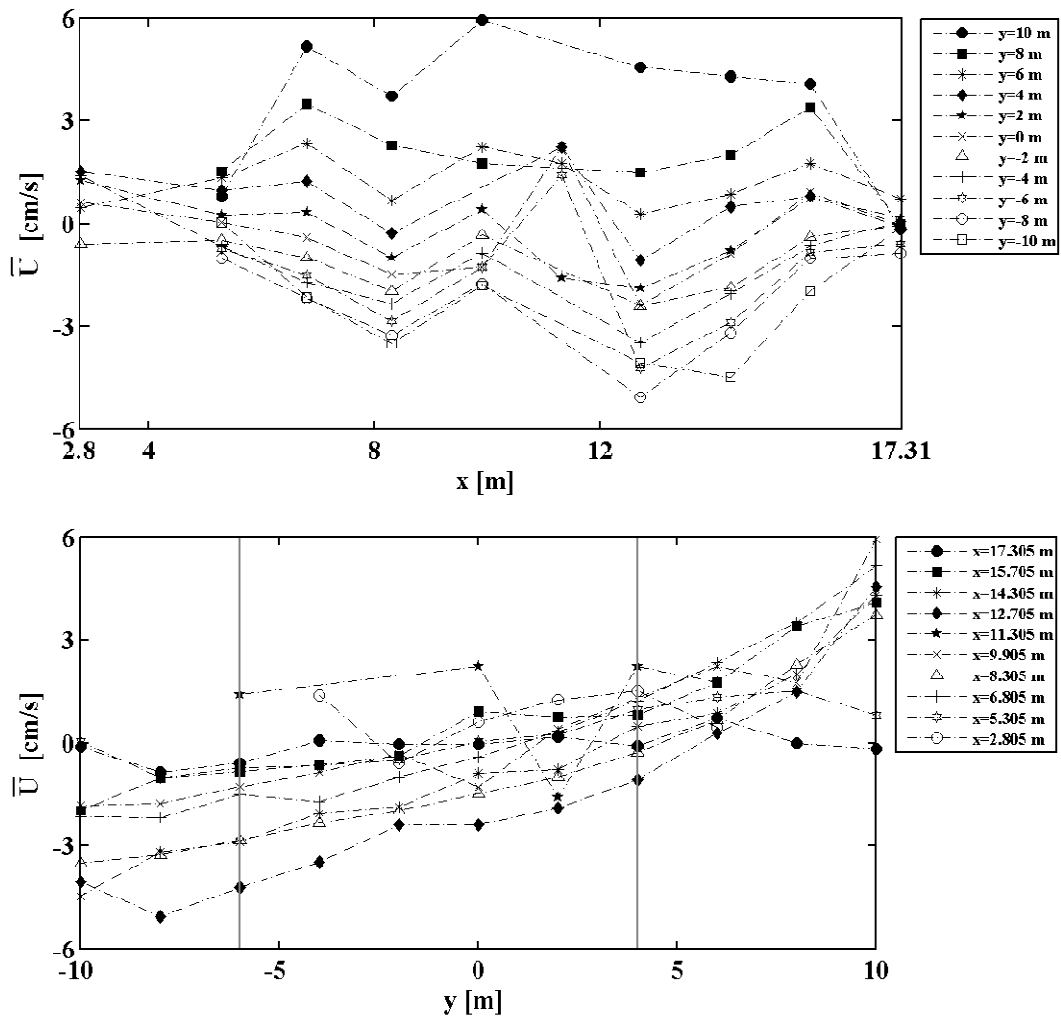


Fig. C-6. Cross-shore and longshore variations of mean cross-shore velocity for test BC3

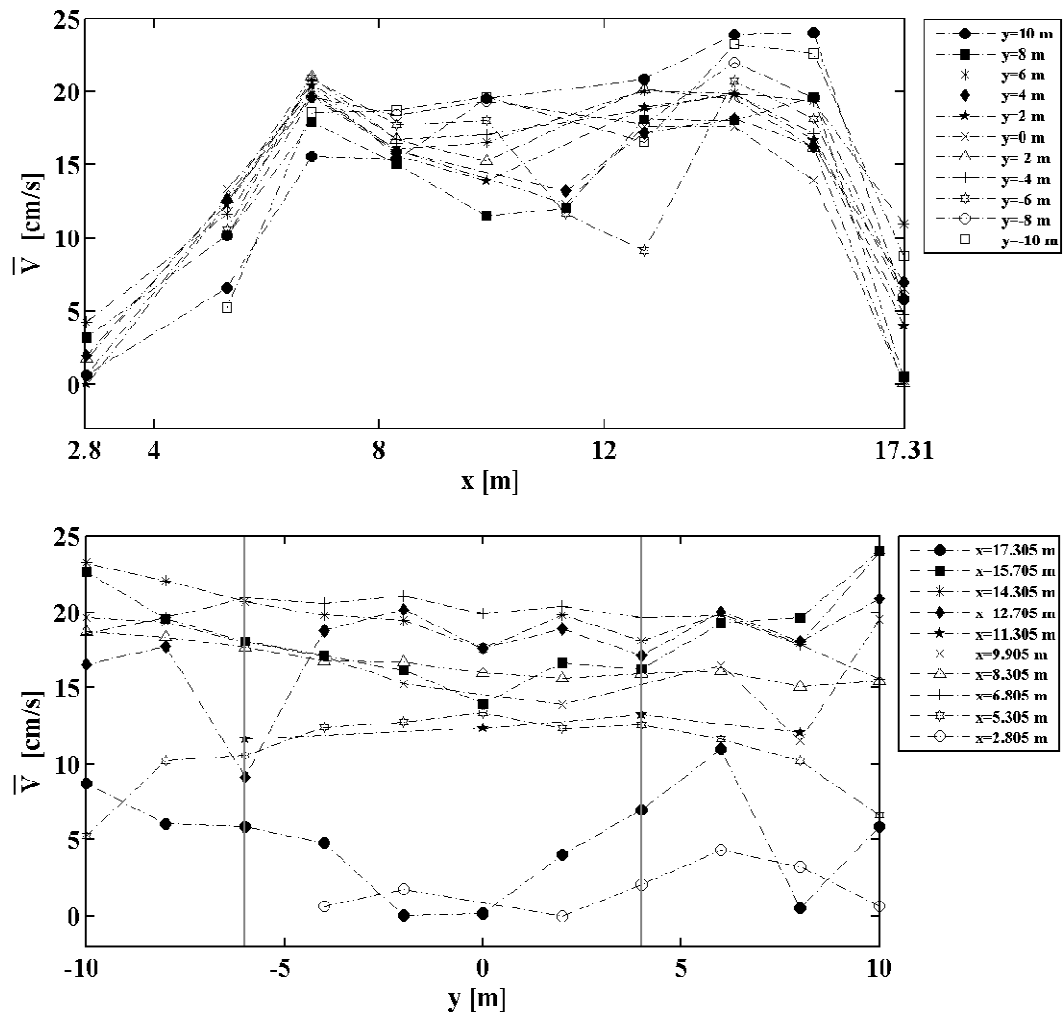


Fig. C-7. Cross-shore and longshore variations of mean longshore velocity for test BC3

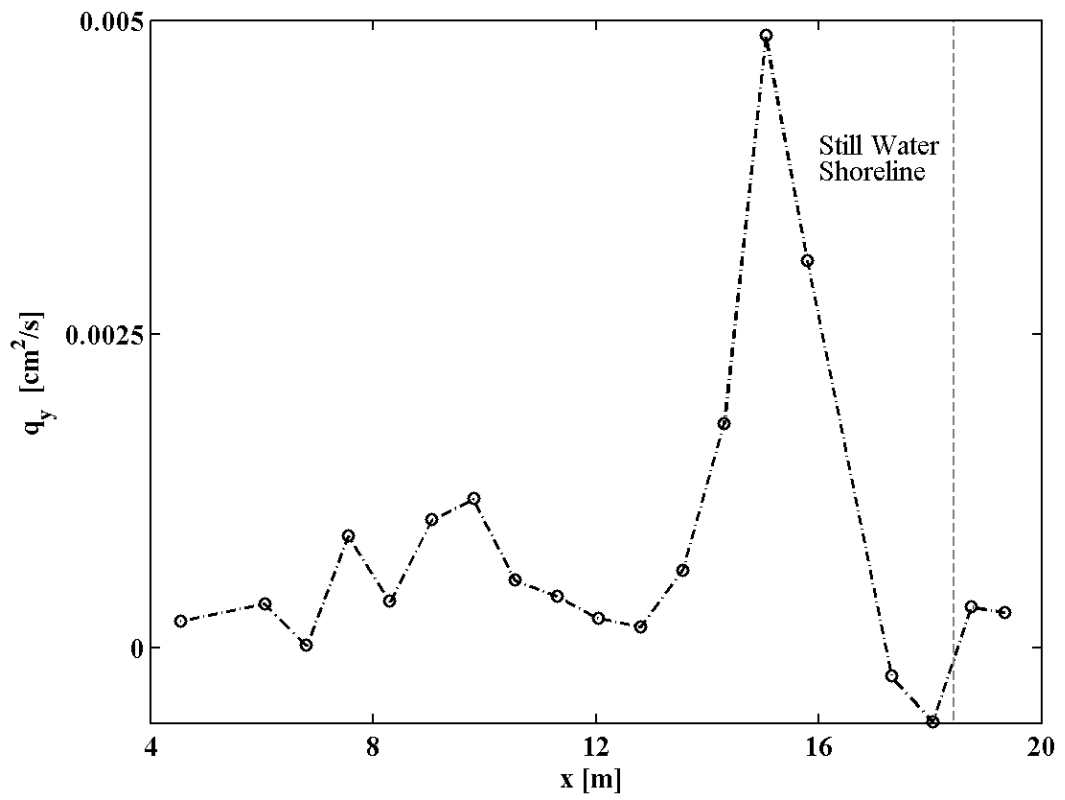


Fig. C-8. Cross-shore distribution of total longshore sediment transport rate q_y for test BC3

APPENDIX D

TEST BC4

Appendix D contains the tables and figures for test BC4.

Table D.1. Still water depth, wave setup, root-mean-square wave height and peak period at given cross-shore and longshore locations for test BC4

<i>y= 10 m</i>					<i>y= 8 m (interpolated)</i>				
<i>x (m)</i>	<i>d (cm)</i>	$\bar{\eta}$ (cm)	H_{rms} (cm)	T_p (s)	<i>x (m)</i>	<i>d (cm)</i>	$\bar{\eta}$ (cm)	H_{rms} (cm)	T_p (s)
0.00	90.00	-0.24	15.90	1.48	0.00	90.00	-0.25	15.88	1.48
5.31	41.65	-0.26	16.69	1.49	5.31	42.15	-0.35	16.41	1.50
6.81	31.54	-0.43	14.18	1.45	6.81	33.43	-0.32	14.21	1.48
8.31	34.33	0.09	12.50	1.57	8.31	35.41	-0.01	12.44	1.53
9.91	30.62	-0.15	11.70	1.42	9.91	30.63	-0.14	11.75	1.45
11.31	24.20	-0.08	11.35	1.59	11.31	24.55	-0.10	11.31	1.55
12.71	17.68	0.10	10.41	1.59	12.71	18.15	0.07	10.08	1.55
14.31	14.39	-0.07	10.29	1.49	14.31	15.30	-0.13	10.40	1.49
15.13	13.76	NR	NR	1.58	15.13	15.33	NR	NR	1.58
16.23	14.67	0.34	5.98	1.58	16.23	12.07	0.36	6.00	1.72
17.31	7.72	0.25	4.68	1.73	17.31	7.83	0.33	4.40	1.80

$y = 6\text{ m}$					$y = 4\text{ m}$				
$x\text{ (m)}$	$d\text{ (cm)}$	$\bar{\eta}\text{ (cm)}$	$H_{rms}\text{ (cm)}$	$T_p\text{ (s)}$	$x\text{ (m)}$	$d\text{ (cm)}$	$\bar{\eta}\text{ (cm)}$	$H_{rms}\text{ (cm)}$	$T_p\text{ (s)}$
0.00	90.00	-0.26	15.86	1.47	0.00	90.00	-0.15	15.83	1.47
5.31	43.07	-0.43	16.12	1.51	5.31	43.73	-0.40	16.03	1.48
6.81	33.28	-0.22	14.24	1.52	6.81	32.93	-0.64	13.74	1.48
8.31	35.47	-0.12	12.37	1.49	8.31	34.60	-0.07	12.23	1.48
9.91	30.77	-0.12	11.81	1.49	9.91	29.88	-0.31	12.37	1.49
11.31	25.60	-0.11	11.27	1.50	11.31	24.60	-0.14	12.14	1.50
12.71	18.98	0.04	9.74	1.50	12.71	20.19	0.00	9.79	1.51
14.31	16.92	-0.18	10.52	1.48	14.31	16.41	-0.20	10.17	1.49
15.13	14.80	NR	NR	1.58	15.13	15.77	NR	NR	1.85
16.23	11.60	0.37	6.02	1.86	16.23	12.07	0.28	6.73	1.85
17.31	7.13	0.41	4.11	1.87	17.31	7.75	0.49	4.88	1.86

$y = 2\text{ m}$					$y = 0\text{ m}$				
$x\text{ (m)}$	$d\text{ (cm)}$	$\bar{\eta}\text{ (cm)}$	$H_{rms}\text{ (cm)}$	$T_p\text{ (s)}$	$x\text{ (m)}$	$d\text{ (cm)}$	$\bar{\eta}\text{ (cm)}$	$H_{rms}\text{ (cm)}$	$T_p\text{ (s)}$
0.00	90.00	-0.21	15.80	1.46	0.00	90.00	-0.21	15.90	1.46
5.31	43.20	-0.49	15.69	1.49	5.31	42.87	-0.40	17.29	1.46
6.81	32.00	-0.28	13.81	1.48	6.81	33.00	-0.62	14.19	1.51
8.31	35.80	-0.14	12.30	1.50	8.31	35.27	-0.03	12.26	1.50
9.91	30.06	-0.19	12.03	1.50	9.91	30.51	-0.25	12.34	1.50
11.31	25.07	-0.16	11.44	1.57	11.31	24.87	-0.11	11.80	1.48
12.71	18.63	-0.02	9.88	1.51	12.71	22.34	0.08	9.75	1.58
14.31	16.08	-0.21	9.91	1.49	14.31	17.13	-0.19	10.80	1.48
15.13	15.00	NR	NR	1.72	15.13	15.37	NR	NR	1.57
16.23	11.67	0.33	6.62	1.86	16.23	12.07	0.30	6.67	1.74
17.31	7.64	0.41	4.42	1.86	17.31	7.89	0.44	4.68	1.92

<i>y</i> = -2 m					<i>y</i> = -4 m				
<i>x</i> (m)	<i>d</i> (cm)	$\bar{\eta}$ (cm)	H_{rms} (cm)	T_p (s)	<i>x</i> (m)	<i>d</i> (cm)	$\bar{\eta}$ (cm)	H_{rms} (cm)	T_p (s)
0.00	90.00	-0.17	15.79	1.48	0.00	90.00	-0.17	15.84	1.47
5.31	41.20	-0.37	15.87	1.55	5.31	40.85	-0.27	16.23	1.46
6.81	32.73	-0.17	13.74	1.49	6.81	34.03	-0.52	14.00	1.49
8.31	34.60	-0.06	12.32	1.48	8.31	35.27	0.07	12.29	1.57
9.91	30.96	-0.13	12.12	1.50	9.91	30.24	-0.15	12.72	1.48
11.31	25.27	-0.08	12.10	1.57	11.31	25.07	-0.05	12.01	1.49
12.71	21.15	0.00	10.05	1.49	12.71	20.71	0.12	10.19	1.58
14.31	18.10	-0.15	10.45	1.48	14.31	16.05	-0.10	9.86	1.49
15.13	16.27	NR	NR	1.73	15.13	16.60	NR	NR	1.58
16.23	10.95	0.33	6.86	1.75	16.23	11.83	0.35	6.28	1.73
17.31	6.76	0.47	4.29	1.89	17.31	7.28	0.30	4.86	1.89

<i>y</i> = -6 m					<i>y</i> = -8 m (interpolated)				
<i>x</i> (m)	<i>d</i> (cm)	$\bar{\eta}$ (cm)	H_{rms} (cm)	T_p (s)	<i>x</i> (m)	<i>d</i> (cm)	$\bar{\eta}$ (cm)	H_{rms} (cm)	T_p (s)
0.00	90.00	-0.23	15.91	1.47	0.00	90.00	-0.24	15.86	1.47
5.31	42.07	-0.27	15.91	1.52	5.31	42.15	-0.27	15.82	1.51
6.81	32.87	-0.16	14.05	1.57	6.81	32.11	-0.15	13.93	1.56
8.31	36.00	-0.02	12.46	1.48	8.31	36.13	0.00	11.98	1.48
9.91	31.76	-0.10	12.15	1.58	9.91	32.13	-0.11	12.13	1.58
11.31	24.67	-0.05	12.08	1.58	11.31	24.53	-0.06	12.15	1.58
12.71	19.53	-0.02	9.56	1.50	12.71	20.20	-0.02	9.44	1.54
14.31	16.07	-0.09	10.14	1.49	14.31	16.68	-0.10	10.29	1.48
15.13	16.30	NR	NR	1.67	15.13	14.43	NR	NR	1.61
16.23	14.07	0.36	6.65	1.72	16.23	13.23	0.34	6.59	1.72
17.31	7.41	0.39	5.04	1.72	17.31	7.81	0.39	5.04	1.73

<i>y = -10 m</i>				
<i>x (m)</i>	<i>d (cm)</i>	$\bar{\eta}$ (cm)	H_{rms} (cm)	T_p (s)
0.00	90.00	-0.24	15.82	1.48
5.31	42.13	-0.27	15.73	1.49
6.81	31.93	-0.14	13.82	1.54
8.31	35.60	0.01	11.49	1.48
9.91	31.74	-0.13	12.10	1.58
11.31	24.87	-0.08	12.23	1.58
12.71	20.41	-0.03	9.32	1.58
14.31	16.03	-0.12	10.44	1.46
15.13	14.07	NR	NR	1.54
16.23	11.97	0.33	6.52	1.73
17.31	8.49	0.40	5.04	1.73

Table D.2. Still water depth, mean cross-shore and longshore velocity at given cross-shore and longshore locations for test BC4

x (m)	$y=10$ m			$y=8$ m		
	d (cm)	\bar{U} (cm/s)	\bar{V} (cm/s)	d (cm)	\bar{U} (cm/s)	\bar{V} (cm/s)
2.81	68.57	-5.98	0.53	70.70	-0.95	1.37
5.31	41.65	-5.82	6.11	42.15	-3.62	7.68
6.81	31.54	-4.38	11.70	33.43	-4.75	12.67
8.31	34.33	-4.95	13.38	35.41	-5.20	14.54
9.91	30.62	-3.27	17.30	30.63	-2.92	15.95
11.31	24.20	-1.52	16.88	24.55	-1.97	15.23
12.71	17.68	-4.41	16.04	18.15	-5.63	13.78
14.31	14.39	-4.84	19.15	15.30	-5.54	18.16
15.71	12.97	-3.42	19.75	13.33	-3.98	17.49
17.31	7.72	-2.77	16.70	7.83	-2.78	15.75

x (m)	$y=6$ m			$y=4$ m		
	d (cm)	\bar{U} (cm/s)	\bar{V} (cm/s)	d (cm)	\bar{U} (cm/s)	\bar{V} (cm/s)
2.81	72.83	-0.51	NR	74.63	NR	NR
5.31	43.07	-3.06	7.58	43.73	-4.42	7.85
6.81	33.28	-5.46	13.91	32.93	-6.08	13.96
8.31	35.47	-5.95	14.52	34.60	-5.97	14.88
9.91	30.77	-3.73	17.13	29.88	-4.10	15.90
11.31	25.60	-2.73	14.93	24.60	-3.71	14.55
12.71	18.98	-4.86	14.40	20.19	-7.58	13.69
14.31	16.92	-5.31	17.14	16.41	-6.75	17.33
15.71	14.04	-4.36	17.77	13.87	-4.61	15.81
17.31	7.13	-1.89	16.22	7.75	-2.41	16.92

	<i>y= 2 m</i>			<i>y= 0 m</i>		
<i>x (m)</i>	<i>d (cm)</i>	\bar{U} (cm/s)	\bar{V} (cm/s)	<i>d (cm)</i>	\bar{U} (cm/s)	\bar{V} (cm/s)
2.81	73.81	NR	NR	74.63	NR	NR
5.31	43.20	-3.60	7.04	42.87	-4.52	7.30
6.81	32.00	-5.40	14.83	33.00	-7.19	14.09
8.31	35.80	-6.57	14.95	35.27	-7.06	15.00
9.91	30.06	-4.54	16.87	30.51	-5.62	16.11
11.31	25.07	-4.48	15.17	24.87	-4.44	14.31
12.71	18.63	-7.30	15.00	22.34	-7.57	12.84
14.31	16.08	-8.07	18.25	17.13	-6.68	18.11
15.71	13.66	-4.54	16.58	12.64	-4.39	17.72
17.31	7.64	-1.55	15.19	7.89	-3.58	13.45

	<i>y= -2 m</i>			<i>y= -4 m</i>		
<i>x (m)</i>	<i>d (cm)</i>	\bar{U} (cm/s)	\bar{V} (cm/s)	<i>d (cm)</i>	\bar{U} (cm/s)	\bar{V} (cm/s)
2.81	73.97	-1.35	NR	74.46	NR	NR
5.31	41.20	-3.97	6.88	40.85	-4.16	6.04
6.81	32.73	-6.74	14.72	34.03	-7.12	14.30
8.31	34.60	-7.00	15.05	35.27	-6.93	15.31
9.91	30.96	-5.09	17.40	30.24	-4.86	16.07
11.31	25.27	-4.50	14.97	25.07	-3.93	15.01
12.71	21.15	-7.14	14.53	20.71	-7.49	13.75
14.31	18.10	-7.28	19.82	16.05	-7.17	18.99
15.71	12.51	-4.97	19.76	14.38	-5.29	19.39
17.31	6.76	-3.07	11.67	7.28	-3.06	13.08

	<i>y= -6 m</i>			<i>y= -8 m</i>		
<i>x (m)</i>	<i>d (cm)</i>	\bar{U} (cm/s)	\bar{V} (cm/s)	<i>d (cm)</i>	\bar{U} (cm/s)	\bar{V} (cm/s)
2.81	74.13	-1.81	NR	74.46	-2.12	NR
5.31	42.07	-3.33	4.41	42.15	-3.45	4.80
6.81	32.87	-5.98	13.83	32.11	-5.54	13.09
8.31	36.00	-6.76	15.66	36.13	-6.54	15.91
9.91	31.76	-4.98	17.50	32.13	-4.46	16.48
11.31	24.67	-4.39	15.72	24.53	-4.27	16.18
12.71	19.53	-7.23	15.76	20.20	-7.01	14.70
14.31	16.07	-6.62	20.35	16.68	-6.41	20.19
15.71	14.50	-4.50	19.87	14.88	-4.15	19.64
17.31	7.41	-3.15	14.41	7.81	-3.18	14.58

	<i>y= -10 m</i>		
<i>x (m)</i>	<i>d (cm)</i>	\bar{U} (cm/s)	\bar{V} (cm/s)
2.81	74.79	-0.87	NR
5.31	42.13	-3.10	3.02
6.81	31.93	-4.92	12.45
8.31	35.60	-6.16	15.88
9.91	31.74	-3.44	18.38
11.31	24.87	-2.76	16.28
12.71	20.41	-6.91	16.81
14.31	16.03	-6.49	22.37
15.71	13.98	-4.30	19.76
17.31	8.49	-3.96	10.86

Table D.2. Mean water depth, fitted profile coefficients, suspended sediment volumes and correlation coefficients at given cross-shore and longshore locations for test BC4

<i>y=10 m</i>		<i>Exponential</i>				<i>Power</i>			
<i>x (m)</i>	\bar{h} (cm)	c_b (g/l)	l_c (cm)	V_s (cm)	<i>CC</i>	c_a (g/l)	<i>m</i>	V_s (cm)	<i>CC</i>
9.91	30.47	9.95	1.76	0.0037	0.98	15.19	2.74	0.0033	0.97
12.23	19.81	8.72	2.30	0.0049	0.92	6.52	1.12	0.0062	0.96
12.71	17.77	21.75	1.13	0.0038	0.99	69.77	4.19	0.0083	0.90

<i>y=8 m</i>		<i>Exponential</i>				<i>Power</i>			
<i>x (m)</i>	\bar{h} (cm)	c_b (g/l)	l_c (cm)	V_s (cm)	<i>CC</i>	c_a (g/l)	<i>m</i>	V_s (cm)	<i>CC</i>
9.91	30.49	9.06	1.50	0.0026	0.92	22.76	3.49	0.0035	1.00
12.23	20.28	9.56	1.94	0.0042	0.95	6.85	1.34	0.0048	0.98
12.71	18.22	12.81	1.62	0.0042	0.99	27.17	2.88	0.0055	0.89

<i>y=6 m</i>		<i>Exponential</i>				<i>Power</i>			
<i>x (m)</i>	\bar{h} (cm)	c_b (g/l)	l_c (cm)	V_s (cm)	<i>CC</i>	c_a (g/l)	<i>m</i>	V_s (cm)	<i>CC</i>
9.91	30.65	10.63	1.74	0.0039	0.95	29.21	3.06	0.0054	0.99
12.23	20.91	10.91	2.00	0.0050	0.96	8.21	1.33	0.0059	0.99
12.71	19.02	10.39	1.31	0.0024	1.00	35.37	3.89	0.0047	0.92

<i>y=4 m</i>		<i>Exponential</i>				<i>Power</i>			
<i>x (m)</i>	\bar{h} (cm)	<i>c_b</i> (g/l)	<i>l_c</i> (cm)	<i>V_s</i> (cm)	<i>CC</i>	<i>c_a</i> (g/l)	<i>m</i>	<i>V_s</i> (cm)	<i>CC</i>
9.91	29.57	244.79	0.95	0.0304	0.92	1275.08	5.17	0.1173	0.88
12.23	20.95	13.13	1.69	0.0046	0.96	8.88	1.53	0.0050	0.98
12.71	20.19	16.59	1.51	0.0049	0.99	59.87	3.53	0.0090	0.88

<i>y=2 m</i>		<i>Exponential</i>				<i>Power</i>			
<i>x (m)</i>	\bar{h} (cm)	<i>c_b</i> (g/l)	<i>l_c</i> (cm)	<i>V_s</i> (cm)	<i>CC</i>	<i>c_a</i> (g/l)	<i>m</i>	<i>V_s</i> (cm)	<i>CC</i>
9.91	29.88	180.85	0.73	0.0127	0.98	596.51	5.77	0.0483	0.96
12.23	20.58	13.49	1.63	0.0045	0.96	9.21	1.61	0.0048	0.99
12.71	18.60	13.78	1.20	0.0027	0.99	31.96	3.77	0.0044	0.94

<i>y=0 m</i>		<i>Exponential</i>				<i>Power</i>			
<i>x (m)</i>	\bar{h} (cm)	<i>c_b</i> (g/l)	<i>l_c</i> (cm)	<i>V_s</i> (cm)	<i>CC</i>	<i>c_a</i> (g/l)	<i>m</i>	<i>V_s</i> (cm)	<i>CC</i>
9.91	30.26	9.74	1.46	0.0027	0.94	22.54	3.52	0.0034	0.99
12.23	23.01	151.29	0.94	0.0184	0.97	74.20	2.76	0.0159	1.00
12.71	22.42	13.90	1.55	0.0043	0.99	29.27	2.97	0.0056	0.91

<i>y=-2 m</i>		<i>Exponential</i>				<i>Power</i>			
<i>x (m)</i>	\bar{h} (cm)	<i>c_b</i> (g/l)	<i>l_c</i> (cm)	<i>V_s</i> (cm)	<i>CC</i>	<i>c_a</i> (g/l)	<i>m</i>	<i>V_s</i> (cm)	<i>CC</i>
9.91	30.83	10.92	1.60	0.0035	0.95	27.63	3.31	0.0045	0.99
12.23	22.20	16.31	1.36	0.0040	0.96	9.84	1.89	0.0039	0.99
12.71	21.15	6.46	1.25	0.0014	0.99	14.06	3.57	0.0021	0.90

<i>y=-4 m</i>		<i>Exponential</i>				<i>Power</i>			
<i>x (m)</i>	\bar{h} (cm)	<i>c_b (g/l)</i>	<i>l_c (cm)</i>	<i>V_s (cm)</i>	<i>CC</i>	<i>c_a (g/l)</i>	<i>m</i>	<i>V_s (cm)</i>	<i>CC</i>
9.91	30.09	4.04	1.48	0.0011	0.96	10.29	3.55	0.0015	0.99
12.23	22.32	13.42	1.45	0.0037	0.96	8.29	1.76	0.0037	0.98
12.71	20.83	8.71	1.80	0.0034	0.99	16.32	2.55	0.0040	0.90

<i>y=-6 m</i>		<i>Exponential</i>				<i>Power</i>			
<i>x (m)</i>	\bar{h} (cm)	<i>c_b (g/l)</i>	<i>l_c (cm)</i>	<i>V_s (cm)</i>	<i>CC</i>	<i>c_a (g/l)</i>	<i>m</i>	<i>V_s (cm)</i>	<i>CC</i>
9.91	31.66	41.37	1.24	0.0086	0.94	124.00	4.23	0.0147	1.00
12.23	20.89	15.45	1.34	0.0037	0.96	9.42	1.92	0.0036	0.99
12.71	19.51	8.42	1.34	0.0020	0.99	23.34	3.69	0.0033	0.91

<i>y=-8 m</i>		<i>Exponential</i>				<i>Power</i>			
<i>x (m)</i>	\bar{h} (cm)	<i>c_b (g/l)</i>	<i>l_c (cm)</i>	<i>V_s (cm)</i>	<i>CC</i>	<i>c_a (g/l)</i>	<i>m</i>	<i>V_s (cm)</i>	<i>CC</i>
9.91	32.01	6.87	1.42	0.0018	0.93	19.75	3.75	0.0027	1.00
12.23	21.10	15.57	1.37	0.0039	0.97	9.85	1.91	0.0038	0.99
12.71	20.18	26.78	1.37	0.0067	0.97	97.60	3.84	0.0131	0.99

<i>y=-10 m</i>		<i>Exponential</i>				<i>Power</i>			
<i>x (m)</i>	\bar{h} (cm)	<i>c_b (g/l)</i>	<i>l_c (cm)</i>	<i>V_s (cm)</i>	<i>CC</i>	<i>c_a (g/l)</i>	<i>m</i>	<i>V_s (cm)</i>	<i>CC</i>
9.91	31.61	91.34	1.24	0.0190	0.97	293.26	4.27	0.0343	0.98
12.23	21.26	24.81	1.07	0.0039	0.97	12.81	2.38	0.0035	1.00
12.71	20.38	8.10	1.36	0.0020	0.99	22.78	3.66	0.0033	0.91

Table D.4. Coefficients a and b corresponding to wave setup longshore gradient and correlation coefficient CC between data and fitted line at given cross-shore locations for tests BC4

x	a	b	CC
0	3.37E-05	-0.0019	0.41
5.31	-0.00019	-0.0039	0.85
6.81	-0.00031	-0.0043	0.53
8.31	-0.00012	-0.0005	0.66
9.91	-1.81E-04	-0.0021	0.87
11.31	-1.16E-04	-0.0011	0.94
12.71	-3.75E-05	0.0002	0.23
14.31	-1.35E-04	-0.0017	0.95
15.13	NR	NR	NR
16.23	-7.20E-05	0.0032	0.87
17.31	1.12E-04	0.0043	0.63

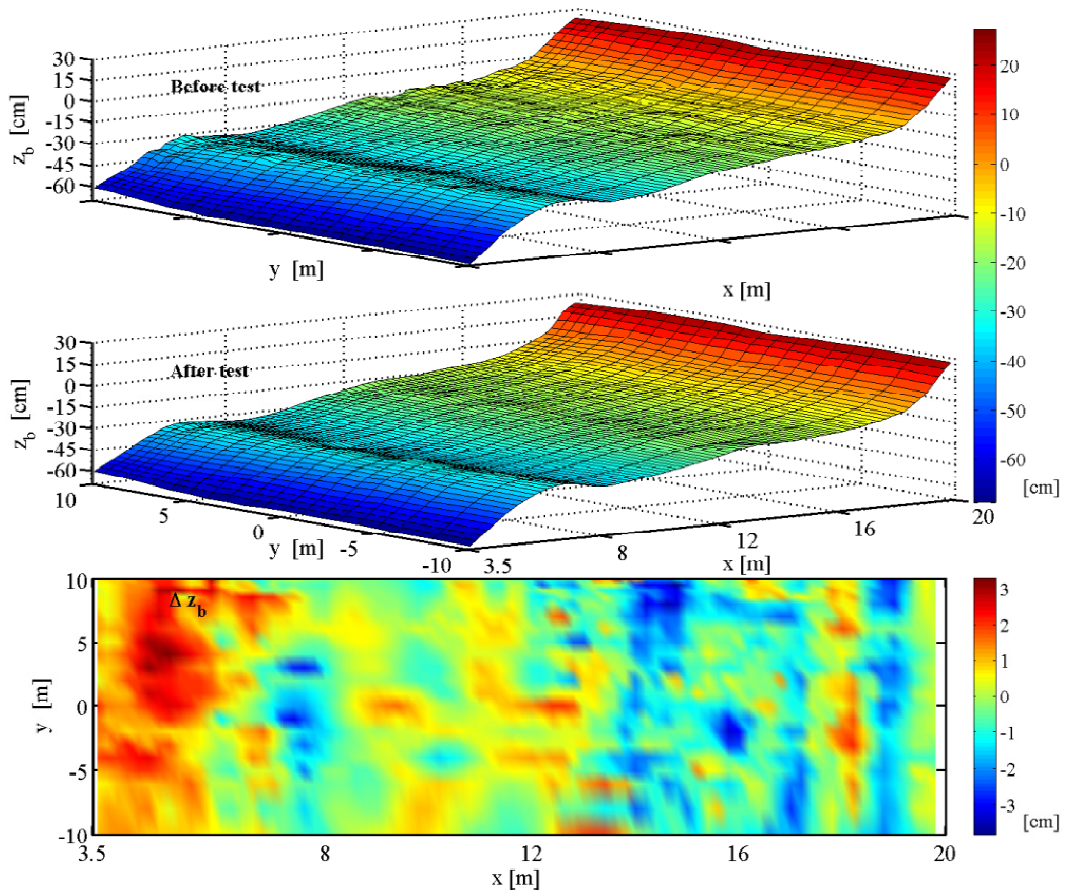


Fig. D-1. Measured initial and final profiles and change in bottom elevation for test BC4

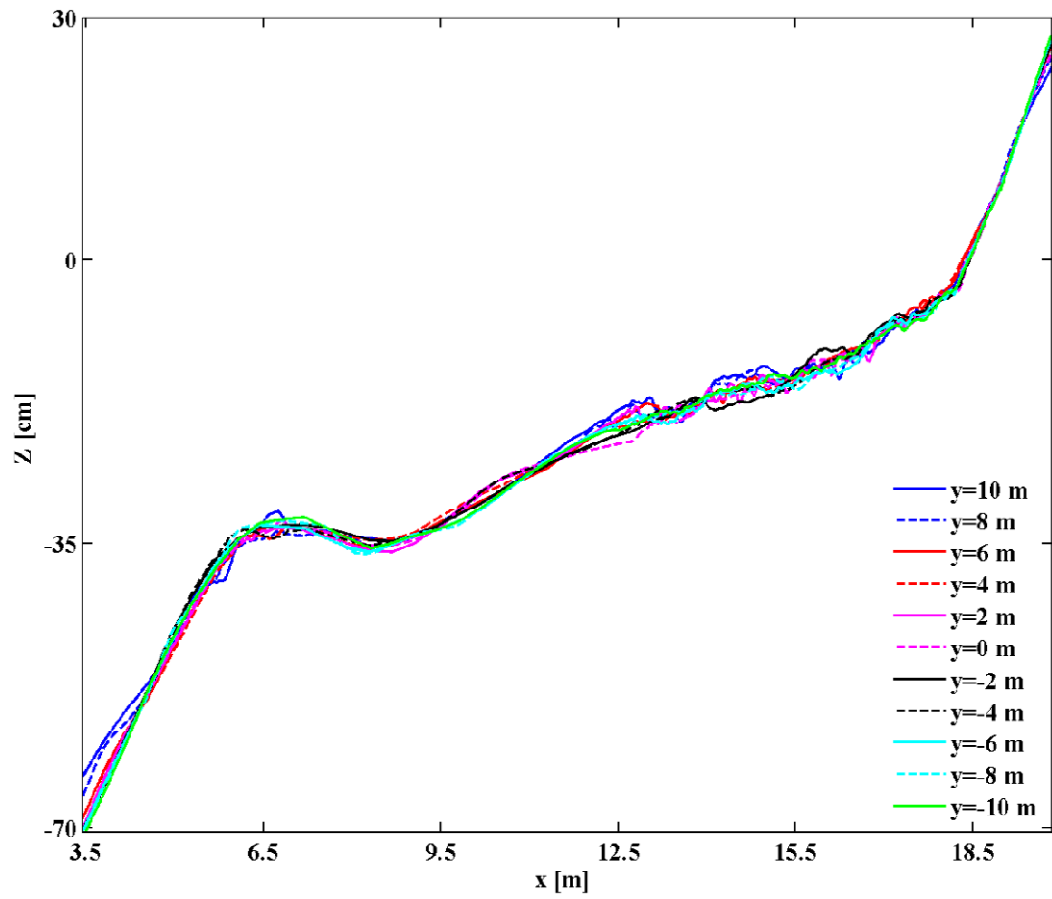


Fig. D-2. Measured initial cross-shore profiles for test BC4

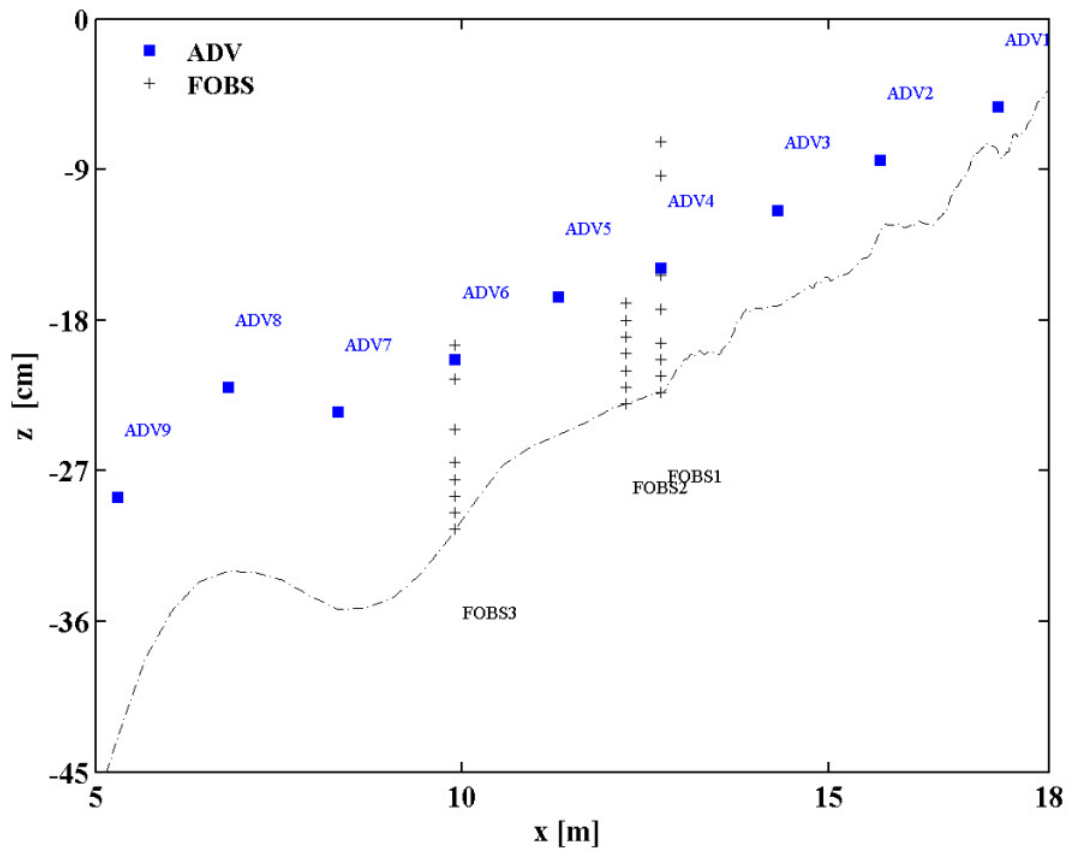


Fig. D-3. Cross-shore positioning of ADVs and FOBS at $y = 0$ for test BC4

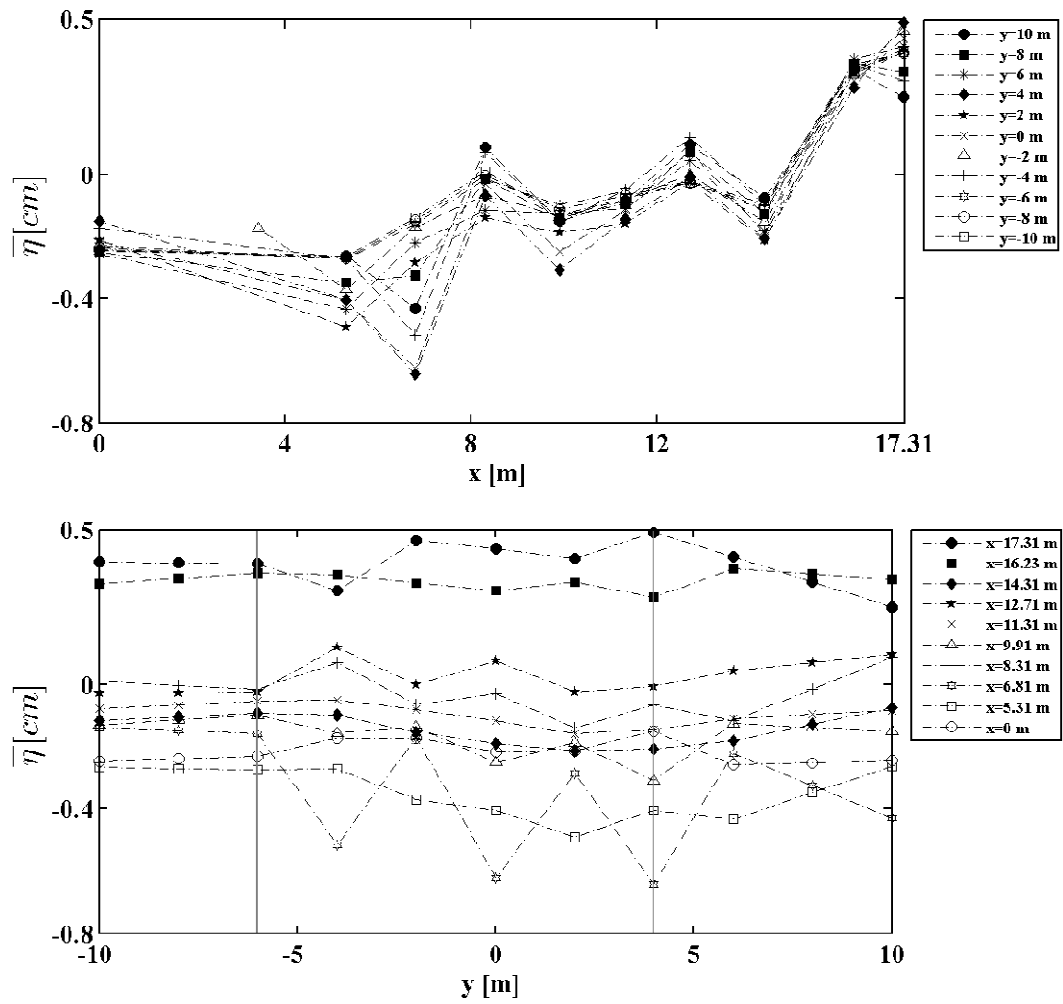


Fig. D-4. Cross-shore and longshore variations of wave setup for test BC4

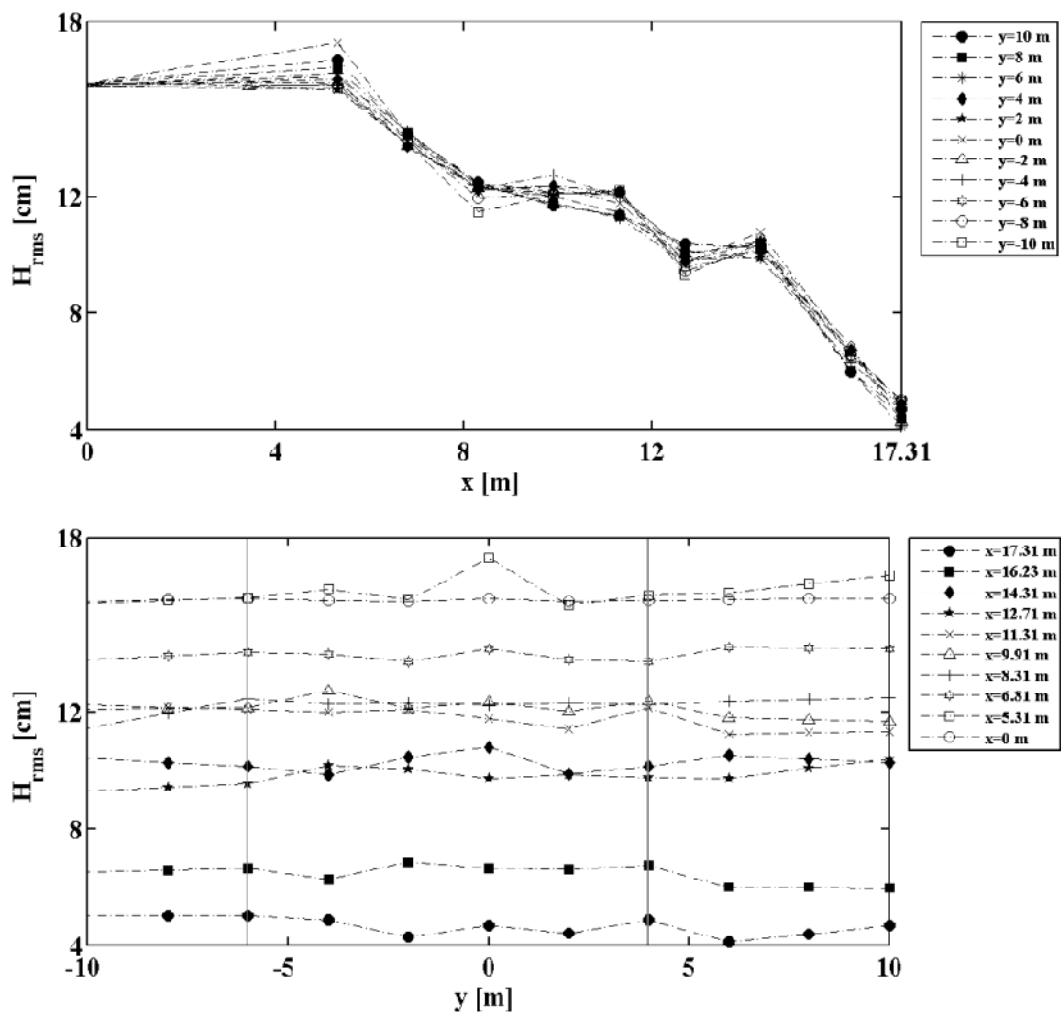


Fig. D-5. Cross-shore and longshore variations of RMS wave height for test BC4

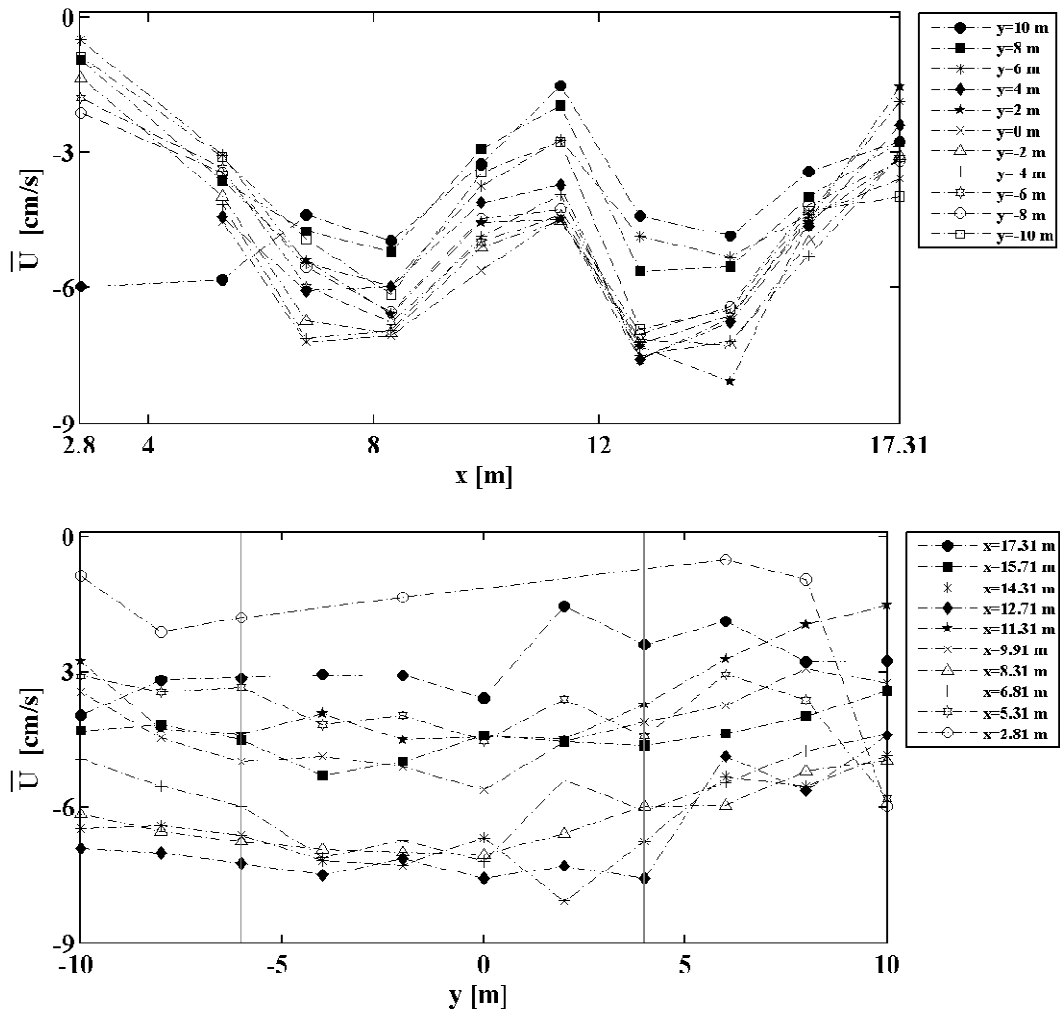


Fig. D-6. Cross-shore and longshore variations of mean cross-shore velocity for test BC4

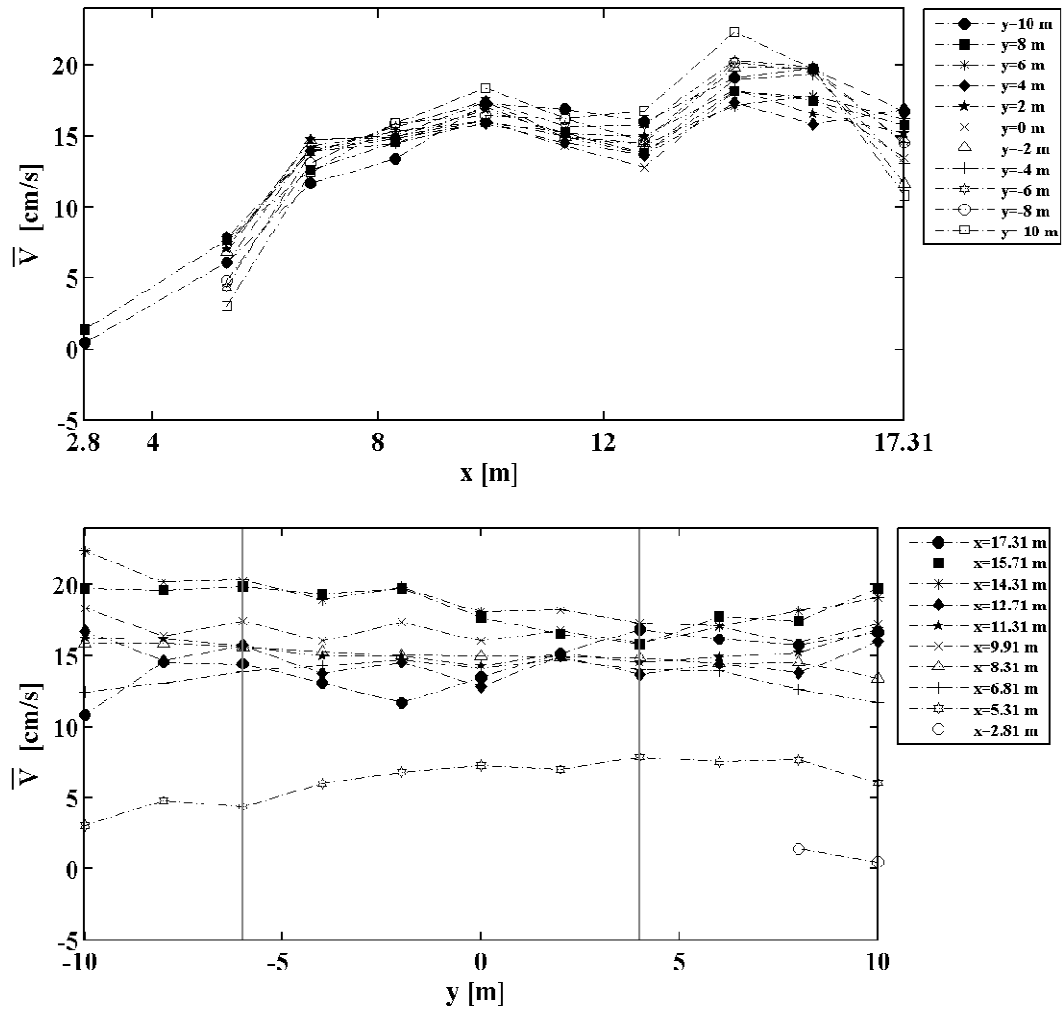


Fig. D-7. Cross-shore and longshore variations of mean longshore velocity for test

BC4

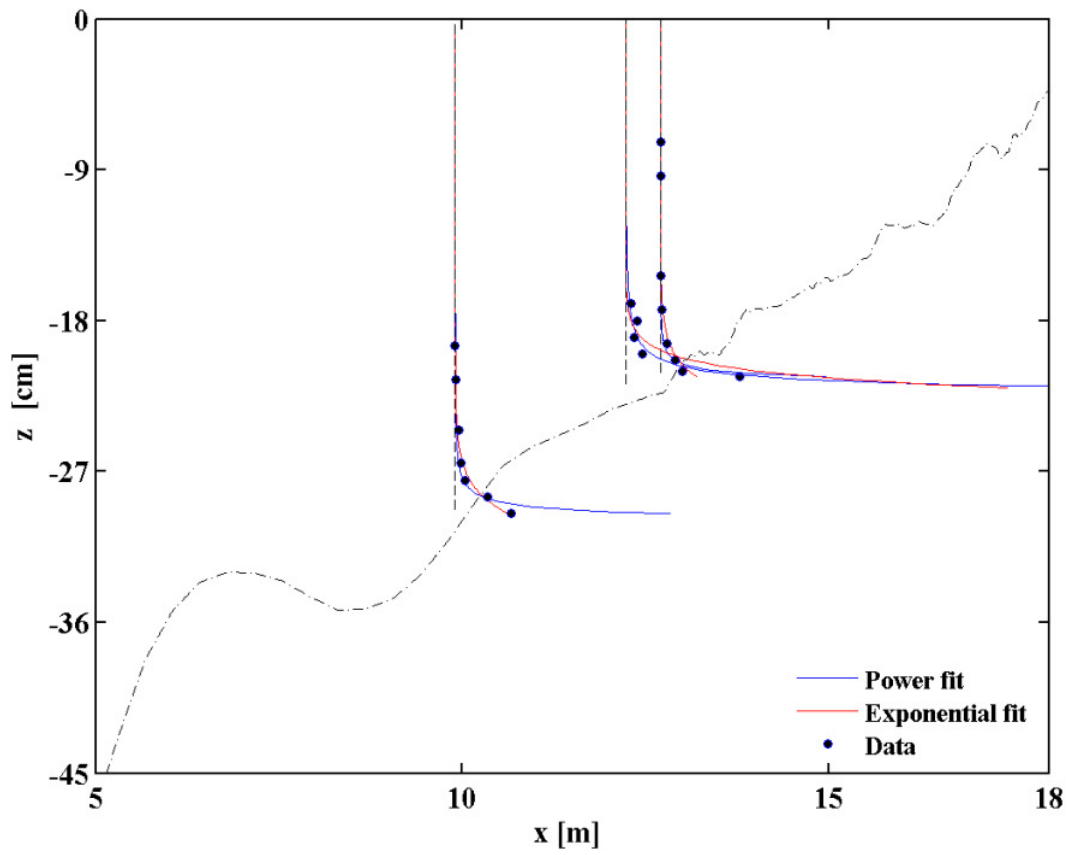


Fig. D-8. Sediment concentration data and power-form and exponential profiles at $y = 0$ for test BC4

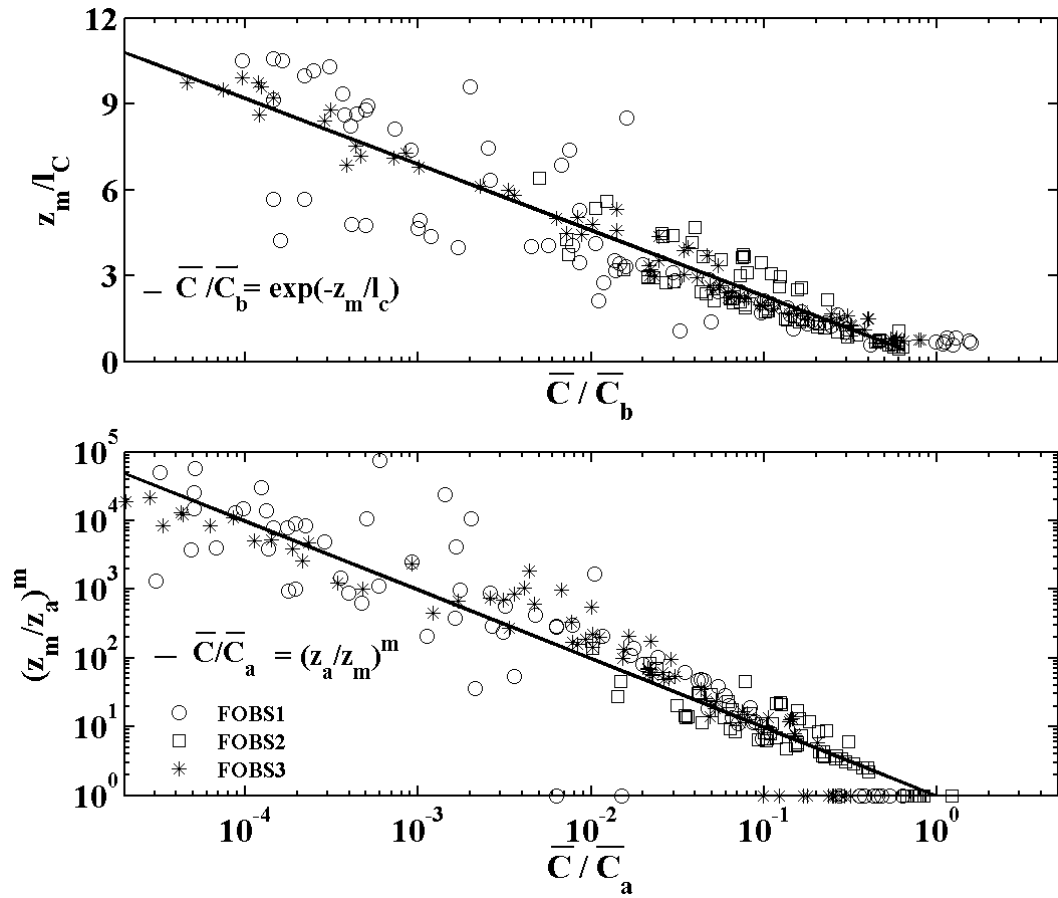


Fig. D-9. Vertical distributions of mean concentration \bar{c} using exponential and power-form profiles for each FOBS for test BC4

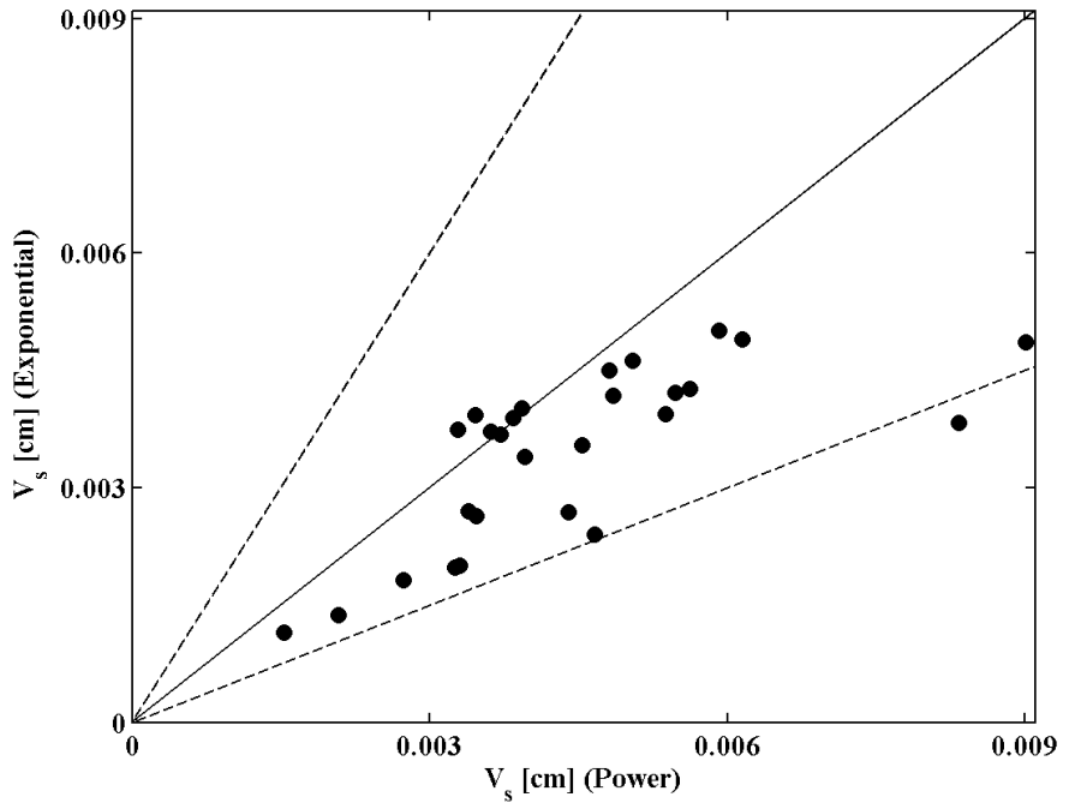


Fig. D-10. Comparison of suspended sediment volume per unit horizontal area using power-form and exponential profiles for all locations in test BC4

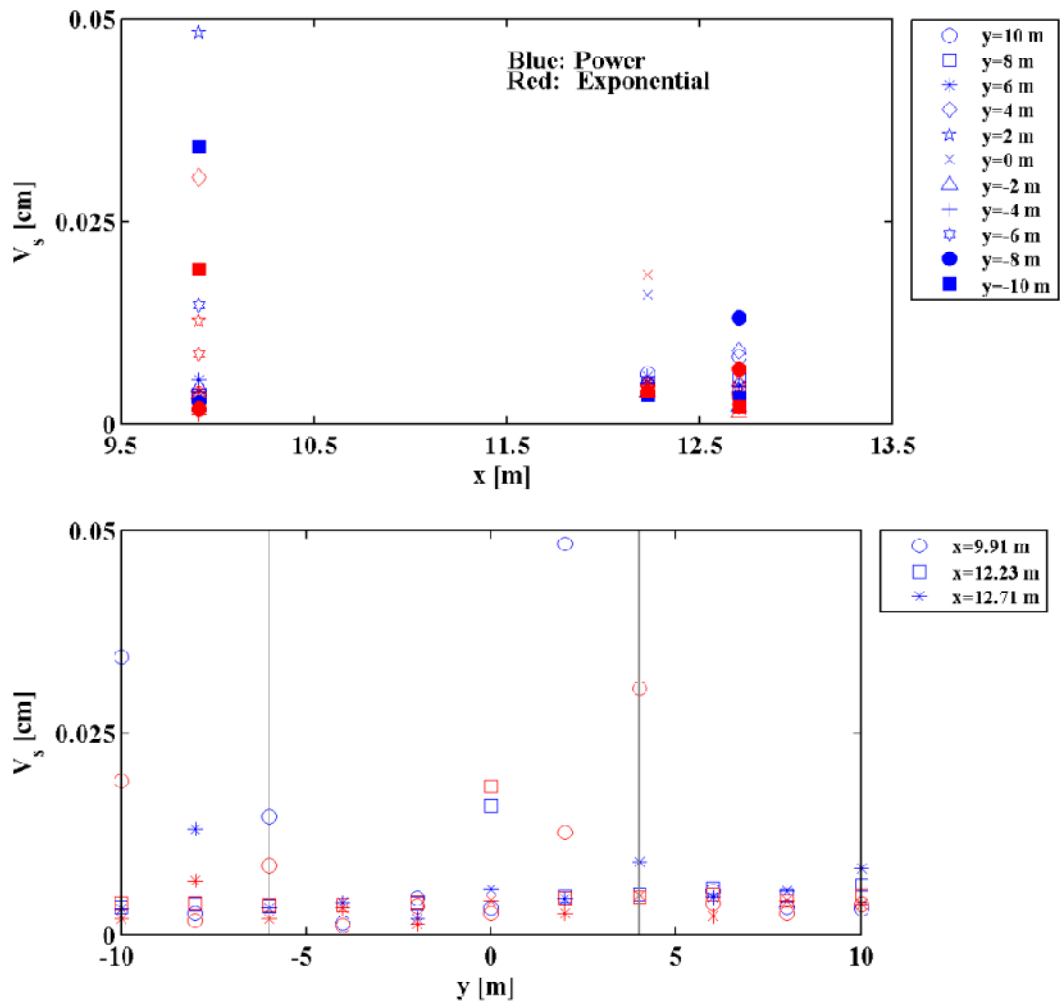


Fig. D-1. Cross-shore and longshore distributions of suspended sediment volume per unit horizontal area using power-form and exponential profiles at all locations for test BC4

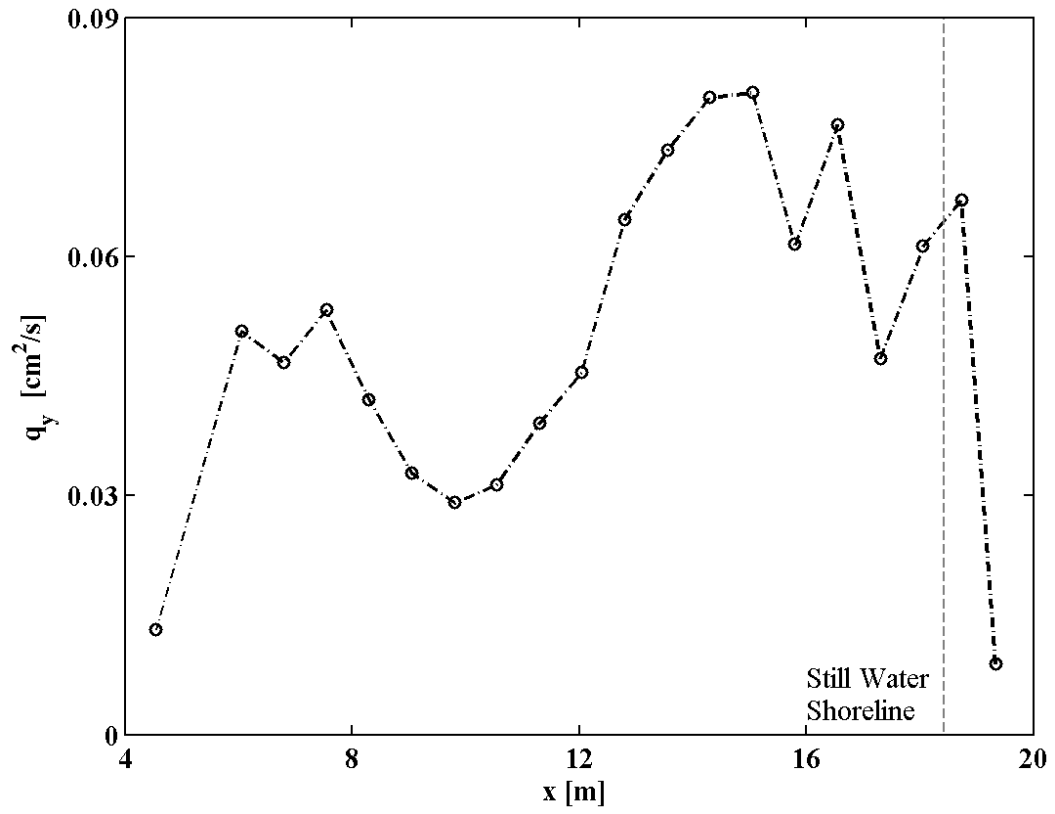


Fig. D-2. Cross-shore distribution of total longshore sediment transport rate q_y for test BC4

APPENDIX E

TEST BC5

Appendix E contains the tables and figures for test BC5.

Table E.1. Still water depth, wave setup, root-mean-square wave height and peak period at given cross-shore and longshore locations for test BC5

<i>y= 10 m</i>					<i>y= 8 m</i>				
<i>x (m)</i>	<i>d (cm)</i>	$\bar{\eta}$ (cm)	<i>H_{rms}(cm)</i>	<i>T_p (s)</i>	<i>x (m)</i>	<i>d (cm)</i>	$\bar{\eta}$ (cm)	<i>H_{rms}(cm)</i>	<i>T_p (s)</i>
0.00	90.00	-0.59	15.81	1.47	0.00	90.00	-0.36	15.82	1.48
5.31	45.23	-0.23	15.52	1.50	5.31	44.30	-0.16	14.74	1.48
6.81	32.21	-0.16	15.49	1.50	6.81	34.61	-0.23	14.04	1.50
8.31	33.27	0.02	13.36	1.50	8.31	34.37	0.18	12.11	1.58
9.91	31.10	0.12	12.24	1.59	9.91	31.09	0.31	11.46	1.58
11.31	25.83	0.32	11.58	1.59	11.31	25.47	0.51	11.00	1.58
12.71	19.88	0.14	10.30	1.59	12.71	20.52	0.32	10.03	1.59
14.31	17.03	0.37	8.08	1.71	14.31	17.07	0.60	8.34	1.73
15.13	15.27	0.39	6.91	1.73	15.13	15.80	0.62	7.42	1.85
16.23	12.93	0.56	6.16	1.84	16.23	13.20	0.79	6.95	1.86
17.31	8.61	0.67	5.24	1.85	17.31	8.82	0.83	5.80	1.86

<i>y= 6 m</i>					<i>y= 4 m</i>				
<i>x (m)</i>	<i>d (cm)</i>	$\bar{\eta}$ (cm)	<i>H_{rms}(cm)</i>	<i>T_p (s)</i>	<i>x (m)</i>	<i>d (cm)</i>	$\bar{\eta}$ (cm)	<i>H_{rms}(cm)</i>	<i>T_p (s)</i>
0.00	90.00	-0.52	15.80	1.48	0.00	90.00	-0.25	15.68	1.48
5.31	42.71	-0.37	15.91	1.51	5.31	42.99	-0.27	15.43	1.47
6.81	34.85	-0.30	14.58	1.52	6.81	34.24	-0.36	14.12	1.44
8.31	34.62	-0.09	12.83	1.50	8.31	34.31	0.05	12.42	1.49
9.91	31.08	0.04	11.83	1.50	9.91	31.82	0.13	12.10	1.50
11.31	25.76	0.24	11.43	1.51	11.31	25.57	0.33	12.12	1.49
12.71	21.17	0.09	10.16	1.56	12.71	20.61	0.15	10.44	1.59
14.31	17.28	0.39	7.88	1.71	14.31	17.28	0.47	8.02	1.72
15.13	16.23	0.42	6.64	1.72	15.13	15.90	0.48	7.17	1.85
16.23	13.20	0.58	6.00	1.86	16.23	13.30	0.64	6.53	1.85
17.31	8.99	0.66	5.26	1.87	17.31	9.05	0.63	5.66	1.86

<i>y= 2 m</i>					<i>y= 0 m</i>				
<i>x (m)</i>	<i>d (cm)</i>	$\bar{\eta}$ (cm)	<i>H_{rms}(cm)</i>	<i>T_p (s)</i>	<i>x (m)</i>	<i>d (cm)</i>	$\bar{\eta}$ (cm)	<i>H_{rms}(cm)</i>	<i>T_p (s)</i>
0.00	90.00	-0.40	15.73	1.48	0.00	90.00	-0.26	15.72	1.48
5.31	43.63	-0.43	15.06	1.49	5.31	42.24	-0.27	16.35	1.48
6.81	35.13	-0.40	14.25	1.49	6.81	34.72	-0.35	14.73	1.51
8.31	34.81	-0.12	12.98	1.51	8.31	34.30	0.09	12.48	1.50
9.91	31.38	-0.01	11.86	1.51	9.91	31.54	0.17	11.91	1.50
11.31	25.95	0.19	11.50	1.58	11.31	25.68	0.39	11.72	1.42
12.71	20.59	0.01	10.28	1.58	12.71	20.78	0.17	10.02	1.59
14.31	17.40	0.35	7.95	1.72	14.31	17.18	0.50	8.03	1.58
15.13	16.27	0.37	6.91	1.86	15.13	15.67	0.50	7.08	1.72
16.23	13.43	0.54	6.23	1.86	16.23	13.47	0.68	6.46	1.87
17.31	9.37	0.60	5.41	1.94	17.31	9.03	0.68	5.66	1.92

<i>y= -2 m</i>					<i>y= -4 m</i>				
<i>x (m)</i>	<i>d (cm)</i>	$\bar{\eta}$ (cm)	<i>H_{rms}(cm)</i>	<i>T_p (s)</i>	<i>x (m)</i>	<i>d (cm)</i>	$\bar{\eta}$ (cm)	<i>H_{rms}(cm)</i>	<i>T_p (s)</i>
0.00	90.00	-0.36	15.83	1.48	0.00	90.00	-0.20	15.67	1.48
5.31	41.96	-0.33	15.54	1.50	5.31	41.53	-0.14	15.52	1.46
6.81	34.33	-0.36	13.85	1.49	6.81	34.45	-0.23	14.62	1.49
8.31	34.48	-0.02	12.58	1.43	8.31	34.99	0.20	12.55	1.57
9.91	31.21	0.07	11.73	1.49	9.91	31.28	0.28	12.36	1.48
11.31	25.59	0.23	11.72	1.50	11.31	25.16	0.52	12.24	1.49
12.71	20.98	0.07	10.06	1.49	12.71	20.82	0.25	10.56	1.58
14.31	17.03	0.37	8.08	1.72	14.31	17.43	0.58	8.24	1.57
15.13	15.83	0.40	7.16	1.73	15.13	15.87	0.57	6.92	1.49
16.23	13.77	0.55	6.65	1.72	16.23	13.80	0.74	6.31	1.88
17.31	8.62	0.59	5.43	1.88	17.31	8.89	0.71	5.75	1.88

<i>y= -6 m</i>					<i>y= -8 m</i>				
<i>x (m)</i>	<i>d (cm)</i>	$\bar{\eta}$ (cm)	<i>H_{rms}(cm)</i>	<i>T_p (s)</i>	<i>x (m)</i>	<i>d (cm)</i>	$\bar{\eta}$ (cm)	<i>H_{rms}(cm)</i>	<i>T_p (s)</i>
0.00	90.00	-0.40	15.68	1.47	0.00	90.00	-0.22	15.84	1.48
5.31	41.37	-0.19	15.65	1.51	5.31	41.03	-0.09	16.07	1.49
6.81	32.64	-0.27	14.49	1.57	6.81	33.89	-0.23	14.55	1.46
8.31	34.08	0.08	12.94	1.49	8.31	35.28	0.25	12.88	1.57
9.91	30.85	0.13	12.16	1.58	9.91	30.75	0.31	11.49	1.42
11.31	25.38	0.29	12.03	1.58	11.31	25.20	0.53	11.56	1.59
12.71	20.71	0.09	9.92	1.50	12.71	20.86	0.25	10.71	1.59
14.31	17.63	0.37	8.09	1.59	14.31	17.41	0.57	8.29	1.59
15.13	15.70	0.41	7.46	1.60	15.13	15.67	0.57	6.69	1.58
16.23	13.67	0.54	6.78	1.71	16.23	13.30	0.75	6.10	1.73
17.31	9.17	0.54	5.50	1.88	17.31	9.25	0.69	5.63	1.88

<i>y = -10 m</i>				
<i>x (m)</i>	<i>d (cm)</i>	$\bar{\eta}$ (cm)	H_{rms} (cm)	T_p (s)
0.00	90.00	-0.41	15.75	1.48
5.31	41.07	-0.22	15.40	1.50
6.81	32.50	-0.31	14.02	1.56
8.31	34.63	0.02	12.09	1.48
9.91	30.46	0.09	12.38	1.58
11.31	25.51	0.27	12.35	1.50
12.71	21.03	0.06	9.46	1.50
14.31	17.13	0.34	8.25	1.52
15.13	15.93	0.38	7.30	1.52
16.23	13.33	0.51	6.57	1.72
17.31	9.33	0.51	5.64	1.88

Table E.2. Still water depth, mean cross-shore and longshore velocity at given cross-shore and longshore locations for test BC5

x (m)	$y=10$ m			$y=8$ m		
	d (cm)	\bar{U} (cm/s)	\bar{V} (cm/s)	d (cm)	\bar{U} (cm/s)	\bar{V} (cm/s)
5.31	45.23	-5.77	5.47	44.30	-3.60	6.87
6.81	32.21	-5.20	12.48	34.61	-4.13	12.82
8.31	33.27	-5.05	21.70	34.37	-4.57	21.94
9.91	31.10	-2.63	16.83	31.09	-2.26	16.87
11.31	25.83	-2.18	15.54	25.47	-1.92	14.95
12.71	19.88	-4.46	12.56	20.52	-4.74	11.60
14.31	17.03	-3.89	19.83	17.07	-4.61	18.24
15.13	15.27	-3.87	13.93	15.80	-4.94	14.84
16.23	12.93	-4.09	19.16	13.20	-4.64	17.47
17.31	8.61	-1.29	16.80	8.82	-1.86	15.32

x (m)	$y=6$ m			$y=4$ m		
	d (cm)	\bar{U} (cm/s)	\bar{V} (cm/s)	d (cm)	\bar{U} (cm/s)	\bar{V} (cm/s)
5.31	42.71	-3.12	7.10	42.99	-4.47	7.47
6.81	34.85	-5.26	13.89	34.24	-5.70	14.17
8.31	34.62	-5.37	22.21	34.31	-5.77	22.72
9.91	31.08	-3.08	17.50	31.82	-3.64	17.26
11.31	25.76	-3.14	15.23	25.57	-3.88	14.03
12.71	21.17	-5.01	12.45	20.61	-6.80	12.08
14.31	17.28	-4.79	17.90	17.28	-6.93	17.37
15.13	16.23	-5.39	15.02	15.90	-5.03	13.09
16.23	13.20	-4.90	17.02	13.30	-4.82	14.69
17.31	8.99	-1.94	15.84	9.05	-2.06	15.28

	<i>y</i> = 2 m			<i>y</i> = 0 m		
<i>x</i> (m)	<i>d</i> (cm)	\bar{U} (cm/s)	\bar{V} (cm/s)	<i>d</i> (cm)	\bar{U} (cm/s)	\bar{V} (cm/s)
5.31	43.63	-3.71	6.87	42.24	-4.30	7.35
6.81	35.13	-5.27	14.52	34.72	-5.78	14.42
8.31	34.81	-5.74	22.90	34.30	-6.45	23.08
9.91	31.38	-4.30	17.20	31.54	-4.18	17.01
11.31	25.95	-4.43	14.75	25.68	-4.28	14.19
12.71	20.59	-6.88	12.46	20.78	-7.18	12.09
14.31	17.40	-6.66	18.55	17.18	-6.41	17.86
15.13	16.27	-5.47	15.08	15.67	-5.05	14.61
16.23	13.43	-5.18	16.61	13.47	-4.84	16.15
17.31	9.37	-1.77	16.28	9.03	-2.65	14.28

	<i>y</i> = -2 m			<i>y</i> = -4 m		
<i>x</i> (m)	<i>d</i> (cm)	\bar{U} (cm/s)	\bar{V} (cm/s)	<i>d</i> (cm)	\bar{U} (cm/s)	\bar{V} (cm/s)
5.31	41.96	-3.91	6.37	41.53	-4.23	5.80
6.81	34.33	-5.68	14.96	34.45	-6.21	14.43
8.31	34.48	-6.10	23.15	34.99	-6.08	23.06
9.91	31.21	-4.03	17.48	31.28	-4.25	16.88
11.31	25.59	-4.19	14.94	25.16	-4.56	14.07
12.71	20.98	-7.29	12.51	20.82	-7.40	11.86
14.31	17.03	-7.20	19.23	17.43	-6.69	19.09
15.13	15.83	-5.75	15.78	15.87	-4.94	14.72
16.23	13.77	-5.46	17.06	13.80	-4.66	16.99
17.31	8.62	-2.19	15.95	8.89	-3.06	12.68

	<i>y= -6 m</i>			<i>y= -8 m</i>		
<i>x (m)</i>	<i>d (cm)</i>	\bar{U} (cm/s)	\bar{V} (cm/s)	<i>d (cm)</i>	\bar{U} (cm/s)	\bar{V} (cm/s)
5.31	41.37	-4.01	5.04	41.03	-3.61	4.64
6.81	32.64	-5.78	13.99	33.89	-5.79	13.08
8.31	34.08	-6.57	23.24	35.28	-5.99	22.81
9.91	30.85	-4.81	17.55	30.75	-4.26	16.89
11.31	25.38	-4.61	15.49	25.20	-3.95	15.54
12.71	20.71	-7.48	13.12	20.86	-5.69	12.82
14.31	17.63	-6.34	21.19	17.41	-5.49	20.60
15.13	15.70	-5.05	15.96	15.67	-2.32	NR
16.23	13.67	-5.23	18.06	13.30	-3.68	17.08
17.31	9.17	-2.98	15.33	9.25	-3.06	12.67

	<i>y= -10 m</i>		
<i>x (m)</i>	<i>d (cm)</i>	\bar{U} (cm/s)	\bar{V} (cm/s)
5.31	41.07	-3.79	3.01
6.81	32.50	-5.50	12.31
8.31	34.63	-6.00	23.85
9.91	30.46	-3.29	18.59
11.31	25.51	-3.33	16.17
12.71	21.03	-6.38	14.56
14.31	17.13	-5.00	22.43
15.13	15.93	-2.66	NR
16.23	13.33	-4.13	16.68
17.31	9.33	-3.75	10.49

Table E.3. Coefficients a and b corresponding to wave setup longshore gradient and correlation coefficient CC between data and fitted line at given cross-shore locations for tests BC5

x	a	b	CC
0	4.07E-05	-0.0031	0.18
5.31	-0.00018	-0.0029	0.64
6.81	-0.00013	-0.0034	0.78
8.31	-0.00015	0.0003	0.50
9.91	-1.12E-04	0.0012	0.42
11.31	-8.93E-05	0.0032	0.28
12.71	-4.89E-05	0.0012	0.22
14.31	-8.87E-06	0.0044	0.04
15.13	-1.93E-05	0.0045	0.10
16.23	8.48E-06	0.0062	0.04
17.31	2.43E-05	0.0063	0.14

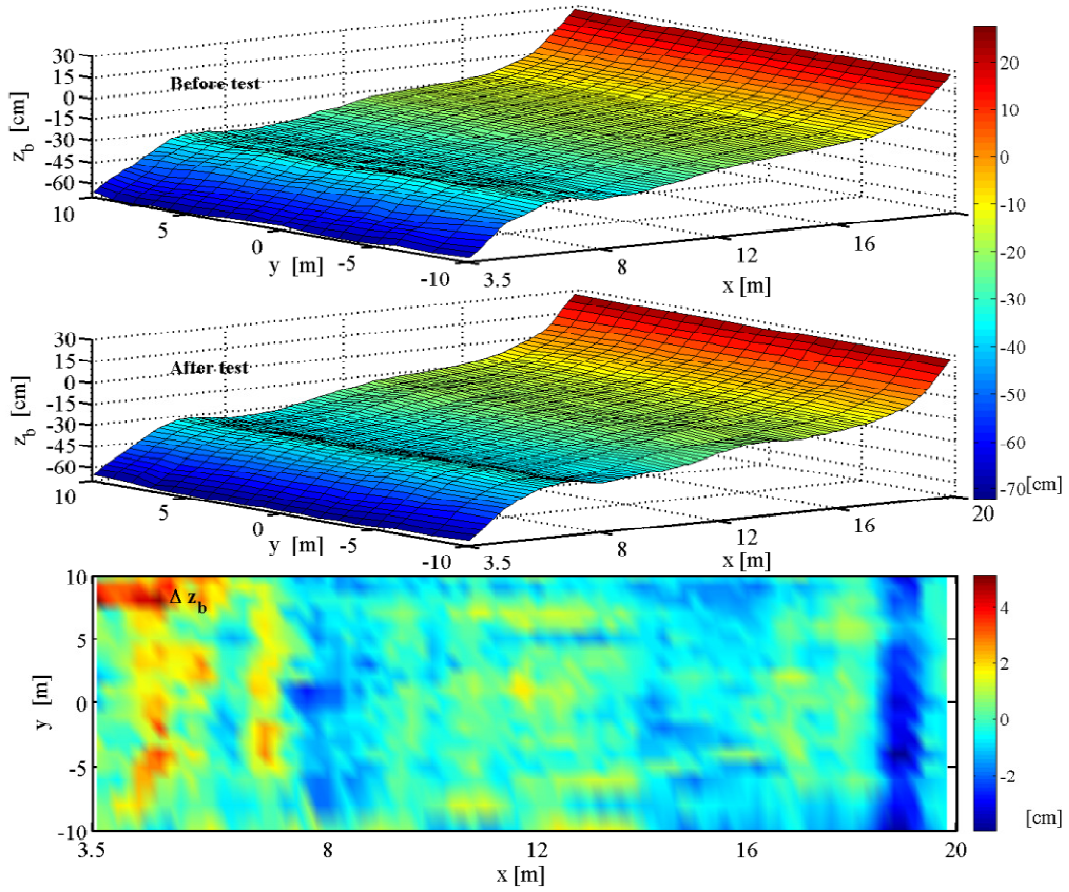


Fig. E-1. Measured initial and final profiles and change in bottom elevation for test BC5

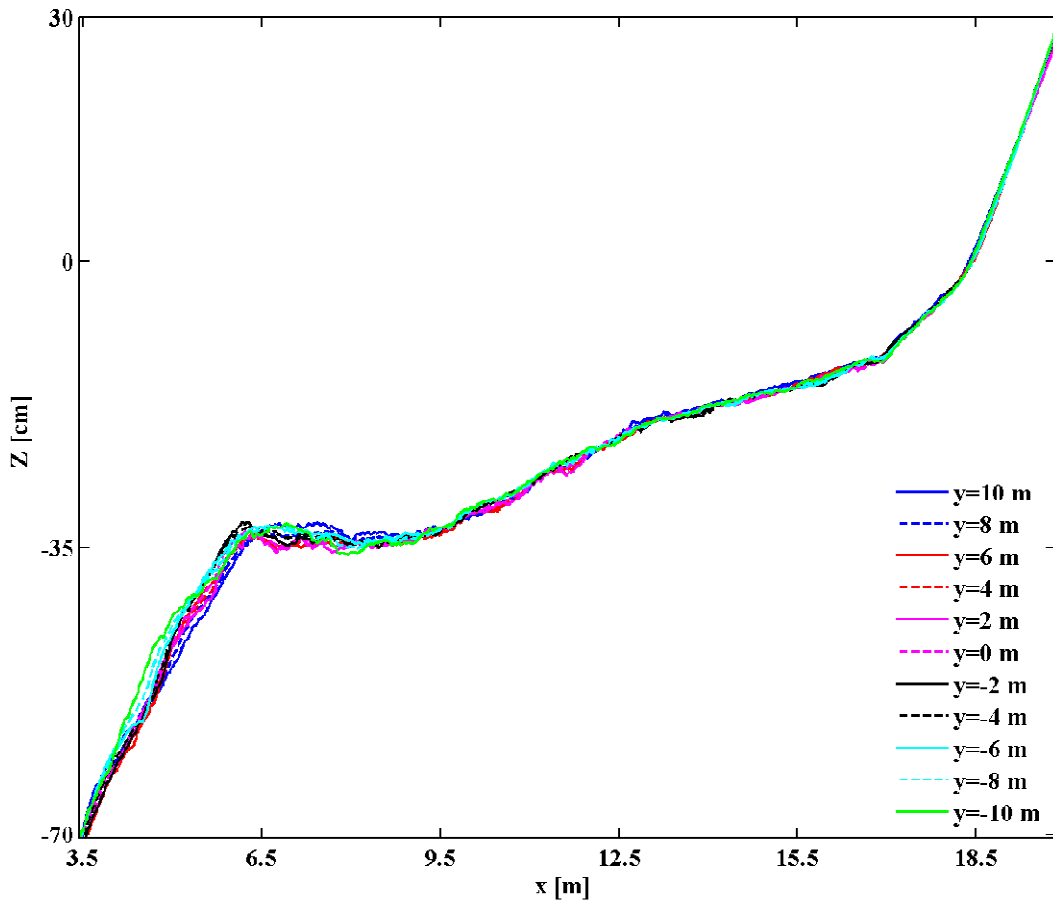


Fig. E-2. Measured initial cross-shore profiles for test BC5

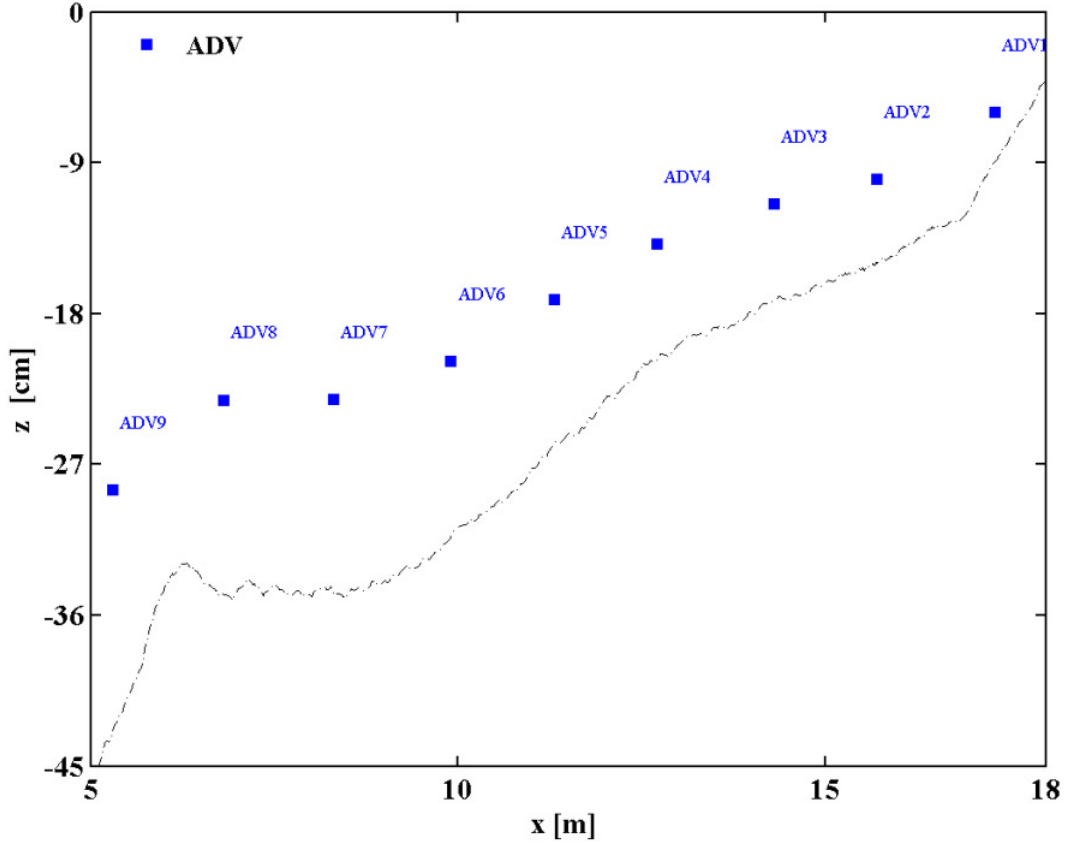


Fig. E-3. Cross-shore positioning of ADVs at $y = 0$ for test BC5

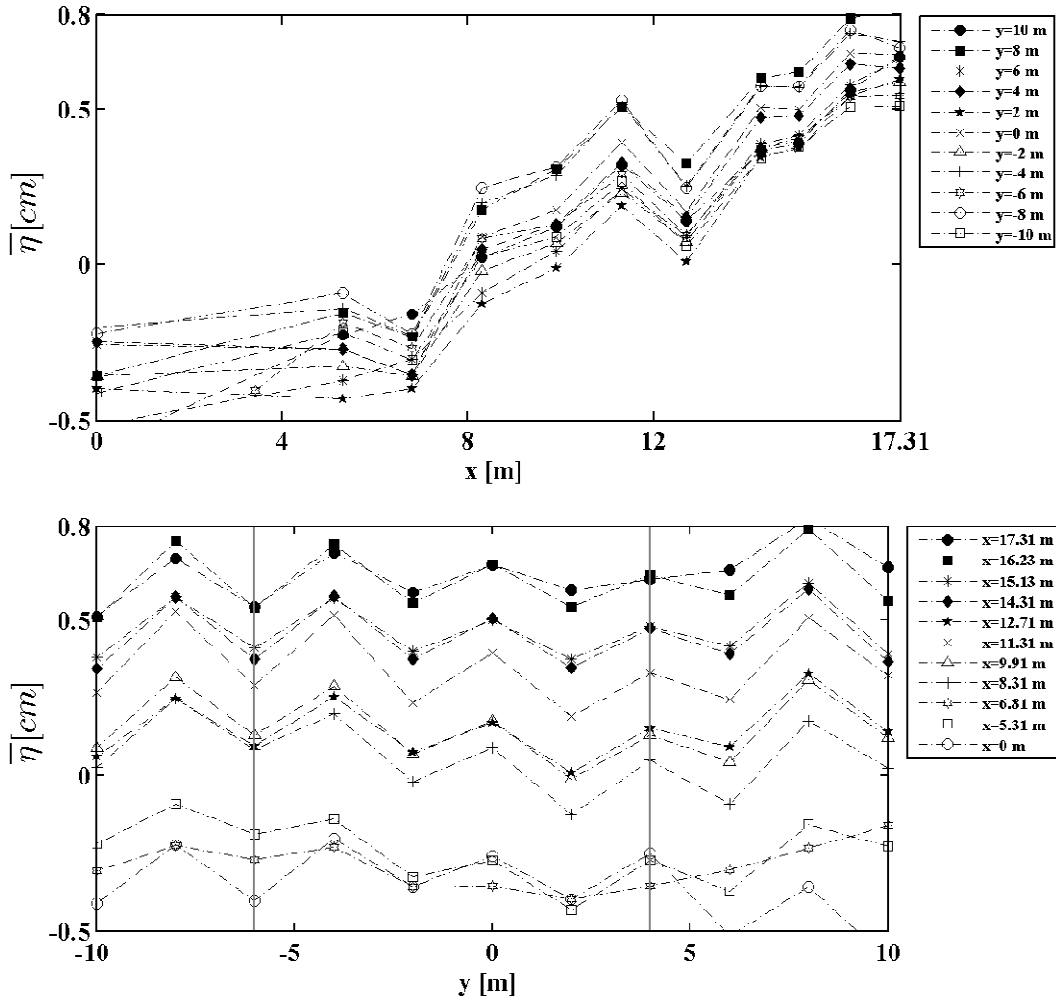


Fig. E-4. Cross-shore and longshore variations of wave setup for test BC5

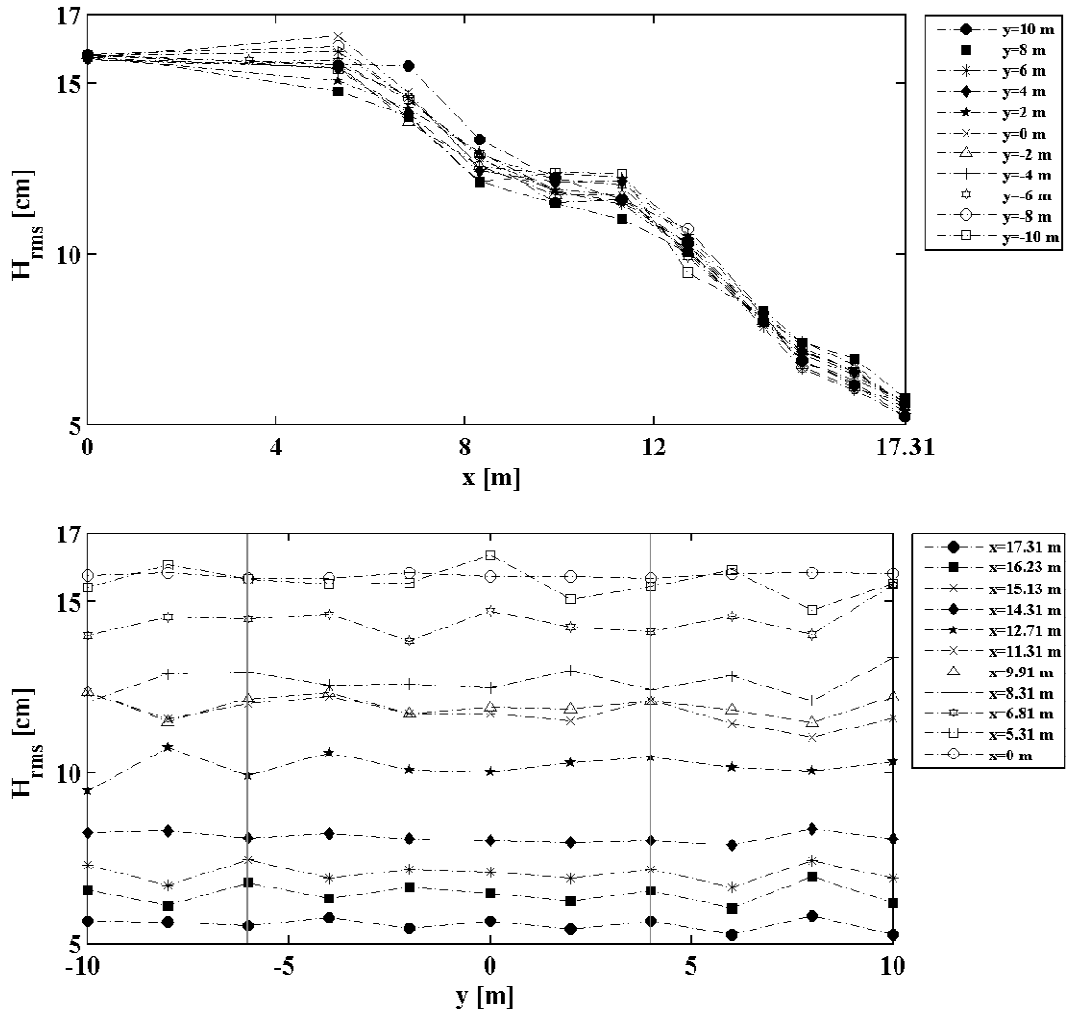


Fig. E-5. Cross-shore and longshore variations of *RMS* wave height for test BC5

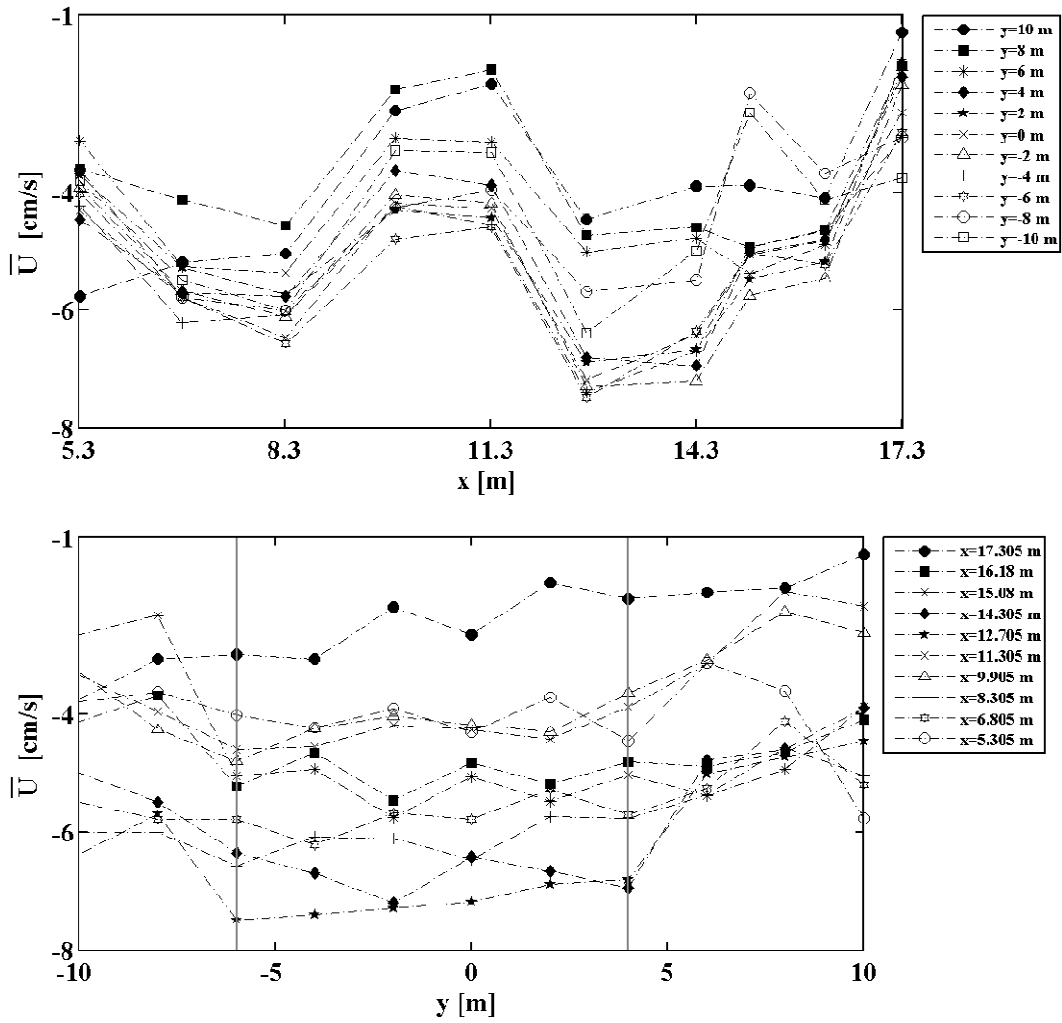


Fig. E-6. Cross-shore and longshore variations of mean cross-shore velocity for test BC5

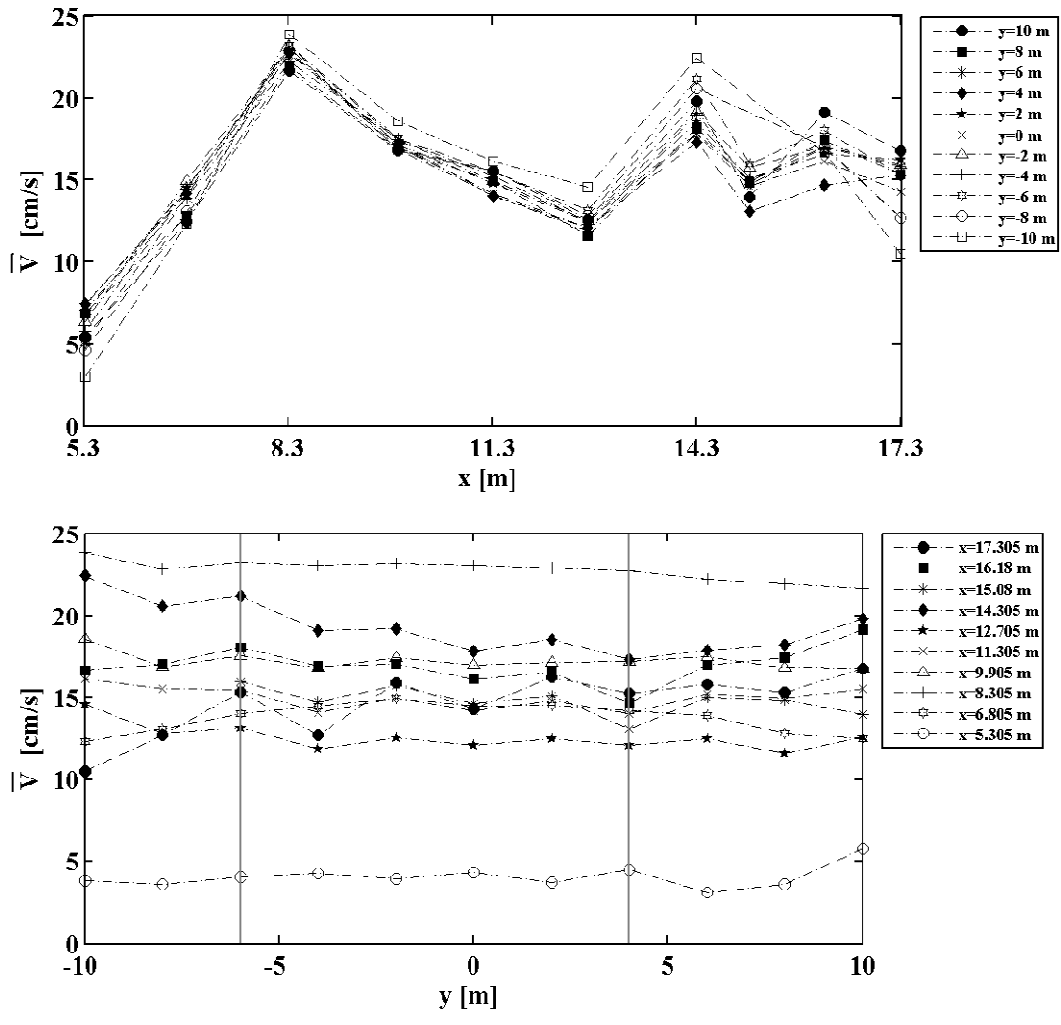


Fig. E-7. Cross-shore and longshore variations of mean longshore velocity for test BC5

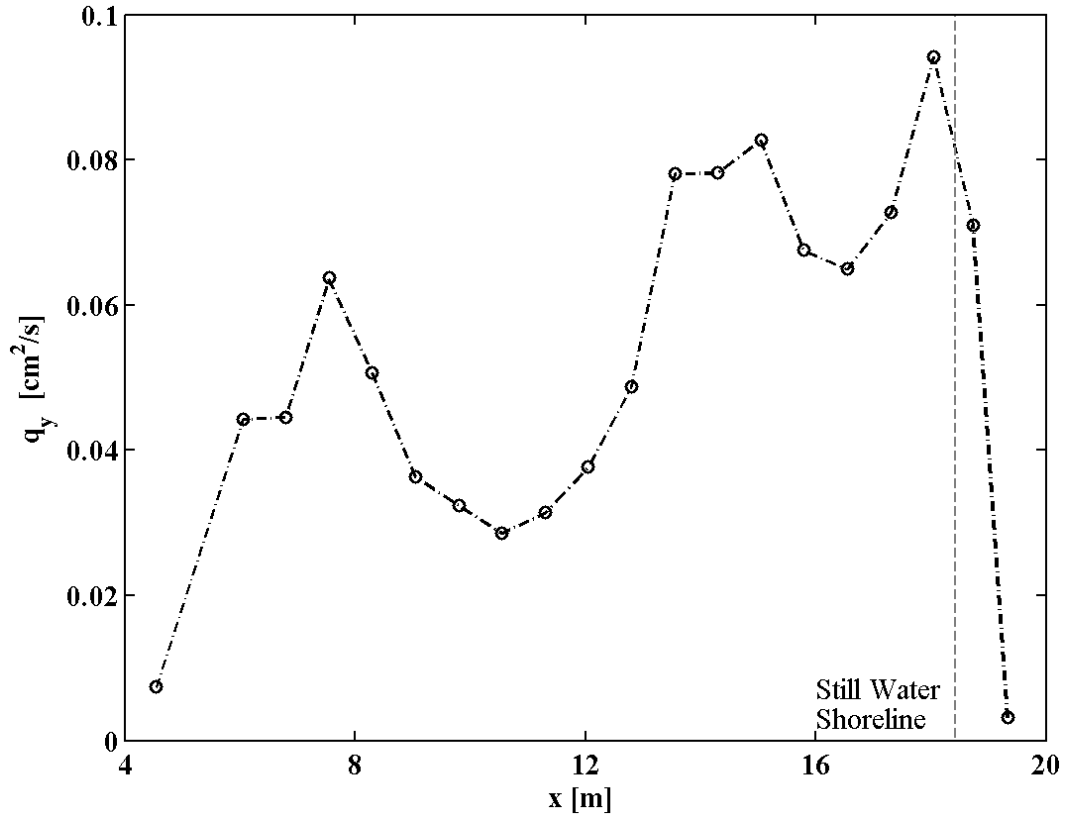


Fig. E-8. Cross-shore distribution of total longshore sediment transport rate q_y for test BC5